University of Malta

Faculty of Medicine and Surgery

MECHANISMS OF ASPIRIN-INDUCED APOPTOSIS IN REDOX-COMPROMISED YEAST CELLS:

THE EFFECT OF ASPIRIN ON THE CELL CYCLE AND GLUTAMATE METABOLISM

A thesis submitted in partial fulfillment for the degree of

Doctor of Philosophy

Maria Azzopardi

March 2020

Principal Supervisor: Professor Rena Balzan

Co-Supervisor: Professor Godfrey Grech

AUTHOR'S DECLARATION

I hereby declare that the work presented in this Ph.D. thesis is based on the results of original research carried out by myself, under the supervision of Professor Rena Balzan (principal supervisor) and Professor Godfrey Grech (co-supervisor), after having registered for a Ph.D. degree. The contents of this thesis are my own composition.

Signature: _____   Date: _____

ABSTRACT

Various non-steroidal anti-inflammatory drugs (NSAIDs) including aspirin (acetylsalicylic acid, ASA), are deemed chemopreventive. This is due to their anti-proliferative effects particularly on early-stage cancer cells, which are redox-compromised due to their reduced expression of the antioxidant enzyme manganese superoxide dismutase (MnSOD). The mechanisms by which ASA induces cell death in redox-compromised cells are not yet fully elucidated. In this study, the redox-compromised MnSOD-deficient *Saccharomyces cerevisiae* EG110 cells and the wild-type MnSOD-proficient EG103 cells, grown aerobically in ethanol medium, were used as suitable models to study the effect of ASA on the cell cycle and glutamate metabolism in redox-compromised eukaryotic cells.

The significant ASA-induced downregulation of the genes *SNO1* and *SNZ1* in EG110, but not in EG103 yeast cells, which was previously determined by microarray analysis at 48 hours of cultivation, was validated by qRT-PCR analyses. Since the proteins encoded by these two genes together catalyse the deamination of glutamine into glutamate, this study confirmed that ASA-treated EG110 yeast cells, but not their untreated counterparts, cultivated for 96 hours in ethanol medium, suffer a highly significant decline in the intracellular levels of glutamate and of its immediate metabolic products α-ketoglutarate and reduced glutathione (GSH), which are involved in mitochondrial function and redox homeostasis, respectively. Also, at 96 hours of cultivation, ASA-treated EG110 cells were observed to die, as determined by growth curves and viability assays. Flow-cytometric DNA content analysis performed in this work revealed that ASA induces a G0/G1 cell-cycle arrest in EG110 cells, whereas their untreated counterparts accumulate at the G2/M phase. Notably, the deleterious effects of ASA on EG110 yeast cells were reversed by exogenous L-glutamate. In fact, the addition of 200 mM L-glutamate to ASA-treated EG110 yeast cells

(i) restored their level of α-ketoglutarate, (ii) increased their level of GSH such that their redox balance was restored, as determined by the GSH/GSSG ratio, and (iii) protected the cells against cell cycle arrest and apoptotic cell death.

These results indicated that glutamate depletion is a critical event in ASA-induced apoptosis in redox-compromised yeast cells. Since early-stage cancer cells are also considered to be redox-compromised and heavily rely on glutamate metabolism to proliferate rapidly and uncontrollably, these findings may (i) throw light on a potential chemopreventive mechanism by which aspirin selectively commits cancer cells to apoptosis, and (ii) contribute to the development of ASA-like drugs for chemoprevention.

ACKNOWLEDGEMENTS

CONTENTS

LIST OF FIGURES

LIST OF TABLES

LIST OF ABBREVIATIONS

4-HNE – 4-hydroxynonenal

5-ASA – 5-aminosalicylic acid, mesalazine

ACD – Accidental cell death

ADP – Adenosine diphosphate

ALS – Amyotrophic lateral sclerosis

ANOVA – Analysis of variance

APC – Anaphase-promoting complex

ASA – Acetylsalicylic acid, aspirin

Atg – Autophagy-related

ATM – Ataxia telangiectasia mutated

ATP – Adenosine triphosphate

BPTES – Bis-2-(5-phenylacetamido-1,3,4-thiadiazol-2-yl)ethylsulfide

COX - Cyclooxygenase

CuZnSOD – Cupper-zinc superoxide dismutase

cAMP – Cyclic adenosine monophosphate

CDK – Cyclin-dependent kinase

cDNA – Complementary DNA

CFU – Colony-forming unit

CLS – Chronological lifespan

CoA – Coenzyme A

Ct – Cycle threshold

DEM – Diethylmaleate

DF – Dilution factor

DMSO – Dimethylsulfoxide

DNA – Deoxyribonucleic acid

DNase – Deoxyribonuclease

DON – 6-diazo-5-oxo-L-norleucine

DTNB – 5,5'-dithiobis-(2-nitrobenzoic acid)

DTT - Dithiothreitol

EDTA – Ethylenediaminetetraacetic acid

ERK – Extracellular-signal-regulated kinase

FACS - Fluorescence-activated cell sorting

FAD – Flavin adenine dinucleotide (oxidised form)

$FADH_2$ – Flavin adenine dinucleotide (reduced form)

FITC - Fluorescein isothiocyanate

Fkh – Forkhead

FSC – Forward scatter

GABA – Gamma-aminobutyrate

gDNA – Genomic DNA

GLR – Glutathione reductase

GLS – Glutaminases

GOGAT – Glutamate synthase

GPX – Glutathione peroxidase

GRX – Glutaredoxin

GSH – Glutathione (reduced form)

GSSG – Glutathione disulfide (oxidised form)

IAP – Inhibitor of apoptosis

IMS – Intermembrane space (mitochondrial)

L-asp – L-aspartate

L-glu – L-glutamate

MetO – Methionine sulfoxide

$MetO_2$ – Methionine sulfone

MLKL – Mixed lineage kinase domain-like

MMR – Mismatch repair

MnSOD - Manganese superoxide dismutase

mRNA – Messenger RNA

MUFA – Monounsaturated fatty acid

MWCO – Molecular weight cut off

NAC – N-acetylcysteine

$NAD(P)^+$ - Nicotinamide adenine dinucleotide (phosphate) (oxidised form)

NAD(P)H – Nicotinamide adenine dinucleotide (phosphate) (reduced form)

NO-ASA – Nitric oxide-releasing ASA

no-RT – No reverse transcriptase

NOX – NADPH oxidase

NRQ – Normalised relative quantities

NSAID – Non-steroidal anti-inflammatory drug

NTC – No-template control

OD – Optical density

OMM – Outer mitochondrial membrane

OSCC – Oral squamous cell carcinoma

PBS – Phosphate buffer saline

PCD – Programmed cell death

PCR – Polymerase chain reaction

PGE_2 – Prostaglandin E_2

PI – Propidium iodide

P_i – Inorganic phosphate

PI3K – Phosphatidylinositol 3-kinase

PKA – Protein kinase A

PMSF – Phenylmethylsulfonyl fluoride

PMT – Photomultiplier tube

PRX – Thioredoxin peroxidase, Peroxiredoxin

PUFA – Polyunsaturated fatty acids

qPCR – Quantitative PCR

qRT-PCR – Quantitative reverse transcription-PCR

RCD – Regulated cell death

ROH – Organic alcohol

ROOH – Alkyl hydroperoxide

ROS - Reactive oxygen species

RNA – Ribonucleic acid

RNase - Ribonuclease

RNR – Ribonucleotide reductase

RT – Reverse transcriptase / Reverse transcription

SCCHN – Squamous cell carcinoma of the head and neck

SD – Standard deviation

SDS – Sodium dodecyl sulfate

SEM – Standard error of the mean

SOD – Superoxide dismutase

SSA – Sulfosalicylic acid

SSC – Side scatter

TAE – Tris-acetate EDTA

TCA – Tricarboxylic acid

TNB – 2-nitro-5-thiobenzoic acid

TNF – Tumour necrosis factor

TRR – Thioredoxin reductase

TRX – Thioredoxin

YEPD – Yeast extract peptone dextrose

YPE – Ethanol-based

CHAPTER ONE

GENERAL INTRODUCTION

Yeasts are unicellular fungi found colonising various habitats. Studies exploring their physiology have shown that they can grow on a broad set of carbon sources (Rodrigues *et al.* 2006). In the laboratory, different yeasts were observed to grow under various conditions ranging from both fermentable to non-fermentable carbon sources as well as in the presence or absence of oxygen (Turcotte *et al.* 2009).

Saccharomyces cerevisiae cells are able to grow on fermentable carbon sources such as glucose. Once glucose becomes depleted in the growth medium, cells undergo a diauxic shift whereby yeast cells avail themselves of the accumulated fermentation products to respire aerobically. Such products include the non-fermentable carbon source ethanol as well as some amounts of glycerol and acetate (Turcotte *et al.* 2009).

Aerobic respiration involves harvesting energy from the oxidation of carbon-containing molecules while molecular oxygen acts as a terminal electron acceptor on the mitochondrial electron transport chain (ETC) (Fernie *et al.* 2004). This process is used to generate the energy-rich molecule adenosine triphosphate (ATP) critical for cells to carry out energy-demanding metabolic reactions for their survival (Lemasters *et al.* 2002, Skulachev 2006, Zhou *et al.* 2012).

In the laboratory, yeast cells may be grown on ethanol as the sole carbon source for ATP production (Figure 1.1). Ethanol increases the membrane fluidity, and thereby enters the cell by passive diffusion (Jones, Greenfield 1987, Lloyd *et al.* 1993, Navarro-Tapia *et al.* 2018). Upon entry into the cell, ethanol is oxidised into acetaldehyde while nicotinamide adenine dinucleotide (NAD^+) is reduced to NADH (de Smidt *et al.* 2008).
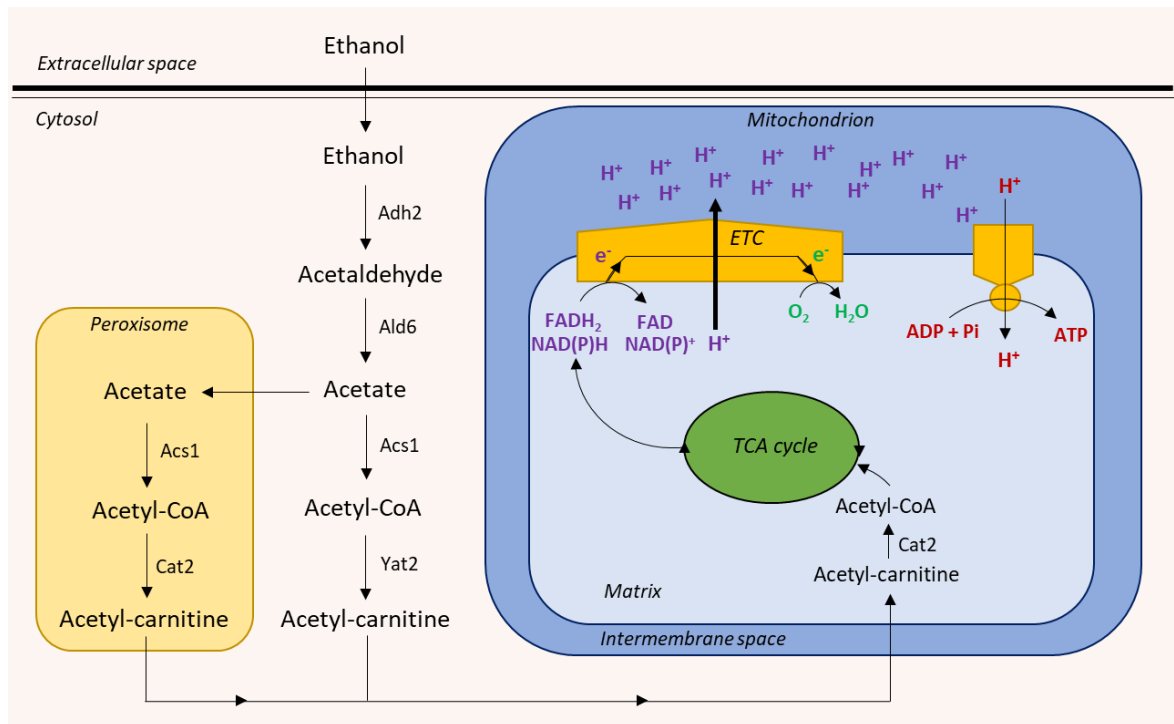
Figure 1.1 Ethanol utilisation pathway in *Saccharomyces cerevisiae*. Ethanol enters the cell by passive diffusion and undergoes oxidation into acetaldehyde and then into acetate, by alcohol dehydrogenase (Adh2) and acetaldehyde dehydrogenase (Ald6), respectively. Acetate found in peroxisomes and in the cytosol is then used for the synthesis of acetyl-Coenzyme A (acetyl-CoA), a reaction catalysed by the acetyl-CoA synthetase enzyme Acs1. The transport of acetyl-CoA into the mitochondria necessitates the involvement of carnitine acetyltransferases (Cat2 and Yat2) to facilitate the entry of the acetyl group into the mitochondria, where it is subsequently oxidised in the tricarboxylic acid (TCA) cycle. This cycle generates electron donors, namely reduced nicotinamide adenine dinucleotide (phosphate) NAD(P)H and reduced flavin adenine dinucleotide (FADH$_2$), which transfer their electrons onto the electron transport chain (ETC), while they are oxidised in the process. This drives a series of energy-yielding redox reactions at the ETC that pump H$^+$ ions from the matrix to the intermembrane space, until electrons are ultimately accepted by molecular oxygen, which is reduced to water. The H$^+$ gradient that is established across the inner mitochondrial membrane is coupled to the phosphorylation of adenosine diphosphate (ADP) to yield energy-rich adenosine triphosphate (ATP).

This reaction is catalysed by the alcohol dehydrogenase enzyme Adh2, a protein which is active at low levels of glucose or in its absence (Verdone *et al.* 2002, Walther, Schüller, 2001; Yaacob *et al.* 2016). Acetaldehyde is then converted into acetate *via* the cytosolic acetaldehyde dehydrogenase Ald6 (Meaden *et al.* 1997), which uses oxidised nicotinamide adenine dinucleotide phosphate (NADP$^+$) as a coenzyme (Saint-Prix *et al.* 2004). In turn, acetate is subsequently converted into acetyl-coenzyme A (acetyl-CoA) *via* acetyl-CoA synthetase, Acs1 (Kratzer, Schüller 1995). Carnitine acetyl transferases shunt cytosolic and peroxisomal acetyl-CoA into the mitochondria (Elgersma *et al.* 1995, Swiegers *et al.* 2001), where the acetyl group is subsequently oxidised in the tricarboxylic acid (TCA) cycle to generate carbon dioxide (CO_2), as well as the electron donors NADH and flavin adenine dinucleotide ($FADH_2$).

These electron donors are reoxidised by transferring electrons onto the ETC located in the inner mitochondrial membrane. Here, a series of energy-yielding redox reactions take place until electrons are accepted by molecular oxygen which is subsequently reduced to water. The energy harvested by reactions of the ETC is used to pump H^+ ions from the mitochondrial matrix to the intermembrane space. The established H^+ gradient across the inner mitochondrial membrane is coupled to the phosphorylation of adenosine diphosphate (ADP), synthesising ATP, in a process known as oxidative phosphorylation (Dickinson, Schweizer 1999).

In order to carry out such reactions efficiently and maximise ethanol utilisation, yeast growing on ethanol as the sole carbon source upregulate genes involved in mitochondrial function, energy metabolism and in the glyoxylate and TCA cycles (Brauer *et al.* 2005, DeRisi *et al.* 1997). Interestingly, yeast cells grown in ethanol medium also upregulate the

expression of genes involved in stress response. This finding shows the close association between respiratory metabolism and the generation of reactive species, which are key players in oxidative stress (Brauer *et al.* 2005, DeRisi *et al.* 1997, Klein *et al.* 2017).

1.1   Reactive oxygen species, oxidative stress and cellular damage

Over 2.2 billion years ago, the evolution of cyanobacteria and their ability to synthesise food by photosynthesis, resulted in an atmosphere which started accumulating significant amounts of molecular oxygen (Lane 2002). The ability of living organisms to adapt to an aerobic mode of life imposed the need for cellular redox homeostasis due to reactive oxygen species (ROS) generated when cells respire aerobically.

ROS are small, oxygen-derived radicals, ions and molecules. These are generated as reduction by-products, whenever oxygen is used during the energy generation process. The overall level of ROS in a cell at any given time is a consequence of the sum of activity of all ROS production and detoxification systems (Poljsak *et al.* 2013). This redox homeostasis is especially important since in normal cells, the effects of ROS on the cell are usually dose-dependent, ranging from beneficial to detrimental, a phenomenon known as hormesis (Davies *et al.* 1995, Martins *et al.* 2011).

ROS are involved in the regulation of signalling processes of cell division (see section 1.3.2), immune regulation (Chen *et al.* 2016b; Yarosz, Chang 2018), autophagy (Azad *et al.* 2009, Filomeni *et al.* 2015), inflammation (Canli *et al.* 2017, Mittal *et al.* 2014) and the stress-related response (see section 1.2). However, the cell's antioxidant capacity to maintain redox homeostasis may be exceeded by high levels of ROS, resulting in oxidative stress (Schieber, Chandel 2014; Ghosh *et al.* 2018). Oxidative stress is characterised by the

oxidation of several biomolecules in the cell which causes oxidative cellular damage and is a common underlying player in a multitude of diseases (de Araújo *et al.* 2016). These include: neurodegenerative disorders such as Alzheimer's disease (Ahmad *et al.* 2017), Huntington's disease (Zheng *et al.* 2018, Covarrubias-Pinto *et al.* 2015), Parkinson's disease (Blesa *et al.* 2015, Dias *et al.* 2013) and amyotrophic lateral sclerosis (ALS) (Barber *et al.* 2006), cardiovascular diseases (Madamanchi *et al.* 2005), ocular diseases (Nita, Grzybowski 2016), as well as other diseases such as diabetes (Ahmad *et al.* 2017, Maiese, 2015), rheumatoid arthritis (Phull *et al.* 2018) and cancer (Kumari *et al.* 2018, Yang *et al.* 2018b).

1.1.1 Mechanisms of ROS generation in *S. cerevisiae*

Amongst different reactive species which occur in cells, the most widely studied ROS include the superoxide and hydroxyl radicals as well as the non-radical hydrogen peroxide (H_2O_2).

Superoxide radicals

The superoxide anionic radical ($O_2{}^{\bullet-}$) is a common and highly-abundant ROS in cells respiring aerobically. Essentially, superoxide radicals are either formed at membranes or inside mitochondria of cells. Cytosolic superoxide radicals are formed by the action of membrane-bound NADPH oxidases (NOXs), which catalyse the oxidation of NADPH using oxygen (Nauseef 2008). In yeast, this reaction is catalysed by the NADPH oxidase, Yno1 (originally referred to as Aim14), which is located in the endoplasmic reticulum (Rinnerthaler *et al.* 2012). This study confirmed that ROS production by Yno1 is independent of mitochondrial respiration and of the source of ROS production in the mitochondria (Rinnerthaler *et al.* 2012). At the mitochondria, aerobic respiration takes place by oxidative

phosphorylation. This highly efficient process entails the tetravalent reduction of molecular oxygen to generate two molecules of water. However, 1-2% of molecular oxygen is not fully reduced to water (Boveris, Chance 1973). This occurs as a result of the univalent reduction of molecular oxygen by electrons which 'leak' while being transferred from one complex to another along the ETC, generating superoxide radicals.

Unlike most eukaryotes, *S. cerevisiae cells* lack complex I of the ETC (Nosek, Fukuhara 1994), but instead contain three rotenone-insensitive NADH:ubiquinone oxidoreductases (Ndi1, Nde1 and Nde2) (de Vries, Grivell 1988, Luttik *et al.* 1998, Small, McAlister-Henn, 1998), which were shown to restore the NADH oxidase activity of complex I in complex I-deficient mammalian cells (Seo *et al.* 1998, 1999). These NADH oxidoreductases together with complex III (ubiquinone cytochrome *c* reductase complex) are located on the inner mitochondrial membrane and are the main sites of mitochondrial superoxide radical production (Fang, Beattie 2003, Li *et al.* 2006), similar to most higher eukaryotes (Bleier, Dröse 2013, Dröse, Brandt 2012; Wenz *et al.* 2007).

In yeast, external dehydrogenase enzymes Nde1 and Nde2 face the intermembrane space and catalyse the oxidation of NADH in this cellular compartment. Hence, these yeast dehydrogenases generate superoxide radicals only in the intermembrane space (Fang, Beattie 2003) unlike complex I in mammalian skeletal cell mitochondria, which releases superoxide radicals to both sides of the inner mitochondrial membrane (Muller *et al.* 2004). On the other hand, the internal counterpart of the external dehydrogenases, Ndi1, faces the mitochondrial matrix and catalyses the oxidation of the NADH produced inside the mitochondrial matrix (Marres 1991). During this reaction, a distinct pool of superoxide radicals is generated in the mitochondrial matrix since the inner mitochondrial membrane is

impermeable to superoxide anions (Gus'kova *et al.* 1984, Takahashi, Asada 1983).

Overexpression of *NDI1* in a mutant yeast strain which lacks the antioxidant enzyme Sod2, causes cell lethality in both fermentable and semi-fermentable media (Li *et al.* 2006). Moreover, in the presence of exogenous stress factors, Ndi1 is also implicated in cell death by apoptosis (Cui *et al.* 2012).

NADH dehydrogenases are optimally located on the inner mitochondrial membrane to oxidise NADH by reducing ubiquinone. Unlike their mammalian counterparts, these dehydrogenases do not pump electrons across the inner mitochondrial membrane (de Vries, Marres 1987, Gonçalves, Videira 2015). Apart from collecting electrons from NADH, the ubiquinone pool also collects electrons from $FADH_2$ generated at the succinate:quinone oxidoreductase (complex II) upon conversion of succinate into malate (Lemire, Oyedotun 2002). Ubiquinol then donates its electrons to cytochrome *c via* ubiquinol:cytochrome *c* oxidoreductase (also known as bc_1 complex or complex III), a key site of superoxide radical formation in the intermembrane space (St. Pierre *et al.* 2002, Rottenberg *et al.* 2009). The ultimate transfer of electrons from cytochrome *c* onto molecular oxygen is catalysed by cytochrome *c* oxidase (complex IV). The energy associated with electron transfer is used to pump protons from the mitochondrial matrix to the intermembrane space. Hence, this energy is stored as an electrochemical proton gradient across the inner mitochondrial membrane. The resulting protonmotive force is then exploited by cells, namely to synthesise ATP *via* ATP synthase (complex V) (Jonckheere *et al.* 2012).

The radical nature of the superoxide anion and the fact that it has limited lipid solubility makes it difficult to cross membranes. As a result, superoxide radicals tend to remain compartmentalised wherever they are generated, until they are metabolised into other ROS.

In fact, the superoxide radical is a precursor of most other radical and non-radical ROS in the cell, including the peroxyl radical by protonation (de Grey 2002), the hydroxyl radical by the Fenton/Haber-Weiss reaction (Fenton 1894, Haber, Weiss 1934), and hydrogen peroxide by dismutation.

Hydrogen peroxide

Dismutation of superoxide ions into hydrogen peroxide and oxygen can take place spontaneously or catalysed by superoxide dismutase enzymes (SODs) (see section 1.2.2). Superoxide radicals are a major source of hydrogen peroxide *in vivo* (Perrone *et al.* 2008). However, hydrogen peroxide can also be generated by other enzyme-catalysed reactions, namely *via* oxidases. For instance, in yeast, hydrogen peroxide is generated by the action of the fatty-acyl coenzyme A oxidase, Pox1, during the oxidation of fatty acids in the peroxisomes (Hiltunen *et al.* 2003).

The non-radical nature of hydrogen peroxide makes it far more inert than the superoxide radical and thus is relatively longer-lived (Halliwell, Gutteridge 2015). In addition to its stability, the chemical properties of hydrogen peroxide enable it to diffuse easily across biological membranes before it is metabolised in locations close or far from its point of origin.

Hydrogen peroxide may be immediately broken down into unharmful water *via* several enzymes, namely catalases and peroxidases (see section 1.2.2). Moreover, unlike superoxide radicals, the reactivity of hydrogen peroxide is rather selective and may thus act as a second messenger or as an oxidative stress agent in a dose-dependent manner (Marinho *et al.* 2014).

At relatively low concentrations, hydrogen peroxide may mildly oxidise cysteine residues of thiol groups belonging to protein-tyrosine phosphatases or kinases which are important signal transducer proteins, to induce a transcriptional response and signalling programs in the presence of hydrogen peroxide (Fomenko *et al.* 2011, Marinho *et al.* 2014). Mild oxidation of signalling proteins may be reversed by antioxidant enzymes (see section 1.2.2), and this is key for the signal transduction process. However, at high concentrations of hydrogen peroxide, the reductive power of the cell may not be sufficient to reverse and reduce these oxidised signalling proteins. Thus, hydrogen peroxide activates transcription factors that regulate the expression of genes involved in the oxidative stress response (Delaunay *et al.* 2000, 2002, Wemmie *et al.* 1997), including that of the antioxidant genes *TRX2* (thioredoxin) (Kuge, Jones 1994), *GLR1* (glutathione reductase) (Grant *et al.* 1996a) and *GSH1* (glutathione synthase) (Gasch *et al.* 2000, Wu, Moye-Rowley 1994). If the oxidative stress response is futile, hydrogen peroxide may react with other biomolecules and give rise to other ROS, including the highly-damaging hydroxyl radical.

Hydroxyl radicals

In the presence of superoxide radicals and ferrous ions (Fe^{2+}), hydrogen peroxide takes part in the Fenton/Haber-Weiss reaction (Fenton 1894, Haber, Weiss 1934) and gives rise to the very reactive hydroxyl radical, $HO^{\bullet}$.

$$Fe^{3+} + O_2^{\bullet-} \longrightarrow Fe^{2+} + O_2$$

$$Fe^{2+} + H_2O_2 \longrightarrow Fe^{3+} + OH^- + HO^{\bullet}$$

$$\underline{\text{Net reaction}}: \quad O_2^{\bullet-} + H_2O_2 \longrightarrow OH^- + HO^{\bullet} + O_2$$
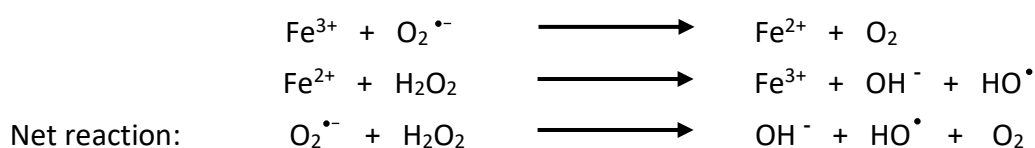
These reactions are cyclic and generate an infinite supply of hydroxyl radicals, especially since there is no enzymatic mechanism which eliminates them. Due to their highly powerful oxidant nature, hydroxyl radicals can only be metabolised by indiscriminately oxidising cellular biomolecules such as nuclear and mitochondrial DNA, proteins and membrane lipids. This causes cellular damage (see section 1.1.2) and may ultimately lead to cell death (Vranovà *et al.* 2002).

1.1.2 The role of ROS in oxidative cellular damage

The increased production of endogenous ROS is associated with apoptosis (see section 1.4.2), to the extent that levels of ROS are commonly used as apoptotic markers (Fröhlich *et al.* 2007). High levels of ROS in the cell facilitate the oxidation of key biomolecules in the cell (Halliwell, Gutteridge 2015). In fact, Muller *et al.* (2007) have shown that a correlation exists between the levels of ROS and the levels of oxidatively damaged biomolecules, namely lipids, proteins and nucleic acids.

1.1.2.1 ROS and lipid peroxidation in S. cerevisiae

Lipid molecules are amongst the targets of ROS in the cell. Yeast cells undergoing oxidative stress due to the presence of the superoxide generator menadione (Kim *et al.* 2011) or hydrogen peroxide (Reekmans *et al.* 2005) were reported to suffer of lipid peroxidation.

Lipid peroxidation is the process by which membrane phospholipids are oxidatively degraded by ROS into products, which confer further oxidative damage to cell biomolecules (Halliwell, Gutteridge 2015). The main products of lipid peroxidation include the highly unstable and toxic lipid peroxides and hydroperoxides. These are key mediators of cellular

disease and death by generating alkoxy radicals and highly reactive aldehydes such as 4-hydroxynonenal (4-HNE) (Gaschler, Stockwell 2017). 4-HNE is an inducer of oxidative stress (Uchida 2003) and limits cellular proliferation in budding yeast (Wonisch *et al.* 1998). The *de novo* synthesis of glutathione after exposure to 4-HNE reversed this restrictive growth effect, due to the ability of glutathione to form adducts (Falletti *et al.* 2007), thus preventing it from covalently modifying DNA and proteins and causing further damage to the cells (Esterbauer *et al.* 1991).

The extent of lipid oxidation is dependent on the amount of ROS (Vazquéz *et al.* 2018), the lipid composition, as well as the degree of unsaturation. In fact, poly-unsaturated fatty acids (PUFAs) are far more susceptible to oxidation than mono-unsaturated fatty acids (MUFAs), due to the presence of two or more double bonds (Ayala *et al.* 2014). Upon oxidation, changes in membrane phospholipids influence the fluidity and shape of the cell membrane. Consequently, the integrity of the membrane is compromised and the function of many membrane-bound proteins are affected (Cortés-Rojo *et al.* 2009). Such effects may lead to growth arrest and cell death (Ayala *et al.* 2014).

Several studies have implied that the mitochondria may be involved in the mechanism by which lipid peroxidation leads to apoptosis. Cardiolipin, a membrane lipid which anchors cytochrome *c* to the intramitochondrial membrane, is very susceptible to oxidation (Horvath, Daum 2013). The degree of cardiolipin oxidation and/or peroxidation alters the mitochondrial morphology and affects the retention of cytochrome *c*. In fact, cardiolipin oxidation has been implicated in cell death (Horvath, Daum 2013, Kagan *et al.* 2005, Shidoji *et al.* 1999), particularly in response to pro-apoptotic Bax-related proteins that may be

exogenously expressed in yeast to confer cell death (Korytowski *et al.* 2011, Manon 2004, Priault *et al.* 2002).

1.1.2.2 ROS and protein oxidation in S. cerevisiae

Protein molecules are amongst the targets of ROS or their products, including those which arise from the oxidative degradation of lipids (see section 1.1.2.1). Excessive protein oxidation affects the activity of proteins including enzymes involved in energy production and antioxidant defences (Kim *et al.* 2010). Failure to maintain cellular proteostasis is associated with decreased replicative lifespan in budding yeast (Yi *et al.* 2018).

All amino acids are susceptible to oxidation. A select few, namely arginine, lysine, proline and threonine form carbonyl groups upon oxidation (Stadtman, Levine 2003). This modification is irreversible (Federova *et al.* 2014, Gonos *et al.* 2018) and carbonylated proteins are largely irreparable (Nyström 2005). The sulfur-containing amino acid residues, cysteine and methionine, tend to be more prone to oxidation compared to other amino acids (Bin *et al.* 2017). Under normal physiological conditions, sulfur-containing amino acids contain protonated thiol groups (-SH). However, during stress, high levels of ROS may abstract the hydrogen of thiol groups and generate a highly reactive thiolate anion (-S$^-$) (Finkel 2000). This in turn forms a disulfide bond (-S-S-) with another thiol-containing protein or low molecular weight thiol such as glutathione, γ-glutamylcysteine, cysteine (Grant *et al.* 1999) and coenzyme A (CoA) (delCardayré *et al.* 1998). These reversible S-thionylation reactions (or S-glutathionylation if GSH is involved) result in mixed protein disulfides and are vital to protect proteins from irreversible protein oxidation during oxidative stress (Gallogly, Mieyal 2007). Disulfide bonds may be further oxidised into the relatively unstable sulfenic acid groups (-SOH) which are irreversibly oxidised into sulfinic

(-SO$_2$H) and sulfonic acid groups (-SO$_3$H) (Moskovitz *et al.* 1999). Similarly, methionine residues may be oxidised into methionine sulfoxide (MetO), a reaction which may be enzymatically reversed. However, MetO may be irreversibly oxidised into methionine sulfone (MetO$_2$) (Le Moan *et al.* 2006).

Protein oxidation can occur both at the backbone or at amino acid side groups, and may target amino acid residues which are at or close to the active site. The oxidation of amino acids that make up the protein backbone drastically change the conformation of the protein. ROS or other free radicals may either introduce new covalent bonds, leading to hydrophobic interactions or protein cross-linking, or break covalent bonds causing protein fragmentation and/or unfolding (Korovila *et al.* 2017). In any case, the activity of oxidised proteins may be affected and the protein must be degraded to maintain cellular proteostasis (Cecarini *et al.* 2006, Nyström, 2005, Wolff, Dean 1986).

Hydrogen peroxide and menadione-generated superoxide radicals, produced in aerobically respiring yeast cells, target mitochondrial proteins, namely those involved in the TCA cycle and in the ETC. Such proteins include, α-ketoglutarate dehydrogenase, aconitase and succinate dehydrogenase (Cabiscol *et al.* 2000, McLain *et al.* 2011). In a similar study, Le Moan *et al.* (2006) identified proteins which could form disulfide bridges in the presence of hydrogen peroxide. The identified proteins included enzymes involved in scavenging ROS as well as in carbohydrate and energy metabolism. Similarly, plant proteins involved in energy generation pathways, such as glycolysis and the TCA cycle are also affected by reactive species (Dumont, Rivoal 2019). Since such enzymes are pertinent to energy generation, their inactivation by reactive species results in energy depletion and growth arrest. Furthermore, excessively high levels of ROS may bring about cell death in oxidatively

damaged yeast cells by oxidising actin microtubules at two cysteine residues, forming an intracellular disulfide bond and subsequently bringing about the hyperstabilisation of the actin cytoskeleton (Farah, Amberg 2007).

1.1.2.3 ROS and oxidative damage to DNA in S. cerevisiae

Nucleic acids, DNA in particular, are also a critical target of ROS in the cell. Upon exposure to certain oxidants, cells may activate their DNA repair mechanisms and induce cell cycle arrest (Santa-Gonzalez *et al.* 2016). However, excessive levels of ROS may cause DNA replication stress which leads to DNA damage and genomic instability, contributing to the chronological ageing process (Burhans, Weinberger 2009) as well as cell death (Burhans *et al.* 2003, Marchetti *et al.* 2006).

DNA can only be directly oxidised by very strong oxidants such as hydroxyl radicals or singlet oxygen (Cadet *et al.* 1999). In fact, superoxide radicals or hydrogen peroxide may only oxidise DNA indirectly, by forming hydroxyl radicals in the Fenton/Haber-Weiss reaction (Fenton 1894, Haber, Weiss 1934) (see section 1.1.1).

Hydroxyl radicals may target the phosphate-sugar backbone and results in DNA fragmentation due to single-strand breaks and/or double-strand breaks (Breen, Murphy 1995, Dizdaroglu 1991). This scenario is similar to the process of apoptosis which involves cleavage of the DNA backbone by nucleases. In fact, if left unrepaired, strand breaks can result in cell death (Jeggo, Löbrich 2007). Unlike DNA fragmentation, most reactive oxygen radicals may directly oxidise and modify DNA bases (Cadet *et al.* 1999). For instance, the DNA base guanine is the most likely to be oxidised of all four bases and is a precursor of 8-oxoguanine, among other products of oxidation. This product is so common that it is usually

used as a biomarker for oxidative DNA damage in the cells. 8-oxoguanine is not a bulky

lesion and hence will not distort the DNA helix. As a result, it is efficiently bypassed by RNA

polymerases *in vitro* (Chen, Bogenhagen 1993). However, during transcription, an incorrect

base is thus incorporated opposite the site of damage (Beard *et al.* 2010), leading to a

mutant transcript that could direct the synthesis of mutant proteins during translation

(Saxowsky, Doetsch 2006). Mutant proteins, similar to oxidised proteins (see section

1.1.2.2), may exhibit impaired activity and are thus unable to perform their cellular function

efficiently. Cellular damage which arises due to the lack of proteostasis maintenance has

major implications on the cell's response to oxidative stress and may lead the cell to activate

cell death pathways (Santra *et al.* 2019).

During oxidative stress, both nuclear DNA as well as mitochondrial DNA may be targeted

by ROS. Mitochondrial DNA was thought to be particularly more susceptible to oxidation

due to the lack of protective histones, inefficient DNA proof-reading and repair mechanisms,

as well as due to the closer proximity of mitochondrial DNA to ETC-generated ROS (Miquel

1991). Mitochondrial DNA largely encodes proteins involved in oxidative phosphorylation.

Hence, oxidation of mitochondrial DNA compromises the respiratory ability of cells. In fact,

the addition of pro-oxidants to aerobically-grown yeast *sod2Δ* mutants, unable to eliminate

mitochondrial superoxide radicals, induced a high proportion of these cells to suffer of

respiratory deficiencies (Piper 1999). Similarly, Doudican *et al.* (2005) reported that the

presence of hydrogen peroxide in a respiration-deficient strain showed a complete loss of

mitochondrial DNA which was prevented by overexpressing Sod2. This shows that oxidative

mitochondrial DNA damage resulting from ROS, was the major contributor to mitochondrial

genomic instability.

1.2 Cellular responses to oxidative stress and maintenance of redox homeostasis in yeast

Together with other reactive species which do not necessarily contain oxygen, ROS play a critical signalling role in the cell (Breitenbach *et al.* 2018, Moldogazieva *et al.* 2018, Veal *et al.* 2007), particularly in pathways regulating cell division and stress response systems (Chiu, Dawes 2012, Schieber, Chandel 2014). They do so by bringing about the oxidation of biomolecules which monitor the cellular redox environment. This sensory function is ongoing, such that it may bring about a response to oxidative stress once a prooxidant-antioxidant imbalance occurs in favour of the former (Kehrer 2000), thereby maintaining redox homeostasis.

The oxidative stress response is ROS-specific (Evans *et al.* 1998, Jamieson 1992, Turton *et al.* 1997). However, Thorpe *et al.* (2004) identified core cellular functions that were commonly induced upon exposure to various oxidants and were thereby needed for general oxidative stress resistance. They highlighted the need for (i) changes in the gene expression *via* transcription factors, (ii) concomitant changes in protein synthesis, processing and trafficking of response proteins encompassing both enzymatic and non-enzymatic antioxidant systems, as well as (iii) the need to remove damaged proteins.

1.2.1   The role of transcription factors in the oxidative stress response

The oxidative stress response is primarily brought about by the activation of key transcription factors which sense ROS *via* oxidation of their protein segments, and in turn bring about the *de novo* transcription of critical antioxidant players (see section 1.2.2). Mutants deficient of RNA polymerase II complex, which catalyses the transcription of DNA,

were sensitive to most oxidants, meaning that transcription is essential to activate the oxidative stress response (Thorpe *et al.* 2004).

The oxidative stress-induced transcription factor Yap1 is a cytosolic protein containing a cysteine-rich C-terminal domain. This redox active domain is critical in the regulation of Yap1 since it may either be oxidised and activated by ROS or reduced by thioredoxin (Delaunay *et al.* 2000, Izawa *et al.* 1999). A wide array of oxidants, including hydrogen peroxide (Kuge, Jones 1994, Schnell *et al.* 1992), diamide (Kuge, Jones 1994) and other inducers, can oxidise Yap1 and induce its translocation from the cytosol to the nucleus (Coleman *et al.* 1999, Kuge *et al.* 1997, Wiatrowski, Carlson 2003). While in the nucleus, Yap1 accumulates and induces several antioxidant enzymatic and non-enzymatic systems (see section 1.2.2).

Yap1 does not act by itself to mediate oxidative stress response but cooperates with Skn7 (Lee *et al.* 1999, Morgan *et al.* 1997). Skn7 is a transcription factor which acts in response to various environmental stresses (Lee *et al.* 1999). Evidence of a protein-protein interaction between Yap1 and Skn7 was reported by Mulford and Fassler (2011), who stated that this interaction guarantees the availability of Skn7, when Yap1 protein accumulates in the nucleus. Both Yap1 and Skn7 were essential for the viability of yeast cells exposed to all forms of oxidative stress (Krems *et al.* 1996, Thorpe *et al.* 2004) and act in the same pathway (Ng *et al.* 2008). Yeast cells lacking both Yap1 and Skn7 exhibited high levels of carbonylated proteins when treated with hydrogen peroxide. These proteins included a key antioxidant enzyme, namely the copper, zinc superoxide dismutase enzyme, Sod1 (or CuZnSOD) (see section 1.2.2), which was thus implicated in hydrogen peroxide-induced cell death (Costa *et al.* 2002). Interestingly, Sod1 was deemed to act as a nuclear transcription factor in its own

right, in response to elevated endogenous and exogenous ROS, namely hydrogen peroxide, paraquat and menadione (Tsang *et al.* 2014). In this study, Sod1 was found to activate genes involved in cellular defence against ROS or other cellular stress inducers, genes involved in the DNA damage response as well as in the maintenance of the cellular redox state.

Furthermore, Skn7 also cooperates with the yeast heat shock factor Hsf1 to induce heat shock genes, in response to oxidative stress (Raitt *et al.* 2000). The authors indicate that in response to *t*-butyl hydrogen peroxide, Skn7 may either dimerise or physically interact with Hsf1 to form a Skn7-Hsf1 complex. These Skn7-containing complexes may then bind to the same consensus sequence as Hsf1 alone, to induce heat shock genes in response to oxidative stress.

In addition to activating heat shock genes, yeast cells may also avail themselves of another set of stress-inducible genes which may be activated by the transcription factor Msn2 and its homolog Msn4 (Gasch *et al.* 2000, Martinez-Pastor *et al.* 1996). These two proteins relocate from the cytoplasm to the nucleus upon stress induction (Martinez-Pastor *et al.* 1996), including nutritional stress indicated by low levels of cAMP and PKA activity (Görner *et al.* 1998).

1.2.2 The role of enzymatic and non-enzymatic players on ROS and the cellular redox balance

The stress-induced transcription factors discussed in section 1.2.1 are critical to bring about the oxidative stress response in an attempt to maintain redox homeostasis. This is so since they activate a large array of biochemicals, both enzymatic and non-enzymatic, which in turn control the quantity of ROS in the cell (Jamnik, Raspor 2005).

Superoxide dismutases (SODs)

Eukaryotic cells express two SOD proteins: the CuZnSOD (or Sod1) enzyme encoded by

SOD1 is found in the cytosol and mitochondrial intermembrane space, whereas the

manganese superoxide dismutase enzyme (MnSOD or Sod2), encoded by *SOD2,* is located in

the mitochondrial matrix. The most prominent function of superoxide dismutase enzymes is

the dismutation of superoxide radicals into hydrogen peroxide and molecular oxygen (Figure

1.2), thereby preventing the accumulation of superoxide radicals and their deleterious

effects on cell biomolecules (see section 1.1.2) (Costa *et al.* 2007) and the cell's function

(Longo *et al.* 1999).

$$2\ O_2^{\bullet-}\ +\ 2\ H^+\ \xrightarrow{\ SOD\ }\ H_2O_2\ +\ O_2$$
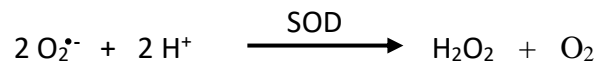
Yeast cells lacking either CuZnSOD or MnSOD were observed to have a shorter lifespan

(Longo *et al.* 1996).   In the absence of MnSOD in *S. cerevisiae* EG110 cells grown in ethanol

medium, mitochondrial superoxide dismutation is impaired and cells grow slower than the

wild-type MnSOD-proficient EG103 cells (Balzan *et al.* 2004).   In addition to this function,

Sod2 is also essential for the expression of antioxidant genes that are induced by the

accumulation of Yap1 in the nucleus (Zyrina *et al.* 2017).   In fact, these authors showed that

sod2-deficient yeast cells failed to activate Yap1 and chaperone it into the nucleus to

activate its antioxidant targets in response to oxidative stress (see section 1.2.1).

Catalases and Peroxidases

Catalases and peroxidases are involved in the detoxification of hydrogen peroxide and

alkyl hydroperoxides (ROOH) into unharmful products, namely dioxygen and water or
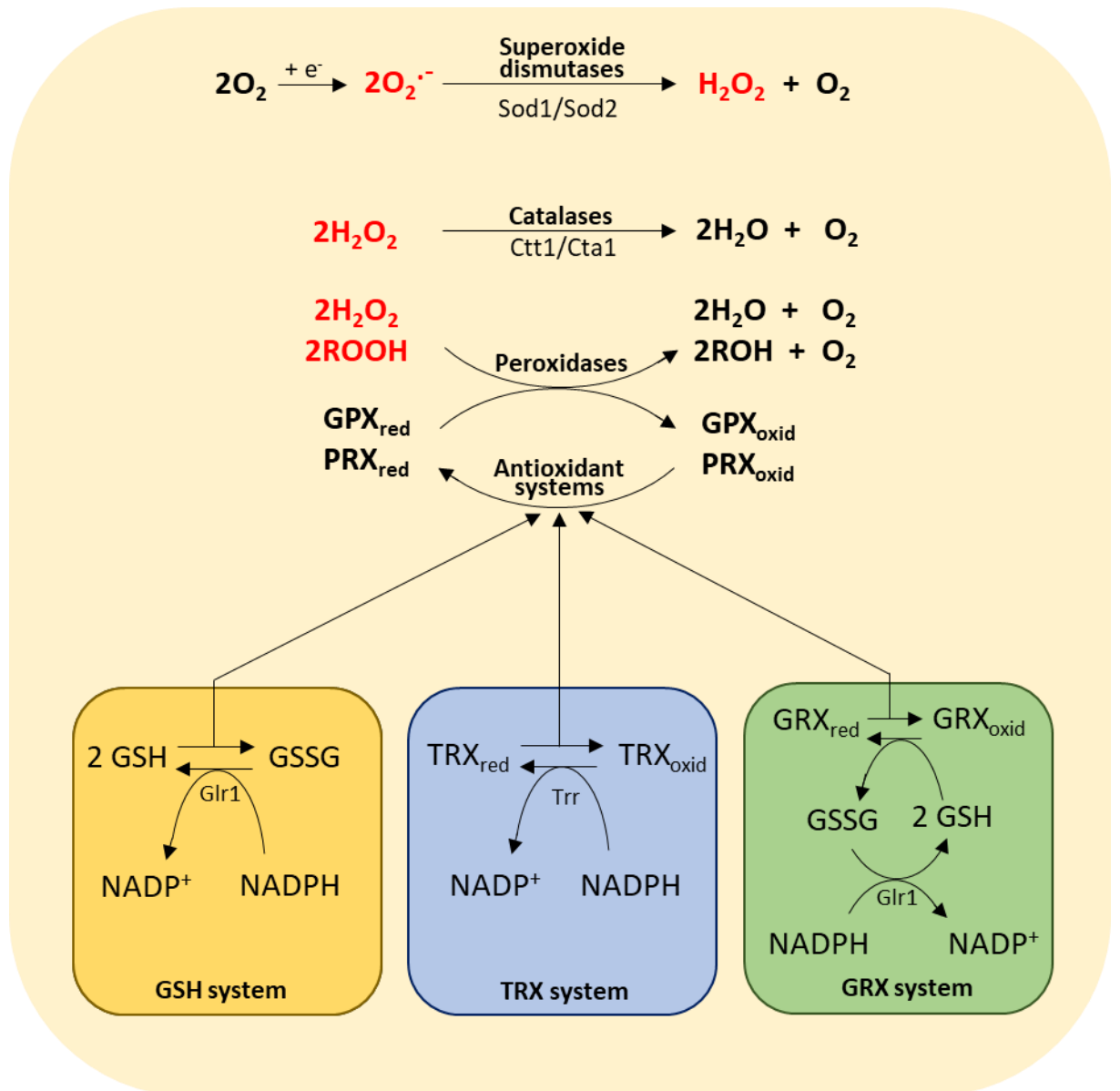
Figure 1.2: Key enzymatic and non-enzymatic antioxidant defences in budding yeast against harmful reactive oxygen species (ROS). Superoxide radicals ($O_2^{.-}$) and hydroperoxides, namely hydrogen peroxide (H_2O_2) and organic hydroperoxides (ROOH), are harmful ROS (shown in red) which must be detoxified. Superoxide dismutases (Sod1 and Sod2) catalyse the dismutation of the $O_2^{.-}$ that are generated by the univalent reduction of molecular oxygen, into H_2O_2. Catalases (Ctt1 and Cta1) detoxify H_2O_2 into water and molecular oxygen. Similarly, peroxidases (glutathione peroxidase (GPX) and thioredoxin peroxidase (PRX)) detoxify both H_2O_2 and ROOH, into unharmful water and alcohols (ROH), by donating their electrons. Hence, peroxidases are oxidised in the process (GPX_{oxid}/PRX_{oxid}). Antioxidant systems, namely glutathione (GSH), thioredoxin (TRX) and glutaredoxin (GRX), reduce peroxidases back to their reduced state (GPX_{red}-/PRX_{red}), while they are oxidised in the process into GSSG, TRX_{oxid} and GRX_{oxid}, respectively. GSSG and TRX_{oxid} may be reduced back to GSH and TRX_{red} by glutathione reductase (Glr1) and thioredoxin reductase enzymes (Trr), respectively, using electrons from reduced nicotinamide adenine dinucleotide phosphate (NADPH). In the absence of a glutaredoxin reductase enzyme, GRX_{oxid} is reduced back to GRX_{red} by the glutathione system.

organic alcohols (ROH), respectively (Figure 1.2).

Hydrogen peroxide: $2\ H_2O_2 \xrightarrow{\textbf{Catalase/Peroxidase}} O_2\ +\ 2\ H_2O$

Hydroperoxides: $2\ ROOH \xrightarrow{\textbf{Peroxidase}} O_2\ +\ 2\ ROH$
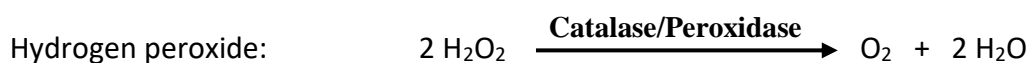
Yeast cells express two catalase proteins, one encoded by *CTT1* and is found in the cytosol and, and another encoded by *CTA1* and is located in peroxisomal and mitochondrial matrices (Cohen *et al.* 1985, Petrova *et al.* 2004). Catalases were induced to protect yeast cells from acetic acid-induced cell death (Giannattasio *et al.* 2005) due to their ability to protect proteins from oxidative modification (Luschak, Gospodaryov 2005). Furthermore, the level of catalase was observed to decline during aspirin-induced apoptosis in redox-compromised yeast cells grown in ethanol medium (Sapienza, Balzan 2005).

In addition, several peroxidases exist in yeast. For instance, glutathione peroxidases (GPX) and thioredoxin peroxidases (PRX, also known as peroxiredoxins) are known to reduce hydrogen peroxide or other hydroperoxides, while they are oxidised in the process (Figure 1.2). To be able to further catalyse such reactions, peroxidases are reduced back to their original state by other cellular antioxidant systems discussed in the following sections, namely glutathione, thioredoxins and glutaredoxins (Figure 1.2). Thus, through such reactions, catalases and peroxidases remove deleterious ROS and minimise cell damage caused by oxidative stress to facilitate the maintenance of redox homeostasis.

Glutathione (GSH) antioxidant system

An important antioxidant system comprises the non-enzymatic tripeptide glutathione
(GSH) which is made up of glutamate, cysteine and glycine. The synthesis of GSH occurs in
two steps in yeast and is partly regulated by the presence of glutamate, glutamine and lysine
in the medium (Stephen, Jamieson 1997). The first step of GSH synthesis involves the
condensation of glutamic acid to cysteine, a step catalysed by γ-glutamylcysteine synthetase,
encoded by *GSH1*. This is followed by the addition of glycine to γ-glutamylcysteine which is
catalysed by glutathione synthetase, encoded by *GSH2*.

glutamate	**Gsh1**		**Gsh2**	glutathione
+	$\longrightarrow$	γ-glutamylcysteine	$\longrightarrow$	(reduced)
cysteine			glycine	
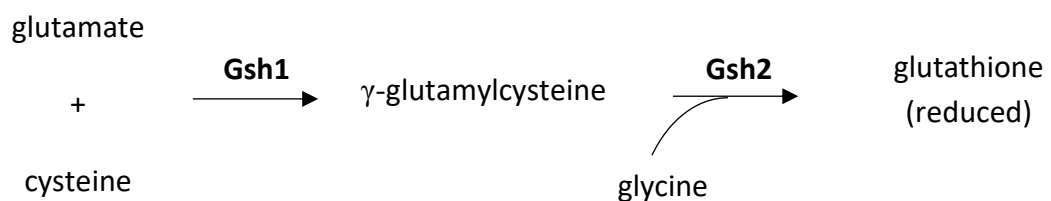
In the absence of Gsh1, the yeasts *S. cerevisiae* (Grant *et al.* 1996b, Madeo *et al.* 1999, Wu,
Moye-Rowley 1994) and *Candida albicans* exhibited GSH auxotrophy (Baek *et al.* 2004). This
shows GSH's vital role in yeast.

GSH can directly scavenge various ROS (Galano, Alvarez-Idaboy 2011, Grant *et al.* 1996a),
including harmful hydroxyl radicals (Fiser *et al.* 2013, Sjöberg *et al.* 1982) and superoxide
radicals (Winterbourn, Metodiewa 1999) as well as non-radical oxidants such as
hypochlorous acid (HOCl) (Haenen, Bast 2014) and H_2O_2 molecules (Winterbourn,
Metodiewa 1999). When the yeast *Pachysolen tannophilus* was subjected to ethanol stress
and supplemented with the three amino acids which constitute GSH, the intracellular GSH
concentration was increased and the cell acquired resistance against ethanol induced-
oxidative stress (Saharan *et al.* 2010).

GSH may also ensure cellular redox homeostasis *via* its role in cell proliferation by changing its cellular distribution in mammalian cells (Markovic *et al.* 2007), possibly in response to cell-cycle checkpoints (Pallardó *et al.* 2009*)*. This phenomenon was also exhibited in the plant *Arabidopsis thaliana,* whereby GSH co-localised with nuclear DNA during cell proliferation (Vivancos *et al.* 2010). The depletion of GSH causes an arrest of the cell cycle at the G1-phase in plant (Vernoux *et al.* 2000), yeast (Spector *et al.* 2001) and mammalian cells (Dethlefsen *et al.* 1988, Russo *et al.* 1995).

The GSH system comprises two enzymes which are key to the redox equilibrium of GSH's oxidised and reduced forms (Berndt *et al.* 2014). GSH acts as a source of electrons for glutathione peroxidase which in turn catalyses the reduction of hydroperoxides, using two GSH molecules as a reductant, such that it forms one molecule of oxidised glutathione (GSSG) (Figure 1.2). In yeast, glutathione peroxidase activity is encoded by *GPX1, GPX2* and *GPX3* (Inoue *et al.* 1999, Avery, Avery 2001). Glutathione reductase, encoded by Glr1, reduces GSSG back to GSH to maintain a high reduced-oxidised ratio in the cell, *via* electrons acquired from reduced nicotinamide adenine dinucleotide phosphate (NADPH), which is in turn oxidised to $NADP^+$ in the process (Figure 1.2). GSH's relatively high concentration and its low redox potential (- 240 mV) explains why it is the major cellular redox buffer and why the redox state of the GSH/GSSG redox couple is often taken as an indicator of the cellular redox environment (Jones 2002, Schafer, Buettner 2001).

Thioredoxin and Glutaredoxin antioxidant systems

Two other NAD(P)H-dependent antioxidant systems are the thioredoxin and glutaredoxin systems which facilitate the reduction of oxidatively-damaged side chains in proteins (Grant

24

2001). Glutaredoxins and thioredoxin are small dithiol proteins $(-SH)_2$ which contain a redox-active disulfide group in their active site to function in electron transfer.

Thioredoxins and glutaredoxins act as antioxidants by donating electrons to oxidised cysteine residues of proteins, thus converting them back to their original reduced state (Grant 2001) (Figure 1.2). Oxidised thioredoxin is then reduced back by electrons originating from NADPH and this reaction is catalysed by thioredoxin reductase enzymes (Trr) encoded by *TRR1* and *TRR2* (Figure 1.2). Unlike the thioredoxin system, glutaredoxins do not have a specific oxidoreductase which catalyses their reduction. Nevertheless, this reduction is still brought about by the oxidation of GSH to GSSG, which is in turn reduced back to GSH by glutathione reductase (Glr1) in the presence of NADPH (Figure 1.2). A specific example of this is the thioredoxin or glutaredoxin-mediated reduction of peroxidases, which in turn are needed in the reduced form to bring about the reduction of hydrogen peroxide or other hydroperoxides into water and alcohols, respectively (Figure 1.2).

Thioredoxins and glutaredoxins are highly involved in the glutathione-dependent synthesis of deoxyribonucleotides from ribonucleotides, a reaction catalysed by the enzyme ribonucleotide reductase (RNR) (Sengupta, Holmgren 2014). In fact, the deletion of the yeast thioredoxin genes *TRX1* and *TRX2,* decreased the activity of the enzyme RNR and thus limited the supply of deoxyribonucleotides. This phenomenon resulted in a prolonged S phase of the cell cycle at the expense of a shorter G1 phase (Muller, 1991). A subsequent study by Muller (1996) showed that these cell cycle effects observed in *trx1trx2Δ* mutants were accompanied by a marked increase in the level of GSSG (Muller 1996), and this further confirms that the depletion of nuclear GSH concentration limits DNA synthesis and cell

proliferation (Dethlefsen *et al.* 1988, Russo *et al.* 1995, Spector *et al.* 2001, Vernoux *et al.* 2000).

Indications of oxidative stress are obtained from ratios of intracellular GSH/GSSG or less accurately NAD(P)$^+$/NAD(P)H (Schafer, Buettner 2001). These two systems must be studied together since NAD(P)H is crucial for donating electrons to reduce GSSG and thioredoxin in reactions catalysed by the enzymes glutathione reductase and thioredoxin reductase, respectively, thereby maintaining the redox potential of the GSH/GSSG system

.

Other antioxidants in yeast

A wide variety of vitamins are known to exhibit antioxidant properties and prevent death of yeast cells exposed to oxidative stress (Branduardi *et al.* 2007, Wolak *et al.* 2014).

Pyridoxine (vitamin B6) is confirmed to be a potent antioxidant capable of quenching ROS in mammals, plants and fungi. For instance, it was shown to counteract singlet oxygen (Bilski *et al.* 2000, Ehrenshaft *et al.* 2001, Padilla *et al.* 1998)*,* quench superoxide radicals (Jain, Lim 2001, Rodríguez-Navarro *et al.* 2002) and prevent lipid peroxidation (Kannan, Jain 2004). Similarly, ascorbic acid (vitamin C) was also shown to protect yeast mutants deficient in key antioxidant enzymes, namely superoxide dismutase (*sod1Δ),* catalase (*cta1Δ),* old yellow enzyme 2 and glutathione reductase (*oye2Δglr1Δ)* (Amari *et al.* 2008)*.* The yeast analogue of ascorbic acid is D-erythroascorbate. Yeast mutants unable to synthesise erythroascrobate were sensitive to hydrogen peroxide and the superoxide anion (Huh *et al.* 1998), confirming its antioxidant properties. Interestingly, Winkler *et al.* (1994) had shown that ascorbic acid pairs up with glutathione to act as a redox couple. An ascorbate-glutathione pathway was identified in plants, and is an important component of their ROS homeostasis mechanism

(Pandey *et al.* 2015). However, this pathway has not been recorded yet in yeast. The antioxidant nature of ascorbic acid was further confirmed in yeast when ascorbic acid reduced oxidised cysteine residues on thioredoxin peroxidases that had been oxidised upon peroxide exposure (Greetham, Grant 2009, Monteiro *et al.* 2007).

Another interesting antioxidant molecule identified in yeast cells is cytochrome *c*. Giannattasio *et al.* (2008) showed that during the early phases of acetic acid-induced cell death, cytochrome *c* is released from intact mitochondria to act as a ROS scavenger and an electron donor. The authors report that the cytochrome *c* released is functional since it could transfer reducing equivalents from ascorbate and/or superoxide anions to cytochrome *c* oxidase for energy generation, before it was ultimately degraded.

1.2.3   The elimination of oxidatively-damaged biomolecules and organelles to maintain redox homeostasis

The enzymatic and non-enzymatic antioxidant systems described in section 1.2.2 may be overwhelmed if oxidative stress is uncontrollably sustained. Redox imbalance due to an oxidising environment within cells results in irreparable oxidative damage to biomolecules (see section 1.1.2) and organelles, such as the mitochondria. In order to maintain cellular homeostasis, yeast cells contain other antioxidant defence systems to eliminate irreversibly oxidised biomolecules, such as cross-linked or unfolded proteins, which are detrimental for cell survival. Elimination of irreparably oxidised components in yeast is mainly brought about by vacuolar proteolysis, proteasomal degradation and autophagy.

Vacuolar proteolysis

Vacuoles of yeast cells are hydrolytic compartments whereby macromolecules are detoxified and recycled. Vacuolar proteolysis is a key cellular process, brought about by proteases located inside the vacuole, by which excess, long-lived or damaged proteins are non-specifically degraded to preserve proteostasis. Hence, vacuoles also play a central role in responding to various stresses. Several studies showed that genes encoding vacuolar proteases or genes associated with protein sorting into the vacuole are upregulated after oxidative damage (Godon *et al.* 1998, Marques *et al.* 2006, Thorpe *et al.* 2004). In fact, vacuolar proteases, such as Pep4, are involved in degrading proteins damaged by endogenously-generated ROS. For example, the overexpression of *PEP4* in yeast cells at the stationary phase enhanced the removal of oxidised proteins (Marques *et al.* 2006*)*. Similarly, Pereira *et al.* (2010) reported the release of Pep4 from the vacuole of yeast cells exposed to acetic acid and demonstrated that Pep4 has an important protective role in mitochondrial degradation during the apoptotic process. In fact, they show that yeast cells deficient in *PEP4* could not bring about mitochondrial degradation which led to accelerated acetic acid-induced cell death. Similarly, Marques *et al.* (2006) also showed that a deficiency of Pep4 in yeast, decreased the cell's capacity to degrade and remove oxidised proteins and caused an accumulation of oxidised proteins, which resulted in a shorter yeast lifespan.

Proteasomal degradation

Another effective antioxidant defence which results in the degradation of short-lived, misfolded and oxidatively damaged proteins is *via* multicatalytic protease complexes known as proteasomes. Yeast contain two major forms of the proteasome, namely the 20 S and the

26 S, and genes encoding these proteasomal subunits were upregulated in response to hydrogen peroxide (Godon *et al.* 1998, Lee *et al.* 1999).

The 26 S proteasome, consisting of one 20 S core particle and two 19 S regulatory particles, is involved in degrading ubiquitinated proteins in an ATP-dependent manner and is largely involved in degrading cell cycle regulatory proteins. Studies have reported that oxidative stress induced a decrease in 26 S and a concomitant increase in 20 S (Wang *et al.* 2010b). This was explained by the fact that in the presence of ROS, which was either generated by protein aggregates (Livnat-Levanon *et al.* 2014, Maharjan *et al.* 2014) or by hydrogen peroxide (Wang *et al.* 2010b), the 26 S proteasome disassociated into its constituent particles, and this inhibited its proteolytic activity and resulted in the accumulation of ubiquitinated substrates. In fact, *ubi4Δ* mutants, deficient in targeting damaged proteins for degradation, were more sensitive to hydrogen peroxide (Cheng *et al.* 1994) and suffer of mitochondrial dysfunction such that they undergo early apoptosis and exhibit shortened replicative lifespan, which is only counteracted by the overexpression of *SOD2* (Zhao *et al.* 2018). Furthermore, proteasomal dysfunction or inhibition has also been associated with cell death due to amino acid scarcity (Suraweera *et al.* 2012).

Unlike the 26 S proteasome, the 20 S core particle specifically degrades oxidised proteins independent of ATP or ubiquitination (Wang *et al.* 2010b) and is key for cellular recovery from oxidative stress in response to hydrogen peroxide (Davies 2001, Wang *et al.* 2010b). In fact, the 20 S core particle proteasome was deemed the major player to degrade oxidised biomolecules since *rpn9Δ* yeast mutants, defective in assembling the 26 S proteasome but still containing the 20 S core particle, were more resistant to hydrogen peroxide since they

could degrade carbonylated proteins more efficiently than in the presence of the 26 S proteasome (Inai, Nishikimi 2002).

Autophagy

Another defence mechanism by which yeast may resist oxidative stress is autophagy (Thorpe *et al.* 2004). Autophagy is an evolutionary-conserved mechanism which involves the intracellular degradation and recycling of long-lived proteins and organelles to provide nutrients and energy (Yin *et al.* 2016). For instance, yeast cells depleted of nutrients such as carbon, nitrogen and single amino acids show autophagic bodies in their vacuoles and cause cell cycle arrest (Takeshige *et al.* 1992). Autophagy is induced once an imbalance between ROS production and thiol redox state occurs and contributes towards clearing cells of irreversibly oxidised biomolecules. In fact, decreased autophagy leads to a decline in proteostasis and this was shown in yeast *atg3Δ* mutants, defective in autophagy, which were more sensitive to oxidative stress compared to wild-type yeast (Thorpe *et al.* 2004).

Autophagy aids homeostasis by removing defective or excess organelles under both normal and stressful physiological conditions. In particular, autophagy is a key regulator of organellar homeostasis, particularly of mitochondria, in a special form of autophagy known as mitophagy (Lemasters 2005). During stationary phase, while yeast cells respire, excess mitochondria are removed since the cells decrease their energy requirement. This limits the extent of ROS production and accumulation (Kanki, Klionsky 2008). Furthermore, during oxidative stress, dysfunctional mitochondria that have lost their membrane potential are also eliminated since they are likely to release ROS and other molecules which trigger cell death (Bin-Umer *et al.* 2014, Priault *et al.* 2005).

1.3   The eukaryotic cell cycle and its role in oxidative tstress response

The cell cycle and the oxidative stress response have been studied in several eukaryotic cells, since proliferation inevitably imposes a requirement for cellular energy (Kalucka *et al.* 2015), which is generated through a series of redox reactions that give rise to deleterious ROS (see section 1.1.1).

To ensure that DNA replication and cell division only occur when sufficient cellular energy reserves have accumulated, the yeast metabolic cycle and the cell division cycle are tightly connected (Burnetti *et al.* 2016). A direct link exists between the presence of the key metabolite involved in energy generation, acetyl-CoA, and cell-cycle progression in *S. cerevisiae* (Shi, Tu 2013). The authors report that acetyl-CoA induces the transcription of the key G1 phase cyclin *CLN3* to promote entry into the cell cycle.

Conversely, a G1/S cell cycle delay in mammalian cells is associated with low ATP and low ROS levels, both mediated by the anti-apoptotic protein, Bcl-2 (Du *et al.* 2017), a protein involved in both oxidative stress resistance (Hockenbery *et al.* 1993, Kane *et al.* 1993) and cell cycle progression (Janumyan *et al.* 2003, 2008, Linette *et al.* 1996).

The pleiotropic effect of oxidative stress on the cell cycle is crucial and largely dictate the cell's fate (Shackelford *et al.* 2000). The timely stress-induced arrest of the cell cycle at checkpoints allows for the transcriptional reprogramming and repair of cellular damage, until conditions are made favourable once again (Ho *et al.* 2018). This shows that the cell cycle is a critical component of the cell's response towards physiological stress.

1.3.1 An overview of the cell cycle in *S. cerevisiae*

The eukaryotic cell cycle encompasses an evolutionarily conserved sequence of events that occur in a growing cell to duplicate all of its components. These include not only the nuclear genome but all intracellular organelles, which are divided between the two daughter cells so that they are suitably equipped to repeat the replication process (Imoto *et al.* 2011, Nurse 2000, Tyson, Novak 2008).

The cell cycle is tightly regulated and involves the alternation of DNA synthesis and DNA segregation (Hartwell, Weinert 1989). These orderly phases of the cell cycle are governed by the CDK Cdc28 in *S. cerevisiae*, which is in turn activated by, and complexes to phase-specific cyclin molecules (as reviewed by Mendenhall, Hodge 1998). Once cells attain a critical size and have sufficient nutrients at their disposition, they start a cycle of cell division which starts with the emergence of the bud at the transition from late G1 into S phase (Hartwell *et al.* 1974) (Figure 1.3). At this point, DNA synthesis also takes place and the yeast cell replicates its spindle pole bodies and begins preparations for mitosis at the G2 phase (Figure 1.3). The mitotic spindle is built and the replicated chromosomes align at the metaphase plate. The G2/M nucleus migrates to the neck of the bud and orients itself with one pole of the mitotic spindle in the mother cell and the other pole in the bud. During anaphase, the replicated chromosomes are segregated into two groups, one enters the mother cell whereas the other enters the bud. Nuclear division is then followed by cytokinesis at the neck of the bud to give rise to two unequal cells (Figure 1.3). If conditions are adverse or become unfavourable during cell division, the cells activate cell cycle checkpoints which delay or arrest cell cycle progression. Interference with cell cycle progression allows cells to initiate the appropriate responses or allow time for conditions to become favourable once again.
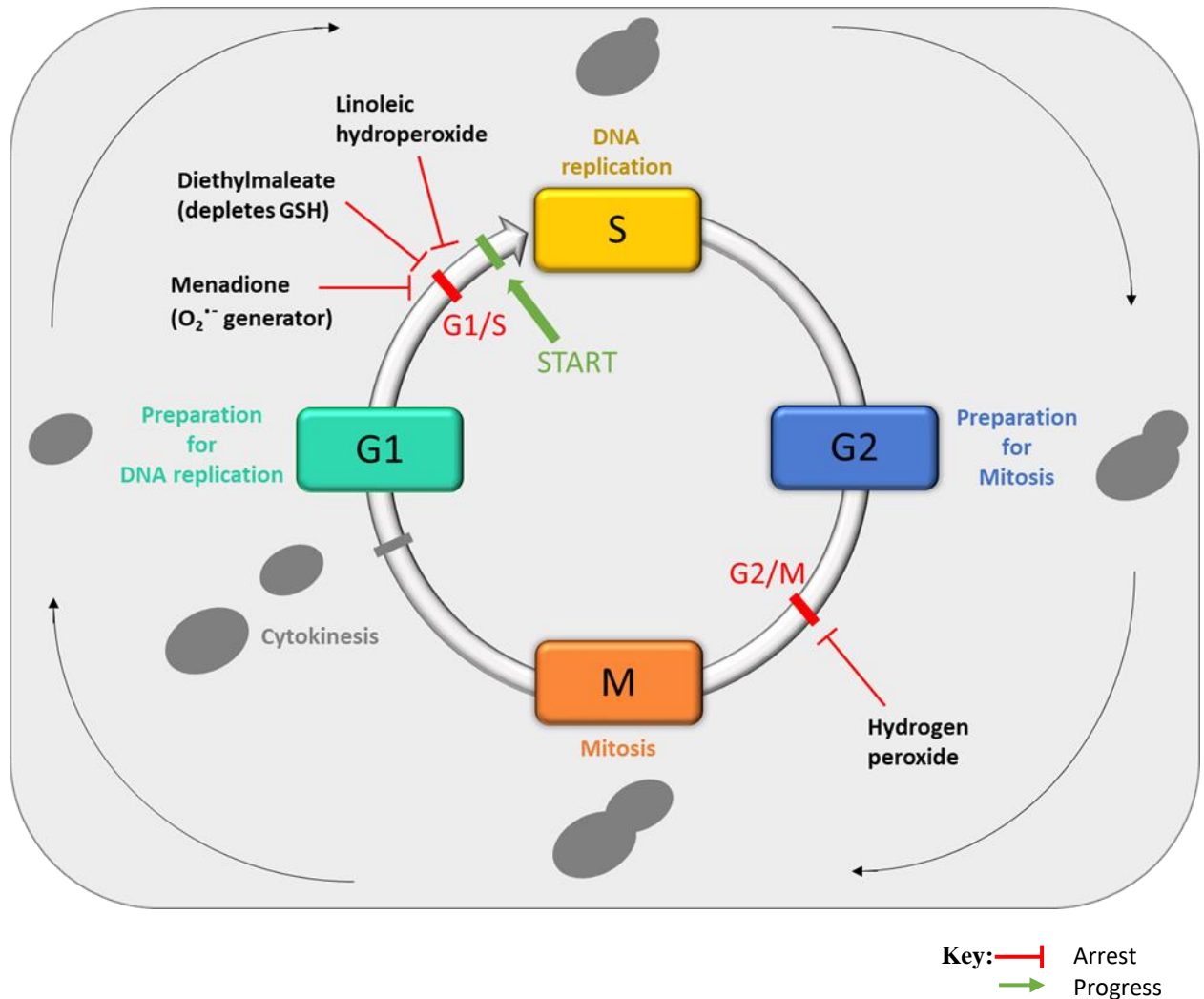
Figure 1.3   The effects of a number of ROS-generating agents on the cell cycle of the budding yeast _Saccharomyces cerevisiae_. Menadione (a superoxide radical generator), diethylmaleate (a glutathione-depleting agent) and linoleic hydroperoxide (a ROS-derived lipid peroxide) arrest the budding yeast cell cycle at the G1/S checkpoint prior to START, which marks the onset of DNA synthesis and bud emergence. On the other hand, hydrogen peroxide causes the cell cycle of budding yeast cells to stop at the G2/M checkpoint, prior to mitotic nuclear division. Morphologically, G2/M arrested budding yeast cells appear as large cells with medium to large buds. DNA, deoxyribonucleic acid; GSH, glutathione; ROS, reactive oxygen species.

This ensures the removal or repair of cellular damage for the maintenance of healthy daughter cells (Barnum, O'Connell 2014).

1.3.2   The effect of oxidative stress on the cell cycle in *S. cerevisiae*

The presence of oxidative stress in cells, due to both exogenous and endogenous sources, is closely linked to cell-cycle progression. For example, in *S. cerevisiae*, low concentrations of hydrogen peroxide induce a S phase delay followed by a G2/M arrest (Flattery-O'Brien, Dawes 1998, Leroy *et al.* 2001), whereas menadione, a superoxide radical generator, induces a G1 arrest (Flattery-O'Brien, Dawes 1998) (Figure 1.3). This shows that different ROS activate different cell-cycle checkpoints *via* different pathways.

A study conducted by Shapira *et al.* (2004) showed why menadione- and hydrogen peroxide-treated yeast cells were arrested at different cell cycle checkpoints. The authors reported that the G2/M transcription regulatory complex involving the forkhead (Fkh) transcription factors Fkh1 and Fkh2, is involved in the hydrogen peroxide-induced cell cycle arrest in yeast. Hydrogen peroxide interferes with the assembly of this complex onto the promoters of its G2/M target genes. Hence, these genes cannot be activated. Conversely, menadione has no effect on this complex since menadione-treated cells progressed through G2 to M phase, until they were then arrested at the subsequent G1/S checkpoint. However, when *fkh1fkh2Δ* cells were treated with menadione, these mutant yeast cells did not arrest at the G1/S checkpoint like their wild-type counterparts. Instead, they stopped at the G2/M checkpoint as hydrogen peroxide-treated wild-type cells.

These Fkh transcription factors are also responsible for the transcriptional activation of the anaphase-promoting complex (APC) which is a cell cycle regulator. The function of the APC under normal physiological conditions entails eliminating mitotic proteins such as the

anaphase inhibitor Pds1, to promote the transition of mitosis into the G1 phase (Cohen-Fix *et al.* 1996). However, under stressful conditions, the APC is also involved in counteracting stress by eliminating inhibitors of the oxidative stress response (Ahlskog *et al.* 2010). The roles of Fkh1, Fkh2 and the APC in overcoming oxidative stress was confirmed in a study carried out by Postnikoff *et al.* (2012) who showed that in the presence of hydrogen peroxide, a triple deletion mutant *apc5^{CA}fkh1fkh2Δ* was extremely sensitive to oxidative stress compared to single mutants or to the wild-type yeast strain.

Hcm1, another Fkh transcription factor that plays a major cell cycle role in the transcriptional activation of chromosome segregating genes (Pramila *et al.* 2006), has also been implicated in oxidative stress resistance in response to hydrogen peroxide, and especially menadione in *S. cerevisiae* cells (Rodriguez-Colman *et al.* 2010). The budding yeast cyclin-dependent kinase (CDK) Cdc28 regulates the cytoplasm-to-nucleus translocation of Hcm1 so that it can perform its cell cycle function (Ubersax *et al.* 2003). Rodriguez-Colman *et al.* (2010) showed that upon addition of hydrogen peroxide or menadione, the nuclear translocation of Hcm1 was enhanced. This phenomenon is in compliance with the microarray gene expression data also presented in the same study which showed that the overexpression of Hcm1 upregulated antioxidant genes (catalase and *SOD2*), and genes involved in: (i) mitochondrial metabolism and biogenesis, (ii) *de novo* biosynthesis of NAD$^+$ and (iii) alternative energy resources, namely to replenish TCA cycle intermediates. This gene expression data also showed that the overexpression of Hcm1 differentially expressed genes involved in cell cycle progression.

Ras2 is another protein which mediates cell cycle arrest when cells suffer of oxidative stress. In fact, a diethylmaleate (DEM)-mediated GSH depletion caused cells to arrest in the

G1 phase of the cell cycle (Figure 1.3) in a RAS-dependent manner (Wanke *et al.* 1999). Ras2 protects yeast, particularly when grown on non-fermentable carbon sources (Breviario *et al.* 1986, Tatchell *et al.* 1985), by mediating pleiotropic responses *via* the cyclic adenosine monophosphate/protein kinase A (cAMP/PKA) pathway (Bissinger *et al.* 1989), which in turn regulates various functions including cell-cycle progression (Kataoka *et al.* 1984, Mizunuma *et al.* 2013, Toda *et al.* 1985). In response to oxidative stress generated by hydrogen peroxide, Ras2 becomes proteolytically depleted (Leadsham *et al.* 2009) and this reduces Ras-cAMP-PKA signalling which in turn allows cell-cycle arrest together with stress response activation (Charizanis *et al.* 1999, Petkova *et al.* 2010). Furthermore, lack of Ras2 in cells was associated with the degradation of the NADH oxidase Yno1, which is a superoxide radical generator in yeast cells (Leadsham *et al.* 2013) (see section 1.1.1).

Linoleic hydroperoxide, an ROS-derived lipid hydroperoxide, was also reported to induce a G1/S cell cycle delay in *S. cerevisiae* cells (Alic *et al.* 2001) (Figure 1.3). A screen of genes involved in the G1 cell cycle delay following linoleic hydroperoxide treatment of yeast cells showed that the G1/S transcription factor Swi6 is highly implicated in response to this oxidant (Fong *et al.* 2008). A subsequent study by Chiu *et al.* (2011) confirmed that Swi6 contains a redox-sensitive thiol group at Cys-404 which can be oxidised into sulfenic acid to act as a stress sensor that detects oxidative stress and downregulates the expression of G1 cyclins (necessary for the G1 to S phase transition in the cell cycle) and of genes involved in DNA replication.

The timely arrest of the cell cycle, to give sufficient time for oxidative stress response, allows for the reparative actions of cellular antioxidant mechanisms, which reduce ROS. In fact, several studies have shown that low ROS levels induced longevity in several organisms,

including *C. elegans* (Schulz *et al.* 2007, Yang, Hekimi 2010), yeast (Mesquita *et al.* 2010) and mice (Hekimi *et al.* 2011). Furthermore, these cellular antioxidant mechanisms, eliminate oxidatively damaged and/or irreparable biomolecules and organelles (see section 1.2), thereby promoting cell survival (Finkel 2011, Groeger *et al.* 2009). However, if conditions still remain unfavourable, a select number of readily-available cell cycle-related proteins may exert their pro-death effects in response to overwhelming stress (as reviewed by Azzopardi *et al.* 2017). This ensures the demise of defective cells (King, Cidlowski 1998).

1.4 Oxidative stress and cell death

Cells exposed to unfavourable conditions cannot carry out their normal physiological functions. This in turn leads to their demise. Cell death may take place *via* several pathways, and death by any one of them is dependent on the ability of the cell to cope with the conditions to which it is exposed, namely the pro-death trigger/s and/or the physiological state of the cell (Fulda *et al.* 2010).

Cells subjected to acute injuries, which arise from exposure to chemical agents, mechanistic injuries or pathogens, die *via* a rapid, uncontrolled and unavoidable mechanism of cell death termed accidental cell death (ACD), often equated with unregulated necrosis (Galluzzi *et al.* 2018). This type of cell death is characterised by (i) increased cell volume (oncosis), (ii) flocculent chromatin, (iii) degradation of nucleic acids and proteins, (iv) complete disintegration of subcellular structures, and (v) early permeabilisation and rupturing of the cell membrane, releasing proteases and cellular contents in the process. The observation of these characteristics, in the absence of typical markers of other forms of cell death such as apoptosis and/or autophagy, confirms unregulated necrosis (Eisenberg *et al.* 2010, Zhivotosky, Orrenius 2001).

Regulated cell death (RCD), unlike ACD, is an orderly process of cell elimination in response to internal and external pro-death stimuli which can be genetically or pharmacologically modulated (Galluzzi *et al.* 2018). Studies have shown that RCD may serve a defence purpose to remove old, infertile or otherwise damaged cells, particularly those which fail to maintain cellular homeostasis in response to unfavourable conditions (Green, Llambi 2015). RCD also removes potentially dangerous cells harbouring deleterious mutations particularly involved in cell cycle regulation, which may lead to uncontrollable cell proliferation and onset of neoplasia (Evan, Vousden 2001). Furthermore, RCD may serve a role in the developmental stages of organisms by removing unwanted cells. This form of cell death is specifically referred to as programmed cell death (PCD) (Galluzzi *et al.* 2018).

Oxidative stress causes extensive cellular damage (see section 1.1.2) and inevitably affects fundamental cellular processes which regulate the execution of cell death, including the cell cycle (see section 1.3.2) and mitochondrial metabolism (Eisenberg *et al.* 2007). ROS-induced dysregulation of cell death has been the crux of several diseases including aging (Davalli *et al.* 2016), neurodegenerative diseases (Singh *et al.* 2019) and cancer (Kumari *et al.* 2018, Yang *et al.* 2018b).

Several studies have shown that different forms of cell death may arise when cells are treated with oxidants, in a dose-dependent manner. In the presence of excessively high concentrations of oxidants, *S. cerevisiae* cells suffered of overwhelming damage to their cellular components and concomitantly died of accidental necrosis (Ludovico *et al.* 2001, Madeo *et al.* 1999). Conversely, these same studies showed that cells treated with relatively lower doses of oxidants resorted to apoptosis, one of the RCD pathways discussed in section 1.4.1.

1.4.1 Mechanisms of regulated cell death

RCD encompasses various forms of cell death; each form displays characteristic morphological features that are induced by distinct mechanisms. These include autophagy, a specific type of regulated necrosis termed necroptosis, as well as apoptosis.

Autophagy

Autophagy is a highly controlled degradative mechanism, which relays both pro-survival and pro-death signals. In section 1.2.3, autophagy was described as a pro-survival mechanism to bring about nutrient recycling during starvation conditions and to eliminate oxidatively damaged biomolecules and organelles which, if left to accumulate, could potentially trigger cell death. However, excessive autophagy, which may arise due to the disruption of termination signals that normally restore autophagy to basal levels (Liu, Chen 2016), could result in a cell devoid of organelles. For instance, excessive mitophagy mediated by the overexpression of PINK1 or Parkin, which are proteins recruited to impaired mitochondria to trigger mitophagy, results in a cell which is unable to generate sufficient energy for its physiological functions (Narendra *et al.* 2008, 2010).

Galluzzi *et al.* (2018) defined autophagy-dependent cell death as a form of RCD which is executed by the autophagy machinery without involving other alternative cell death pathways. The autophagy machinery, which in *S. cerevisiae* mainly consists of autophagy-related (Atg) proteins, is necessary to synthesise the characteristic double-membraned vesicles known as autophagosomes (Suzuki *et al.* 2007). These vesicles engulf cytoplasmic contents which are degraded once autophagosomes fuse with lysosomes or vacuoles, in metazoans or yeast, respectively (Feng *et al.* 2014).

Yu *et al.* (2006) suggest that the specificity of the cargo sequestered in autophagosomes determines the cell's fate. The selective sequestration and ultimate degradation of proteins required for cell homeostasis and viability facilitate cell death. Such proteins include catalase (Yu *et al*. 2006) and inhibitor of apoptosis (IAP) proteins (He *et al.* 2014, Xu *et al.* 2016), amongst others. Furthermore, when autophagy is highly activated, but is defective in its termination stages, it may be rerouted towards apoptosis or necroptosis (Choi *et al.* 2016). In fact, the membranes of autophagosomes may act as scaffolds for the assembly of death-inducing complexes involved in necroptosis (Basit *et al.* 2013, Goodall *et al.* 2016, Kharaziha *et al.* 2015) and apoptosis (Young *et al.* 2012).

Necroptosis

Necroptosis is a lytic form of cell death which is regulated and displays a necrotic phenotype. In particular, it is characterised by the regulation of cell membrane leakage and rupturing in response to a variety of signals, such as death receptor ligands belonging to the tumor necrosis factor (TNF) family (e.g. TNF-α and Fas ligands) (Holler *et al.* 2000), under apoptotic-deficient conditions, such as in T lymphocyte cells deficient for caspase-8 (Ofengeim *et al.* 2015) or when exposed to caspase inhibitors (Zhang *et al.* 2009). These ligands lead to the activation of the receptor-interacting protein kinases RIPK1 and RIPK3, which regulate necroptosis. Ultimately, RIPK3 phosphorylates and activates the pseudokinase mixed lineage kinase domain-like (MLKL) protein which subsequently translocates to the plasma membrane and compromises the integrity of the plasma membrane (Dondelinger *et al.* 2014) to bring about cell lysis and necrotic cell death (Wang *et al.* 2014). The exact mechanism by which MLKL protein brings about the permeabilisation and rupturing of the plasma membrane is still obscure (Galluzzi *et al.* 2018). Studies

proposed that MLKL may do so by forming membrane-disrupting pores (Wang *et al.* 2014) or by allowing a sudden influx of extracellular Na$^+$ ions into the cell, thereby increasing the intracellular osmolality which lead cells to burst (Chen *et al.* 2016a, Xia *et al.* 2016).

In *S. cerevisiae*, the vacuolar protease Pep4 (previously described in section 1.2.3 as a protease which proteolytically eliminates oxidatively-damaged proteins) was shown to perform another cytoprotective function by extending the chronological lifespan (CLS) and inhibiting necroptotic cell death *via* its non-proteolytic function at the pro-peptide stage (Carmona-Gutierrez *et al.* 2011). The authors report that the anti-necrotic activity of Pep4 is associated with hypoacetylation of histone H3 and is dependent on the biosynthesis of polyamines, which are largely implicated in cellular survival and longevity (Eisenberg *et al.* 2009). However, the exact mechanism by which Pep4 exerts its anti-necrotic function is yet largely unknown (Carmona-Gutierrez *et al.* 2011).

Apoptosis

Apoptosis is one of the most widely studied forms among RCD pathways. Apoptosis is morphologically identified by (i) the externalisation of the lipid phosphatidylserine, which is normally present in the inward-facing leaflet of the phospholipid bilayer of the plasma membrane (Fadok *et al.* 1992, Martin *et al.* 1995), (ii) chromatin condensation (pyknosis), (iii) reduction in cellular volume due to water loss from the cell, and (iii) plasma membrane blebbing followed by karyorrhexis (nuclear fragmentation) which result in the appearance of apoptotic bodies (Madeo *et al.* 1997). During the late stages of apoptosis, DNA fragmentation (Bortner *et al.* 1995) and protein cross-linking (Nemes *et al.* 1996) are other apoptotic biochemical features which are observed.

Apoptosis is regulated by several protein families, including caspase cysteine proteases and the Bcl-2 family of proteins. Caspases selectively cleave vital proteins at aspartic acid residues (Thornberry, Lazebnik 1998), committing the cell to death in the process. Procaspases (inactive precursors of caspases) are activated (i) by their aggregation in response to death stimuli or (ii) by other caspases. This activation allows for the amplification of a caspase cascade effect (Logue, Martin 2008). Depending on their role in the cascade, caspases are broadly categorised into initiator caspases and effector caspases. Initiator caspases activate downstream effector caspases, which in turn cleave target proteins and bring about the disassembly of cells (Thornberry, Lazebnik 1998). In addition to caspases, proteins belonging to the Bcl-2 family are also critical metazoan apoptotic regulators which exert their actions directly on the outer mitochondrial membrane to regulate mitochondrial permeability (Chipuk *et al.* 2006).

Intracellularly-generated death signals (see section 1.4.2.1), including DNA damage and ROS accumulation, induce apoptosis, which may be mediated by two signalling pathways, namely the extrinsic (death receptor-induced) pathway (Green, Llambi 2015) and the intrinsic pathway (mitochondrial pathway) (Ferri, Kroemer 2001). Triggers which induce cell death by generating excessive ROS levels often impair mitochondrial respiratory complexes and/or overwhelm antioxidant systems. Such events further increase ROS levels. In turn, accumulated ROS induce (i) the permeabilisation of the outer mitochondrial membrane (Guaragnella *et al.* 2010b, Ludovico *et al.* 2002, Sapienza *et al.* 2008, Yamaki *et al.* 2001), (ii) the release of cytochrome *c* from the mitochondria, (Giannattasio *et al.* 2008, Guaragnella *et al.* 2010b, Ludovico *et al.* 2002, Sapienza *et al.* 2008, Yamaki *et al.* 2001) and (iii) mitochondrial fragmentation (Fannjiang *et al.* 2004), all of which transduce pro-apoptotic signalling. The direct activation of the pro-apoptotic Bcl-2 proteins, Bax and Bak, triggers the

release of several mitochondrial proteins into the cytoplasm, including cytochrome *c,* which

induces the formation of the apoptosome complex to activate caspases and the apoptotic

cell death cascade (Li *et al.* 1997).

1.4.2 Oxidative stress and apoptosis in *S. cerevisiae*

The reason for the evolutionary conservation of the basal apoptotic machinery in

unicellular organisms, such as yeasts, was far less clear until studies established that yeasts

naturally co-exist in colonies and have the ability to form biofilms when nutrients become

depleted (Váchová, Palková 2005, Zara *et al.* 2002). It then became evident that the

elimination of chronologically aged cells (Herker *et al.* 2004, Laun *et al.* 2001), or of infertile,

stressed or otherwise damaged yeast cells, lead to the redistribution of nutrients to younger,

healthier cells, thereby increasing their odds of survival (Büttner *et al.* 2006, Herker *et al.*

2004, Knorre *et al.* 2005). In fact, when Váchová and Palková (2005) removed from the

centre of the colony, old mother cells that displayed high ROS levels amongst other

apoptotic markers, the survival of yeast cells decreased, indicating that the younger cells at

the periphery of the colony benefitted from the inner, aged cells.

Yeast cells displaying phenotypic changes associated with apoptosis were first observed in

cdc48 mutants, deficient in AAA-ATPase which has roles in cell division, protein degradation

and vesicle trafficking (Madeo *et al.* 1997). Yeast cells lacking this protein displayed similar

apoptotic features as mammalian cells, including the exposure of phosphatidylserine at the

outer layer of the plasma membrane, DNA fragmentation as well as extensive chromatin

condensation and fragmentation. In addition to these features, the release of cytochrome *c*

from the mitochondria was another key feature observed in yeast undergoing apoptotic

yeast cell death subjected to ROS or ROS-generating sources (Eisenberg *et al.* 2007,

Giannattasio *et al.* 2008, Ludovico *et al.* 2002, Madeo *et al.* 1999, Manon *et al.* 1997,

Sapienza *et al.* 2008, Yang *et al.* 2008).

1.4.2.1 ROS-generating sources trigger apoptosis in S. cerevisiae

ROS have long been deemed as potent regulators of cell death (Chandra *et al.* 2000,

Simon *et al.* 2000, Ludovico *et al.* 2001, Madeo *et al.* 1999). Their accumulation is a key

event which occurs in yeast cells dying by apoptosis. In fact, aged mother cells dying by

apoptosis displayed high ROS levels when stained with dihydroethidium (Váchová, Palková

2005). In addition, several studies have been carried out to decipher which ROS, or sources

of ROS, trigger apoptosis. Triggers were found to be either (i) exogenous, namely *via*

chemical or physical sources, or *via* the heterologous expression of human pro-apoptotic

proteins, or (ii) endogenous, by activating pro-death signal transduction pathways, for

example in response to mutations.

Exogenous sources

Apoptosis preceded by ROS accumulation may result from exposure to ROS-generating

exogenous agents including hydrogen peroxide (Madeo *et al.* 1999), acetic acid (Ludovico *et

al.* 2001, Giannattasio *et al.* 2005, Fannjiang *et al.* 2004), valproic acid (Mitsui *et al.* 2005),

acetylsalicylic acid (Balzan *et al.* 2004, Sapienza, Balzan 2005, Farrugia *et al.* 2013),

pheromones (Severin, Hyman 2002), heavy metals (Du *et al.* 2007, Liang, Zhou 2007,

Nargund *et al.* 2008), drugs (Almeida *et al.* 2008) and ultraviolet radiation (Del Carratore *et

al.* 2002). The heterologous expression of human pro-apoptotic proteins such as Bax also

promotes ROS generation in the mitochondria of budding yeast (Ligr *et al.* 1998). In turn,

the resultant ROS accumulation may cause a wide array of cellular damage (see section

1.1.2) which if uncontrolled triggers internal pathways which overlap with pathways

activated by the following endogenous sources.

Endogenous sources

The presence of mutations which interfere with the cell's ability to maintain cellular

homeostasis are endogenous sources which result in apoptotic cell death. Defects which

arise from such mutations cause cellular dysfunction and result in the subsequent activation

of pro-death pathways (Weinberger *et al.* 2005). Mutations which cause defects in

mitochondrial oxidative phosphorylation such as respiratory-deficient mutants lacking

mitochondrial DNA, as well as mutants with a depleted intramitochondrial ATP pool due to

inhibition of mitochondrial respiration, die *via* an apoptosis-like cell death, involving ROS

accumulation (Trancíková *et al.* 2004).

Furthermore, gene deficiencies or defects associated with the oxidative stress response

machinery also trigger cell death by apoptosis and shorten the replicative lifespan during

oxidative stress (Odat *et al.* 2007, Zhao *et al.* 2018). For instance, mutations which result in

glutamate or GSH depletion result in cell death by apoptosis. This occurs due to glutamate's

vital cellular roles in the synthesis of the (i) metabolite α-ketoglutarate, which is necessary

for the bioenergetic and biosynthetic functions of the TCA cycle, and (ii) major cellular

antioxidant GSH which plays a key role in maintaining redox homeostasis for cells to thrive.

Yeast mutant cells which suffer of glutamate depletion, including *gdh3Δ* cells (lacking a

NADP+-dependent glutamate dehydrogenase) (Lee *et al.* 2012) and *cit1Δ* cells (lacking

mitochondrial citrate synthase) (Lee *et al.* 2007), display apoptotic features accompanied by

high levels of ROS. Similarly, Madeo *et al.* (1999) showed that yeast cells lacking *GSH1,*

encoding the first enzyme involved in GSH biosynthesis, γ-glutamylcysteine synthetase, also

displayed apoptotic markers. These markers include DNA breakage, chromatin condensation and margination and phosphatidylserine translocation.

Moreover, DNA damage and replication failure, potentially induced by mutations acquired during chronological and replicative aging, often result in cell cycle dysfunction due to checkpoint abrogation (Shimada *et al.* 2002, Shirahige *et al.* 1998) or impairment in DNA repair and synthesis, followed by cell death (Iraqui *et al.* 2009, Weinberger *et al.* 2005).

1.4.2.2   *ROS-dependent apoptotic cell death occurs both in the presence and absence of caspase-like proteases*

Yeast cells undergo apoptotic cell death accompanied by characteristic morphological features as observed in mammalian cells (see section 1.4.1). As described in section 1.4.1, caspases are the key molecular players which bring about apoptosis in mammalian cells. Similarly, yeast cells contain caspase-like proteases which execute apoptotic cell death in an analogous manner to mammalian caspases. However, studies of ulterior apoptotic pathways independent of caspase activity have also been extensively reported and studied (Burhans, Weinberger 2007, Büttner *et al.* 2006, Susin *et al.* 1996, 1999, Wissing *et al.* 2004).

Apoptotic yeast cell death in the presence of caspase-like proteases

Studies revealing the key molecular players involved in the mechanisms of apoptotic yeast cell death described several caspase-like proteases. All caspase-like proteases were shown to cleave target proteins which are involved in the signal transduction of the apoptotic cell death pathway. Such caspase-like proteases include the yeast metacaspase protein Yca1 (Madeo *et al.* 2002), the separase protein Esp1 (Yang *et al.* 2008) and the nuclear protease Nma111 homologous to HtrA2 in mammalian cells (Fahrenkrog *et al.* 2004).

Yca1 is a metacaspase which contains a caspase-like fold (Uren *et al.* 2000). Yca1 is a highly important molecule since it is required both during normal physiological conditions as well as during cellular stress, due to its non-death and pro-death roles. This dual role of Yca1 confirms the ease by which a cell may transform an adaptive response into cell death using machinery which is readily available.

A non-death role of Yca1 entails upregulating the proteasomal activity to eliminate damaged proteins which would have been previously ubiquitinated (Khan *et al.* 2005, Lee *et al.* 2010). Furthermore, Yca1 also plays a non-death role in cell cycle regulation by activating the G2/M checkpoint (Lee *et al.* 2008) essential for ensuring the absence of any lesions associated with DNA synthesis during the S phase (Magiera *et al.* 2014). However, in the presence of several exogenous and endogenous pro-apoptotic factors, Yca1 is also closely linked with ROS generation and the onset of apoptosis in yeast (Madeo *et al.* 2002; Ludovico *et al.* 2002, Weinberger *et al.* 2005) (Figure 1.4). In fact, *yca1Δ* yeast cell mutants showed increased survival by evading apoptosis induced by H_2O_2 (Madeo *et al.* 2002) or by acetic acid (Ludovico *et al.* 2002), even though Khan *et al.* (2005) reported that such mutants yeast cells contained higher levels of oxidised protein carbonyl groups when compared to wild-type yeast cells. Moreover, this phenomenon was exacerbated by treatment with hydrogen peroxide.

Yeast cell death triggered independently of Yca1 has been reported, and may involve other caspase-like proteases (as reviewed by Wilkinson, Ramsdale 2011). One such protein is separase, Esp1, which under normal conditions is a cell cycle-related protein that brings about the onset of anaphase (Baskerville *et al.* 2008). The destruction of the separase inhibitor Pds1, during late metaphase, by the Cdc20-activated anaphase promoting complex
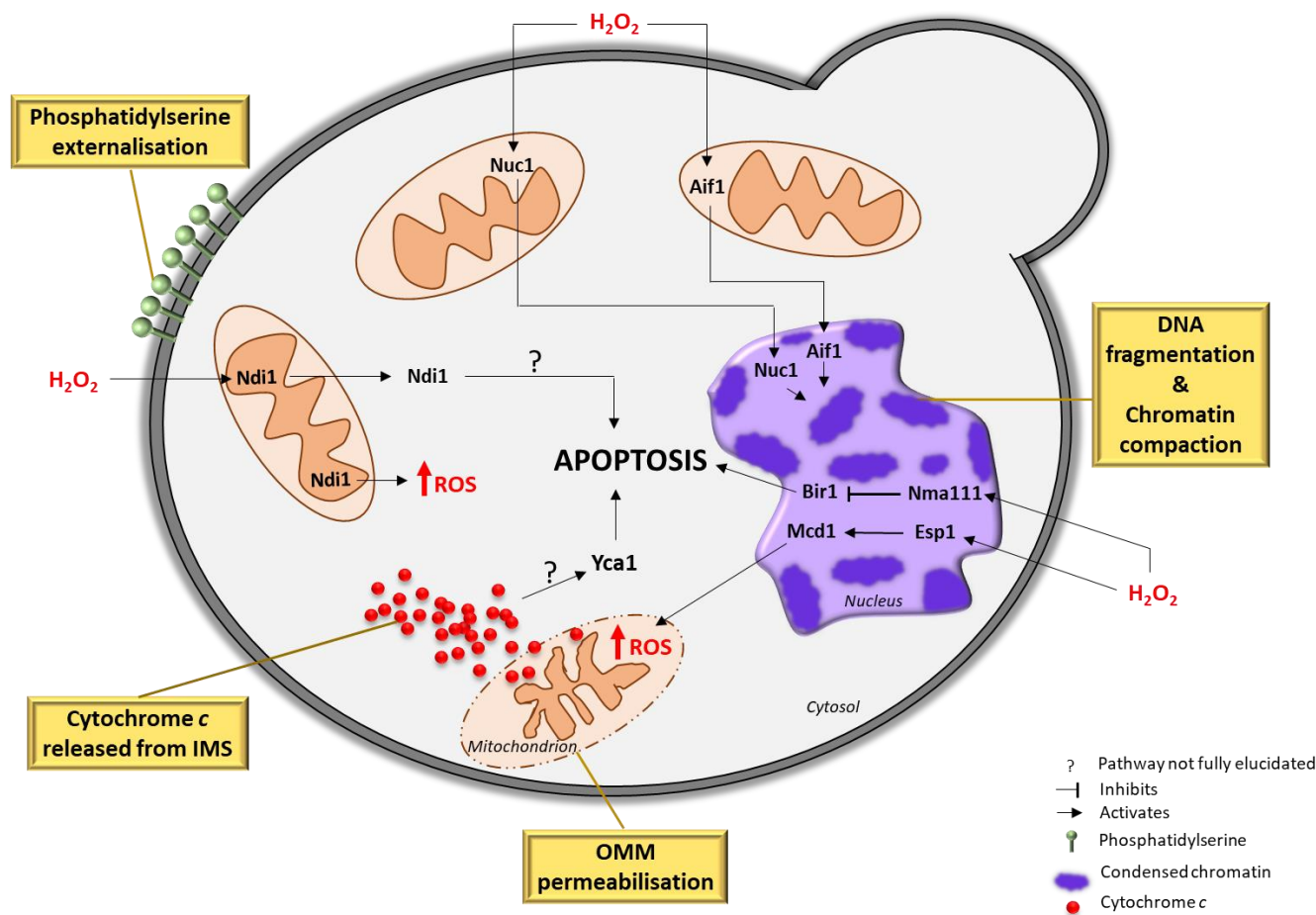
Figure 1.4 The molecular machinery and phenotypic features of a budding yeast cell undergoing apoptotic cell death. Pro-apoptotic triggers such as hydrogen peroxide (H_2O_2) and other reactive oxygen species (ROS), induce apoptotic cell death *via* pathways involving either caspase-like proteases, such as the yeast metacapase Yca1, the separase protein Esp1 and the nuclear protease Nma111, or in their absence *via* the yeast mitochondrial apoptosis-inducing factor Aif1, the mitochondrial nuclease Nuc1 and/or the internal NADH dehydrogenase Ndi1. These pathways result in a characteristic apoptotic phenotype which includes the externalisation of phosphatidylserine at the cell membrane, DNA fragmentation and chromatin compaction in the nucleus, as well as the permeabilisation of the outer mitochondrial membrane (OMM) and release of cytochrome *c* from the mitochondrial intermembrane space (IMS).

(APC), activates Esp1. The activated Esp1 cleaves the cohesin subunit Mcd1, which is responsible for joining sister chromatids together. Thus, Esp1 mediates the dissociation of Mcd1 from sister chromatids such that these can separate during anaphase (Uhlmann *et al.* 1999). In the presence of H_2O_2, the activation of Esp1 mediates further cleavage of the Mcd1's C-terminal and the truncated Mcd1 is translocated from the nucleus to the mitochondria, acting as a nuclear signal for cytochrome *c*-dependent cell death (Yang *et al.* 2008), *via* a Yca1-dependent mechanism which is not yet fully elucidated (Ludovico *et al.* 2002) (Figure 1.4). The proteolytic activity of Esp1 is similar to that of caspases. In fact, the protein sequence of Esp1 is analogous to that of the human caspase-1 protein (Uhlmann *et al.* 2000). This observation was confirmed when Esp1's proteolytic activity was inhibited by a caspase-1 inhibitor (Yang *et al.* 2008).

Another pro-apoptotic protease identified in yeast is Nma111, which is homologous to HtrA2 in human cells. HtrA2 is known to induce apoptosis by antagonising inhibitor of apoptosis (IAP) proteins (Hegde *et al.* 2002, Suzuki *et al.* 2001, Yang *et al.* 2003, Verhagen *et al.* 2002). Similarly, the nuclear serine protease Nma111 was associated with apoptotic induction in yeast since upon treatment with hydrogen peroxide, *nma111Δ* null mutants failed to display characteristic apoptotic features unlike their wild-type counterparts. Moreover, the overexpression of Nma111 caused their wild-type counterparts to die by apoptosis (Fahrenkrog *et al.* 2004). In the presence of oxidative stress, Nma111 acts on the IAP protein Bir1, making yeast cells more sensitive to apoptotic cell death, similar to yeast cells lacking *bir1* (Walter *et al.* 2006) (Figure 1.4).

Apoptotic yeast cell death in the absence of caspase-like proteases

Apoptotic pathways dependent on caspase-like proteases only make up 40% of investigated cell death scenarios (Madeo *et al.* 2009). Most other scenarios involve other apoptogenic factors, most of which are located in the mitochondria to promote pro-apoptotic signalling. Mitochondrial factors which are involved in mediating Yca1-independent apoptotic cell death include Aif1 (homolgous to AIF in mammals) (Susin *et al.* 1996, 1999, Wissing *et al.* 2004), Ndi1 (homologous to AMID in mammals) and Nuc1 (homologous to endonuclease G in mammals) (Burhans, Weinberger 2007, Büttner *et al.* 2006). All of these proteins have dual cellular roles, depending on whether the cell is triggered to undergo cell death or not.

Aif1 is a mitochondrial NADH-dependent oxidoreductase involved in oxidative phosphorylation (Amigoni *et al.* 2016) and its absence in mammalian cells caused a severe decline in the activity of respiratory complexes (Vahsen *et al.* 2004). Upon mitochondrial membrane permeabilisation triggered by the presence of oxidants or during aging, Aif1 migrates to the nucleus (Susin *et al.* 1999, Wissing *et al.* 2004, Yu *et al.* 2009) whereby it is critical to bring about chromatin condensation and DNA degradation, two key features of apoptotic cell death (Figure 1.4). This observation was confirmed by the higher survival rates of *aif1Δ* deletion mutants, when treated with oxidants or during aging (Wissing *et al.* 2004).

The mitochondrial NADH-dependent oxidoreductase Ndi1, which also participates in respiration, is another pro-apoptotic molecule which may bring about cell death in a metacapase-independent manner in yeast (Cui *et al.* 2012). The oxidoreductase function of Ndi1 during respiration is linked with ROS generation (see section 1.1.1), especially when

NDI1 is overexpressed or if respiration is enhanced by growth on glucose-limited media, especially in *sod2*-deficient cells (Li *et al.* 2006) (Figure 1.4). Cui *et al.* (2012) showed that Ndi1's pro-apoptotic property is separable from its role in respiration. In fact, the authors show that when yeast cells are subjected to various pro-apoptotic stimuli, such as hydrogen peroxide, Ndi1 is activated by cleavage of its N-terminal, and this is in turn translocated to the cytoplasm to execute its apoptotic activity (Figure 1.4). Yet, further studies are needed to elucidate the pro-apoptotic pathway which follows the release of Ndi1 from the mitochondria (Cui *et al.* 2012).

Another mitochondrial apoptogenic factor which is involved in stress response and Yca1-independent apoptotic cell death is Nuc1 (Büttner *et al.* 2006). Treatment of yeast cells with hydrogen peroxide triggers the translocation of Nuc1 from the mitochondria to the nucleus to induce apoptosis in a Yca1-independent manner (Büttner *et al.* 2007) (Figure 1.4). In fact, the deletion of the mitochondrial localisation sequence promoted its pro-apoptotic activity since Nuc1 was expelled from mitochondria. Once inside the nucleus, Nuc1 interacts with the histone protein H2B and digests nuclear DNA in the absence of caspase activity (van Loo *et al.* 2002) (Figure 1.4). H2B has been highly implicated in hydrogen peroxide-induced cell death since it directly mediates apoptotic chromatin compaction (Ahn *et al.* 2005, 2006). Interestingly, *nuc1Δ* mutants grown in non-fermentable media evade apoptotic cell death, unlike if grown on fermentable media whereby they die by necrotic death. This indicated that Nuc1 may protect, or sensitise yeast cells to cell death depending on whether they respire or not (Bütttner *et al.* 2007).

1.4.3 Evasion of apoptosis and carcinogenesis

Tissue homeostasis in multicellular organisms or the maintenance of a healthy colony of unicellular organisms is ensured by the maintenance of a healthy balance between proliferation and removal of cells by apoptosis (Green, Evan 2002, Lowe, Lin 2000). Mutations or cellular events which lead to the dysregulation of the cell cycle (Lau *et al.* 2007) or evasion of apoptosis (Fulda 2010, Sharma *et al.* 2019) result in rapid and uncontrolled cellular proliferation which leads to carcinogenesis. In fact, cancer cells alter their genetic expression, namely by upregulating anti-apoptotic proteins (Mallick *et al.* 2009, Lee *et al.* 2019) and downregulating pro-apoptotic proteins (Manoochehri *et al.* 2014, Pompeia *et al.* 2004).

However, to keep on proliferating indefinitely, cancer cells need a constant supply of nutrients, such as glucose and glutamine, to be able to meet their biosynthetic and bioenergetic requirements. This characteristically altered metabolism in cancer cells generates higher levels of ROS as compared to normal cells, and thus cancer cells, particularly in their early stages of altered metabolism, are more prone to suffer from oxidative stress (El Sayed *et al.* 2013). This key difference between normal cells and early-stage cancer cells is being therapeutically exploited to selectively induce apoptosis in cancer cells but not in normal, healthy cells (see section 1.5).

1.5 Non-steroidal anti-inflammatory drugs (NSAIDs) and chemoprevention

NSAIDs such as salicylates, are being extensively studied to understand their effects on cells, particularly on transformed, malignant cells. NSAIDs are a group of drugs which are primarily used to control fever, pain and inflammation since they possess antipyretic,

analgesic and anti-inflammatory properties. Like steroids, NSAIDs reduce inflammation by inhibiting the cyclooxygenase enzymes COX-1 and COX-2, which catalyse the conversion of arachidonic acids into pro-inflammatory prostaglandins (Vane 1971). It has long been hypothesised that the origin of cancer occurs at sites of chronic inflammation where cell proliferation is promoted and this increases the risk for tumour initiation (Trinchieri 2012, Virchow 1863).

Studies have shown that prolonged or dysregulated inflammation may trigger changes in the expression of oncogenes, tumour suppressor genes and/or pro-inflammatory genes (Landskron *et al.* 2014, Rao *et al.* 2010), all of which play a role in malignant transformation. For instance, tumorigenesis is mediated by high levels of the pro-inflammatory prostaglandin E2 (PGE2) which in turn stimulate cancer cell proliferation and invasion (Ke *et al.* 2016, Kawamori *et al.* 2003). Furthermore, Roberts *et al.* (2011) showed that glucose deprivation of colorectal tumour cells increases the expression of COX-2 and concomitantly increases the levels of PGE2 which facilitates the adaptation and survival of tumours in a glucose-deprived environment.

The anti-inflammatory properties of NSAIDs are well-documented in the literature. However, since inflammation and tumorigenesis are intimately linked, interest grew to unravel the potential of NSAIDs in cancer prevention. In fact, several epidemiological studies indicated that the regular use of NSAIDs is associated with reduced risk of incidence and mortality from several cancer types to different extents (Algra, Rothwell 2012, Bosetti *et al.* 2012, Harris *et al.* 2005). These include breast cancer (Dierssen-Sotos *et al.* 2016, Kim *et al.* 2015, Harris *et al.* 2003), colorectal and gastrointestinal cancer (Baron *et al.* 2003, Benamouzig *et al.* 2003, Burn *et al.* 2011a, Burn *et al.* 2011b, Friis *et al.* 2015; Ishikawa *et al.*

2013, Logan *et al.* 2008, Rothwell *et al.* 2010, Ruder *et al.* 2011, Sandler *et al.* 2003), lung

cancer (Olsen *et al.* 2008, Harris *et al.* 2002, Ye *et al.* 2019), prostate cancer (Doat *et al.*

2017, Vidal *et al.* 2015), ovarian cancer (Baandrup *et al.* 2015, Prizment *et al.* 2010, Trabert

et al. 2014) and head and neck cancer (Shi *et al.* 2017) among others.

The majority of the above-mentioned epidemiological studies concluded that a daily,

long-term use of a low-dose of NSAID in senior people, reduced the risk of incidence and

mortality from cancer, or of relapse. This hypothesis warranted further experimental studies

to provide solid evidence for the indicative results gathered by epidemiological studies. In

spite of the fact that numerous studies were and are still being carried out to understand the

underlying chemopreventive mechanisms and anti-tumour activity of NSAIDs, these are still

not fully elucidated. However, most studies showed that various NSAIDs exerted an anti-

proliferative effect which was often followed by cell death in malignant cells, as discussed in

the following section.

1.5.1 The anti-proliferative properties of aspirin and other NSAIDs

Sustained proliferation is critical in cancer development and progression. In fact,

malignant cells alter their physiology to adapt to a highly-proliferative mode of life by

altering the expression of key cellular regulators, such as cell cycle regulators and molecules

involved in energy generation and lipid biosynthesis, to meet the high metabolic demands of

such cells. Thus, the capacity of cancer cells to evade growth control and to proliferate

rapidly, is a key survival strategy for them to outcompete normal, untransformed cells.

Hence, novel cancer preventive measures and cancer therapies are focussing on identifying

anti-proliferative drugs and molecular targets involved in cellular proliferation pathways, in

an attempt to control or impede cancer cell growth. Various studies have shown how

different NSAIDs exhibited anti-proliferative activity on different cancer cells. The

mechanisms employed by NSAIDs to exert their chemopreventive, anti-proliferative

behaviour may be dependent or independent of their ability to inhibit COX enzymes and

suppress inflammation.

1.5.1.1   COX-dependent mechanisms of NSAID chemoprevention

The chemopreventive properties of NSAIDs, are in part due to their ability to counteract

inflammation and suppress cell proliferation, an important hallmark in tumour formation

(Chang *et al.* 2009). The COX-inhibiting role of NSAIDs is particularly effective for

chemoprevention since various cancer cell types were found to overexpress COX enzymes

(Eberhart *et al.* 1994, Ferrandina *et al.* 2002, Hida *et al.* 1998, Hwang *et al.* 1998, Koga *et al.*

1999, Roelofs *et al.* 2014, Tucker *et al.* 1999), which increase resistance of cancer cells to

apoptosis (Sun *et al.* 2002, Wang *et al.* 2019), stimulate angiogenesis (Hu *et al.* 2017) and

promote invasion and metastasis, amongst other effects (Tsuji *et al.* 1997).

Studies have reported that NSAIDs suppress inflammation and proliferation of

transformed cells by: (i) inhibiting cancer cells from upregulating the expression of COX

enzymes (Al-Nimer *et al.* 2015), (ii) inhibiting COX activity and prostaglandin formation (see

section 1.5), or by (ii) accumulating arachidonic acid, which in various colorectal cancer cell

lines has led to the induction of apoptosis through the activation of pro-apoptotic molecules

including caspase-3 (Monjazeb *et al.* 2006) and ceramides (Chan *et al.* 1998).

Furthermore, sulindac sulfide reversed the inhibition of apoptosis that had been observed

in mammalian cells overexpressing the human cyclocoxygenase-2 (COX-2) gene (Tsuji,

DuBois 1995) and also induced apoptosis in human colorectal adenocarcinoma (HT-29) cells

which similarly express COX-2 (Piazza *et al.* 1995, Shiff *et al.* 1995). In addition, the anti-proliferative effect of the NSAID metamizole on human breast adenocarcinoma MCF-7 cells and on colorectal adenocarcinoma HT-29 cells, was at least partly due to the induction of apoptosis and suppression of cell migration (Nikolova *et al.* 2018). Metamizole also inhibited the growth of the pancreatic cancer cell lines PaTu 8988 and Panc-1 (Malsy *et al.* 2017) and lung carcinoma A549 cells (Shao, Feng 2013). However, in both studies, the authors failed to indicate the mechanism by which metamizole suppressed their growth.

1.5.1.2   COX-independent mechanisms of NSAID chemoprevention

NSAIDs may also induce apoptosis independent of their ability to suppress COX and thus inflammation (Elder *et al.* 1997, Luciani *et al.* 2007, Yin *et al.* 2006, Yip-Schneider *et al.* 2001). These COX-independent mechanisms by which NSAIDs exert their chemopreventive properties were initially demonstrated *in vitro* whereby NSAIDs could inhibit proliferation and/or induce apoptosis in several tumour cell lines irrespective of their COX expression and ability to synthesise prostaglandins (Hanif *et al.* 1996). In fact, supplementation of cancer cells with prostaglandins, did not reverse the anti-proliferative effect of NSAIDs (Chan *et al,* 1998, Hanif *et al.* 1996). Also, the sulfone metabolite of sulindac, which does not inhibit COX enzymes, still induced apoptosis in HT-29 cells (Piazza *et al.* 1997, Reddy *et al.* 1999). Hence, these observations and other studies clearly confirm that NSAIDs may limit the proliferation and induce apoptosis in several human cancer cell lines *via* COX- independent pathways (Elder *et al.* 1997, Luciani *et al.* 2007, Yin *et al.* 2006, Yip-Schneider *et al.* 2001).

Studies delineating COX-independent mechanisms found that aspirin may induce transcriptional changes to exert its chemopreventive properties, such as by changing the expression of cell cycle regulatory proteins (Chang *et al.* 2009, Cheng *et al.* 2017, Dachineni

et al. 2016, Goel *et al.* 2003, Shiff *et al.* 1995) (see section 1.5.2.1) or by changing the expression and levels of pro-apoptotic and anti-apoptotic proteins. For instance, aspirin and other NSAIDs decreased the expression and protein levels of the anti-apoptotic proteins Bcl-2 and survivin in various human cancer cells (Bank *et al.* 2008, Ding *et al.* 2014, Greenspan *et al.* 2011, Lai *et al.* 2008, Lu *et al.* 2008, Pathi *et al.* 2012, Sankpal *et al.* 2012, Yang *et al.* 2011). Aspirin also reduced cancer cell proliferation by (i) increasing the translocation of Bcl-2 to the nucleus whereby it led to apoptotic cell death of breast cancer cells MCF-7 (Choi *et al.* 2013), and by (ii) inhibiting the migration and invasion of oral squamous cell carcinoma (OSCC) cells (Zhang *et al.* 2018). On the other hand, NSAIDs increased the expression of the pro-apoptotic proteins Bax and caspase-3 (Bank *et al.* 2008, Ding *et al.* 2014, Lai *et al.* 2008). The indomethacin-mediated upregulation of Bax in oesophageal adenocarcinoma cells, resulted in mitochondrial cytochrome *c* translocation (Aggarwal *et al.* 2000). Furthermore, the aspirin-mediated activation of Bax and caspase8/Bid was also involved in the apoptosis of the gastric cancer cells AGS and MKN-45 (Gu *et al.* 2005). Bax levels were also increased by the aspirin-mediated inhibition of the cellular ubiquitin proteasome degradation pathways in human lung cancer cells (Huang *et al.* 2002) and in neuroblastoma cells (Dikshit *et al.* 2006). The latter cells were observed to contain severe mitochondrial abnormalities, including membrane depolarisation, cytochrome *c* release from the mitochondria and caspase activation.

Caspases are often involved in the mechanisms by which NSAIDs bring about cell death in malignant cells. Aspirin and other NSAIDs were reported to reduce proliferation and induce apoptosis in HT-29 colon adenocarcinoma cells mediated by caspases (see section 1.5.1). In fact, the addition of caspase inhibitors to aspirin-treated HT-29 cells rescued these cells from death by apoptosis (Castaño *et al.* 1999). Similarly, treatment of squamous cell carcinoma of

the head and neck (SCCHN) with celecoxib and sulindac sulfide activated caspase-3 and

subsequently induced apoptosis after 48 hours of treatment (Bock *et al.* 2007*).*

Moreover, aspirin prevents the binding of c-Raf with Ras in A549 human lung cancer cells

(Pan *et al.* 2008). The binding of c-Raf with Ras is important to activate the extracellular-

signal-regulated kinase (ERK) signalling pathway. This pathway is involved in cellular

proliferation, differentiation and survival and is highly activated in cancers (as reviewed by

Bos 1989). Aspirin also interfered with the interaction between the mammalian proto-

oncogenic protein K-ras and the enzyme p110α and this inhibited the proliferation of human

uterine leiomyoma cells (Gao *et al.* 2017). p110α is the Ras-binding catalytic subunit of the

type I phosphatidylinositol 3-kinase (PI3K), which is involved in the regulation of RAS-

mediated cell growth, cell cycle entry and cell survival (Castellano, Downward 2011). The

disruption of the RAS-PI3K interaction is associated with reduced growth and survival of

malignant cells, which in turn inhibits the onset of tumorigenesis (Murillo *et al.* 2018).

1.5.2   NSAIDs and cell cycle arrest

Anti-proliferative mechanisms are often brought about by stopping the cell cycle for

repair or cell death, to prevent genetically defective cells, like cancer cells, from proliferating

uncontrollably. The anti-proliferative characteristics of NSAIDs bring about cell cycle arrest

mediated by the induction or inhibition of cell cycle regulatory players. For instance, a G1

cell cycle arrest was followed by apoptosis in (i) human MG32 osteosarcoma cells treated

with the NSAIDs aspirin, indomethacin and nimesulide (De Luna-Bertos *et al.* 2012, Díaz-

Rodríguez *et al.* 2012) and in (ii) A549 human lung carcinoma cell line treated with the NSAID

metamizole (Shao, Feng 2013). Similarly, the NSAIDs celecoxib and sulindac sulfide were

observed to inhibit cell cycle progression of the squamous cell carcinoma of the head and

neck (SCCHN) at the G1 phase, followed by apoptosis (Bock *et al.* 2007*).* Evidence in this study showed that these NSAIDs mediated cell cycle arrest by: (i) inducing the G1 CDK inhibitor p21, and by (ii) inhibiting the G1 cyclin D1 and the G1/S transcription factor E2F. Similarly, aspirin was also found to downregulate the transcription factor E2F in ovarian cancer, to induce a G1 cell cycle arrest (Valle *et al.* 2013).

1.5.2.1. *Mechanisms of aspirin-induced cell cycle arrest*

Aspirin causes a G1 arrest followed by apoptosis in the pancreatic cancer cell lines BxPC3 and Panc-1 (Perugini *et al.* 2000), in the liver cancer cell line HEPG2 (Hossain *et al.* 2012, Raza *et al.* 2011), as well as in several colorectal cancer cell lines (Luciani *et al.* 2007, Pathi *et al.* 2012) including HT-29 (Castaño *et al.* 1999, Qiao *et al.* 1998, Piazza *et al.* 1995, Shiff *et al.* 1996), HCT116 (Goel *et al.* 2003) and in SW480 (Lai *et al.* 2008).

Aspirin's ability to cause a G1 cell-cycle arrest in mammalian cells is partially dependent on its ability of activating ataxia telangiectasia mutated kinase (ATM) (Luciani *et al.* 2007) and of upregulating the CDK inhibitor gene, *p21* (Hardwick *et al.* 2004, Jung *et al.* 2015, Luciani *et al.* 2007). The activation of the G1/S checkpoint, dependent on ATM, is independent of aspirin's ability of inducing oxidative stress or of its anti-inflammatory properties (Luciani *et al.* 2007). The activation of ATM results in the phosphorylation and activation of its substrates, including the tumour suppressor p53 and the G2/M CDK protein, CHK2. However, in p53-deficient cells, cells bypass the G1/S checkpoint and accumulate at the CHK2-mediated G2/M checkpoint (Luciani *et al.* 2007). The activation of both p53 and CHK2 increases the levels of p21, which is in turn critical to bring about the aspirin-induced G1 arrest in colorectal cells (Hardwick *et al.* 2004, Hirao *et al.* 2000*,* Luciani *et al.* 2007).

Hardwick *et al.* (2004) showed that aspirin repressed other genes involved in the regulation of the cell cycle, namely cyclin proteins. This was also shown in other studies (Dachineni *et al.* 2016, Yip-Schneider *et al.* 2001). The absence of specific cyclins prevents the cell cycle from proceeding from one phase to the next, thus arresting the cell cycle at different checkpoints. Furthermore, aspirin may also target proteins involved in DNA synthesis and repair, and upregulates their expression in cancer cells. These proteins, particularly mismatch repair (MMR) proteins, may inhibit cell growth by interfering with cell-cycle progression and induce the G1/S checkpoint or by promoting apoptosis (Goel *et al.* 2003). By doing so, genomic integrity is maintained since cells have an increased chance of repairing DNA damage or induce apoptosis in genetically-defective cells.

However, the literature contains a number of studies which report a G2/M cell cycle arrest in response to treatment with aspirin or aspirin derivatives. Subbegowda and Frommel (1998) reported evidence of aspirin retarding cell cycle progression through the S and G2/M phases in the human colonic tumour cells SW620 and HT-29. However, this anomalous arrest could be attributed to the fact that in this study, these cells died by necrosis since no cells in the population bound annexin V alone.

A similar NSAID which also induced a G2/M cell cycle arrest in colorectal cancer cells is mesalazine (also known as 5-aminosalicylic acid, 5-ASA) (Reinacher-Schick *et al.* 2003). Unlike most NSAIDs, mesalazine had no effect on the expression of the G1 CKI *p21*, and the authors attribute this arrest to an anti-mitotic effect which is specific to this drug. In fact, a subsequent study by Koelink *et al.* (2010) reported that treatment of colorectal cancer cells with 5-ASA induced apoptosis and abnormal spindle organisation that led to mitotic catastrophe.

Moreover, a modified aspirin molecule, containing a nitric oxide-releasing group (NO-ASA) was also shown to inhibit cell growth and induce a G2/M arrest in several human cancer cells, accompanied by high intracellular ROS levels (Gao, Williams 2012). The authors linked this arrest with NO-ASA-induced oxidative stress since the addition of the antioxidant N-acetylcysteine prevented this arrest. However, keeping in mind that aspirin treatment in cancer cells also generates oxidative stress (Raza *et al.* 2011), the mechanism by which NO-ASA induces a G2/M arrest is still unclear. In fact, generation of oxidative stress in cancer cells by other nitro-derivatives of aspirin such as NCX4040 (Chinnapaka *et al.* 2019), NCX-4016 (Selvendiran *et al.* 2008) and NOSH-aspirin (Kashfi 2015) still induced a G0/G1 cell cycle arrest (Chinnapaka *et al.* 2019, Selvendiran *et al.* 2008).

1.5.3 NSAIDs and oxidative stress

The oxidative metabolism in cancer cells is highly distinctive from that of normal cells, since cancer cells alter their metabolism to facilitate their rapid proliferation (Warburg 1956). During, the early stages of their development, cancer cells often suppress the expression and protein levels of the mitochondrial antioxidant enzyme MnSOD in a p53-dependent manner (Dhar *et al.* 2011, Oberley, Buettner 1979) before MnSOD expression is reelevated during tumour development to counteract elevated ROS levels generated by their increased metabolic activity. Low levels of MnSOD in early-stage cancer cells inconceivably result in elevated levels of mitochondrial ROS and injury (see section 1.1.2), at which point malignant cells are more prone to suffer from oxidative stress compared to normal, healthy cells (El Sayed *et al.* 2013, Pelicano *et al.* 2004, Szatrawski, Nathan 1991). Thus, NSAIDs are often deemed chemopreventive since they conveniently exploit this marked difference in MnSOD levels to inhibit the growth of early-stage cancer cells. This was also confirmed in

yeast cells whereby aspirin caused apoptotic cell death in the MnSOD-deficient EG110 yeast

cells grown in ethanol medium, which like early-stage cancer cells are redox-compromised,

but not in their wild-type counterparts which like normal, healthy cells are not redox-

compromised (Balzan *et al.* 2004).

Various studies have shown how NSAIDs induce oxidative stress to mediate cell death in

early-stage cancer cells. In fact, it has been widely confirmed that NSAIDs target

mitochondria and mitochondrial proteins to induce ROS accumulation (Farrugia *et al.* 2013,

Gu *et al.* 2005, Pathi *et al.* 2012, Marimuthu *et al.* 2011). In fact, most mechanisms of

NSAID-induced cell death involve the loss of mitochondrial membrane potential, subsequent

mitochondrial dysfunction and apoptosis (Marchetti *et al.* 2009, Raza *et al.* 2011, Sapienza *et

al.* 2008), mediated by mitochondrial Bcl-2 proteins and other mitochondrial apoptogenic

proteins (see section 1.4.2.2). NSAIDs also induce ROS accumulation by: (i) inhibiting

mitochondrial respiratory complexes (Sandoval-Acuña *et al.* 2012, van Leeuwen *et al.* 2011),

(ii) inhibiting the activity of MnSOD (Albano *et al.* 2013) or by (iii) activating Akt (Rai *et al.*

2015), a signalling molecule involved in regulating cell survival, proliferation and

metabolism, often found elevated in cancer cells (Crowell *et al.* 2007). Furthermore, NSAIDs

also mediate cell death by targeting mitochondrial membrane proteins involved in ion

exchange and calcium uptake (Núñez *et al.* 2006, Tewari *et al.* 2017).

In general, salicylates have proved to exhibit both pro-oxidant (Battaglia *et al.* 2005,

Hermann *et al.* 1999, Klessig *et al.* 2000) and antioxidant properties (Baltazar *et al.* 2011,

Grosser, Schroder 2003, Yiannakopoulou, Tiligada 2009) and thus can be regarded as

potential modulators of the oxidative stress response. In fact, a high concentration of

salicylic acid promoted ROS production, induced oxidative stress and reduced the stress

tolerance in plants (Herrera-Vásquez *et al.* 2015). Furthermore, salicylic acid mediated the

inhibition of the hydrogen peroxide detoxifying enzymes catalase and ascorbate peroxidase,

which also promoted ROS accumulation (Chen *et al.* 1993, Durner, Klessig 1995). On the

other hand, salicylic acid may also act as an antioxidant, particularly when it acts in concert

with GSH, to control the transcription of defence genes against biotic and abiotic stress and

the scavenging of ROS (Herrera-Vásquez *et al.* 2015).

1.5.3.1   *Aspirin and oxidative stress*

The ability of aspirin, a derivative of salicylic acid, to modulate the redox state in the cell

allows it to exhibit both cytoprotective properties as well as chemopreventive properties.

Aspirin was shown to scavenge ROS and behave as an antioxidant in normal cells

(Ayyadevara *et al.* 2013, Baltazar *et al.* 2011, Yiannakopoulou, Tiligada 2009). This was also

shown in *S. cerevisiae*, whereby the growth of the wild-type EG103 cells in aspirin-treated

YPE medium showed an increase in the level of mitochondrial NAD(P)H (Farrugia *et al.* 2013).

However, aspirin was observed to have a pro-oxidant role in cells with compromised

mitochondrial redox balance. In fact, aspirin induced apoptosis in mitochondrial MnSOD-

deficient EG110 yeast cells grown aerobically in ethanol medium (Balzan *et al.* 2004), which

are suitable models of early-stage cancer cells due to their lack of MnSOD (Dhar *et al.* 2011).

The aspirin-induced apoptosis in EG110 yeast cells was accompanied by (i) an increase in

mitochondrial and cytosolic superoxide radicals in conjunction with the oxidation of

mitochondrial NAD(P)H levels (Farrugia *et al.* 2013), (ii) a decrease of catalase levels and

GSH/GSSG ratio (Sapienza, Balzan 2005), as well as (iii) the release of mitochondrial

cytochrome *c* followed by a drop in mitochondrial membrane potential (Sapienza *et al.*

2008). Furthermore, in the redox-compromised EG110 cells, aspirin downregulated the

expression of several genes encoding the enzymes involved in the synthesis and transport of acetyl-CoA (Farrugia *et al.* 2019*)*, a key mitochondrial metabolite required by all cells for energy generation and metabolite synthesis, particularly in cancer cells (DeBerardinis, Chandel 2016). However, the overexpression of *ADH2*, the gene which encodes the enzyme that catalyses the conversion of ethanol into acetaldehyde that is later used for acetyl-CoA synthesis, did not rescue EG110 cells from aspirin-induced apoptosis (Farrugia *et al.* 2019). Thus, further investigation was required to identify other key targets of aspirin which mediate apoptotic cell death in these mutant, redox-compromised yeast cells but not in their wild-type counterparts.

Conclusions from further studies on aspirin-treated MnSOD-proficient and deficient *S. cerevisiae* cells, which are suitable models of normal, healthy cells and early-stage cancer cells respectively (Dhar *et al.* 2011, Farrugia *et al.* 2019), will shed more light on the underlying mechanisms by which aspirin acts as a chemopreventive drug and helps in the development of novel aspirin-like drugs.

Indeed, various studies on survival and death pathways in eukaryotic cells including cancer cells, employ yeast as a suitable model organism due to its numerous practical benefits (Petranovic *et al.* 2010). It is very easy to handle since it has relatively simple and cheap growth requirements and together with its rapid cell division and thus short generation time, can be easily cultivated in large populations (Mager, Winderickx 2005; Nurse 2000, Simon, Bedalov 2004).

Despite being phylogenetically distant from humans, yeast and humans share conserved key regulatory elements (Petranovic *et al.* 2010). In fact, several studies have employed yeast to better understand basic cellular and molecular processes in higher eukaryotes.

These include cell-cycle control (Forsburg, Nurse 1991, Hartwell *et al.* 1970) and cell death pathways (Battaglia *et al.* 2005, Büttner *et al.* 2007, Fahrenkrog *et al.* 2004, Kazemzadeh *et al.* 2012, Madeo *et al.* 1997, 1999, 2002, 2004, Wissing *et al.* 2004). Yeast has greatly aided our understanding of mitochondrial-mediated apoptosis. In addition, one of the most important benefits of using yeast is that studies are performed *in vivo* (Petranovic, Nielsen 2008, Petranovic *et al.* 2010, Simon, Bedalov 2004). Yeast has proved to be a very simple and powerful tool for eukaryotic systems biology studies, the results from which can be extrapolated to more complex mammalian systems (Petranovic *et al.* 2010, Simon, Bedalov 2004).

1.6   Principal aim and objectives of this study

The principal aim of this study is to delineate other possible mechanisms by which aspirin induces apoptosis in the redox-compromised MnSOD-deficient EG110 yeast cells grown aerobically in ethanol medium, but not in the wild-type MnSOD-proficient EG103 cells, thereby further characterising aspirin's role in chemoprevention (see section 1.5.3). Specifically, this work entails:

(i)   validating by quantitative reverse transcription-polymerase chain reaction (qRT-PCR), published aspirin-induced changes in the expression of a select number of genes (Farrugia *et al.* 2019) in EG110 yeast cells, but not in EG103 cells, which are involved in oxidative stress and the cell cycle. Such genes include the highly-downregulated genes *SNO1* and *SNZ1*, which together catalyse the deamination of glutamine to form glutamate;

(ii)   investigating the effect of aspirin on the cell cycle distribution of EG103 and EG110 yeast cells grown in aspirin-treated and untreated ethanol medium, as well as the effect of L-glutamate on the cell cycle distribution of aspirin-treated EG110 yeast cells, to further characterise the anti-proliferative mechanisms of aspirin on these cells;

(iii)   exploring the effect of aspirin on the glutamate metabolism of redox-compromised yeast cells by measuring the intracellular level of glutamate in aspirin-treated and untreated EG110 yeast cells grown in ethanol medium;

(iv)   determining the effect of aspirin on the immediate metabolic products of glutamate in redox-compromised yeast cells, by measuring the intracellular levels of α-ketoglutarate and GSH in EG110 yeast cells grown in aspirin-treated and untreated ethanol medium;

(v)   measuring the intracellular redox balance in aspirin-treated and untreated EG110 yeast cells grown in ethanol medium, as given by the GSH/GSSG concentration ratio.

CHAPTER TWO

THE EFFECT OF ASPIRIN ON THE

EXPRESSION OF GENES INVOLVED IN

OXIDATIVE STRESS AND THE CELL CYCLE

2.1 Introduction

Salicylates have proved to exhibit both pro-oxidant (Battaglia *et al.* 2005, Hermann *et al.* 1999, Klessig *et al.* 2000) and antioxidant properties (Baltazar *et al.* 2011, Grosser and Schroder 2003, Yiannakopoulou, Tiligada 2009) and thus can be regarded as potential modulators of the oxidative stress response. Evidence in the literature has frequently shown that the nature and concentration of ROS, as well as the duration of their exposure, affect the cell cycle (Byun *et al.* 2008, Könczöl *et al.* 2013, Márton *et al.* 2018, Preya *et al.* 2017, Pyo *et al.* 2013). ROS may facilitate the progression of the cell cycle (Fehér *et al.* 2008) but it may also induce a transient cell cycle arrest for repair or a permanent cell cycle arrest leading to RCD (Verbon *et al.* 2012).

2.1.1 ROS-related genes as potential targets of aspirin

Aspirin's ability to modulate the redox state in the cell allows it to exhibit both cytoprotective properties as well as chemopreventive properties. Aspirin was shown to scavenge ROS and behave as an antioxidant in normal, wild-type cells (Ayyadevara *et al.* 2013, Chen *et al.* 2012, Yiannakopoulou, Tiligada 2009). This was also shown in *S. cerevisiae*, whereby the growth of the wild-type EG103 cells in aspirin-treated YPE (ethanol-based) medium showed a decrease in the level of mitochondrial superoxide radicals and an increase in the level of mitochondrial NAD(P)H (Farrugia *et al.* 2013). However, aspirin was observed to have a pro-oxidant role in cells with a compromised mitochondrial redox balance. In fact, aspirin induced apoptosis in mutant EG110 yeast cells lacking the mitochondrial antioxidant enzyme MnSOD, when grown aerobically in ethanol medium (Balzan *et al.* 2004). This observation was associated with an increase in mitochondrial and cytosolic superoxide radicals in conjunction with the oxidation of mitochondrial NAD(P)H levels (Farrugia *et al.*

2013), and the release of mitochondrial cytochrome c followed by a drop in mitochondrial membrane potential (Sapienza *et al.* 2008). This shows that genes which somehow have an influence on the oxidative environment within the cell may be potential targets of aspirin and thus determine whether yeast cells survive or die. Such potential ROS-related gene targets of aspirin include *SNO1, SNZ1, OYE2* and *OYE3*.

In spite of the vast literature on the pro-oxidant and antioxidant properties of aspirin and other NSAIDs (see section 1.5.3), the effects of aspirin on the expression of these ROS-related genes have not yet been studied in any cell type. Aspirin-induced gene expression data obtained by microarray analysis (Farrugia *et al.* 2019) have indicated that *SNO1* and *SNZ1* are downregulated ~4.5-fold in the redox-compromised EG110 yeast cells but not in the wild-type EG103 yeast cells. This makes them the most highly affected genes amongst those which were selected in this study, and so will be discussed further below.

2.1.1.1 SNO1 and SNZ1

The *S. cerevisiae* genes *SNO1* and *SNZ1* are simultaneously expressed under nitrogen-limiting conditions (Braun *et al.* 1996, Fuge *et al.* 1994; Padilla *et al.*, 1998). The proximal location of these two genes to each other, as well as the homologues of their gene products, have been evolutionary conserved in other fungi (Benabdellah *et al.* 2009) and plants (Chen, Xiong 2005). Yet, these genes are still unidentified in animals. The reason for this may be that animals are unable to survive frequent, severe starvation conditions, unlike plants which may grow in poor soils or experience drought (Padilla *et al.* 1998).

Galperin and Koonin (1997) observed that Sno and Snz proteins have sequence similarity to glutamine amidotranferases, most of which are involved in both purine and pyrimidine biosynthesis (Neuhard, Kelln 1996, Zalkin, Nygaard 1996). Padilla *et al.* (1998) showed that

the gene products of *SNO1* and *SNZ1* interact to form a protein complex, and in the absence

of such a complex, *sno1snz1*-null mutants were sensitive to 6-azauracil, a drug which inhibits

purine and pyrimidine biosynthesis and thus lowers nucleotide pools in the cell. In addition,

these double mutants were also sensitive to methylene blue, a producer of singlet oxygen.

Thus, the authors suggested that *SNO1* and *SNZ1* are expressed in response to a depleted

carbon source and a low concentration of nucleotides, as well as to counteract oxidative

stress. Rodríguez-Navarro *et al.* (2002) showed that *sno*-deficient and *snz*-deficient mutants

were also sensitive to menadione, a superoxide radical generator.

Snz-related proteins in other organisms have been found to play a role in stress tolerance

or in its mitigation. For example, these proteins were induced in response to stress in several

plant species (Dell'Aglio *et al.* 2017, Moccand *et al.* 2014, Raschke *et al.* 2011,

Sivasubramaniam *et al.* 1995, Titiz *et al.* 2006), in the bacterium *Bacillus subtilis* (Antelmann

et al. 1997), in the protozoan parasite *Plasmodium falciparum* (Knöckel *et al.* 2012) and in

the fungal parasite *Cercospora nicotianae* (Ehrenshaft, Daub 2001).

A more in-depth function of *S. cerevisia*e's *SNO1* and *SNZ1* was elucidated by Dong *et al.*

(2004), who showed that these two genes were expressed simultaneously and behaved as a

glutamine amidotransferase with comparable specific activity to other glutamine

amidotransferases. They observed that Sno1 served as the glutaminase, although this

glutaminase activity was barely detectable in the absence of Snz1. This Sno1-Snz1 complex

catalyses the deamination of glutamine to give rise to glutamate and an ammonium ion.

$$\text{Glutamine} \xrightarrow{\text{Sno1-Snz1}} \text{Glutamate} + \text{NH}_4^+$$
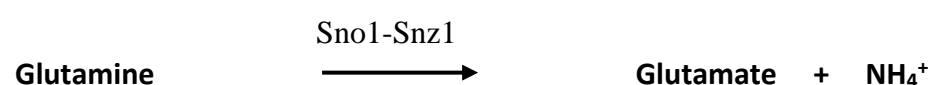
In addition to the synergistic roles of Sno1 and Snz1 in counteracting ROS, Sno1 contains a conserved 16 amino acid sequence which resembles the anti-apoptotic TSC22 motif. Yang *et al.* (2006) showed that the human TSC22 protein counteracts ROS and behaves as a suppressor of yeast cell death mediated by the pro-apoptotic Bax protein. It is well known that the mechanisms involved in Bax-mediated cell death in yeast are similar to the processes that take place in mammalian cells (Jürgensmeier *et al.* 1997, Ligr *et al.* 1998, Manon *et al.* 1997, Priault *et al.* 2003, Zha *et al.* 1996). In fact, the overexpression of Sno1, containing the anti-apoptotic TSC22 motif, also delayed Bax-mediated cell death in yeast when Bax was ectopically expressed (Khoury *et al.* 2008).

2.1.2   Cell cycle-related genes as potential targets of aspirin

Although aspirin and other NSAIDs have been widely implicated in the modulation of cell-cycle progression in mammalian cells, particularly in cancer cells (see section 1.5.2) , the literature is rather limited as regards to the effect of aspirin on the cell cycle of *S. cerevisiae*. The fact that oxidative stress has been linked to the cell cycle in yeast (see section 1.3.2) suggests that aspirin induces apoptotic cell death in redox-compromised yeast cells (Balzan *et al.* 2004) by targeting cell cycle-related proteins as previously shown in mammalian cancer cells (see section 1.5.2.1). This indicates that gene products which are somehow involved in cell-cycle progression, or its regulation, may be potential targets of aspirin and may be critical in determining whether yeast cells survive or die. Such potential cell cycle-related gene targets include *RAS2, CDC6, YCA1, ESP1* and *MCD1*.

In this chapter, the effect of aspirin on the expression of a select number of genes pertinent to oxidative stress and the cell cycle in redox-compromised EG110 and wild-type EG103 *S. cerevisiae* cells cultivated in ethanol medium, was investigated. Quantitative

reverse transcription-polymerase chain reaction (qRT-PCR) experiments were performed to validate published aspirin-induced microarray gene expression data obtained from Farrugia *et al.* (2019) of: (i) the ROS-related genes *OYE2*, *OYE3*, *SNO1* and *SNZ1*, and (ii) the cell cycle-related genes *RAS2, CDC6, YCA1, ESP1* and *MCD1.*

2.2 Materials

2.2.1 Chemicals

β-mercaptoethanol, acetylsalicylic acid (ASA), agarose, disodium hydrogen phosphate, ethylenediaminetetraacetic acid (EDTA) disodium salt dihydrate, potassium dihydrogen phosphate and Trizma® base were obtained from Sigma-Aldrich, Darmstadt, Germany. General BDH® chemicals, including glacial acetic acid and hydrochloric acid were obtained from VWR International Ltd., UK.

The kits used in this part of the research study were the following: QuantiTect® Reverse Transcription Mini Kit, QuantiTect® SYBR® Green PCR and RNeasy® Mini Kit were obtained from Qiagen (Hilden, Germany). GeneRuler™ 50 bp DNA ladder, GeneRuler™ 100 bp DNA ladder and 2x ReddyMix™ PCR Master Mix with 1.5 mM $MgCl_2$ were obtained from ThermoScientific™ (Massachusetts, USA).

2.2.2 Yeast strains

The *Saccharomyces cerevisiae* strains used were the wild-type strain EG103 (*MATα leu2-3 112 his3Δ1 trp1-289α ura3-52 GAL+*) and the redox-compromised MnSOD-deficient strain EG110 (EG103 *sod2Δ :: TRP1*) kindly provided by Edith Gralla of the University of California, Los Angeles and Valeria C. Culotta of Johns Hopkins University, Baltimore.

2.2.3 Media for yeast cell cultures

Yeast nitrogen base without amino acids was obtained from Difco™, Becton, Dickinson and Company, USA. Bacteriological agar, bacteriological peptone and yeast extract were obtained from Oxoid Limited, Hampshire, UK. BDH® absolute ethanol was obtained from VWR International Ltd., UK. Amino acids and glucose were obtained from Sigma-Aldrich, Darmstadt, Germany.

2.2.3.1 *Synthetic complete medium*

Synthetic complete medium was prepared by dissolving 0.67% (w/v) yeast nitrogen base without amino acids, 2% (w/v) glucose, 100 µg/ml L-histidine-HCl, 20 µg/ml L-methionine, 30 µg/ml L-lysine (mono-HCl), 120 µg/ml leucine, 40 µg/ml adenine and 25 µg/ml uracil in distilled water. Since EG103 yeast cells are auxotrophic for tryptophan, 40 µg/ml of tryptophan were also added to the minimal medium for EG103 cells. This solution was filter-sterilised using 0.2 µm Nalgene™ disposable sterilisation filters.

To prepare solid synthetic complete media for plates, a 2% (w/v) bacteriological agar suspension was prepared in distilled water and autoclaved at 120 °C for 20 min. This was mixed with the filter-sterilised complete medium, poured into sterile petri dishes and allowed to solidify at room temperature.

2.2.3.2 YPE medium

YPE medium is an ethanol-based medium containing 1% (w/v) yeast extract, 2% (w/v) bacteriological peptone and 3% (v/v) ethanol dissolved in distilled water. This solution was filter-sterilised using 0.2 μm Nalgene™ disposable sterilisation filters and stored at room temperature.

2.2.4 Buffer and reagent solutions

2.2.4.1 0.5 M Ethylenediaminetetraacetic acid (EDTA)

A 0.5 M solution was prepared by dissolving 18.61 g of EDTA disodium salt dihydrate (MW = 372.24 g/mol) in 100 ml of deionised water while stirring at room temperature. The pH of the solution was adjusted with 1 M NaOH to the pH of interest. The solution was autoclaved at 120 ^{o}C for 20 min and stored at 4 ^{o}C.

2.2.4.2 Phosphate buffer saline (PBS)

Sterile PBS was prepared by dissolving 8.0 g of NaCl, 0.2 g of KCl, 1.44 g of Na_2HPO_4 and 0.24 g of KH_2PO_4 in 800 ml of distilled water. The pH of the resulting solution was adjusted to 7.4 with 1 M hydrochloric acid or sodium hydroxide and topped up to a volume of 1 litre using deionised water. This volume was aliquoted, autoclaved at 120 ^{o}C for 20 min and stored at room temperature.

2.2.4.3 Tris-acetate EDTA (TAE) electrophoresis buffer

A 50x stock solution was prepared by adding 242 g of Trizma$^®$ base (MW = 121.14 g/mol), 57.1 ml glacial acetic acid (MW = 60.05 g/mol) and 100 ml of 0.5 M EDTA (pH 8.0) (MW = 372.24 g/mol) (see section 2.2.4.1) to deionised water, bringing the final volume to 1 litre.

The buffer was stored at room temperature. Dilutions were made to prepare working solutions accordingly.

2.2.4.4   1 M Trizma® base

A 1 M solution of Trizma® base (MW = 121.14 g/mol) was prepared by dissolving 60.57 g in 500 ml of distilled water. The solution was aliquoted, autoclaved at 120 °C for 20 min and stored at room temperature.

2.2.5   Software programmes

The following software programmes were used for this part of the study:

Primer3Plus software (Untergasser *et al.* 2007), Primer-BLAST (Ye *et al.* 2012), qbase+ (Biogazelle, Gent, Belgium), Rotor-Gene® Q Software 2.1.0.9 (Qiagen, Hilden, Germany) and SPSS® Statistics v25 (IBM, New York, USA).

2.3   Methods

2.3.1   Preparation and cultivation of *S. cerevisiae* cell cultures

Primary cultures of yeast cells that were previously grown on solid 2% (w/v) agar minimal media petri dishes (see section 2.2.3.1) for four days at 28 °C, were prepared in 5 ml YPE medium (see section 2.2.3.2) and incubated with shaking (250 rpm) for four days at 28 °C in a Unitron Infors AG orbital incubator. Aliquots from these 5 ml primary cultures were then used to prepare secondary cultures of the desired volumes, such that all initial cultures had an equal optical density at 600 nm (OD_{600}) (BioPhotometer Eppendorf spectrophotometer, Hamburg, Germany) for comparison. Secondary yeast cell cultures were incubated at 28 °C with constant shaking (250 rpm), for the desired span of time.

2.3.2 Monitoring the growth of *S. cerevisiae* cells in the absence and presence of aspirin

Primary yeast cell cultures were used to inoculate 5 ml secondary cultures as described in section 2.3.1. Yeast cell growth was measured as the OD_{600} at 24-hour intervals. For OD_{600} measurements greater than 1.0, cultures were diluted as necessary. A growth curve of OD_{600} against time in hours was then plotted.

Similarly, the growth of yeast cells was also monitored when cultivated in 5 ml of YPE medium which was supplemented with 15 mM of aspirin (acetylsalicylic acid), the pH of which was adjusted to 5.50 with 1 M Trizma® base (see section 2.2.4.4), according to Balzan *et al.* (2004). The specific dose of 15 mM aspirin was used since it is the lowest dose that consistently and reproducibly induces apoptotic cell death in EG110 yeast cells. A growth curve of OD_{600} against time in hours was then plotted.

2.3.3 Harvesting of yeast cells and extraction of total RNA

Aspirin-treated and untreated yeast cell cultures grown in YPE medium were withdrawn from the incubator and harvested, after 48 hours of growth.

Purification of total RNA from yeast cells by mechanical digestion

The total RNA from yeast cells was extracted and purified using the RNeasy® mini kit (see section 2.2.1). After measuring the OD_{600} for each cell culture of aspirin-treated and untreated yeast cells grown in YPE medium, 10 ml of each cell culture were centrifuged at 1,000 g for 5 min at 4 °C and the supernatant was discarded. The cell pellets were resuspended and washed in an equal volume of PBS (see section 2.2.4.2).   The cell pellets were then resuspended in PBS to give a final OD_{600} of 10 and the pellets were placed on ice.

Two 1 ml aliquots of the aspirin-treated and untreated cell cultures of OD_{600} = 10, were spun down at 1,000 g for 5 min at 4 ^oC. The PBS supernatant was removed and the pellets were resuspended in 600 µl of a 1:100 (v/v) mixture of β-mercaptoethanol and Buffer RLT (provided in the kit). Cell lysis was carried out in lysis chambers which were half-filled with acid-washed glass beads of diameter 0.45-0.55 µm, using the µ-minibeadbeater beadmill for two rounds of 60 s with an interval of 1 min. 350 µl of lysate were spun down at 1,000 g for 5 min at 4 ^oC. An equal amount of 70% (v/v) ice-cold ethanol was added to the homogenised lysate and mixed well. The whole volume was transferred to a RNeasy® spin column and centrifuged at 8,000 g for 15 s at 4 ^oC. The column was then washed with 350 µl of Buffer RW1 (provided in the kit). An on-column DNase digestion step was carried out by adding 80 µl of a 7:1 (v/v) mixture of cold Buffer RDD (provided in the kit) and DNase I to each column and these were incubated at room temperature for 15 min. Another 350 µl of Buffer RW1 (provided in the kit) was added to each column and these were centrifuged at 8,000 g for 30 s at 4 ^oC. The columns were washed with 500 µl of RPE buffer (provided in the kit) and were then spun down at 8,000 g for 15 s at 4 ^oC. This washing step was repeated twice. Elution was carried out by applying 50 µl of RNase-free water to the column and by centrifugation at 8,000 g for 1 min at 4 ^oC. The Nanodrop™ 2000 spectrophotometer (Thermo Fischer Scientific™, Massachusetts, USA) was used to quantify the amount of RNA eluted and determine its purity. The eluted RNA was stored at -80 ^oC.

2.3.4 Complementary DNA (cDNA) synthesis

In order to be able to amplify by polymerase chain reaction (PCR) the full-length transcripts, 700 ng of total RNA were reverse-transcribed into cDNA using the QuantiTect® Reverse Transcription Kit (see section 2.2.1).

To do so, the total RNA was first subjected to a genomic DNA (gDNA) elimination reaction. To a microfuge tube the following were added successively: (i) RNase-free water, (ii) the appropriate amount of 7x gDNA Wipeout Buffer (provided in the kit) to give a 1x final concentration, and (iii) 700 ng of total RNA. The total volume of the reaction mixture was that of 14 µl. This reaction mixture was mixed well by pipetting and incubated for 2 min at 42 °C and then immediately placed on ice.

To this reaction, the reverse-transcriptase (RT) mixture consisting of 1 µl of the enzyme Quantiscript Reverse Transcriptase, 4 µl of 5x Quantiscript RT Buffer (so as to give a 1x final concentration), and 1 µl of RT Primer Mix, was added and mixed well to give a total volume of 20 µl. All chemicals of this mixture were provided in the kit. A no-reverse transcriptase (no-RT) control was also prepared which consisted of the above mixture except for the enzyme Quantiscript Reverse Transcriptase, which was replaced with an equal volume of RNase-free water. This was set up to ensure that the initial RNA template in the samples is indeed RNA, as well as to ensure that the gDNA Wipeout buffer was effective and no contaminant gDNA was present in the sample.

The samples and the no-RT control were then incubated in the thermocycler for 30 min at 42 °C to facilitate effective reverse transcription of the RNA template. Following this, the samples and controls were incubated for a further 3 min at 95 °C to inactivate the Quantiscript Reverse Transcriptase enzyme. The resulting cDNA was then amplified by PCR (see section 2.3.5) using an intron-spanning primer set to check for cDNA integrity and for the presence of any contaminant gDNA. The remaining cDNA was stored at -20 °C for downstream techniques.

2.3.5   Polymerase chain reaction (PCR)

PCR is a molecular biology technique which is used to amplify specific DNA lengths by using a specific primer set. This was carried out using the ThermoScientific™ 2x ReddyMix™ PCR Master Mix, with 1.5 mM $MgCl_2$ (see section 2.2.1) and the appropriate primer set and template DNA to be amplified.

To a 0.2 ml RNase-free PCR tube the following were added successively to a total volume of 25 μl: (i) RNase-free water needed to bring to the required volume, (ii) the appropriate 2x ReddyMix™ PCR Master Mix (so as to give a 1x final concentration), (iii) 0.5 μM of the forward primer, (iv) 0.5 μM of the reverse primer, and (v) 1 μl of the template cDNA to be amplified. In another 0.2 ml RNase-free PCR tube, a no template control (NTC) was prepared by preparing an identical reaction mixture except for the cDNA template which was replaced by an equal volume of RNase-free water. This control ensured the absence of any contaminant cDNA template in the reaction buffer, primers or in the RNase-free water. The tubes were placed in Biometra's TProfessional Standard PCR thermocycler (Göttingen, Germany) and PCR was performed using the thermal cycling conditions outlined in Table 2.1.

2.3.6   Agarose gel electrophoresis

Agarose gels were prepared by melting agarose powder in an appropriate volume of 1x Tris-acetate EDTA (TAE) electrophoresis buffer (see section 2.2.4.3). A 1% (w/v) agarose gel was prepared when analysing PCR products larger than 500 bp. When a higher resolution was required to visualise smaller PCR products, a 2% (w/v) agarose gel was prepared. 7.5 μl of ethidium bromide per 100 ml agarose solution were added to the agarose solution. This solution was allowed to solidify in a gel cast at room temperature. The solid agarose gel was placed in an electrophoretic chamber containing 1x TAE as the electrophoretic buffer.

Table 2.1 The thermal cycling conditions required for the amplification of template DNA using the 2x ReddyMix™ PCR Master Mix, with 1.5 mM MgCl$_2$.

Step	Temperature (ºC)	Time	No. of cycles
Initial Denaturation	95.0	2 min	1
Denaturation	95.0	25 s	
Annealing*	48.0-63.0	35 s	35
Extension	72.0	65 s	
Final extension	72.0	5 min	1
Hold	4.0	∞	/

*The annealing temperature was changed depending on the optimal annealing temperature of the primer set which was used.

10 μl of each PCR product was loaded in different wells alongside 5 μl of the appropriately-sized GeneRuler™ DNA ladder (see section 2.2.1). Once the wells of the gel were loaded, a constant voltage of 130 V was passed through the electrophoretic chamber. The DNA bands were visualised under UV light, since the ethidium bromide binds to DNA and renders it fluorescent.

2.3.7   Design of Primers

Oligonucleotide primers for both reference genes and genes of interest were designed for quantitative PCR (qPCR) using Primer3Plus software (see section 2.2.5). These primers were designed according to the following criteria: (i) a product size of 100-150 bp, (ii) primer size between 18-24 bp, (iii) a primer melting temperature (T_m) of 58.0–62.0 °C, (iv) a primer GC content of 20-60%. Once designed, the primer sequences were blasted in Primer-BLAST (see section 2.2.5) to check for specificity. The designed primers were synthesised by Integrated DNA Technologies (Iowa, USA) and were received in lyophilised form. These were then reconstituted in RNase-free water to obtain 100 μM stock solutions.

2.3.8   Gradient PCR

To determine the optimal annealing temperature of each newly-designed primer set for qPCR analysis, six identical PCR reactions were set up for each primer set, using the 2x ReddyMix™ PCR Master Mix, with 1.5 mM $MgCl_2$ (see section 2.3.5). Each of the six PCR reactions was subjected to a different annealing temperature, namely 50.3, 52.4, 55.2, 58.2, 60.8 and 62.0 °C. A no template control (NTC) which contained RNase-free water instead of cDNA template was also prepared to ensure that no contaminant cDNA template was

present in the buffer, primer solutions or in the RNase-free water. All six reactions together with the NTC were placed in the Biometra's TProfessional Standard PCR thermocycler (Göttingen, Germany) and were subjected to the thermal cycling conditions which are outlined in Table 2.1, but using the annealing temperatures specified above.

2.3.9 Quantitative Reverse Transcription–PCR (qRT-PCR)

mRNA levels in aspirin-treated and untreated EG103 and EG110 yeast cells grown in YPE medium for 48 hours were determined by qRT-PCR using the 72-well rotor of the Rotor-Gene® Q Series Thermocycler (Qiagen, Hilden, Germany). Experiments were carried out using three independent biological samples of each aspirin-treated and untreated yeast strain, with three technical replicates each. Qiagen's QuantiTect® SYBR® Green PCR kit (see section 2.2.1) was used for quantification.

A master mix was prepared by adding: (i) RNase-free water needed to bring to the required volume, (ii) 0.5 µM of the reverse primer, (iii) 0.5 µM of the forward primer and (iv) the appropriate volume of SYBR Green 2x (to give a final concentration of 1x) to a volume of 19 µl for each reaction. 1 µl of the appropriate cDNA was then added to sample tubes whereas a NTC control was prepared by adding 1 µl of RNase-free water instead of the cDNA. Sample tubes and the NTC were subjected to the thermal cycling conditions outlined in Table 2.2.

The amplification of a target cDNA in each sample was monitored in real time since during each qPCR run, the Rotor-Gene Q Series Software (version 2.1.0.9) plots an amplification plot of normalised fluorescence against cycle number. This plot shows the

Table 2.2 The thermal cycling conditions required for the amplification of cDNA fragments using the QuantiTect® SYBR® Green PCR kit.

Step	Temperature (ºC)	Time	Ramp Rate (ºC/s)*	No. of cycles
Initial Activation	95.0	15 min	20	1
3-step cycling				
Denaturation	94.0	15 s	20	
Annealing	55.2	30 s	20	40
Extension**	72	30 s	20	

* The ramp rate is the time it takes for the thermocycler to reach a certain temperature as dictated by the thermal profile during the PCR reaction.

** Data acquisition was taken at this step after each cycle since the fluorescence generated from the incorporation of SYBR Green I into the newly-synthesised double-stranded DNA is at its maximum.

fluorescence given off by SYBR Green I after the extension step of each cycle during PCR. SYBR Green I is a dye which fluoresces at a higher intensity when it binds to double-stranded DNA (which is highly prevalent during the extension step). The subsequent fluorescence measurements after each cycle give rise to a curve which represents the accumulation of product over the course of the real-time PCR experiment. Thus, quantification of qPCR double-stranded products was performed in the log-linear phase of the reaction by measuring the cycle threshold (Ct) value which is the intersection between an amplification curve and a threshold line (Figure 2.1). This value represents the number of cycles required for the fluorescence of the sample to significantly rise above the fluorescence given off by the NTC, which contains no cDNA, and thus cross the threshold line. This was followed by melt-curve analysis (performed using the Rotor-Gene® Q software version 2.1.0.9) to ensure that the desired amplicon was detected, rather than any primer dimers or contaminating DNA. In principle, during melt-curve analysis, the temperature is increased such that the DNA starts to denature into single strands. Since SYBR Green I binds preferentially to double-stranded DNA, there is a resulting characteristic drop in fluorescence, which gives a melt-curve profile specific to each amplicon (Supplementary Figures 1 and 2).

The software qbase+ (see section 2.2.5) was used to calculate the normalised relative quantification (NRQ) values by comparing Ct values of target genes to those of the reference genes *GLC7*, *SMD2* and *TFC1*. Log$_2$ transformed NRQ values were used to calculate and plot graphs of the Log$_2$ fold changes in aspirin-treated and untreated samples. Significant aspirin-induced changes in the expression of target genes were determined using statistical tests which analyse pairwise comparisons (see section 2.3.10). These results were compared to the gene expression data from a microarray study published by Farrugia *et al.* (2019), so as to confirm the effect of aspirin on the levels of mRNA transcripts from the genes of interest.
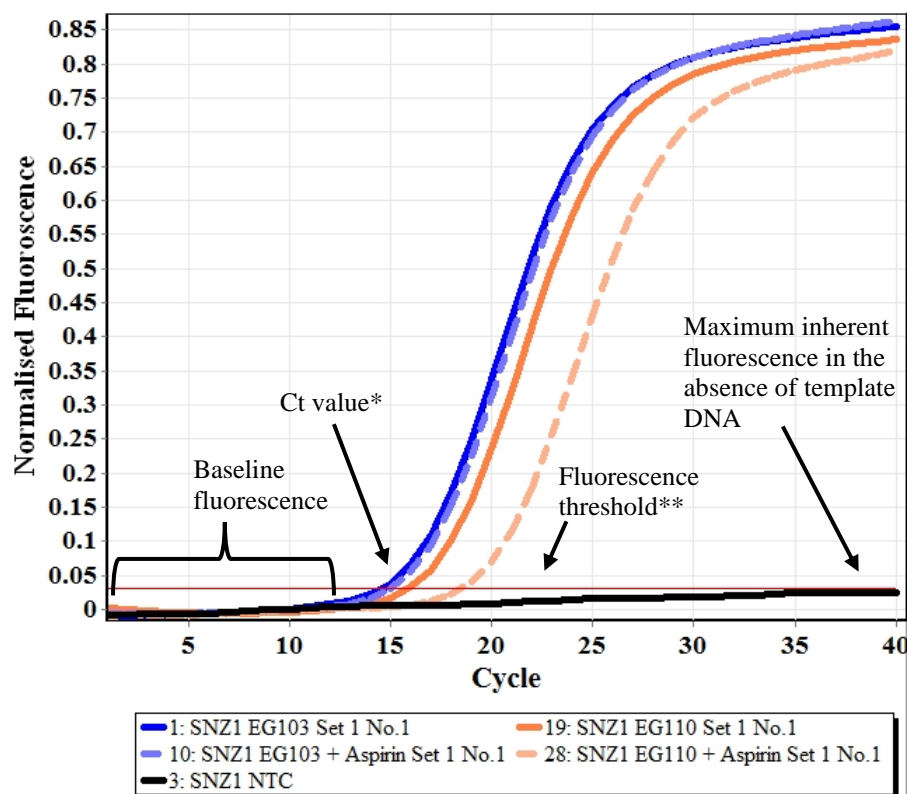
Figure 2.1 The change in fluorescence given off by the dye SYBR Green I when it binds to double-stranded DNA during the extension step of each PCR cycle against the number of cycles. This plot monitors in real time the amplification of a target cDNA as exemplified by cDNA from aspirin-treated (orange, dashed curve) and untreated samples of EG110 (orange, solid curve) and aspirin-treated (blue, dashed curve) and untreated samples of EG103 (blue, solid curve) yeast cells grown in YPE for 48 h. During the first few cycles the target cDNA is in relatively very low abundance. However, PCR amplifies DNA exponentially and the number of target molecules doubles with each amplification cycle, at least theoretically. As a result, the fluorescence given off by the target double-stranded DNA molecules increases exponentially, until a stationary phase is reached due to saturation of primers. Ct, cycle threshold; NTC, no template control; PCR, polymerase chain reaction.

* Ct value: The cycle number at which the amplification curve intersects with the threshold line due to a significant rise in fluorescence compared to the baseline fluorescence.

** Fluorescence Threshold: This is set right above the maximum baseline fluorescence so as to eliminate any inherent fluorescence which is not due to template DNA in the reaction.

2.3.10   Statistical analyses

Experimental datasets were tested for (i) normality using the Shapiro-Wilk test, which is appropriate for small sample sizes, and for (ii) equality of variances using the Levene's test. Subsequently, datasets obtained from treatments and controls that were normally distributed (i.e. $p > 0.05$ as determined by the Shapiro-Wilk test) and had equal population variances (i.e. $p > 0.05$ as determined by the Levene's test) were compared using the unpaired, two-tailed t-test for pairwise comparisons or the one-way analysis of variance (ANOVA) followed by Bonferroni post-hoc tests for multiple comparisons. Datasets which were normally distributed (i.e. $p > 0.05$ as determined by the Shapiro-Wilk test) but did not have equal population variances (i.e. $p \leq 0.05$ as determined by the Levene's test) were compared using the Welch t-test for pairwise comparisons or the Welch's ANOVA followed by Games-Howell post-hoc tests for multiple comparisons. Datasets which were not normally-distributed (i.e. $p \leq 0.05$ as determined by the Shapiro-Wilk test) were compared using the non-parametric test Mann-Whitney U for pairwise comparisons, or the non-parametric test Kruskal-Wallis followed by Bonferroni post-hoc tests for multiple comparisons.

Significance was accepted at a p-value ≤ 0.05 (i.e. 5% probability of rejecting a true null hypothesis). Significance levels are denoted by ns, not significant, $p > 0.05$; *, slightly significant, $p \leq 0.05$; **, moderately significant, $p \leq 0.01$; and ***, highly significant, $p \leq 0.001$.

2.4 Results

2.4.1 Selection of genes of interest which show altered aspirin-induced expression in the mutant EG110 *S. cerevisiae* cells, but not in the wild-type EG103 *S. cerevisiae* cells

To identify novel targets and/or pathways by which aspirin induces apoptosis in the redox-compromised EG110 yeast cells, but not in their wild-type EG103 counterparts, a select number of yeast genes were selected based on (i) their association with either ROS or the cell cycle and (ii) their aspirin-induced fold change, as determined by microarray analysis (Farrugia *et al.* 2019), which had to be greater than 1.5.

The shortlisted ROS-related genes were *OYE2, OYE3, SNO1* and *SNZ1,* wherea*s* the shortlisted cell-cycle-related genes were *CDC6, ESP1, MCD1, RAS2* and *YCA1*. Although the mRNA expression of the cell cycle-related gene *YCA1* was less than 1.5, as determined by microarray analysis (Farrugia *et al.* 2019), this gene was still shortlisted since it encodes for the yeast metacaspase which has been highly implicated in regulated cell death by apoptosis (Madeo *et al.* 2002) and in cell-cycle progression (Lee *et al.* 2008). The metacaspase is also a downstream effector of the gene products of *ESP1* and *MCD1* during apoptosis (Yang *et al.* 2008) (see section 1.4.2.2).

2.4.2 Selection of reference genes for the normalisation of target gene expression data by qRT-PCR

To normalise the change in the expression of the genes of interest (see section 2.4.1), candidate reference genes had to be chosen. A suitable reference gene must be constitutively expressed and should not alter its expression across all experimental conditions (Chervoneva *et al.* 2010). Data from a microarray analysis performed by Farrugia *et al.* (2019) was used to choose a number of genes which exhibited constitutive expression

and an unchanged mRNA expression in aspirin-treated and untreated samples of both EG110 and EG103 yeast strains. These genes are listed in Table 2.3.

2.4.3 Determination of the optimal annealing temperature of each primer set by gradient PCR followed by gel electrophoresis

Oligonucleotide primers for the target genes and reference genes were designed for cDNA amplification as described in section 2.3.7. The primer pair sequences of the reference genes and of the target genes are listed in Table 2.4.

Gradient PCR (see section 2.3.8) was carried out for each primer set to determine the optimal annealing temperature as well as to make sure that a single cDNA product was amplified. This was carried out for the candidate reference genes *ACT1, FBA1, GCN4, GLC7, PDA1, SMD2* and *TFC1* as well as for the genes of interest *CDC6, ESP1, MCD1, OYE2, OYE3, RAS2, SNO1, SNZ1,* and *YCA1*.

A series of annealing temperatures ranging from 50.3 °C to 62.0 °C were applied to six identical PCR reactions. Subsequently, the gradient PCR products of the reference genes (Figure 2.2) and the genes of interest (Figure 2.3) were run on a 2% (w/v) agarose gel (see section 2.3.6). The optimal annealing temperature was chosen based on the band intensity of these PCR products which is in turn a measure of PCR efficiency. The bands which showed a higher intensity, due to more fluorescence given off by ethidium bromide bound to DNA, indicated a greater amount of PCR product. This is a result of a higher efficiency in the annealing of the primers to the template DNA at the subjected annealing temperature. The optimal annealing temperatures for each primer set are shown in Table 2.5. The optimal annealing temperatures of the reference genes *ACT1* and *PDA1* were different from the rest

Table 2.3   Microarray gene expression data of candidate reference genes required for normalisation of the mRNA expression of the target genes by quantitative reverse transcription-polymerase chain reaction (qRT-PCR).

Reference Gene	EG110 + ASA *vs* EG110		EG103 + ASA *vs* EG103	
	Fold change	*p*-value	Fold change	*p*-value
ACT1	+1.04	0.48	+1.08	0.39
FBA1	+1.02	0.73	+1.02	0.84
GCN4	+1.04	0.49	+1.08	0.41
GLC7	-1.08	0.24	-1.05	0.60
PDA1	-1.07	0.25	-1.02	0.83
SMD2	-1.07	0.35	+1.11	0.30
TFC1	-1.14	0.18	-1.15	0.15

This microarray data obtained from Farrugia *et al.* (2019) shows that the mRNA expression of these candidate reference genes shows no change between aspirin (ASA)-treated and untreated samples of both EG110 and EG103 yeast strains, since the fold changes are close to 1. In addition, any slight changes in the fold change are insignificant since the *p*-value is greater than 0.05 for all the listed genes in both strains.

Table 2.4   List of primer pair sequences for a) the reference genes and b) the genes of interest that were designed for gene expression analyses by quantitative reverse transcription-polymerase chain reaction (qRT-PCR). The product size of the amplified complementary DNA (cDNA) products of the respective genes are also shown.

Gene Name	Primers		Product Size of amplified cDNA
	Forward (Left) Sequence (5'→3')	Reverse (Right) Sequence (5'→3')	
a) Reference Genes			
ACT1	CGTTCCAATTTACGCTGGTT	TCAGCAGTGGTGGAGAAAGA	129 bp
FBA1	CCACATGTTGGATTTGTCTGA	CATCTTCTTCACCACCGGTAA	131 bp
GCN4	GACGATGTTTCATTGGCTGA	GAACAGGAGTGGGTAAGAATGAA	106 bp
GLC7	GAGGATCTAAACCTGGTCAACAA	TATTGCCCATGAATGTCACC	148 bp
PDA1	ACCTTTACGCTCCAGGCTTC	GAGGCACCATCACCATACAA	136 bp
SMD2	TGGTGACAAGAACACCTGTGA	GCCCTTCTTCTCTGTCCAAA	131 bp
TFC1	GCTGGAGGAATGCTTGAAAA	GCCCCATTGTGAAACGATAA	149 bp
b) Genes of Interest			
CDC6	TTTGGACAGAGGGTTGTTACC	TCTTTGCTGCGAATTTGATG	140 bp
ESP1	GTGCCTTATGCCGACAATTA	TGCATGTAATAACGCCTGCT	138 bp
MCD1	CCCTCTTGATGATGCTGGAA	ATCCGTAGGCTCCTCAGACA	139 bp
OYE2	GGTTCTAGGTTGGGCTGCTT	TGTGTTGTGGGTTGTTAGCC	131 bp
OYE3	AGAGGACCGACGAATACGG	GCACCCCAGACATACTGTT	148 bp
RAS2	TCTCTTACCAGGACGGGTTG	TGTTGTACTTGCCGCCTTC	141 bp
SNO1	GTCCCTCATCGCTCAAAGAA	ATTGCGCGCTTAAAAAGATG	113 bp
SNZ1	TGGCGCTAAAGACTTAGGTGA	GCACGCCTTTATCTCCTCTG	142 bp
YCA1	TTTGGTCAGGGTTCCCACTA	TCCCCATCCAAATCTTCAGT	132 bp
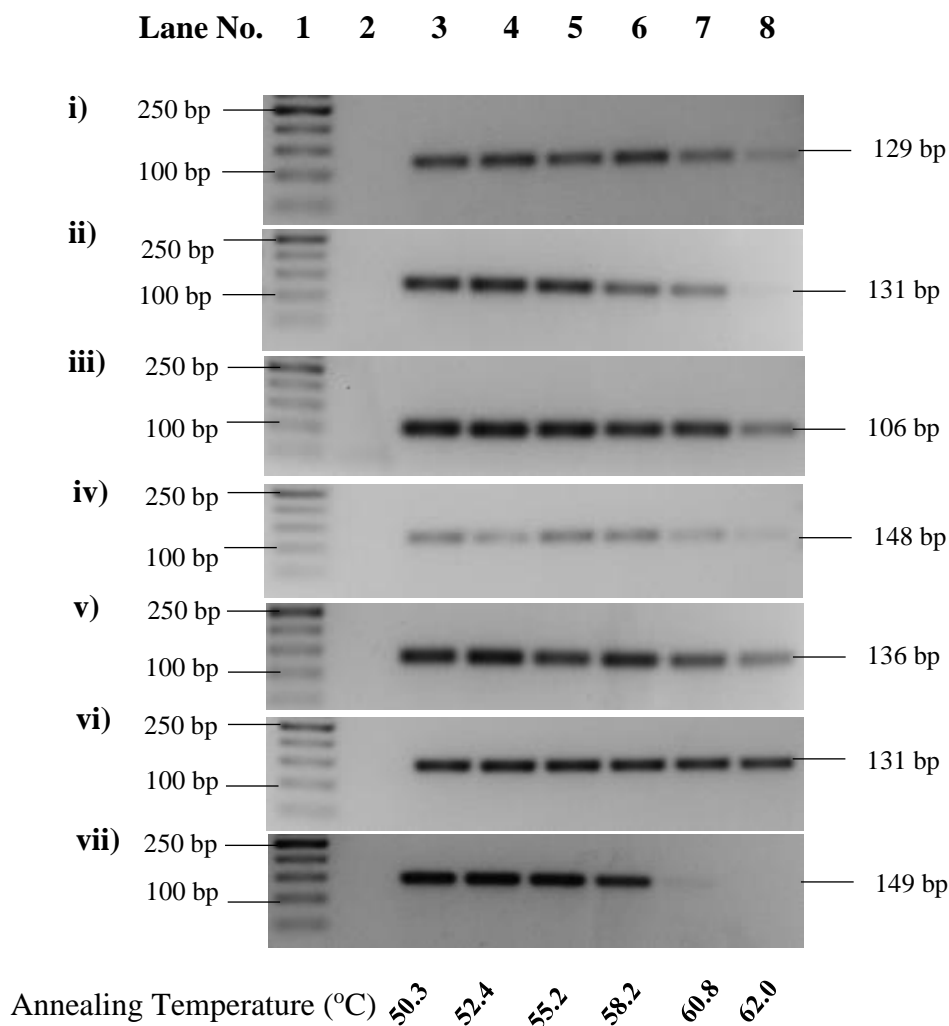
Figure 2.2 Gradient PCR gels to determine the optimal annealing temperatures of the primers for the reference genes i) *ACT1* **ii)** *FBA1* **iii)** *GCN4* **iv)** *GLC7* **v)** *PDA1* **vi)** *SMD2* **and vii)** *TFC1* **using cDNA from RNA of** *S. cerevisiae* **EG103 cells grown on YPE medium for 48 hours.**

Lane 1, 50 bp DNA ladder; Lane 2, no template control; Lanes 3 - 8, amplified cDNA from RNA of *S. cerevisiae* EG103 cells grown on YPE medium for 48 hours at 50.3 ºC, 52.4 ºC, 55.2 ºC, 58.2 ºC, 60.8 ºC and 62.0 ºC, respectively. As expected, no bands were observed in lane 2. In lanes 3 - 8, the amplified cDNA products are shown.

cDNA, complementary DNA; PCR, polymerase chain reaction; RNA, ribonucleic acid; YPE, ethanol-based.

Figure 2.3 Gradient PCR gels to determine the optimal annealing temperatures of primers for the genes of interest i) *CDC6* **ii)** *ESP1* **iii)** *MCD1* **iv)** *OYE2* **v)** *OYE3* **vi)** *RAS2* **vii)** *SNO1* **viii)** *SNZ1* **and ix)** *YCA1* **using cDNA from RNA of** *S. cerevisiae* **EG103 cells grown on YPE medium for 48 hours.**

Lane 1, 50 bp DNA ladder; Lane 2, no template control; Lanes 3 - 8, amplified cDNA from RNA of *S. cerevisiae* EG103 cells grown on YPE medium for 48 hours at 50.3 °C, 52.4 °C, 55.2 °C, 58.2 °C, 60.8 °C and 62.0 °C, respectively. As expected, no bands were observed in lane 2. In lanes 3-8, the amplified cDNA products are shown.

cDNA, complementary DNA; PCR, polymerase chain reaction; RNA, ribonucleic acid; YPE, ethanol-based.

Table 2.5 The optimal annealing temperature for each primer set as determined by gradient PCR.

	Gene Name	Optimal Annealing Temperature (ºC)
Reference genes	*ACT1*	58.2
	FBA1	55.2
	GCN4	55.2
	GLC7	55.2
	PDA1	52.4
	SMD2	55.2
	TFC1	55.2
Genes of interest	*CDC6*	55.2
	ESP1	55.2
	MCD1	55.2
	OYE2	55.2
	OYE3	55.2
	RAS2	55.2
	SNO1	55.2
	SNZ1	55.2
	YCA1	55.2

and thus, were eliminated for qRT-PCR to maintain a constant annealing temperature of 55.2 °C throughout all qRT-PCR experiments.

2.4.4 Confirmation of the specificity of the correct PCR product and optimal performance of each primer set

A trial qRT-PCR run (see section 2.3.9) was carried out to ensure that the cDNA products of the shortlisted reference genes *FBA1, GCN4, GLC7, SMD2* and *TFC1*, as well as of the genes of interest, *CDC6, ESP1, MCD1, RAS2, OYE2, OYE3, SNO1, SNZ1* and *YCA1,* were amplified efficiently at the pre-determined annealing temperature from gradient PCRs. The trial qRT-PCR experiment also ensured that the primers were specific, and amplified just a single cDNA product, as determined by melt-curve analysis (Supplementary Figures 1 and 2). The specificity of the qRT-PCR products was confirmed by loading the qRT-PCR products on a 2% (w/v) agarose gel for electrophoresis (see section 2.3.6) (Figure 2.4). These gels also showed that the qRT-PCR products were of the correct size.

2.4.5 cDNA used for qRT-PCR was of good quality and free of gDNA contamination

Before using the same cDNA synthesised from the mRNA used for the microarray analysis carried out by Farrugia *et al.* (2019), thereby reducing variability amongst techniques, the cDNA was checked for any degradation. This cDNA was amplified by PCR (see section 2.3.5) using the intron-spanning *YRA1* primers to give a cDNA PCR product of 594 bp. The 5' to 3' sequences of the *YRA1* primers are TGTCGGTGGTACTCGTGGTA and TAGTCCGCCATTTCCTTGTC for the forward and reverse primers, respectively. The strength of using an intron-spanning primer set such as this pair lies in the fact that if gDNA was
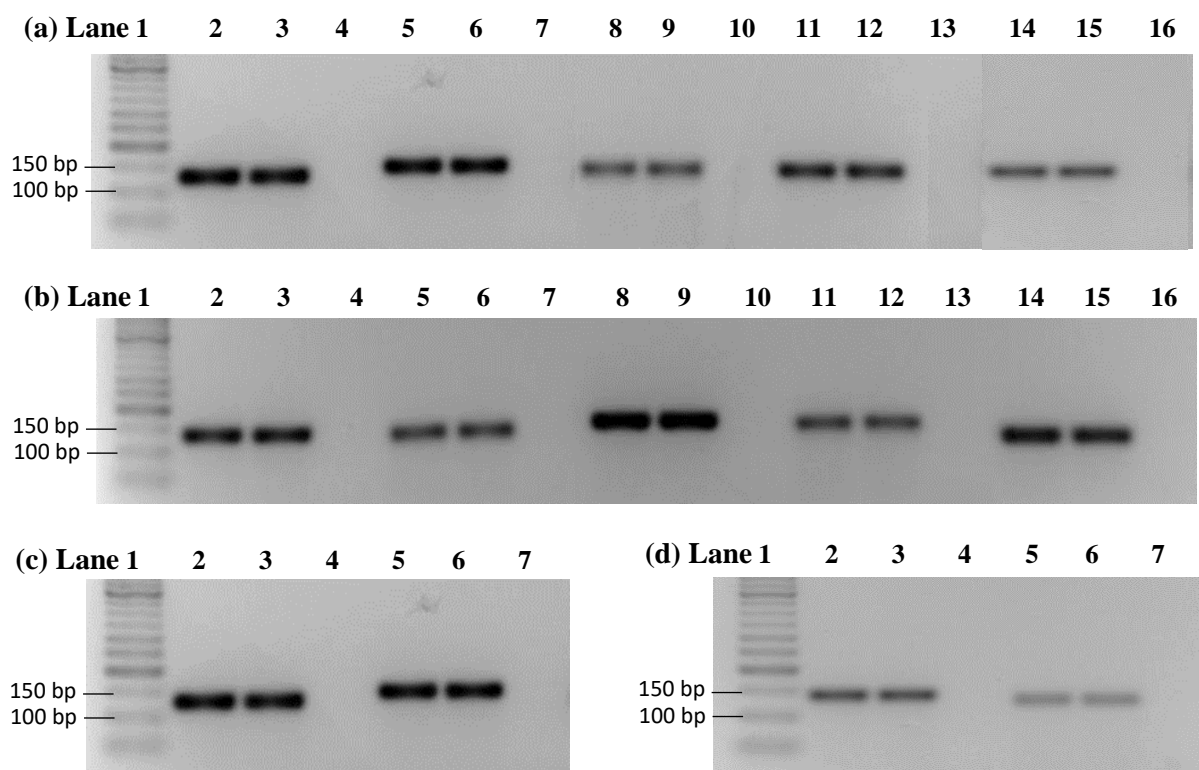
Figure 2.4 Single cDNA qRT-PCR products amplified using primer pairs of both reference genes and target genes. The presence of single bands confirm primer specificity and suitability for use in downstream experiments. The cDNA used was reverse-transcribed from RNA that was extracted from EG103 yeast cells grown in YPE medium.

(a) Lane 1, 100 bp DNA ladder; Lanes 2 and 3 contain two technical replicates of cDNA qRT-PCR products, using *FBA1* primers; Lanes 5 and 6 contain two technical replicates of cDNA qRT-PCR products, using *TFC1* primers; Lanes 8 and 9 contain two technical replicates of cDNA qRT-PCR products, using *CDC6* primers; Lanes 11 and 12 contain two technical replicates of cDNA qRT-PCR products, using *ESP1* primers; Lanes 14 and 15 contain two technical replicates of cDNA qRT-PCR products, using *GCN4* primers. Lanes 4,7, 10, 13 and 16, no template controls.

(b) Lane 1, DNA ladder; Lanes 2 and 3, cDNA qRT-PCR products, using *MCD1* primers; Lanes 5 and 6, cDNA qRT-PCR products, using *OYE2* primers; Lanes 8 and 9, cDNA qRT-PCR products, using *OYE3* primers; Lanes 11 and 12, cDNA qRT-PCR products, using *RAS2* primers; Lanes 14 and 15, cDNA qRT-PCR products, using *SNO1* primers. Lanes 4, 7, 10, 13 and 16, no template controls.

(c) Lane 1, DNA ladder; Lanes 2 and 3, cDNA qRT-PCR products, using *GLC7* primers; Lanes 5 and 6, cDNA qRT-PCR products, using *SMD2* primers. Lanes 4 and 7, no template controls.

(d) Lane 1, DNA ladder; Lanes 2 and 3, cDNA qRT-PCR products, using *SNZ1* primers; Lanes 5 and 6, cDNA qRT-PCR products, using *YCA1* primers. Lanes 4 and 7, no template controls.

As expected, no bands were observed in lanes loaded with no template controls. All the expected cDNA products are of sizes between 100 and 150 bp. The gels confirm the size of the products of interest and ensures primer specificity due to the absence of bands other than those of interest. cDNA, complementary DNA; qRT-PCR, quantitative reverse transcription – polymerase chain reaction; RNA, ribonucleic acid; YPE, ethanol-based.

present, this would give a PCR product of 1360 bp due to the additional presence of a 766 bp intron which is absent in cDNA, since introns are spliced out after transcription.

The cDNA PCR products were loaded on a 1% (w/v) agarose gel (see section 2.3.6) and are shown in Figure 2.5. The gel showed no additional bands or smearing below the bands, which would have been indicative of cDNA degradation. Also, no additional bands were visible above the 1000 bp mark which confirms the absence of gDNA.

2.4.6 Determination of cycle threshold (Ct) values by qRT-PCR analyses

During each qRT-PCR run, an amplification plot of normalised fluorescence (given off by SYBR Green I after the extension step of each cycle) is plotted against cycle number in real time, as was shown in Figure 2.1. Amplification plots of all qRT-PCR runs were used to determine Ct values as described in Section 2.3.9. These values were then processed using the software qbase+ (see section 2.2.5), to calculate NRQs by comparing Ct values of target genes to those of reference genes. Log_2 transformed NRQ values were used to calculate and plot graphs of the Log_2 fold changes in aspirin-treated and untreated samples as described in the following Section 2.4.7 and shown in Figure 2.6.

2.4.7 Gene expression data analyses of aspirin-induced changes in the mRNA expression of the genes of interest in wild-type EG103 and in MnSOD-deficient EG110 *S. cerevisiae* cells

To validate aspirin-induced gene expression data that had been determined by microarray analysis (Farrugia *et al.* 2019), qRT-PCR analysis was carried out using the SYBR green I kit (see section 2.3.9). The mRNA expression of the genes of interest were normalised to the expression of the constitutive genes *GLC7, SMD2* and *TFC1* which showed no changes in mRNA expression upon treatment with 15 mM aspirin. The choice of these
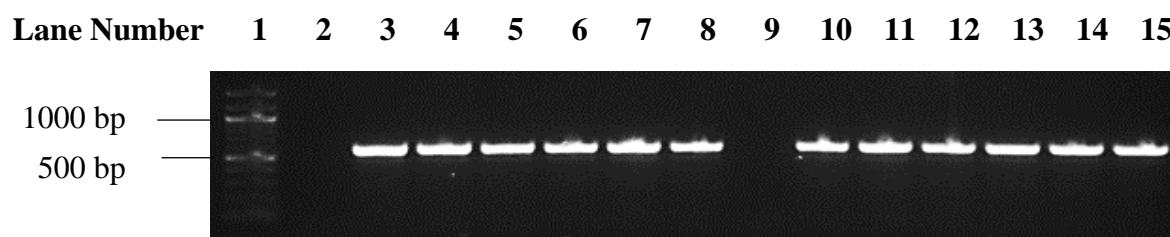
Figure 2.5 **PCR products amplified using *YRA1* primers from template cDNA that was reverse-transcribed from RNA extracted from EG103 and EG110 yeast cells grown in YPE medium in the presence and absence of 15 mM aspirin for 48 hours.**

Lane 1, 100 bp DNA ladder; Lanes 2 and 9, no template controls; Lanes 3 - 5, cDNA PCR products from RNA of EG103 cells (three biological replicates); Lanes 6 - 8, cDNA PCR products from RNA of EG103 cells treated with aspirin (three biological replicates); Lanes 10 – 12, cDNA PCR products from RNA of EG110 cells (three biological replicates); Lanes 13 - 15, cDNA PCR products from RNA of EG110 cells treated with aspirin (three biological replicates). As expected, no bands were observed in lanes 2 and 9. In each of lanes 3 – 8 and 10 - 15, the expected cDNA product of 594 bp is shown. The gel showed no smearing below the bands of interest, which would have been the case if the cDNA had been degraded. Thus, this gel proved that the cDNA was of good quality and could be used for qRT-PCR.

cDNA, complementary DNA; qRT-PCR, quantitative reverse transcription-polymerase chain reaction; YPE, ethanol-based.
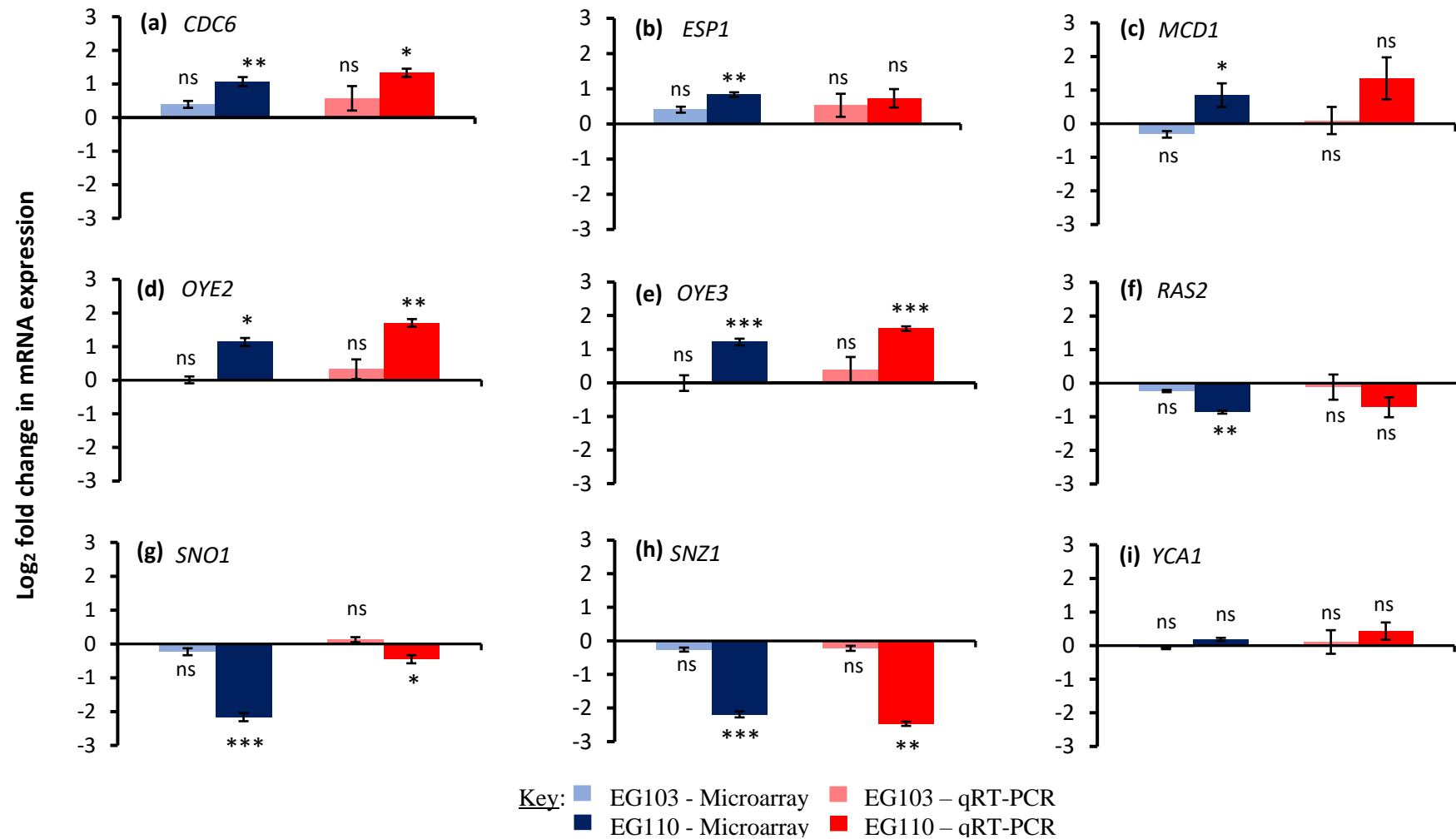
Figure 2.6 Log$_2$ transformed aspirin-induced (aspirin-treated *vs* aspirin-untreated) fold changes in gene expression data of (a) *CDC6* (b) *ESP1* (c) *MCD1* (d) *OYE2* (e) *OYE3* (f) *RAS2* (g) *SNO1* (h) *SNZ1* and (i) *YCA1* as determined by microarray analysis (blue-shaded bars) and by qRT-PCR analyses (red-shaded bars) in wild-type EG103 (light-shaded bars) and MnSOD-deficient EG110 (dark-shaded bars) yeast cells grown on YPE medium in the absence and presence of 15 mM aspirin for 48 hours. MnSOD, manganese superoxide dismutase; mRNA, messenger ribonucleic acid; qRT-PCR, quantitative reverse transcription-polymerase chain reaction; YPE, ethanol-based. Vertical bars represent the mean of three independent determinations. Error bars represent the standard error of the mean. Microarray data was obtained from Farrugia *et al.* (2019). ns, not significant, $p > 0.05$; *, $p \leq 0.05$; **, $p \leq 0.01$; ***, $p \leq 0.001$, unpaired Welch *t*-test, 2-tailed.

three reference genes for normalisation was based on the best score of the stability measure *M* (M = 0.380; Coefficient of Variation = 14.8%). The internal control gene-stability measure *M* is defined as the average pairwise variation of a single reference gene with all other candidate reference genes (Vandesompele *et al.* 2002). The lower the *M* score, the more stable is the expression stability of the control genes and thus the higher is their suitability to be used as internal control genes (Vandesompele *et al.* 2002).

From microarray and qRT-PCR analyses, aspirin induced no significant changes in the mRNA expression of *CDC6, ESP1, MCD1, OYE2*, *OYE3, RAS2, SNO1, SNZ1* and *YCA1* in the wild-type EG103 cells after 48 hours of growth in YPE medium (Figure 2.6). On the other hand, microarray gene expression data of EG110 cells grown for 48 hours in YPE medium showed that aspirin significantly upregulated the mRNA expression of *CDC6, ESP1, MCD1, OYE2* and *OYE3* and significantly downregulated the mRNA expression of *RAS2, SNO1* and *SNZ1* (Farrugia *et al.* 2019; Figure 2.6). Of all the selected target genes, the genes *SNO1* and *SNZ1* were affected the most by aspirin (~4.5-fold) in EG110 yeast cells cultivated for 48 hours in YPE medium (Farrugia *et al.* 2019; Figure 2.6 (g) and (h)). In this study, qRT-PCR analyses validated the aspirin-induced upregulation of *CDC6, OYE2* and *OYE3*, as well as the aspirin-induced downregulation of *SNO1* and *SNZ1* (Figure 2.6). The changes in the gene expression of *ESP1, MCD1, RAS2* and *YCA1,* as determined by qRT-PCR analyses, were not significant (Figure 2.6).

2.5 Conclusion

To better understand and explore the mechanisms by which aspirin induces apoptosis in the redox-compromised EG110 yeast cells, but not in the wild-type EG103 cells, it was important to (i) select key genes of interest which could potentially be targeted by aspirin

due to their association with the cell cycle or oxidative stress, and (ii) validate by qRT-PCR the aspirin-induced gene expression data obtained by microarray analysis (Farrugia *et al.* 2019).

In the present study, aspirin did not alter the expression of the cell-cycle related target genes *ESP1, MCD1, RAS2* and *YCA1* in EG110 yeast cells grown in YPE medium for 48 hours (Figures 2.6 (b), (c), (f) and (i)). However, this result does not exclude the involvement of their gene products in aspirin-mediated apoptosis, which played pro-death roles in yeast cells treated with pro-oxidants, including hydrogen peroxide and acetic acid (Hlavatá *et al.* 2008, Madeo *et al.* 2002, Ludovico *et al.* 2001, Yang *et al.* 2008). Conversely, aspirin enhanced the expression of the cell cycle-related gene *CDC6* in EG110 cells (Figure 2.6 (a)), the gene product of which may induce cell cycle arrest by inhibiting the CDK Cdc28 (Bueno, Russell 1992, Calzada *et al.* 2001, Perkins *et al.* 2001).

Moreover, this study confirms the important role of the compromised redox environment in aspirin-treated EG110 cells, since the aspirin-induced changes in the expression of all the selected ROS-related genes, namely *OYE2*, *OYE3*, *SNO1* and *SNZ1*, were confirmed by qRT-PCR and were found to be statistically significant (Figure 2.6). Aspirin induced the upregulation of *OYE2* and *OYE3* in the MnSOD-deficient EG110 yeast cells but not in the wild-type EG103 yeast cells (Figures 2.6 (d) and (e)), potentially promoting aspirin-induced apoptotic cell death of EG110 yeast cells, through their roles in modulating oxidative stress and regulating yeast cell death (Odat *et al.* 2007). More importantly, of all the aspirin-induced changes in the expression of the selected target genes, the downregulations of *SNO1* and *SNZ1* in EG110 yeast cells were the strongest (~4.5-fold), and both downregulations were validated by qRT-PCR (Figure 2.6 (g) and (h)). Conversely, the

expressions of these genes were not altered by aspirin in the MnSOD-proficient EG103 cells (Figures 2.6 (g) and (h)). Thus, *SNO1* and *SNZ1* were chosen for further studies since this result suggested that aspirin may induce apoptosis in EG110 cells by compromising glutaminolysis, which is catalysed by the gene products of *SNO1* and *SNZ1* (Dong *et al.* 2004)*,* leading to a depleted level of glutamate in these cells. Hence, in this study the main focus was on the effect of aspirin on glutamate metabolism in the redox-compromised EG110 yeast cells. Furthermore, the effect of aspirin on cell cycle progression was also studied to better understand aspirin's effect on the cell cycle distribution of both redox-compromised and wild-type *S. cerevisiae* cells.

CHAPTER THREE

THE EFFECT OF ASPIRIN ON THE CELL CYCLE AND GLUTAMATE METABOLISM IN YEAST CELLS GROWN AEROBICALLY IN ETHANOL MEDIUM

3.1 Introduction

The anti-proliferative role of aspirin has been partly attributed to cell cycle arrest (see section 1.5.2.1), redox imbalance (see section 1.5.3.1) as well as to defects in energy generation. Aspirin inhibits (i) the synthesis and transport of acetyl-CoA into the mitochondria (Farrugia *et al.* 2019), and reduces the pool of CoA (Vessey *et al.* 1996), (ii) enzymes involved in the TCA cycle, namely succinate dehydrogenase and α-ketoglutarate dehydrogenase (Kaplan *et al.* 1954, Nulton-Persson *et al.* 2004), (iii) respiratory complexes (Sandoval-Acuña *et al.* 2012, van Leeuwen *et al.* 2011) and (iv) ATP synthesis (Tomoda *et al.* 1994), all of which are critical for normal mitochondrial function. By targeting mitochondria, which are key sites for oxidative stress response and energy generation in aerobic conditions, aspirin directly compromises the ability of cells to counteract oxidative stress and grow.

Cell growth and proliferation are highly dependent on nutritional status and redox homeostasis (Conrad *et al.* 2014). During nutrient-limitation, cells downregulate growth signalling pathways which inhibit cell cycle progression (Takeshige *et al.* 1992), and upregulate processes such as autophagy (Takeshige *et al.* 1992; Yin *et al.* 2016) and stress resistance (Leadsham *et al.* 2009), until conditions are ameliorated. This is a common scenario during stationary phase of yeast cell growth, at which point yeast cells adapt to nutrient scarcity and reduce the rate of growth, often accompanied by a G1/S arrest (Hartwell *et al.* 1974). The period of time that non-dividing yeast cells remain viable during stationary phase defines the CLS of the population (Fabrizio, Longo 2007). Studies have shown that failure to maintain amino acid homeostasis caused cell death (Suraweera *et al.* 2012), while the availability of amino acids extended the chronological longevity in yeast,

and increased resistance to oxidative and thermal stress during chronological aging (Alvers *et al.* 2009, Gomes *et al.* 2007, Maruyama *et al.* 2016).

3.1.1   Glutamate metabolism and cell growth in *S. cerevisiae*

Glutamate is a highly abundant non-essential amino acid and is critical for cell growth. In fact, the CLS of a mutant yeast cell population unable to synthesise glutamate was significantly reduced, due to very low levels of intracellular glutamate (Hofman-Bang 1999). Glutamate is heavily involved in the synthesis of other amino acids and nucleotides by serving as an amino group donor (Cooper 1982, Magasanik 1992). In the cell, glutamate is mainly derived from α-ketoglutarate or glutamine.

Glutamate may be synthesised from α-ketoglutarate and ammonia, and this reaction is catalysed by the $NADP^+$-dependent glutamate dehydrogenase enzymes Gdh1 (Moye *et al.* 1985) and Gdh3 (Avendaño *et al.* 1997) (Figure 3.1). Gdh1 is important for growth during exponential phase whereas Gdh3 is the more important isoenzyme to mediate glutamate biosynthesis for resistance to stress-induced apoptosis and chronological aging during stationary phase (Lee *et al.* 2012) (see section 3.1.2).

Glutamate may also be synthesised from glutamine *via* two independent pathways mediated by NAD^+-dependent glutamate synthase (Glt1, also known as GOGAT) and glutaminases (GLS) (Figure 3.1). GOGAT catalyses the transfer of an amide group from glutamine onto α-ketoglutarate to generate two molecules of glutamate and is activated in response to amino acid starvation (Valenzuela *et al.* 1998). In fact, this enzyme was deemed a link between energy production and biomass production (Guillamón *et al.* 2001).
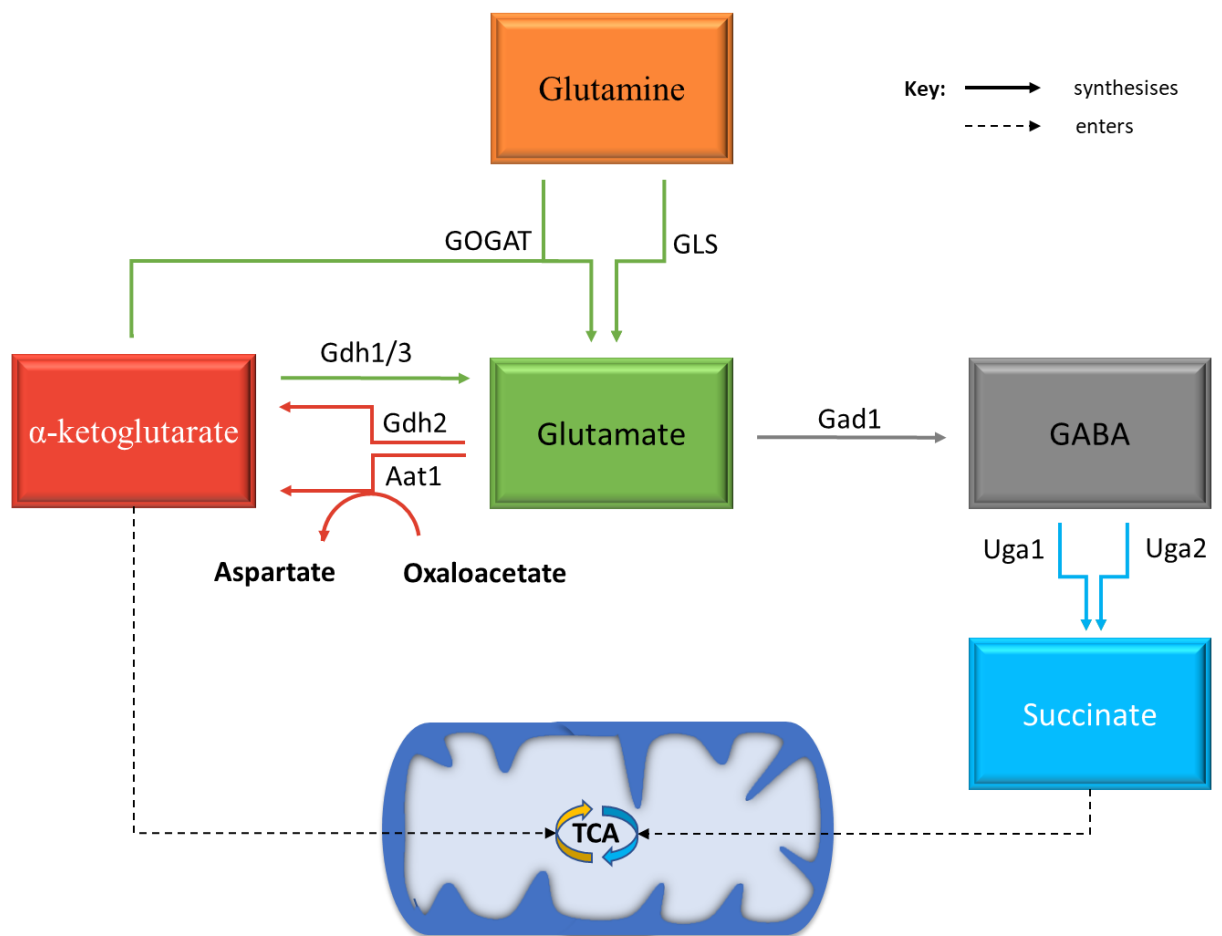
Figure 3.1 Glutamate metabolism for yeast cell growth. Glutamate is synthesised by the deamination of glutamine *via* glutaminase (GLS) or from glutamine and α-ketoglutarate *via* Glt1, an NAD^+-dependent glutamate synthase (also referred to as GOGAT). Glutamate may also be synthesised from α-ketoglutarate by the $NADP^+$-dependent glutamate dehydrogenase enzymes Gdh1 and Gdh3. In turn, glutamate may be converted back to α-ketoglutarate by the NAD^+-dependent glutamate dehydrogenase enzyme Gdh2, or by transamination *via* Aat1, yielding aspartate in the process. Furthermore, glutamate may be decarboxylated into gamma-aminobutyrate (GABA) *via* glutamate decarboxylase (Gad1). GABA may be converted to succinate *via* 4-aminobutyrate aminotransferase (Uga1) and by succinate semialdehyde dehydrogenase (Uga2, also known as Uga5). Glutamate-derived α-ketoglutarate and succinate are used to fuel the mitochondrial tricarboxylic acid (TCA) cycle during aerobic metabolism.

Furthermore, glutamine may be degraded into glutamate and ammonia by the action of GLS (Figure 3.1). Glutamate is often used to fuel the TCA cycle by anaplerosis for cell survival, particularly in glucose-deprived cells (Choo *et al.* 2010, Yang *et al.* 2009). Glutamate may be converted into gamma-aminobutyrate (GABA) by the action of glutamate decarboxylase (Gad1), which in turn may be converted into the TCA cycle intermediate succinate by 4-aminobutyrate aminotransferase (Uga1) and by succinate semialdehyde dehydrogenase (Uga2, also known as Uga5) (Coleman *et al.* 2001) (Figure 3.1).

Glutamate may also be converted back to the TCA cycle intermediate α-ketoglutarate *via* oxidative deamination or transamination. The oxidative deamination of glutamate into α-ketoglutarate is catalysed by the NAD^+-dependent glutamate dehydrogenase enzyme, Gdh2 (Miller, Magasanik 1990) (Figure 3.1). In addition, glutamate may transfer its amino group onto oxaloacetate to generate α-ketoglutarate and aspartate, a transamination reaction catalysed by the aminotransferase Aat1 (Figure 3.1). Glutamate-derived α-ketoglutarate further supports cell growth by supplying carbon to the TCA cycle for the *de novo* synthesis of aspartate (DeBerardinis *et al.* 2007, Son *et al.* 2013). In the murine neuroblastoma cell line Neuro2A, decreased levels of aspartate have been linked with cell death (Profilo *et al.* 2017), especially since aspartate is required for nucleotide, amino acid and protein synthesis, as well as for redox homeostasis (see section 3.1.2).

3.1.2 Glutamate metabolism and oxidative stress

Glutamate is an important player involved in the mitigation of oxidative stress and maintenance of cellular redox homeostasis (Amores-Sáchnez, Medina 1999). Wu *et al.* (2013) observed that glutamic acid extended the CLS in a redox-compromised *sod2*-null

yeast strain. Furthermore, decreased levels of glutamate were associated with yeast cells which suffered from oxidative stress- or thermal stress-induced apoptosis in *gdh3*-null yeast cells (Lee *et al.* 2012). Cell death in these cells was mediated by ROS accumulation, and this was likely due to glutamate's well-known role as a precursor of the main cellular antioxidant GSH (see section 1.2.2). In fact, the apoptotic phenotype of *gdh3*-null yeast cells was suppressed in the presence of exogenous GSH or glutamate or by the deletion of *GDH2* (Lee *et al.* 2012). Similarly, the addition of glutamate, but not of the other precursors of GSH, restored the viability of stressed mutant yeast cells unable of synthesising the TCA cycle intermediate citrate in the cytosol (Lee *et al.* 2007). This result suggested that apoptosis was mediated by glutamate depletion required for the biosynthesis of GSH, to mitigate cellular stress (Lee *et al.*, 2007), and confirmed that glutamate input is the rate-limiting step for GSH synthesis (Grant *et al.* 1997).

Conversely, Hu *et al.* (2010) reported that when glutamate production was increased in H_2O_2-treated mammalian cells, they observed a concomitant increase in the levels of α-ketoglutarate and GSH (see section 1.2.2). Moreover, they reported that the higher levels of α-ketoglutarate and GSH enhanced mitochondrial respiration and ATP generation, as well as reduced ROS levels, thereby showing that glutamate could also mitigate oxidative stress induced by H_2O_2.

Transamination reactions are also important for redox homeostasis and cell survival, particularly in mammalian cells (as reviewed by Hosios, Vander Heiden 2018). As described earlier, the transamination of glutamate generates other useful amino acids such as aspartate, through several redox reactions involving α-ketoglutarate (Fendt *et al.* 2013, Mullen *et al.* 2014, Sullivan *et al.* 2015) (Figure 3.1). In turn, glutamate-derived aspartate

may be involved in redox homeostasis through its involvement in the malate-aspartate shuttle. In mammalian cells, this shuttle is responsible for oxidising cytosolic NADH and exchanging it for mitochondrial NAD^+, since the mitochondrial inner membrane is impermeable to NAD^+ and NADH (Bremer, Davis 1975). Thus, this shunt controls cellular NAD/NADH ratio between the mitochondrial and cytosolic/nuclear pool (Bakker *et al.* 2001) to maintain redox homeostasis. In yeast, the malate-aspartate shuttle is critical for growth on acetate or fatty acids as carbon sources, but not for growth on ethanol (Cavero *et al.* 2003). This may be so since yeast grown on ethanol may compensate for the absence of the malate-aspartate shuttle by activating the ethanol-acetaldehyde shuttle system to reduce the cytosolic NADH/NAD ratio. Furthermore, Bakker *et al.* (2001) indicates that yeast grown on ethanol may regenerate cytosolic NAD+ by the external NADH dehydrogenases Nde1 and Nde2 (Luttik *et al.* 1998, Small, McAlister-Henn 1998) or by the glycerol-3-phosphate shuttle (Larsson *et al.* 1998).

These studies show that reactions involving glutamate may influence the redox balance through the synthesis of reduced GSH, TCA cycle intermediates and reducing equivalents, all of which are essential for mitochondria to function properly and ensure survival of cells. In particular, cancer cells are highly dependent on glutamate metabolism for energy production, biomass synthesis and redox homeostasis, especially under conditions of metabolic stress and oncogenic activation (Choi, Park 2018).

3.1.3 Glutamate metabolism and cancer cells

A key hallmark of cancer metabolism is the breakdown of glutamine into glutamate, termed glutaminolysis (Yang *et al.* 2017). The glutamate synthesised by this reaction allows cancer cells to mitigate excessive ROS levels and keep a functioning TCA cycle to synthesise

ATP, electron donors and other biosynthetic precursors (DeBerardinis *et al.* 2007, 2008). The ability of cancer cells to resort to glutamate metabolism to satisfy their increased metabolic requirements, enables them to proliferate rapidly and uncontrollably (Yang *et al.* 2017). In fact, some cancer cells die rapidly if deprived of glutamate or its precursor glutamine (Cluntun *et al.* 2017, Jiang *et al.* 2019, Yuneva *et al.* 2007, Zhang *et al.* 2017).

The substantial reliance of cancer cells on glutamate has made its metabolism a promising target to pharmacologically control their growth and proliferation. Although several drugs targeting glutamate metabolism have been developed in an attempt to slow down tumour growth and prolong survival (Fung, Chan 2017, Xiang *et al.* 2015), little is known about aspirin's potential to inhibit glutamate metabolism in cancer cells and thereby compromise their ability to proliferate.

In this chapter, studies were carried out to explore the effect of aspirin on glutamate metabolism and the cell cycle in *S. cerevisiae* cells grown in ethanol medium. The intracellular level of glutamate was measured in aspirin-treated and untreated redox-compromised EG110 yeast cells. Furthermore, the effect of aspirin on the immediate metabolic products of glutamate was determined by measuring the intracellular levels of α-ketoglutarate and GSH in EG110 yeast cells grown in aspirin-treated and untreated YPE medium. Additionally, the intracellular redox balance in these cells was measured, as given by the GSH/GSSG concentration ratio. The effect of aspirin on the cell cycle distribution of EG110 and the wild-type EG103 yeast cells grown in YPE medium was also investigated.

3.2 Materials

3.2.1 Chemicals

2-vinylpyridine, 5-sulfosalicylic acid, 5,5'-dithiobis-(2-nitrobenzoic acid) (DTNB or Ellman's reagent), D-sorbitol, dithiothreitol (DTT), L-aspartic acid monosodium salt hydrate, L-glutamic monosodium salt hydrate, reduced glutathione (GSH), nicotinamide adenine dinucleotide phosphate reduced (ß-NADPH), nocodazole, potassium phosphate monobasic and dibasic, propidium iodide (PI), sodium acetate and trisodium citrate dihydrate were obtained from Sigma-Aldrich, Darmstadt, Germany. Phenylmethylsulfonyl fluoride (PMSF) was obtained from Boehringer, Mannheim, Germany. Magnesium chloride and sodium hydroxide were obtained from Fluka, Buchs, Switzerland.

The kits used in this part of the research study were the following: Glutamate assay kit (ab83389) and alpha-KG assay kit (ab83431) were obtained from Abcam (Cambridge, UK). FITC Annexin V Apoptosis Detection Kit I was obtained from BD Pharmingen™ (California, USA).

3.2.2 Enzymes

3.2.2.1 Glutathione reductase

The enzyme glutathione reductase from baker's yeast (*Saccharomyces cerevisiae*) suspended in ammonium sulfate was obtained from Sigma-Aldrich, Darmstadt, Germany. Dilutions of the stock suspension were prepared in phosphate-EDTA buffer solution, pH 7.5 (see section 3.2.5.3). These were stored at 4 $^{\circ}$C and were stable for two weeks.

3.2.2.2 Ribonuclease A from bovine pancreas

Lyophilised ribonuclease A (RNase A) from bovine pancreas (R6513) was obtained from Sigma-Aldrich, Darmstadt, Germany. 1 mg/ml stock solution of RNase A was prepared by dissolving 1 mg of lyophilised enzyme in 1 ml of filtered nuclease-free water (ThermoScientific™, Massachusetts, USA), and was aliquoted and stored at -20 °C.

3.2.2.3 Zymolase®-20T from Arthrobacter luteus

Lyophilised Zymolase®-20T from *Arthrobacter luteus* (120491-1) was obtained from AMS Biotechnology (Abingdon, UK). A fresh solution of the enzyme was prepared on the day of use, in potassium phosphate buffer (see section 3.2.5.1) containing 1.2 M sorbitol (see section 3.2.5.17).

3.2.3 Yeast strains

The yeast strains used were described in section 2.2.2.

3.2.4 Media for yeast cell cultures

The chemicals required to prepare media for yeast cell cultures were described in section 2.2.3.

3.2.4.1 Synthetic complete medium

Synthetic complete medium was prepared as described in section 2.2.3.1.

3.2.4.2 YPE medium

YPE medium was prepared as described in section 2.2.3.2.

3.2.4.3 Yeast extract peptone dextrose (YEPD) medium

YEPD medium was prepared by mixing 1% (w/v) yeast extract and 2% (w/v) bacteriological peptone in distilled water. Separately, 2% (w/v) glucose was dissolved in distilled water. These two solutions were autoclaved separately at 120 $^{\circ}$C for 20 min and mixed afterwards.

Solid YEPD plates were prepared by adding bacteriological agar to the yeast extract and bacteriological peptone solution, to give a final concentration of 2% (w/v). This solution was then autoclaved at 120 $^{\circ}$C for 20 min, mixed with the glucose solution, poured out into sterile petri dishes and allowed to solidify at room temperature.

3.2.5 Buffer and reagent solutions

3.2.5.1 Potassium phosphate buffer

A 1 M solution of potassium dihydrogen phosphate (KH_2PO_4) was prepared by dissolving 27.22 g of KH_2PO_4 in 200 ml of deionised water. A 1 M solution of dipotassium hydrogen phosphate (K_2HPO_4) was prepared by dissolving 34.84 g of K_2HPO_4 in 200 ml of deionised water. Given amounts of these two solutions were then used to prepare a potassium phosphate buffer with the pH of interest according to Sambrooke *et al.* (1989), namely by adding K_2HPO_4 to raise the pH and KH_2PO4 to lower the pH. The 1 M stock solution and any dilutions thereof were aliquoted, autoclaved at 120 $^{\circ}$C for 20 min and stored at 4 $^{\circ}$C.

3.2.5.2 Phosphate buffer saline

PBS was prepared as described in section 2.2.4.2.

3.2.5.3   Phosphate-EDTA solution

A phosphate-EDTA solution (phosphate, 0.125 M; EDTA, 6.3 mM) was prepared by dissolving 3.99 g of dipotassium hydrogen phosphate (K_2HPO_4), 0.43 g of potassium dihydrogen phosphate (KH_2PO_4) and 0.59 g of EDTA disodium salt dihydrate in 250 ml of deionised water. The buffer was adjusted to the desired pH by using 1 M solutions of K_2HPO_4 or KH_2PO_4 to raise or lower the pH, respectively (see section 3.2.5.1). The solution was aliquoted, sterilised by autoclaving at 120 ^{o}C for 20 min and stored at room temperature.

3.2.5.4   Sodium acetate buffer

A 0.01 M solution was prepared by dissolving 82.03 mg of sodium acetate (MW = 82.03 g/mol) in 80 ml of deionised water. The pH was adjusted with glacial acetic acid to the pH of interest after the solution was allowed to cool. The volume was brought to 100 ml with deionised water. The solution was filter-sterilised, aliquoted and stored at room temperature.

3.2.5.5   Sodium citrate buffer

A 0.5 M solution of sodium citrate buffer was prepared by dissolving 14.71 g of trisodium citrate dihydrate (MW = 294.10 g/mol) in 80 ml of nuclease-free water. The pH was adjusted with sodium hydroxide to the pH of interest. The volume was made to 100 ml. The buffer was autoclaved at 120 ^{o}C for 20 min, aliquoted and stored at 4 ^{o}C.

3.2.5.6 Phenylmethylsulfonyl fluoride (PMSF) solution

A 100 mM solution was prepared by dissolving 17.4 mg of PMSF (MW = 174.19 g/mol) in 1 ml of isopropanol in the fume hood, using protective clothing. The solution was filter-sterilised, aliquoted and stored at -20 °C.

3.2.5.7 0.5 M Magnesium chloride

A 0.5 M stock solution was prepared by dissolving 508.25 mg of magnesium chloride ($MgCl_2$) (MW = 203.3 g/mol) in 4 ml of deionised water. The volume was brought to 5 ml with deionised water. The solution was filter-sterilised, aliquoted and stored at -20 °C.

3.2.5.8 1 M Trizma® base

1 M Trizma® base was prepared as described in section 2.2.4.4.

3.2.5.9 Tris-HCl

A 1 M solution of Tris-HCl buffer was prepared by adding concentrated hydrochloric acid to a 1 M Trizma® base solution (see section 2.2.4.4) to the pH of interest. The solution and any dilutions thereof were autoclaved at 120 °C for 20 min and stored at 4 °C.

3.2.5.10 1 M Dithiothreitol (DTT)

A 1 M solution of DTT was prepared by dissolving 772.5 mg of DTT in 5 ml of 0.01 M sodium acetate, pH 5.2 (see section 3.2.5.4). The solution was filter-sterilised and aliquoted into 250 µl aliquots and stored at -20 °C.

3.2.5.11   Tris-DTT buffer

Tris-DTT was freshly prepared by adding 10 mM DTT (see section 3.2.5.10) to 0.1 M Tris-HCl (see section 3.2.5.9). The mixture was filter-sterilised and used immediately.

3.2.5.12   5,5'-dithiobis-(2-nitrobenzoic acid) (DTNB) solution

A 6 mM solution of DTNB (also known as Ellman's reagent) was prepared by dissolving 23.8 mg of DTNB (MW = 396.35 g/mol) in 10 ml of phosphate-EDTA solution (see section 3.2.5.3). The solution was filter-sterilised, stored at 4 $^{\circ}$C and was stable for two weeks.

3.2.5.13   Glutathione stock solution

A 20 mM stock solution of glutathione (GSH) was freshly prepared by dissolving 30.73 mg of GSH (MW = 307.32 g/mol) in 5 ml of deionised water. Any dilutions thereof were also prepared on the day of use and kept on ice.

3.2.5.14   Nicotinamide adenine dinucleotide phosphate (ß-NADPH) solution

A 0.3 mM solution of ß-NADPH was prepared by dissolving 26.6 mg of ß-NADPH, tetrasodium salt in 100 ml solution of phosphate-EDTA solution (see section 3.2.5.3). This was filter-sterilised and stored at 4 $^{\circ}$C for two weeks.

3.2.5.15   Nocodazole solution

1.5 mg of nocodazole were dissolved in 1 ml of dimethyl sulfoxide (DMSO). Heating was required for nocodazole to dissolve completely. The solution was filter-sterilised, aliquoted and stored at -20 $^{\circ}$C.

3.2.5.16   10% (w/v) sodium dodecyl sulfate (SDS)

A 10% (w/v) solution of SDS was prepared by dissolving 10 g of SDS in 80 ml of deionised water and the solution was allowed to stir gently without frothing. Heating was necessary for SDS to dissolve completely. Once the solute had dissolved, the volume of the solution was adjusted to 100 ml with deionised water while mixing. The solution was filter-sterilised and stored at room temperature.

3.2.5.17   2 M Sorbitol

A 2 M solution of D-sorbitol (MW = 182.172 g/mol) was prepared by dissolving 87.44 g in approximately 100 ml of deionised water with continuous stirring. The sorbitol was added little by little to aid dissolution. The volume was made to 240 ml with deionised water and aliquoted into two. The solution was autoclaved at 120 ^{o}C for 20 min and stored at 4 ^{o}C.

3.2.5.18   3.5% (w/v) sulfosalicylic acid (SSA)

A 3.5% (w/v) solution of SSA was prepared by dissolving 14 g of SSA in 400 ml of deionised water, in the fume hood. The resultant solution was aliquoted, autoclaved at 120 ^{o}C for 20 min and stored at 4 ^{o}C.

3.2.6 Software Programmes

The software programmes used for this part of the work were Cell Quest™ Pro, FlowJo™ v10.0.7 from BD Biosciences and SPSS® Statistics v25 from IBM (New York, USA).

3.3 Methods

3.3.1 Colorimetric determination of intracellular glutamate content

To investigate whether aspirin affects the level of glutamate in EG110 cells, the Glutamate assay kit by Abcam was used (see section 3.2.1). The methodology described in the kit's instructions was slightly modified for yeast extracts as described in the following paragraph. The concentration of glutamate was determined by measuring the formation of a colorimetric product (OD_{450}), proportional to the glutamate present in the samples.

Sample Preparation

1×10^6 EG110 cells were cultivated in 5 ml YPE medium, in the presence and absence of 15 mM ASA (see section 2.3.1). After the required time of growth, 4×10^7 cells/ml (OD_{600} = 4) were harvested from each culture and washed in 1 ml of ice-cold PBS (see section 2.2.4.2). The cells were then pelleted (3,000 g for 5 min) and resuspended in 1 ml of room temperature-acclimatised Glutamate Assay Buffer. The cell suspension was transferred to lysis chambers which were half-filled with 400-600 µm glass beads. The cell suspensions were then subjected to two rounds of cell lysis cycles of 30 s each, using the µ-minibeadbeater. The lysates were then incubated for 15 min on ice and transferred to clean microcentrifuge tubes. Samples were centrifuged at 13,000 g for 10 min at 4 °C to remove any insoluble material. Lysates were then transferred to spin filters with a molecular weight cut off (MWCO) of 10 kDa for deproteinisation. This was important to avoid particulate matter, proteins, fats and/or enzymes in the sample from interfering with the assay. Lysates were then centrifuged for 10 min at room temperature at 14,000 g. The filtrate from each sample was collected into clean microcentrifuge tubes.

Assay Procedure and Detection

To perform the assay, 50 μl of filtrate collected from each sample were added in duplicate to a 96-well plate. Standard diluted solutions (ranging from 0 – 10 nmol/well), which were prepared from a 1 mM stock solution of L-glutamate in Glutamate Assay buffer (both provided in the kit), were similarly added in duplicate in separate wells to plot a standard calibration curve (Supplementary Figure 3).   100 μl from a previously prepared master mix, consisting of 90 μl of Glutamate Assay Buffer, 8 μl Glutamate Developer and 2 μl of Glutamate Enzyme Mix (all provided in the kit) were added to each reaction well. The master mix was prepared to avoid variability amongst the samples and standards.

Another similar master mix but without Glutamate Enzyme Mix was added to a separate set of sample wells to serve as a background control. The 96-well plate was briefly shaken horizontally and incubated at 37 $^\circ$C overnight, protected from light. The absorbance at OD_{450} was measured on a Mithras LB940 Multimode Microplate Reader (Berthold Technologies GmbH, Co. KG, Baden-Württemberg, Germany).

Calculations and Statistics

A standard calibration curve of mean absorbance values (OD_{450}) measured for different standard solutions was plotted against their corresponding L-glutamate concentrations (0 – 10 nmol/well) (Supplementary Figure 3). Mean absorbance values of L-glutamate standard solutions were corrected for any inherent absorbance reading of the assay buffer containing no glutamate. Similarly, mean absorbance values of the samples were corrected for inherent absorbance readings of (i) the blank containing no sample and (ii) the background control wells containing no Glutamate Enzyme Mix. Linear regression analysis was used to determine the amount of glutamate (nmol) in 50 μl of each sample. The concentration of

glutamate in nmol/ml was then calculated. To normalise the quantity of glutamate in ASA-treated and untreated samples, the amount of glutamate in nmol/ml per turbidimetric unit of culture was calculated. Pairwise comparisons tests were performed (see section 2.3.10) to determine if the intracellular level of glutamate was reduced in the aspirin-treated EG110 yeast cells when compared to their aspirin-untreated counterparts.

3.3.2   Monitoring the growth of EG110 *S. cerevisiae* cells grown in ASA-treated ethanol medium in the absence and presence of L-glutamate

A primary culture of EG110 cells was used to inoculate 5 ml secondary cultures (see section 2.3.1) of ASA-treated YPE medium containing different amounts of L-glutamic acid monosodium salt hydrate, having the pH adjusted to 5.50 with 1 M Trizma® base (see section 2.2.4.4). All initial secondary cultures had an equal OD_{600} of 0.08 and were incubated at 28 °C with constant shaking (250 rpm). The optical density was measured using a BioPhotometer Eppendorf spectrophotometer (Hamburg, Germany) at 24-hour intervals. Growth curves of OD_{600} against time in hours were plotted to monitor the growth of yeast cells.

3.3.3   Viability assay based on colony-forming units (CFUs) grown on YEPD plates

For cell viability, 500 cells from each 5 ml secondary yeast cell culture (see section 2.3.1) were inoculated onto YEPD plates (see section 3.2.4.3) at 24, 48, 96 and 144 hours of cultivation. The CASY Cell Counter and Analyzer System Model TT (Innovatis) was used to calculate the number of cells. The fold change in cell viability of EG110 yeast cells grown in ASA-treated YPE medium, in the absence and presence of L-glutamate, was obtained by comparing CFU counts of treated cells to those of untreated cells growing only in YPE medium.

Statistically significant changes in the viability of EG110 cells subjected to different treatments were determined using multiple comparisons tests (see section 2.3.10).

3.3.4 Determination of the mode of yeast cell death by flow cytometry using annexin V-FITC / propidium iodide (PI) staining

To confirm that ASA-treated redox-compromised EG110 yeast cells die by apoptosis and to verify whether these cells are rescued by exogenous L-glutamate, cells were double-stained with annexin V-FITC and PI using the FITC Annexin V Apoptosis Detection Kit I (BD Pharmingen™) (see section 3.2.1).

Preparation of spheroplasts

EG110 yeast cell cultures were grown for the desired time in 5 ml of YPE medium only, and in ASA-treated YPE medium in the absence and presence of 200 mM L-glutamate having the pH adjusted to 5.50 with 1 M Trizma® base. For the preparation and cultivation of the yeast cell cultures see section 2.3.1.

Centrifugation of 1×10^7 cells from each cell culture was carried out at 3,000 g for 5 min at 4 °C. The cell pellet was resuspended and washed in 1 ml of phosphate buffer containing 1.2 M sorbitol (see section 3.2.5.17), 35 mM potassium phosphate, pH 6.8 (see section 3.2.5.1) and 0.5 mM $MgCl_2$ (see section 3.2.5.7). Cells were pelleted (3,000 g for 5 min at 4 °C) and resuspended in 1 ml Tris-DTT buffer (see section 3.2.5.11) to break the cysteine bridges in the yeast cell wall. The cell suspensions were incubated with gentle shaking (50 rpm) for 20 min at 30 °C. The cells were then recovered by centrifugation (3,000g for 5 min at 4 °C) and the wet weight of cells was recorded.

To digest the cell wall of the yeast cells, 20 mg of pre-warmed (to 28 °C) Zymolase®-20T (see section 3.2.2.3) per gram wet weight of cells, were dissolved in a volume of sorbitol-containing phosphate buffer which is equivalent to 2 ml per gram wet weight of cells. This volume was used to resuspend the cell pellet, and cells were incubated for 2 hours at 30 °C, with gentle shaking at 50 rpm. After this step, the resultant spheroplasts were treated very gently. The formation of spheroplasts was confirmed by removing an aliquot from the enzyme-exposed suspension, diluting it 10-fold in 10% (w/v) SDS (see section 3.2.5.16), and microscopically examining the suspension for the presence of cells. The absence of cells indicated completion of spheroplast formation. Control cells (not treated with Zymolase®-20T) were treated in the same way. These remained fully-intact cells. The spheroplasts were harvested by centrifugation in a Micro-Centaur centrifuge at 1,000 rpm for 1 min.

Assay procedure and detection

Recovered spheroplasts were washed in 1 ml of 1x sorbitol-containing binding buffer prepared by adding 1.2 M sorbitol (see section 3.2.5.17) to the binding buffer which was provided in the kit. Spheroplasts were spun down again, resuspended in 500 μl of 1x binding buffer and divided into two aliquots. One aliquot was double-stained with 5 μl of annexin V-FITC and 5 μl of PI (both dyes provided in the kit), and incubated for 30 min at room temperature in the dark with continuous gentle mixing. The other aliquot was left unstained and served as a control to ensure that autofluorescence did not present a problem across experimental conditions. Finally, both stained and unstained samples were analysed by flow cytometry on a BD FACS Calibur flow cytometer. Side scatter (SSC) *vs* forward scatter (FSC) plots were constructed to identify and gate spheroplasts using CellQuest™Pro software (BD biosciences) (Figure 3.2).
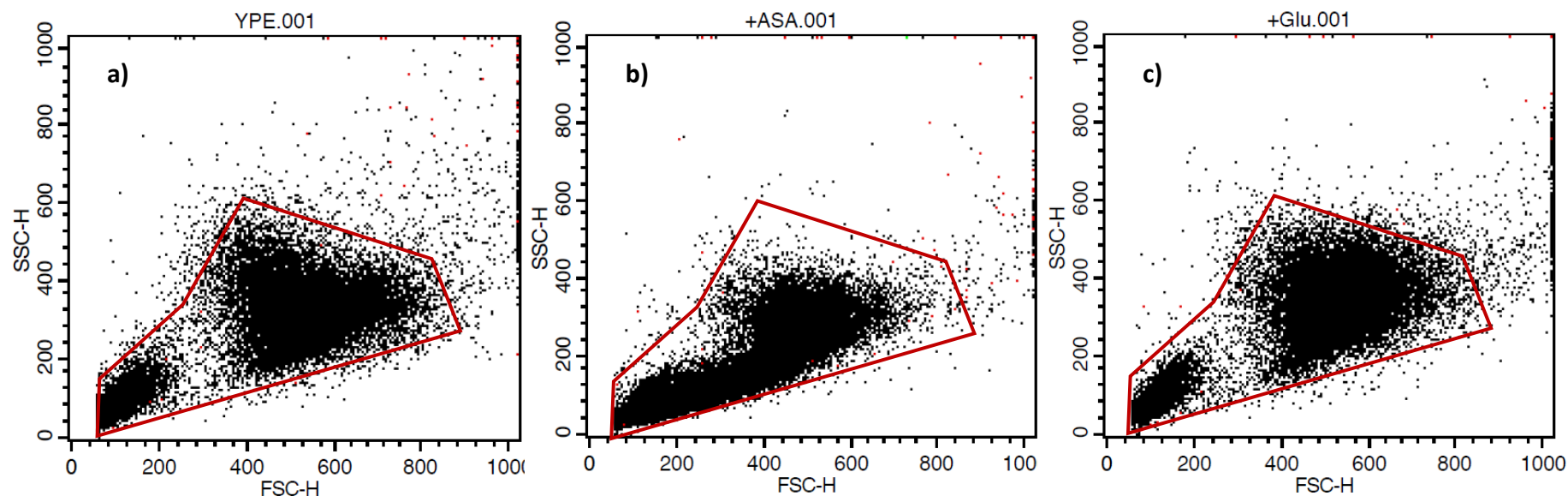
Figure 3.2: Identification of EG110 spheroplasts by side scatter (SSC) *versus* forward scatter (FSC) plots. EG110 spheroplasts that were originally cultivated in a) YPE medium, b) ASA-treated YPE medium and in c) ASA-treated YPE medium in the presence of L-glutamate for 96 hours were identified based on size and granularity (complexity) as indicated by FSC and SSC, respectively. Since cell debris have lower FSC than live cells, they tend to be observed at the lower left corner of the dot plots. However, it is rather difficult to distinguish between cell debris from yeast cell buds. In addition, the SSC *vs* FSC plot of ASA-treated EG110 cells (b) showed no definite boundary between the two seemingly distinct populations observed in a) and c). For this reason, one gate was applied across treatment (as shown by the red polygonal shape), encompassing most of the cell populations irrespective of treatment. The enclosed population was used for analysis. ASA, aspirin; Glu, glutamate; YPE, ethanol-based.

To adjust the settings of the instrument such that the emission spectra of the two fluorochromes did not overlap, positive controls for both dyes were needed. Suspensions of EG110 spheroplasts originally grown in ASA-treated YEPD medium (see section 3.2.4.3) for 96 hours, were used to serve as positive controls for cell death as indicated by the findings of Balzan *et al.* (2004). These suspensions were divided into four aliquots: one aliquot was left unstained; two aliquots were single-stained with either PI or with annexin V-FITC and an aliquot was double-stained with both dyes. Compensation of the instrument was required to exclude overlapping of the two emission spectra (Figure 3.3 (a) and (b)). The instrument settings were kept constant across experimental conditions and included an excitation wavelength of 488 nm, a 530/30 nm bandpass filter for FITC detection, and a 630/22 nm bandpass filter for PI detection. During analyses, gates were set once, such that they could be applied to all samples for comparison, under all experimental conditions (Figure 3.3 (c)).

3.3.5 Cell cycle analyses of yeast cells by flow cytometry using PI

The method used for the flow-cytometric analysis of the DNA content in budding yeast was adapted from the protocol of Haase and Lew (1997). Yeast cells cultivated in 5 ml cultures were grown for the desired time at 28 ^{o}C with shaking at 250 rpm (see section 2.3.1). An aliquot from EG103 cells grown in YPE medium, of OD_{600} = 0.5, was treated with 50 µg/ml nocodazole dissolved in dimethyl sulfoxide (DMSO) (see section 3.2.5.15) as a positive control for cells arrested at the G2/M checkpoint. To ensure that the concentration of DMSO used did not influence the cell cycle distribution of nocodazole-treated cells, a separate aliquot of cells was treated with an equivalent volume of nocodazole-free DMSO.

(a) Annexin V-FITC channel
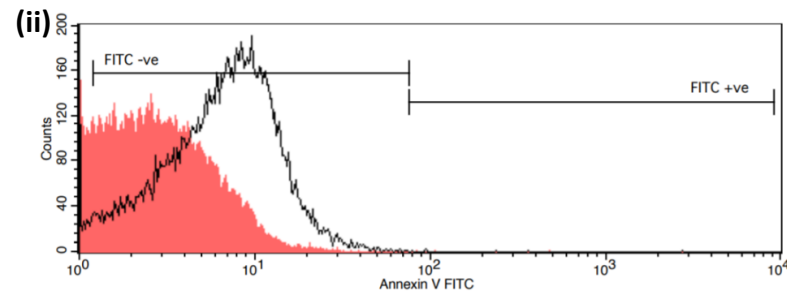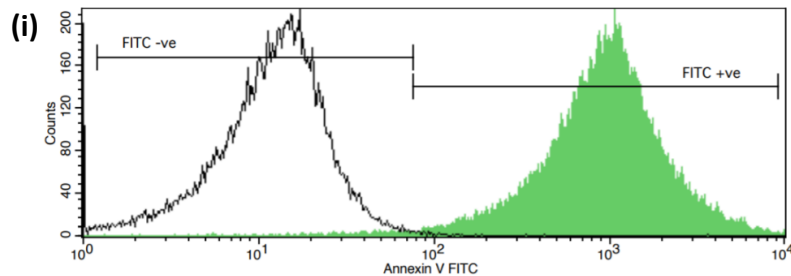
(b) PI channel
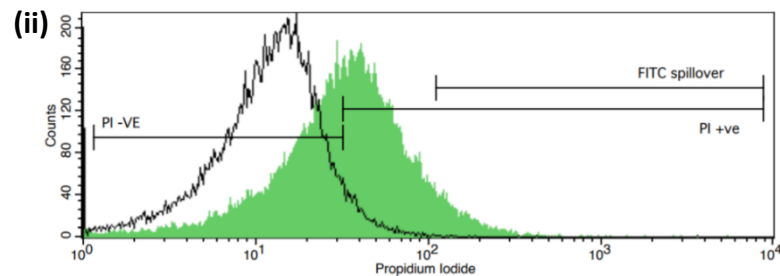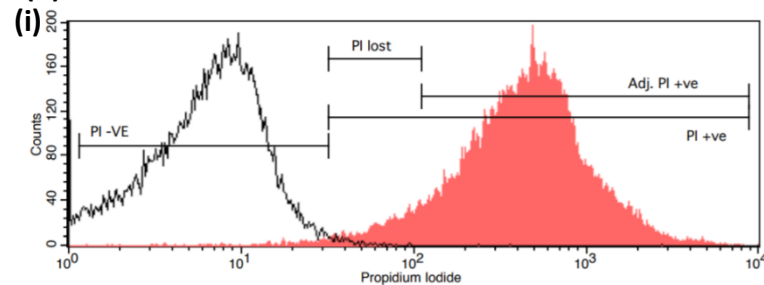
(c) Dot plots
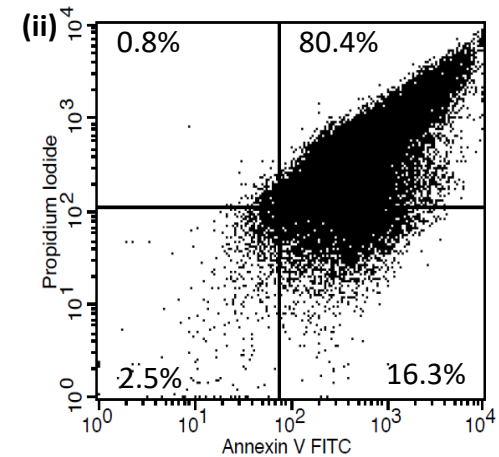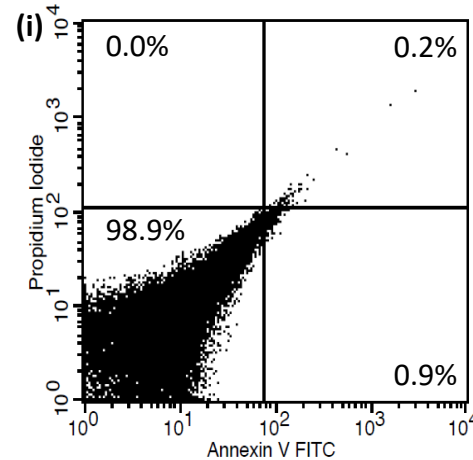
Figure 3.3: **Flow-cytometric compensation and gating strategy for the staining with annexin V-FITC and PI of spheroplasts from aspirin-treated EG110 cells grown in YEPD medium for 96 hours.** Superimposed graphs visualised in (a) the annexin V-FITC channel and (b) the PI channel, are from unstained spheroplasts (left, open black curves) and from spheroplasts that are single-stained with either annexin V-FITC (green-filled curves) or PI (red-filled curves). In the PI channel, as shown in (b)(ii), fluorescence from FITC-stained spheroplasts was observed as spillover in the PI +ve gate. Thus, the left boundary of the adjusted PI +ve gate in (b)(i) was objectively set at the point where the fluorescence signals from annexin V-FITC-stained spheroplasts in (b)(ii), and PI-stained spheroplasts in (b)(i), intersect in the PI channel. By doing so, a compromise was achieved between a false negative signal (PI lost = 6.87%) and a false positive signal (FITC spillover = 5.84%). (c) Dot plots of (i) unstained and (ii) double-stained EG110 spheroplasts that were previously cultivated in aspirin-treated YEPD medium for 96 hours. Graphs in (a) and (b) were used to set gates of dot plots shown in (c). Gates set in dot plots were then applied to all stained and unstained samples for comparison, under all experimental conditions. Quadrants: lower left, FITC -ve/PI -ve; upper left, FITC -ve/PI +ve; lower right, FITC +ve/PI -ve; upper right, FITC +ve/PI +ve.
FITC: fluorescein isothiocyanate; PI, propidium iodide; YEPD: yeast extract peptone dextrose.

Upon treatment, both cell aliquots were returned to the shaking incubator for 2 hours at 28 °C.

After the incubation period of interest, 1×10^7 cells were harvested from each cell culture using the CASY Cell Counter and Analyzer System Model TT (Innovatis). Cells were recovered by centrifugation at 3,000 g for 5 min at 4 °C. Cell pellets were washed twice with 1 ml of 50 mM sodium citrate buffer, pH 7.2 (which limits cell clumping) (see section 3.2.5.5). Recovered cells were then permeabilised and fixed in 70% (v/v) ice-cold ethanol by adding it dropwise to the cell pellet while vortexing. This was important to prevent cell clumping. Cells were then stored at 4 °C at least overnight, to ensure complete fixation and permeabilisation.

Assay procedure and detection

On the next day, permeabilised and fixed cells were recovered by centrifugation at 3,000 g for 10 min at 4 °C and washed twice with sodium citrate buffer, pH 7.2 (see section 3.2.5.5), to ensure the absence of ethanol which influences the quality of the cell cycle profiles. Each cell pellet was then resuspended in 0.5 ml of sodium citrate buffer, pH 7.2 (see section 3.2.5.5), containing 0.1 mg/ml RNase A (see section 3.2.2.2) in nuclease-free water and incubated at 37 °C for 4 hours with gentle shaking (50 rpm). The addition of RNase A ensured that only DNA, not RNA, was stained.

Each RNase-treated sample was divided into two aliquots of 250 µl each. One aliquot was topped up with 250 µl of sodium citrate buffer, pH 7.2 (see section 3.2.5.5) and this served as an unstained control to ensure that any fluorescence observed in the stained cells originated from the PI added. The other aliquot was treated with 250 µl of sodium citrate

buffer, pH 7.2 (see section 3.2.5.5) containing 8 µg/ml PI so that the final concentration of PI

was 4 µg/ml. After thorough mixing, both PI-stained and unstained cells were incubated at 4

°C overnight, in the dark (to ensure saturation with PI), and were processed on the next day.

All cell suspensions were briefly vortexed and then sonicated (sonicator output = 20%) for

2 rounds of 15 s, each with an interval of 30 s on ice using a Soniprep 150. This was done to

separate buds from mother cells and to break up any cell clumps. Finally, the cell

suspensions were transferred into 12 x 75 mm FACS tubes, vortexed briefly right before

being analysed by flow cytometry on a BD FACS Aria III flow cytometer with the aid of

FlowJo™ v10.0.7 software.   At least 30,000 cells from each sample were analysed. The

instrument settings were kept constant across experimental conditions and recorded at a

photomultiplier tube (PMT) voltage of 700 V. The excitation wavelength was set at 488 nm

with a bandpass filter of 630/22 nm for PI detection.

Analyses and Statistics

After identifying and gating yeast cells based on size and complexity with the aid of SSC *vs*

FSC plots (Figure 3.4), cell aggregates were excluded using side scatter (SSC) plots (Figure

3.5) with the aid of FlowJo™ v10.0.7 software. During analyses, gates were set with the aid

of nocodazole-treated cells arrested at the G2/M checkpoint (Figure 3.6). Such gates were

then applied to all samples for comparison, under all experimental conditions. Treatment-

induced changes in the percentage of cells in different phases of the cell cycle were

determined by performing pairwise or multiple comparisons tests (see section 2.3.10),

depending on whether two or more treatments were compared, respectively.
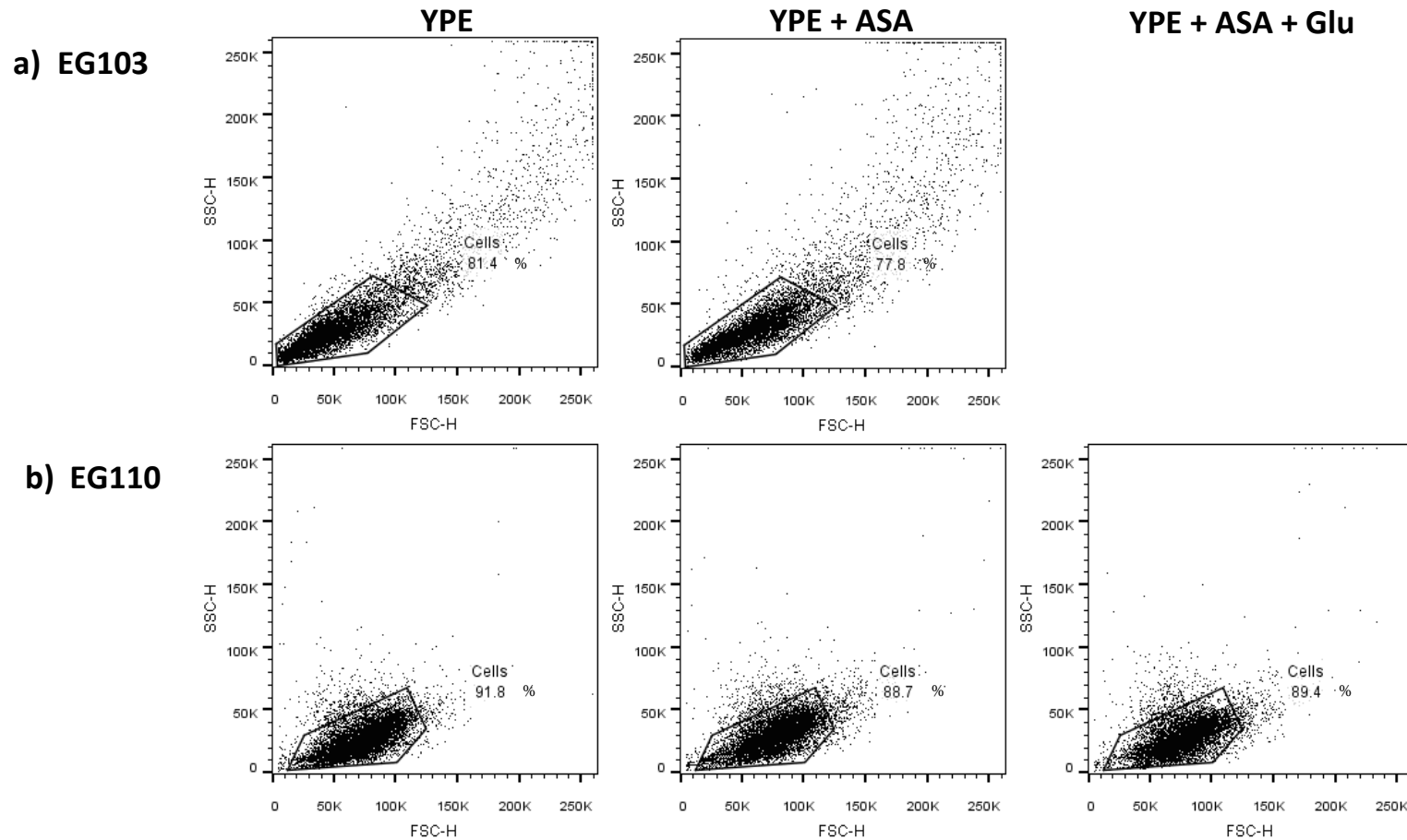
Figure 3.4 Identification of fixed and permeabilised a) EG103 and b) EG110 yeast cells by side scatter (SSC) *versus* forward scatter (FSC) dot plots. Yeast cells cultivated for 168 hours in YPE medium, and in ASA-treated YPE medium in the absence or presence of L-glutamate were identified based on size and granularity (complexity) as indicated by FSC and SSC, respectively. EG103 and EG110 cells revealed differences in SSC *vs* FSC plots and this required a different gate to be set for each strain. Values represent the percentage of cells gated within the polygon. At least 30,000 cells were measured for each sample. Analyses were carried out on a FACS Aria III flow cytometer with the aid of FlowJo™ v10.0.7 software (BD biosciences). ASA, aspirin; Glu, glutamate; YPE, ethanol-based.

127
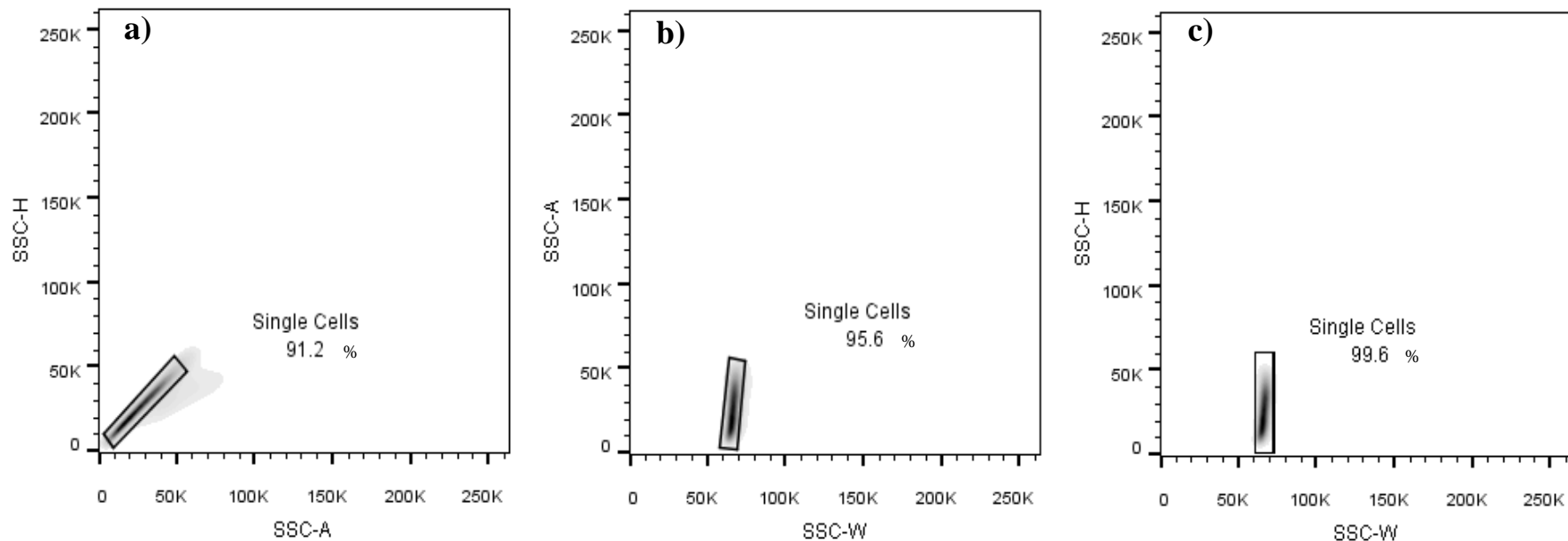
Figure 3.5 Side scatter (SSC) density plots to exclude yeast cell aggregates for flow-cytometric analyses of the cell cycle in yeast cells. The density plot, side scatter-height (SSC-H) *vs* side scatter-area (SSC-A), shown in a) was constructed using the cell population that had originally been gated based on size and complexity (granularity) (SSC *vs* FSC, Figure 3.4). A polygon was drawn around cells which are observed as a thin, linear streak, to exclude cell aggregates. This gated population of single cells was then used to construct the SSC-A *vs* side scatter-width (SSC-W) density plot shown in b). Once again, a polygon was drawn around the thin, linear streak which represented single cells. Similarly, this gated population of single cells was used to plot a final density plot of SSC-H *vs* SSC-W shown in c). Once again, a polygon was drawn to exclude cell aggregates. This step-wise procedure resulted in the identification of the single cell population that was analysed for cell cycle distribution. Values represent the percentage of cells gated within the polygon. Analyses were carried out on a FACS Aria III flow cytometer with the aid of FlowJo™ v10.0.7 software (BD biosciences).

FSC, forward scatter.
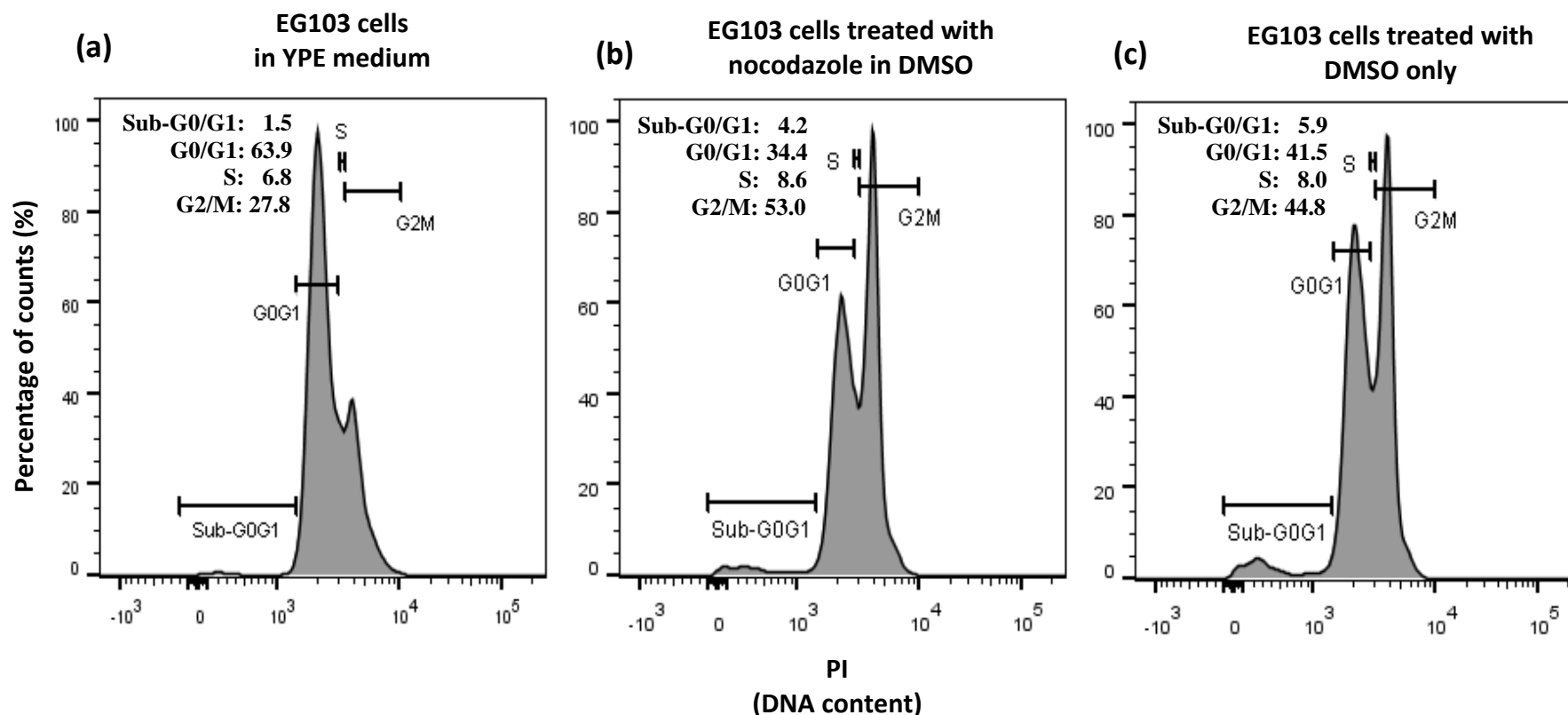
Figure 3.6 Propidium iodide (PI)-stained EG103 yeast cells treated with nocodazole served as a positive G2/M arrest control for flow-cytometric cell cycle analyses. The figure shows fluorescence histograms of exponentially-growing EG103 yeast cells in (a) YPE medium only, in (b) YPE medium to which 50 µg/ml nocodazole in dimethyl sulfoxide (DMSO) were added, and in c) YPE medium to which an equivalent amount of DMSO, as in (b), was added prior to fixation. Nocodazole-treated cells were used as a positive control for cells arrested at the G2/M checkpoint such that samples could be aligned to it for comparison. DMSO-treated cells were used to check whether the concentration of DMSO influences the cell cycle distribution of nocodazole-treated control cells. Values represent the percentage of cells in different phases of the cell cycle. At least 30,000 cells were measured. Analyses were carried out on a FACS Aria III flow cytometer with the aid of FlowJo™ v10.0.7 software (BD biosciences). YPE, ethanol-based.

3.3.6 Colorimetric determination of intracellular α-ketoglutarate content

To investigate whether aspirin affects the level of α-ketoglutarate in EG110 cells the Alpha-KG Assay Kit (ab83431) from Abcam was used (see section 3.2.1). The concentration of α-ketoglutarate was determined by measuring the absorbance at 570 nm of a colorimetric product produced by the pyruvate originally generated from α-ketoglutarate in the samples.

Sample Preparation

EG110 cells were cultivated in 5 ml YPE medium only, and in ASA-treated YPE medium in the absence and presence of 200 mM L-glutamate having the pH adjusted to 5.50 with 1 M Trizma® base (see section 2.2.4.4).

After the desired time of growth, 1×10^8 cells/ml (OD_{600} = 10) were harvested from each culture and washed with 1 ml of ice-cold PBS (see section 2.2.4.2). The cells were then pelleted (3,000 *g* for 5 min at 4 °C) and resuspended in 1 ml of room temperature-acclimatised Alpha-KG Buffer (provided in the kit). The cell suspension was transferred to lysis chambers which were half-filled with 400-600 μm glass beads. The cell suspensions were then subjected to two rounds of cell lysis cycles of 30 s each, with a cooling interval of 30 s, using the μ- minibeadbeater. The lysates were then transferred to clean microcentrifuge tubes and spun down at 13,000 *g* for 10 min at 4 °C to precipitate any yeast cell debris or insoluble material. Lysates were then transferred to spin filters with a molecular weight cut off (MWCO) of 10 kDa (UFC501024, Sigma-Aldrich, Darmstadt, Germany) and centrifuged at 14,000 *g* for 10 min at room temperature for deproteinization. This was important to avoid particulate matter, proteins, fats and/or enzymes in the sample from interfering with the assay. The filtrate from each sample was collected into clean microcentrifuge tubes and used for the assay.

Assay procedure and detection

To perform the assay, 50 μl of filtrate collected from each sample were added in duplicate in a 96-well plate. Standard diluted solutions (ranging from 0 – 10 nmol/well), which were prepared from a 1 nmol/μl stock solution of Alpha-KG standard prepared in assay buffer provided in the kit, were similarly added in duplicate in separate wells to plot a standard calibration curve (Supplementary Figure 4).   50 μl of reaction mix consisting of 44 μl of Alpha-KG Assay Buffer, 2 μl Alpha-KG Converting Enzyme, 2 μl Alpha-KG Enzyme Mix and 2 μl Alpha-KG Probe were added to each sample and standard. To avoid variability amongst samples and standards, a master mix was prepared and a multi-channel pipette was used. Another master mix containing no Alpha-KG Converting Enzyme was added to a separate set of sample wells, to serve as a background control. This control was crucial to ensure that the sample itself did not catalyse the colorimetric reaction. The plate was briefly shaken horizontally and incubated at 37 °C overnight, protected from light. The absorbance at OD_{570} was measured on a Mithras LB940 Multimode Microplate Reader by Berthold Technologies GmbH, Co. KG (Baden-Württemberg, Germany).

Calculations and Statistics

A standard calibration curve of mean absorbance values (OD_{570}) measured for different standard solutions was plotted against their corresponding α-ketoglutarate concentrations (0 – 10 nmol/well) (Supplementary Figure 4). Mean absorbance values of α-ketoglutarate standard solutions were corrected for any inherent absorbance reading of the Alpha-KG Assay Buffer containing no α-ketoglutarate. Similarly, mean absorbance values of the samples were corrected for inherent absorbance readings by means of the following controls: (i) a blank containing no sample, to ensure the absence of α-ketoglutarate in the

reagents, and (ii) a control containing no Alpha-KG Converting Enzyme, to exclude any absorbance which may be due to other enzymes present in the sample. Linear regression analysis was used to determine the amount of α-ketoglutarate (nmol) in 50 µl of sample. The concentration of α-ketoglutarate (nmol/µl) was then converted to nmol/ml. To normalise the quantity of α-ketoglutarate in the total cell extract from EG110 cells grown in YPE only, and in ASA-treated YPE in the presence and absence of L-glutamate, the amount of α-ketoglutarate was expressed in nmol/ml per turbidimetric unit of culture. Statistically significant changes in the intracellular level of α-ketoglutarate in EG110 cells subjected to different treatments were determined by multiple comparisons tests (see section 2.3.10).

3.3.7   Monitoring the growth of EG110 *S. cerevisiae* cells grown in ASA-treated ethanol medium in the absence and presence of L-aspartate

A primary culture of EG110 cells was used to inoculate 5 ml secondary cultures (see section 2.3.1) of ASA-treated YPE medium containing different amounts of L-aspartic acid monosodium salt hydrate, having the pH adjusted to 5.50 with 1 M Trizma® base (see section 2.2.4.4). All initial secondary cultures had an equal OD_{600} of 0.08 and were incubated at 28 °C with constant shaking (250 rpm). The optical density was measured using a BioPhotometer Eppendorf spectrophotometer (Hamburg, Germany) at 24-hour intervals. Growth curves of OD_{600} against time in hours were plotted to monitor the growth of yeast cells.

3.3.8   Spectrophotometric determination of the reduced and oxidised intracellular glutathione content

The cellular levels of GSH and GSSG were determined by the method of Griffith (1985). 5,5'-dithiobis-(2-nitrobenzoic acid) (DTNB) reacts non-enzymatically with GSH to yield GSSG

and 2-nitro-5-thiobenzoic acid (TNB). GSSG is then reduced enzymatically by glutathione

reductase (Glr1), in the presence of NADPH, to regenerate GSH, which reacts again. The

concentrations of DTNB, NADPH and glutathione reductase were chosen such that the rate

of the overall reaction is linearly proportional to the concentration of total glutathione,

which is indicated by the intensity of the yellow product, TNB. The formation of TNB was

followed continuously and spectrophotometrically at 412 nm.

$$2\ GSH\ +\ DTNB\ \longrightarrow\ GSSG\ +\ 2\ TNB$$
$$GSSG\ +\ NADPH\ +\ H^+\ \longrightarrow\ 2\ GSH\ +\ NADP^+$$

Glutathione reductase
(Glr1)

Combined reaction: $DTNB\ +\ NADPH\ +\ H^+\ \xrightarrow[\text{Glr1}]{\text{GSH/GSSG}}\ 2\ TNB\ +\ NADP^+$
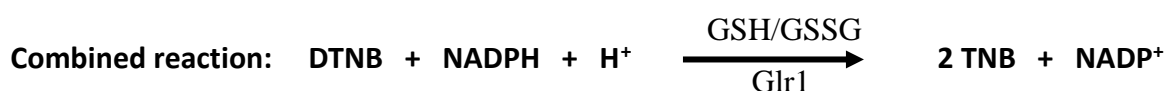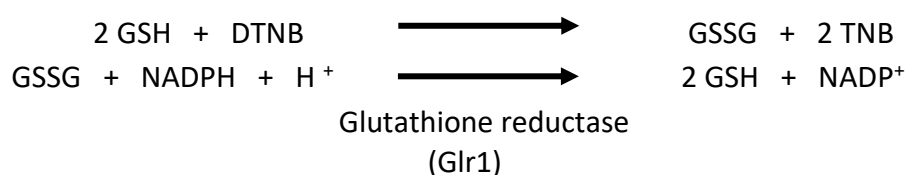
Sample preparation

The yeast strain EG110 was cultivated in 250 ml cultures of YPE medium only, and in ASA-

treated YPE medium in the presence and absence of 200 mM L-glutamate having the pH

adjusted to 5.50 with 1 M Trizma® base (see section 2.2.4.4). Cell cultures were prepared

and cultivated as described in section 2.3.1.

After the desired time of growth, 5×10^9 cells were harvested by centrifugation at 3,000 g

for 10 min at 4 °C. The cells were washed twice with 10 ml of ice-cold deionised water, and

resuspended again in 1 ml deionised water. Next, the cell suspension was divided equally

into two aliquots. One aliquot was used for the determination of GSSG and the other aliquot

was used for the determination of the total glutathione (GSH and GSSG). The cell density of

each aliquot was spectrophotometrically measured (as indicated by OD_{600}) so that the levels

of GSH and GSSG could be compared across samples and treatments. Cells from each aliquot were recovered again by centrifugation and resuspended in an equal volume of 3.5% (w/v) SSA solution (see section 3.2.5.18), which is a protein denaturant. The acidification of cellular extracts was important to inactivate γ-glutamyl transpeptidase and limit GSH degradation, as well as to reduce oxidation of GSH to GSSG and/or to mixed disulfides (Griffith 1980).

Protein-free cell lysates were prepared by transferring the cell suspensions into lysis chambers half-filled with 400-600 μm acid-washed glass beads. The samples were lysed for two rounds of 30 s each in a μ-minibeadbeater with a cooling interval of 30 s. The resultant cell lysate was recovered by two consecutive centrifugation cycles of 15,000 g for 5 min at 4 ^{o}C to remove large, insoluble cell debris followed by a long centrifugation step of 45 min at 18,000 g to further remove any remaining proteins. The protein-free cell lysates which were to be used for the measurement of the total glutathione were stored at 4 ^{o}C until assayed. The protein-free cell lysates which were to be used for the measurement of GSSG were neutralised using 50 mM Tris-HCl, pH 7.5 (see section 3.2.5.9). Subsequently, 2 μl of 2-vinylpyridine were added to 100 μl of the neutralised protein-free cell lysate. The 1 ml vial containing the cell lysate was vortexed vigorously to ensure sample homogeneity, and was left to stand for 1 hour.

Assay Procedure and Detection of the Total Glutathione Content in Protein-Free Yeast Extracts

For the spectrophotometric analysis of the total glutathione content in the cell lysates, the following assay reagents were added to a 1 ml cuvette: 690 μl phosphate-EDTA solution, pH 7.7 (see section 3.2.5.3), 10 μl ß-NADPH solution (see section 3.2.5.14), 100 μl DTNB (see

section 3.2.5.12); 193 µl deionised water together with the sample or GSH standard (see section 3.2.5.13) and 7 µl glutathione reductase (see section 3.2.2.1).

The formation of the yellow product TNB, recorded as the change in absorbance against change in time ($\Delta A/\Delta t$), was monitored at 412 nm on a Perkin-Elmer spectrophotometer at 25 $^{\circ}$C, against a reference cuvette containing deionised water. A blank assay consisting of the above components together with 3.5% (w/v) SSA (see section 3.2.5.18) instead of the sample was carried out.

The GSH calibration curve was constructed by carrying out assays with 1, 2, 3 and 4 µl of a 1.0 mM GSH standard solution (see section 3.2.5.13), corresponding to 1, 2, 3, and 4 nmol GSH. A graph of $\Delta A/\Delta t$ against GSH (nmol) was plotted (Supplementary Figure 5a), and this gave a straight line passing through 0.03 min^{-1} on the ordinate, and $\Delta A/\Delta t$ of 1.0 min^{-1} at 3 nmol GSH. If the rates were not in this range, the amount of glutathione reductase was adjusted accordingly.

Assay Procedure and Detection of the Oxidised Glutathione (GSSG) Content in Protein-free Yeast Extracts

For spectrophotometric analysis of the oxidised glutathione content in cell lysates, the same volumes of assay reagents were added to a 1 ml cuvette as indicated for the measurement of the total glutathione content except for using 35 µl glutathione reductase (see section 3.2.2.1) instead of 7 µl, also adjusting the volume of deionised water. The blank contained 3.5% (w/v) SSA together with 2-vinylpyridine, in proportions similar to the amounts present in the sample assayed.

The GSSG calibration curve was constructed by carrying out assays with 2, 4, 6, 8 and 10

μl of a 0.1 mM GSH standard solution (see section 3.2.5.13), corresponding to 0.2, 0.4, 0.6,

0.8 and 1.0 nmol GSH equivalents. When carrying out the assays of the calibration curve,

the same amounts of 3.5% (w/v) SSA and 2-vinylpyridine were added as was present in the

samples assayed. A graph of ΔA/Δt against GSH (nmol) was plotted (Supplementary Figure

5b), and this gave a straight line passing thorough 0.18 min^{-1} on the ordinate, and ΔA/Δt of

1.3 min^{-1} at 1.0 nmol GSH. The amount of glutathione reductase was adjusted accordingly to

ensure the above rates of reaction.

Calculations and Statistics

Total cellular GSH (GSH$_T$), and GSH reduced from GSSG by glutathione reductase (GSH$_{GSSG}$)

in each sample cuvette was determined from the calibration curves. Next, the concentration

of total GSH, [GSH$_T$], was calculated by multiplying the total cellular GSH in the sample

cuvette by the dilution factor (DF) i.e. the number of times the sample was diluted in the

cuvette. Thus:

$$[GSH_T] = GSH_T \ \times \ DF$$

The concentration of GSH reduced from GSSG, [GSH$_{GSSG}$], was calculated by multiplying

the GSH$_{GSSG}$ in the sample cuvette by the dilution factor (DF), also taking into account the

further dilution of 100 μl of the sample with 2 μl of 2-vinylpyridine.

$$[GSH_{GSSG}] = GSH_{GSSG} \ \times DF \ \times \ (102 / 100)$$

To correct for the fact that one molecule of GSSG gives rise to two GSH$_{GSSG}$ molecules, the

actual concentration of GSSG, [GSSG], was obtained by dividing the [GSH$_{GSSG}$] by two

(Griffith, 1985), using the following equation:

$$[GSSG] = [GSH_{GSSG}] / 2$$

The concentration of GSH, [GSH], was obtained by subtracting [GSSG] from [GSH$_T$]. Thus:

$$[GSH] = [GSH_T] - [GSSG]$$

The concentrations of GSH and GSSG were expressed as nanomoles per A$_{600}$ turbidimetric unit of culture (nmol A$_{600}$ unit^{-1}). For EG103 and EG110 cells, this is equivalent to 1 x10^7 cells per ml as stated by Longo *et al.* (1997, 1999). Statistically significant changes in the levels of GSH and/or GSSG of EG110 cells subjected to different treatments were determined using multiple comparisons tests (see section 2.3.10).

3.4 Results

3.4.1 The intracellular level of glutamate declines in aspirin-treated redox-compromised EG110 yeast cells

The aspirin-mediated downregulation of *SNO1* and *SNZ1* in EG110 yeast cells in the MnSOD-deficient EG110 yeast cells, but not in the wild-type wild-type EG103 cells (Figure 2.6 (g) and (h)), suggested that aspirin depletes the level of glutamate only in the redox-compromised cells. To confirm this hypothesis that aspirin depletes the level of glutamate in EG110 yeast cells, the intracellular level of glutamate was spectrophotometrically measured in yeast cell extracts of aspirin-treated and untreated EG110 yeast cells cultivated for 72 and 96 hours (see section 3.3.1). After 72 hours of cultivation, the level of glutamate in aspirin-treated EG110 cells was not significantly different from that of untreated cells (p = 0.561) (Figure 3.7). However, the level of glutamate in the aspirin-treated cells after 96 hours of cultivation dropped significantly by ~30% ($p \leq$ 0.0001) (Figure 3.7), unlike their aspirin-untreated counterparts. Thus, the presence of aspirin is associated with the intracellular
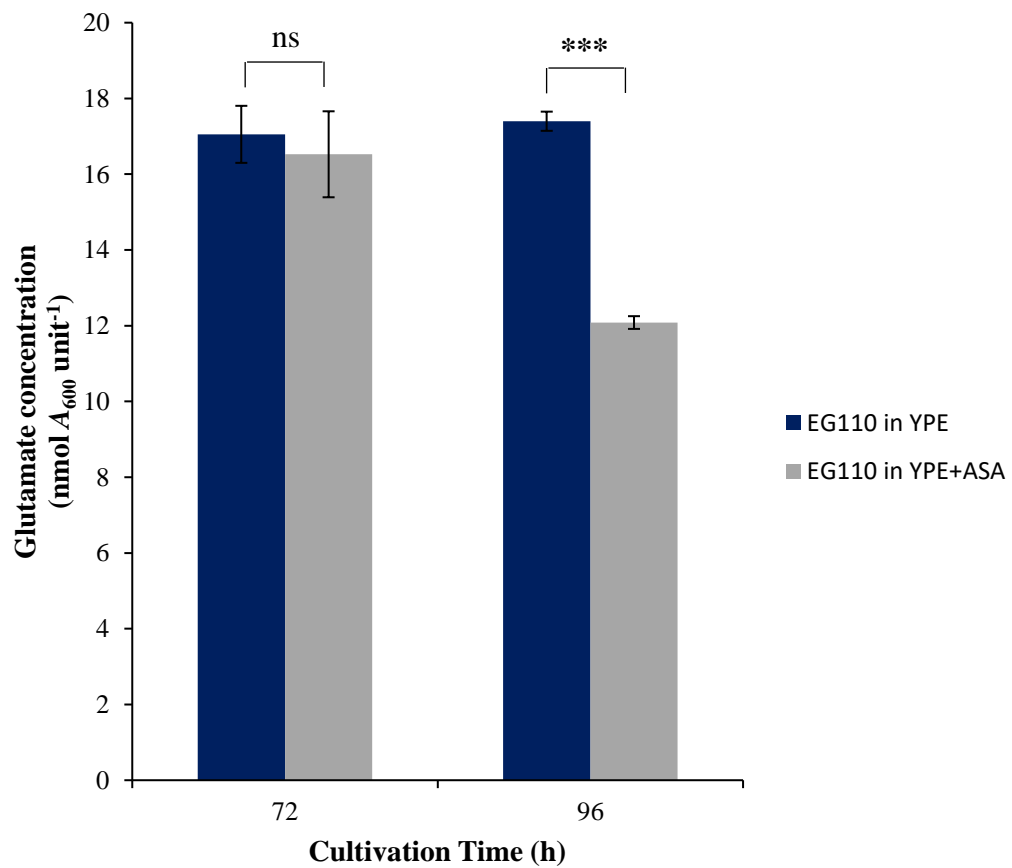
Figure 3.7 Levels of intracellular glutamate in the redox-compromised *Saccharomyces cerevisiae* EG110 cells grown for 72 and 96 hours in aspirin (ASA)-treated and untreated YPE medium. The levels of glutamate are expressed as nanomoles per A_{600} turbidimetric unit of culture, which is equivalent to 1×10^7 cells per ml. Results are the mean ± standard error of the mean (SEM), from three independent biological replicates. ns, not significant ($p > 0.05$); ***, highly significant ($p \leq 0.001$); unpaired *t*-test, 2-tailed. YPE, ethanol-based.

depletion of glutamate in the redox-compromised EG110 cells and this result may be a consequence of the aspirin-induced downregulation of the genes *SNO1* and *SNZ1* in these cells, which together catalyse the conversion of glutamine into glutamate.

3.4.2 L-glutamate restores the growth of aspirin-treated redox-compromised EG110 yeast cells

Considering the critical roles of glutamate in maintaining mitochondrial function, together with previous observations that aspirin-induced cell death of MnSOD-deficient EG110 yeast cells is preceded by a decline in respiratory rate (Sapienza *et al.* 2008) and lowered GSH/GSSG ratio (Sapienza, Balzan 2005), aspirin-treated EG110 yeast cell cultures grown in ethanol medium were supplemented with fixed doses of L-glutamate in an attempt to rescue them from cell death (see section 3.3.2). L-glutamate was supplemented in various concentrations, ranging from 10 to 250 mM, to EG110 yeast cells growing in aspirin-treated YPE medium, to determine whether the addition of L-glutamate rescues these cells. OD_{600} measurements were taken of all L-glutamate-treated and untreated cultures growing in aspirin-treated YPE medium, to monitor the growth of yeast cells over time (Figure 3.8).

The beneficial effect of supplementing 100 mM L-glutamate to aspirin-treated EG110 yeast cells appeared after 48 hours of growth, whereas that of 200 mM L-glutamate was evident after 96 hours. Nevertheless, growth of the 200 mM L-glutamate-treated yeast cells remained well-maintained up to 216 hours, at which point the 100 mM L-glutamate-treated cells showed a much greater decline in growth (Figure 3.8). When the concentration of L-glutamate was further increased to 250 mM, the growth of the aspirin- treated EG110 yeast cells was not ameliorated to the same extent as when 200 mM L-glutamate was added.
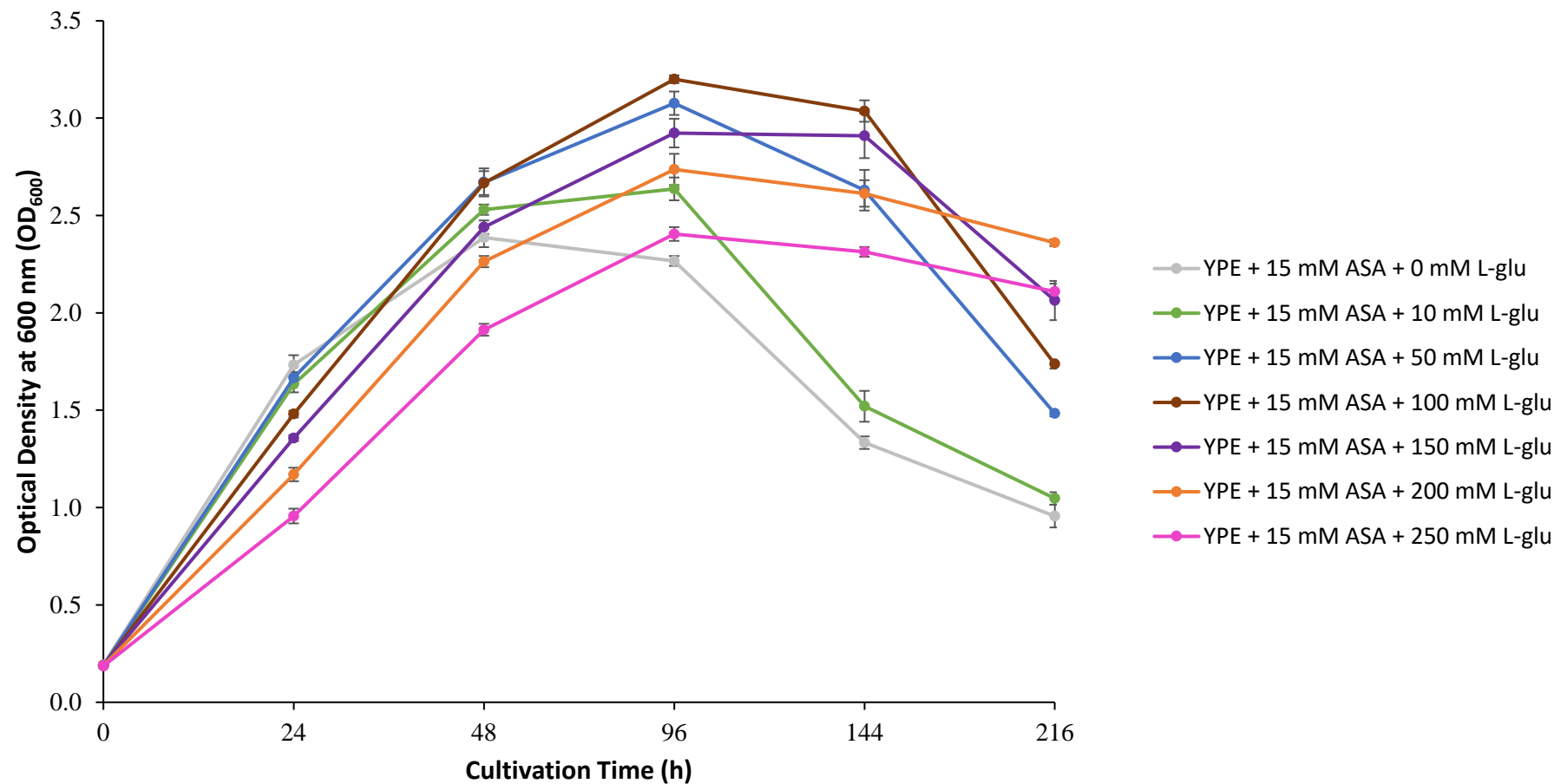
Figure 3.8 Exogenous L-glutamate counteracts the aspirin (ASA)-induced decline in cellular growth of MnSOD-deficient *Saccharomyces cerevisiae* EG110 cells cultivated in YPE medium. The optical density at 600 nm (OD_{600}) of EG110 yeast cells grown in ASA-treated YPE medium, in the presence of different concentrations of L-glutamate (L-glu), was plotted against the cultivation time in hours. Each data point represents the mean of at least three independent biological replicates and error bars represent the standard deviation (SD) from the mean. EG110 yeast cell cultures treated with ASA alone started to decline in growth after 48 hours. At 96 hours, the addition of 100 mM L-glu resulted in the highest OD_{600} measurement recorded across all timepoints. The eventual decline of cell growth was mostly delayed at a glutamate concentration of 200 mM. YPE, ethanol-based.

3.4.3 L-glutamate restores the viability of aspirin-treated redox-compromised EG110 yeast cells

Since OD_{600} measurements are simply an indication of cell density based on turbidity, a viability assay based on colony forming units (CFUs) grown on YEPD plates was carried out to clearly verify whether glutamate actually rescues aspirin-treated EG110 cells (see section 3.3.3). Results showed that the addition of exogenous L-glutamate to aspirin-treated EG110 yeast cells grown in YPE medium considerably improved the yeast cell viability (Figure 3.9). In fact, EG110 yeast cells which were grown in aspirin-treated YPE medium died after 96 hours (p = 0.002), but yeast cell viability was signficantly improved in the presence of 100 mM ($p = 0.005$) and 200 mM ($p \leq 0.0001$) L-glutamate. At most time points assayed, the addition of 200 mM L-glutamate to aspirin-treated EG110 yeast cells maintained the viability of these cells to a greater extent than the viability of the aspirin-untreated EG110 cells grown in YPE medium only (Figure 3.9).

3.4.4 L-glutamate rescues aspirin-treated EG110 yeast cells from apoptosis as determined by annexin V-FITC and PI staining

To determine the mode of cell death from which L-glutamate rescues aspirin-treated cells, EG110 yeast cells grown in YPE medium only, and in aspirin-treated YPE medium in the absence and presence of 200 mM L-glutamate were stained with annexin V-FITC and PI simultaneously (see section 3.3.4). The results displayed in Figure 3.10 show that at 96 hours of growth the majority of EG110 yeast cells grown in YPE medium only were still viable since they did not acquire either of the stains. In fact, 76.7% of these cells are shown in the lower left quadrant (Figure 3.10 (a)). However, as previously shown in Figure 3.9, the addition of 15 mM aspirin caused these redox-compromised cells to die. This result is further confirmed by the significant aspirin-induced 10-fold decrease of viable cells, as observed in
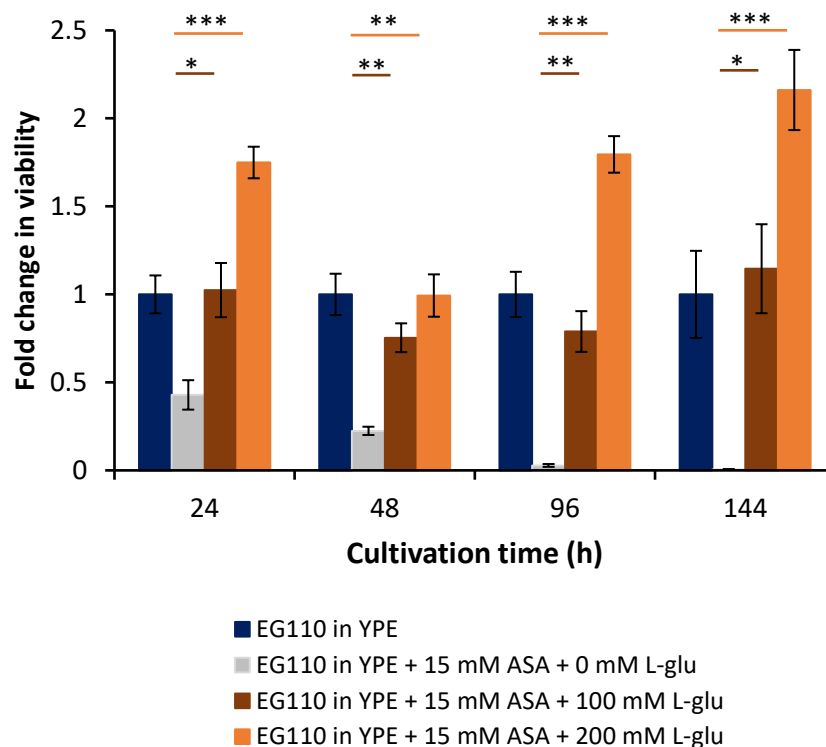
Figure 3.9 L-glutamate restores the cell viability of aspirin-treated EG110 cells. CFU counts on YEPD plates were used to determine fold change in cell viability of the redox-compromised, MnSOD-deficient EG110 yeast cells grown in ASA-treated YPE medium, in the absence and presence of 100 mM or 200 mM L-glu when compared to untreated EG110 yeast cells grown in YPE medium. Vertical bars represent the mean of six independent biological replicates and statistical significance is shown when compared to aspirin-treated EG110 cells. Error bars represent the SEM. Error bars represent the SEM. **, moderately significant ($p \leq 0.01$); ***, highly significant ($p \leq 0.001$) (Welch's ANOVA with Games-Howell post-hoc tests). ASA, aspirin; CFU, colony-forming unit; L-glu, L-glutamate, MnSOD, manganese superoxide dismutase; PI, propidium iodide; SEM, standard error of the mean; YEPD, yeast extract peptone dextrose; YPE, ethanol-based.

the lower left quadrant of Figure 3.10 (b) ($p \leq 0.0001$, Kruskal-Wallis with Bonferroni

correction for multiple comparisons). In the presence of aspirin, EG110 cells are seen to

migrate towards (i) the lower right quadrant indicating cell death by apoptosis (16.1%) and

(ii) upper right quadrant, indicating secondary necrosis (74.7%) which follows apoptosis.

However, the addition of 200 mM L-glutamate to aspirin-treated EG110 cells maintained

their viability such that the percentage of cells recorded in the lower left quadrant (68%) is

not significantly different than that of EG110 cells grown only in YPE medium (p = 0.437,

Kruskal-Wallis with Bonferroni correction for multiple comparisons) (Figure 3.10 (c)).

3.4.5 L-glutamate restores the cell cycle distribution of the redox-compromised MnSOD-deficient EG110 yeast cells treated with aspirin

The aspirin-mediated decrease in cell viability of EG110 yeast cells (Figure 3.9) could likely

be due to an aspirin-induced arrest of cell cycle progression. To investigate whether this

was the case, cell cycle analysis was carried out by flow-cytometry using PI-stained EG110

yeast cells (see section 3.3.5), that were previously cultivated in the presence and absence

of aspirin for 168 hours (see section 2.3.1). The results show that aspirin-treated EG110

cells accumulate in the sub-G0/G1 phase of the cell cycle (35.4%) ($p = 0.012$), which is

indicative of apoptosis, and the G0/G1 phase of the cell cycle (39.0%) (p = 0.007), at the

expense of the G2/M phase (14.7%) ($p = 0.003$), when compared to the aspirin-untreated

EG110 cells (Figure 3.11).

 Flow-cytometric cell cycle analysis was also carried out on ASA-treated EG110 yeast cells,

cultivated for 168 hours in YPE medium supplemented with 200 mM L-glutamate. In

agreement with previous results showing the rescuing effect of L-glutamate, ASA-treated
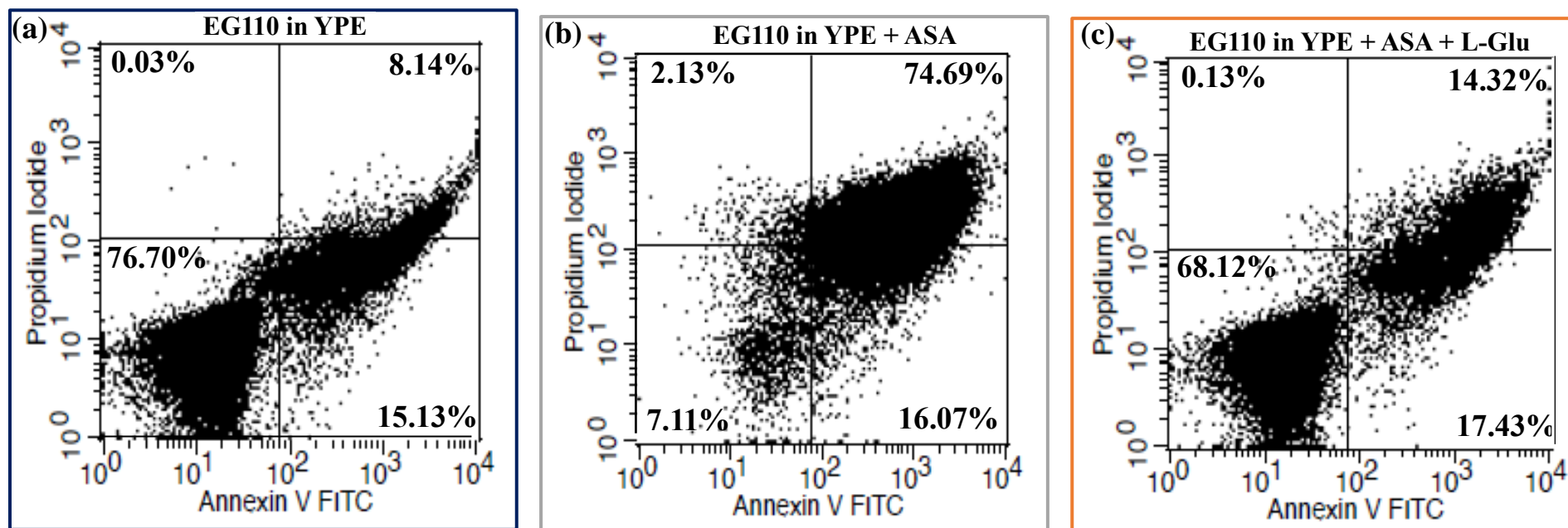
Figure 3.10 **The rescuing effect of glutamate from apoptosis in aspirin (ASA)-treated EG110 cells confirmed by flow-cytometric measurements at 96 hours of growth**. Double-staining with annexin V-FITC and propidium iodide (PI) of ASA-treated EG110 cells, supplemented with 200 mM L-glutamate (L-glu), shows that the addition of L-glu to ASA-treated EG110 yeast cells rescues these cells from apoptosis. The majority of EG110 yeast cells grown in YPE medium only, are still viable since they lie in the lower left quadrant as shown in (a). The lower left quadrant of ASA-treated cells (b) is depleted of cells since these migrate towards the lower and upper right quadrants indicating that these cells die by apoptosis and subsequently undergo secondary necrosis. The addition of 200 mM L-glu restores the viability of ASA-treated EG110 cells, as shown in the lower left quadrant in (c), similar to untreated EG110 cells shown in (a). Representative dot plots show the mean percentage of cells from nine independent biological replicates in each quadrant. YPE, ethanol-based.

Quadrants: lower left, viable cells; lower right, apoptotic cells; upper right, secondary necrotic cells. 30 000 cells were analysed for each sample.
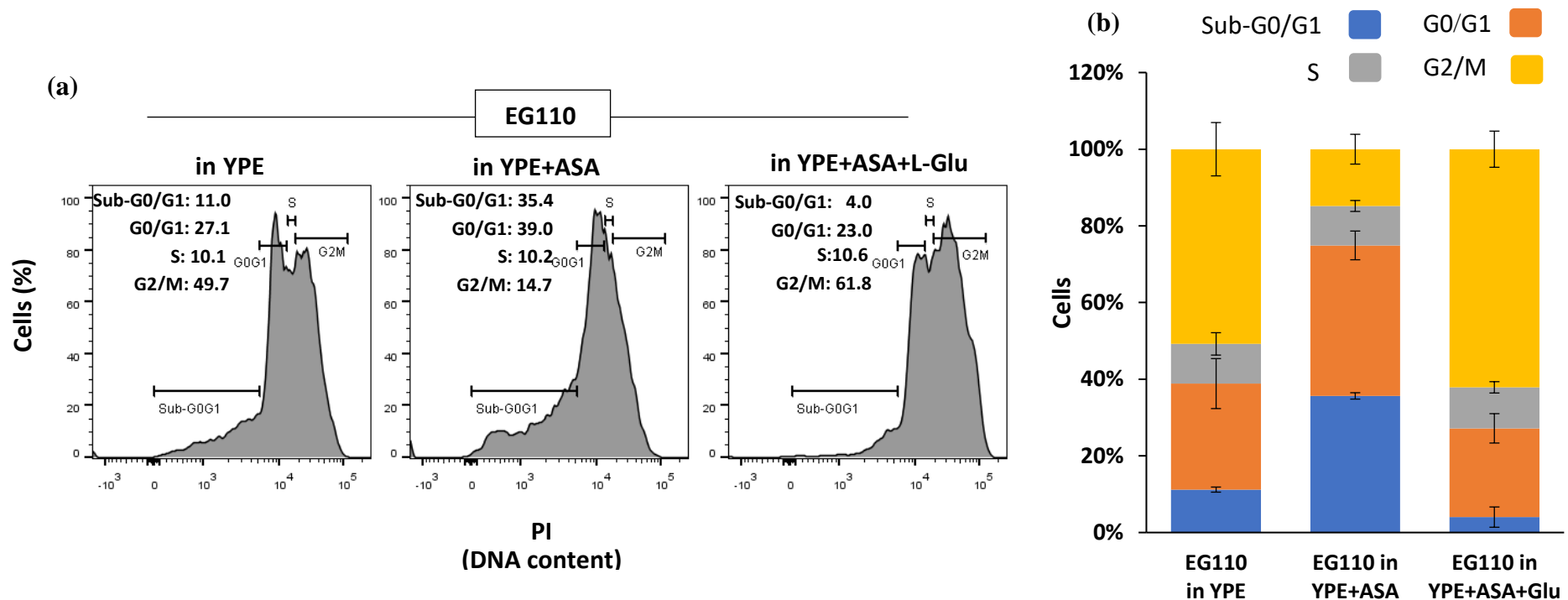
Figure 3.11 L-glutamate (L-glu) restores the cell cycle distribution of the redox-compromised MnSOD-deficient EG110 yeast cells treated with aspirin (ASA). (a) The figure shows representative fluorescence histograms of asynchronous EG110 cells grown for 168 hours in YPE medium (control) and in ASA-treated YPE medium in the absence and presence of 200 mM L-glutamate. The fluorescence signal given off by propidium iodide (PI), which is a measure of DNA content, is shown along the *x*-axis and was analysed using the FL2 detector at a voltage of 700 V on a FACS Aria III and using FlowJo v10.0.7 software (Becton Dickinson). Horizontal bars indicate the peak boundaries, and values represent the mean percentage of cells in different phases of the cell cycle. At least 30 000 counts were measured. (b) Stacked bar graphs show the mean percentage of EG110 yeast cells in each cell cycle phase at 168 hours of cultivation, treated as described in (a). Aspirin-treated EG110 cells accumulate in the sub-G0/G1 ($p \leq 0.0001$) and the G0/G1 ($p = 0.015$) phases, at the expense of the G2/M phase ($p \leq 0.0001$), when compared to their aspirin-untreated counterparts. However, the addition of 200 mM L-glutamate to ASA-treated EG110 cells restores their cell cycle distribution such that the percentage of cells in each phase is similar to that of untreated control cells ($p > 0.05$ for all cell cycle phases) (Welch's ANOVA with Games-Howell post-hoc tests). Error bars represent the standard error of the mean (SEM) of four independent determinations. YPE, ethanol-based, MnSOD, manganese superoxide dismutase.

145

EG110 cells in the presence of L-glutamate had the cell cycle distribution restored to that of untreated control cells growing only in YPE medium ($p > 0.05$) (Figure 3.11).

These results were further compared with the cell cycle distribution of the wild-type strain EG103, grown in aspirin-treated and untreated ethanol medium. Previous results have shown that unlike EG110, aspirin-treated EG103 cells grow similarly to ASA-untreated EG103 cells cultivated in YPE medium (Balzan *et al.* 2004). The flow-cytometric results displayed in Figure 3.12 show that ASA-treated EG103 cells stained with PI do not exhibit an increase in the sub-G0/G1 peak at 168 hours (0.7%), unlike ASA-treated EG110 cells (35.4%) (Figure 3.11). Aspirin-treated EG103 cells, when compared to their aspirin-untreated counterparts, are temporarily arrested at the G2/M checkpoint (62.8%) ($p \leq 0.0001$), mainly at the expense of the G0/G1 fraction (24.1%) ($p = 0.001$) (Figure 3.12). The percentages of ASA-treated EG103 cells in the G2/M and G0/G1 cell cycle phases are not statistically different than those of ASA-treated EG110 cells in the presence of L-glutamate ($p > 0.05$, unpaired *t*-test, 2-tailed) (Figure 3.11).

3.4.6 L-glutamate increases the level of the TCA cycle intermediate α-ketoglutarate in aspirin-treated redox-compromised EG110 yeast cells

In order to determine how glutamate supplementation rescues aspirin-treated EG110 yeast cells, the levels of α-ketoglutarate were measured in aspirin-treated EG110 yeast cells in the absence and presence of 200 mM L-glutamate, as well as in aspirin-untreated EG110 cells (see section 3.3.6). This is because L-glutamate is a direct precursor of the TCA cycle intermediate α-ketoglutarate, which is used to anaplerotically fuel the TCA cycle (Miller, Magasanik 1990).
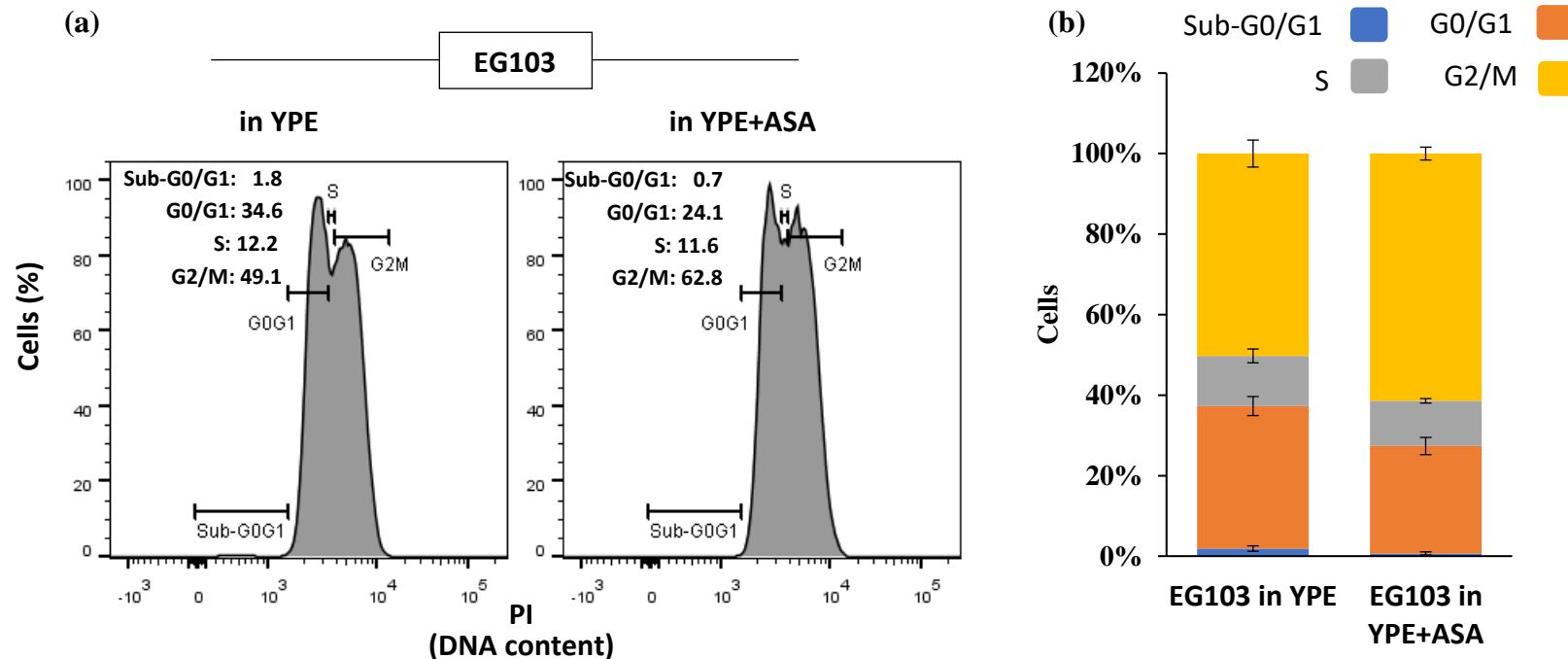
Figure 3.12 The effect of aspirin (ASA) on the cell cycle distribution of the wild-type EG103 yeast cells. (a) The figure shows representative fluorescence histograms of asynchronous EG103 cells grown for 168 hours in ASA-treated and untreated YPE medium. The fluorescence signal given off by propidium iodide (PI), which is a measure of DNA content, is shown along the x-axis and was analysed using the FL2 detector at a voltage of 700 V on a FACS Aria III (Becton Dickinson) and using FlowJo v.10 software (Becton Dickinson). Horizontal bars indicate the peak boundaries, and values represent the mean percentage of cells in different phases of the cell cycle. At least 30 000 counts were measured. (b) Stacked bar graphs show the mean percentage of EG103 yeast cells in each cell cycle phase at 168 hours of cultivation, when treated as described in (a). ASA-treated EG103 cells accumulate in the G2/M ($p \leq 0.0001$) phase at the expense of the G0/G1 phase ($p = 0.001$), when compared to their ASA-untreated counterparts (unpaired t-test, 2-tailed). Error bars represent the standard error from the mean (SEM) of four independent determinations. YPE, ethanol-based.

147

Figure 3.13 shows that at 96 hours of cultivation, the level of α-ketoglutarate in aspirin-treated EG110 yeast cells significantly declines by a factor of two ($p \leq 0.0001$). On the other hand, the addition of 200 mM L-glutamate restored the level of α-ketoglutarate to a level which is not significantly different from that of EG110 yeast cells grown only in YPE medium ($p > 0.05$) (Figure 3.13).

3.4.7 L-aspartate does not rescue aspirin-treated MnSOD-deficient EG110 yeast cells to the same extent as L-glutamate

The conversion of glutamate into α-ketoglutarate may be brought about by the transaminase Aat1 which produces aspartate as a by-product (see section 3.1.2 and Figure 3.1). To investigate the possible involvement of L-aspartate in the glutamate-mediated rescue of aspirin-treated EG110 yeast cells from apoptosis (Figure 3.9), the growth of these cells in the presence of different doses of L-aspartate was monitored by OD_{600} measurements (see section 3.3.7).

Growth curves displayed in Figure 3.14 indicate that that the addition of L-aspartate did not restore the growth of aspirin-treated EG110 cells to the same extent as L-glutamate. In fact, OD_{600} measurements taken at 96 hours indicate that the addition of 100 mM L-glutamate increased the growth of aspirin-treated EG110 cells in YPE medium 18% more than 100 mM L-aspartate at the same time point. Similarly, at 96 hours of growth, the supplementation of 200 mM L-glutamate increased the growth of these cells by 22% more than the supplementation of 200 mM L-aspartate. Furthermore, at 216 hours of cultivation, the addition of 100 mM and 200 mM L-glutamate to aspirin-treated EG110 yeast cells increased their growth by ~37% more than when the same doses of L-aspartate were supplemented ($p \leq 0.0001$, Welch's ANOVA with Games-Howell post-hoc tests).
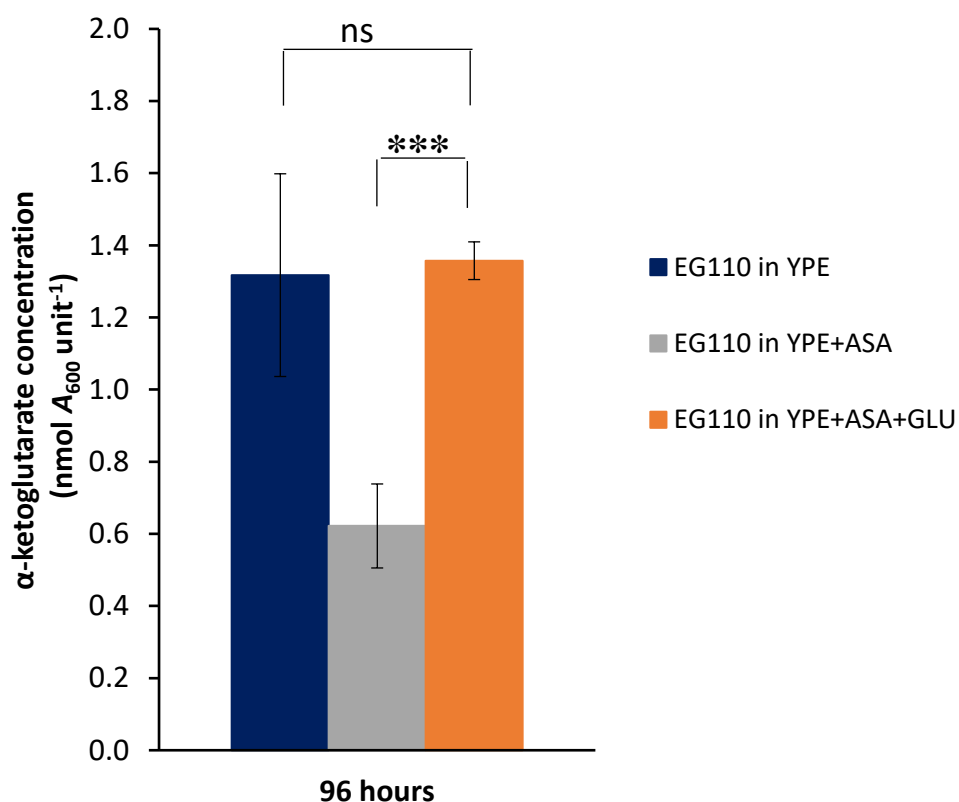
Figure 3.13 L-glutamate increases the level of α-ketoglutarate in aspirin (ASA)-treated EG110 yeast cells. EG110 yeast cells were grown for 96 hours in YPE medium, and in ASA-treated YPE medium in the absence and presence of 200 mM L-glutamate. The levels of α-ketoglutarate are expressed as nanomoles per A_{600} turbidimetric unit of culture, which is equivalent to 1×10^7 cells per ml. Results are the mean ± standard error of the mean (SEM), from three independent biological replicates. ns, not significant ($p > 0.05$); ***, highly significant ($p \leq 0.0001$) (One-way ANOVA with Bonferroni post-hoc tests). YPE, ethanol-based.
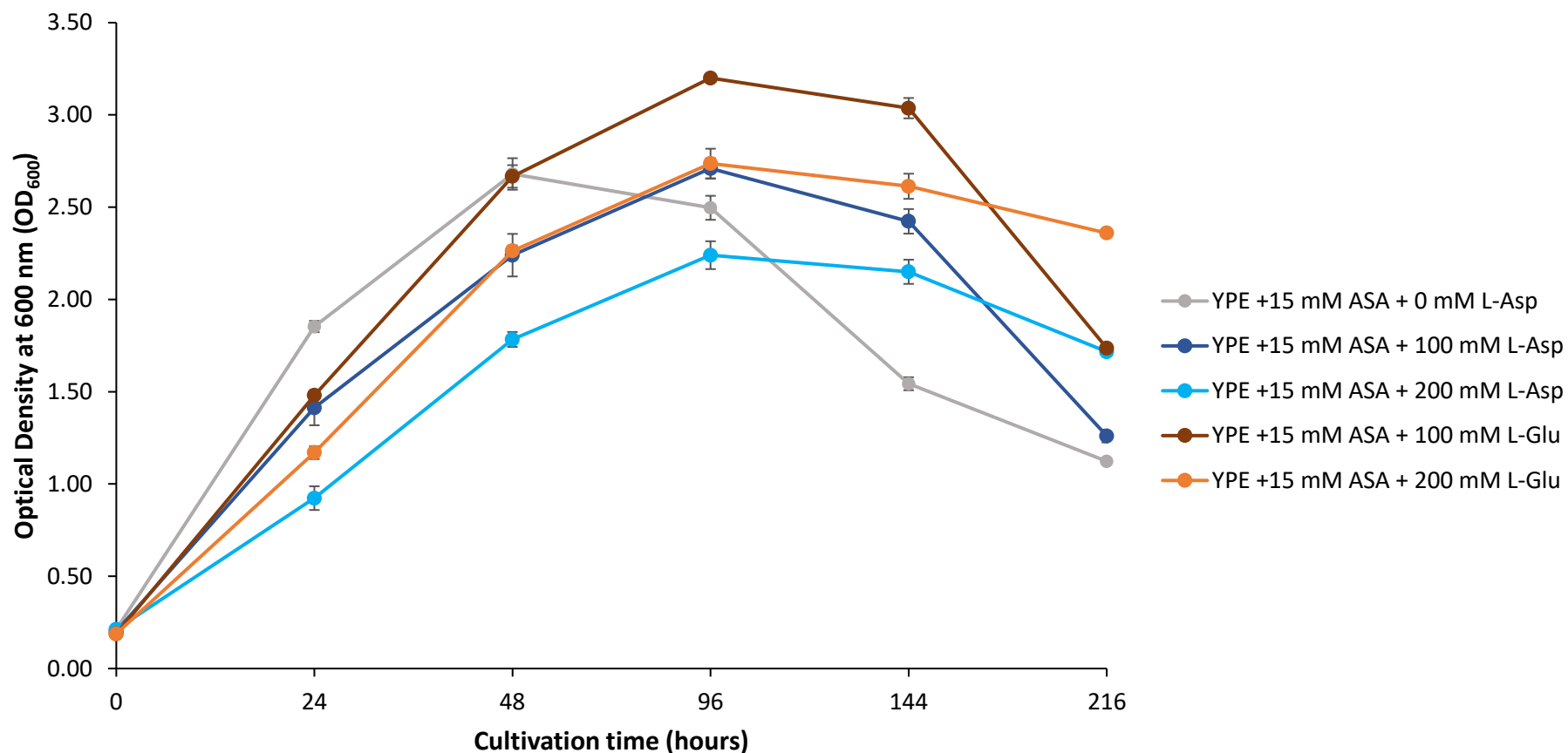
Figure 3.14   Exogenous L-aspartate (L-Asp) does not ameliorate cell growth of aspirin (ASA)-treated EG110 cells to the same extent as L-glutamate (L-Glu). The optical density at 600 nm (OD_{600}) of EG110 yeast cells grown in ASA-treated YPE medium, in the presence of 100 mM and 200 mM L-asp, was plotted against the cultivation time in hours. Each data point represents the mean of at least three independent biological replicates and error bars represent the standard deviation (SD) from the mean. Growth curves of aspirin-treated EG110 yeast cells supplemented with 100 mM and 200 mM L-glutamate are also plotted for comparison. YPE, ethanol-based.

These results confirm that L-glutamate ameliorates the growth of EG110 yeast cells grown in ethanol medium to a much greater extent than L-aspartate.

3.4.8   L-glutamate restores the redox balance of aspirin-treated MnSOD-deficient yeast cells by increasing the level of reduced GSH

Since glutamate is also a direct precursor of the major cellular antioxidant GSH, the levels of reduced and oxidised glutathione in MnSOD-deficient EG110 yeast cells grown in YPE medium, and in aspirin-treated YPE medium in the absence and presence of 200 mM L-glutamate, were determined (see section 3.3.8). This was important to determine whether glutamate supplementation restored the cellular redox balance in aspirin-treated cells, by calculating the GSH/GSSG concentration ratio.

As shown in Table 3.1, EG110 cells cultivated in aspirin-treated YPE medium showed a steady decline in GSH level over time. At 48 hours of cultivation, the GSH level was 2.15 nmol A_{600} unit^{-1}, which decreased by ~15% after 72 hours, and by ~56% after 96 hours. However, when these cells were treated with 200 mM L-glutamate, the GSH level increased over time. GSH measured at 48 hours of cultivation was 2.11 nmol A_{600} unit^{-1} and increased by ~40% after 72 hours, and by ~79% after 96 hours, similar to what was observed for control cells in the absence of any treatment (Table 3.1). The GSSG level in aspirin-treated EG110 cells increased over time, unlike the generally consistent GSSG level in the presence of glutamate.

Taking these results into consideration, the GSH/GSSG ratios of aspirin-treated EG110 cells in the absence and presence of L-glutamate, were relatively similar at 48 hours of cultivation ($p = 0.639$), but not at 72 ($p = 0.036$) and 96 hours ($p = 0.003$) of cultivation.

Table 3.1: Levels of GSH and GSSG in the MnSOD-deficient *Saccharomyces cerevisiae* EG110 cells grown in YPE medium, and in aspirin-treated YPE medium in the absence and presence of 200 mM L-glutamate.

	Cultivation time (h)	Control[a] (nmol A_{600} unit^{-1})	Aspirin-treated[b] (nmol A_{600} unit^{-1})	Aspirin-treated + L-glutamate[c] (nmol A_{600} unit^{-1})[d]
GSH	48	1.81 ± 0.11*	2.15 ± 0.24^{ns}	2.11 ± 0.07
	72	2.31 ± 0.27*	1.82 ± 0.10***	2.95 ± 0.05
	96	2.57 ± 0.18**	0.95 ± 0.09***	3.77 ± 0.06
GSSG	48	0.27 ± 0.03**	0.40 ± 0.09^{ns}	0.42 ± 0.04
	72	0.36 ± 0.05^{ns}	0.54 ± 0.08^{ns}	0.43 ± 0.12
	96	0.23 ± 0.02**	0.83 ± 0.08**	0.35 ± 0.02
GSH/GSSG	48	6.87 ± 0.68*	5.58 ± 1.19^{ns}	5.01 ± 0.59
	72	6.84 ± 0.75^{ns}	3.42 ± 0.41*	7.27 ± 1.70
	96	11.07 ± 1.34^{ns}	1.13 ± 0.10**	10.79 ± 0.71

[a] Cells were cultivated in rich medium containing the non-fermentable carbon source ethanol (YPE) at 28 °C, 250 rpm.

[b] The concentration of aspirin added to YPE medium was 15 mM. The pH was adjusted to 5.50 with 1 M Trizma® base.

[c] The concentration of L-glutamate added to aspirin-treated YPE medium was 200 mM. The pH was already 5.50.

[d] The levels of GSH and GSSG were determined as described in section 3.3.8 and are expressed as nmol per A_{600} turbidimetric unit of culture, which is equivalent to 1×10^7 cells ml^{-1}. Values are the mean of at least three independent determinations ± standard deviation (SD).

ns, not significant ($p > 0.05$); * slightly significant ($p \leq 0.05$); **, moderately significant ($p \leq 0.01$); ***, highly significant ($p \leq 0.001$); comparison with GSH and GSSG levels in aspirin-treated EG110 cells in the presence of L-glutamate (Welch's ANOVA with Games-Howell post-hoc tests).

In fact, the presence of L-glutamate restored the GSH/GSSG ratio of aspirin-treated cells at 72 and 96 hours of cultivation to that of aspirin-untreated control cells grown in YPE medium only (p = 0.692 and p = 0.945, respectively) (Table 3.1).

3.5 Conclusion

The aspirin-induced downregulation of the genes *SNO1* and *SNZ1* in EG110 yeast cells grown for 48 hours in ethanol medium (Figure 2.6 (g) and (h)), suggested that the conversion of glutamine into glutamate may be compromised when these cells are treated with aspirin. This study confirmed that aspirin indeed lowers the intracellular level of glutamate in redox-compromised yeast cells at 96 hours of cultivation (Figure 3.7) and could potentially explain why aspirin compromises the growth of these cells. In fact, the supplementation of L-glutamate considerably improved the growth of aspirin-treated EG110 cells in a dose-dependent manner (Figure 3.8). Supplementation of 200 mM L-glutamate to aspirin-treated EG110 cells was observed to (i) sustain their growth, at least until 216 hours of cultivation (Figure 3.8) and (ii) consistently improve their viability (Figure 3.9).

The observed loss of viability of aspirin-treated EG110 yeast cells is due to the onset of apoptosis in these cells, as determined by annexin V-FITC/PI staining (Figure 3.10 (b)). These findings were corroborated by the accumulation of the aspirin-treated EG110 yeast cells (i) in the sub-G0/G1 phase, indicative of DNA fragmentation, and (ii) in the G0/G1 phase of the cell cycle, at 168 hours of growth (Figure 3.11). The addition of 200 mM L-glutamate to aspirin-treated EG110 cells circumvented the onset of aspirin-induced apoptosis in these cells (Figure 3.10 (c)), and this result was corroborated by the absence of a prominent sub-G0/G1 peak confirming the lack of DNA fragmentation in these cells (Figure 3.11). Thus,

these findings further suggest that glutamate depletion is a critical event in aspirin-induced apoptosis of the redox-compromised EG110 cells.

Furthermore, results showed that at 96 hours of cultivation, aspirin-treated EG110 yeast cells contained lower levels of glutamate's immediate metabolic products, namely α-ketoglutarate (Figure 3.13) and GSH (Table 3.1), both of which were increased when exogenous L-glutamate was added (Figure 3.13, Table 3.1). Also, the addition of 200 mM L-glutamate restored the significantly lowered intracellular redox balance in aspirin-treated EG110 yeast cells, as determined by the GSH/GSSG ratio (Table 3.1). These results confirm that the depletion of glutamate in aspirin-treated EG110 yeast cells compromises their ability to maintain redox homeostasis and to refuel the mitochondrial TCA cycle, both of which contribute to their demise.

CHAPTER FOUR

GENERAL DISCUSSION

This study involved the identification of novel targets of aspirin, to delineate mechanisms by which aspirin mediates apoptotic cell death in redox-compromised *S. cerevisiae* cells but not in healthy yeast cells. Aspirin-induced gene expression data published by Farrugia *et al.* (2019) revealed significant changes in the expression of a number of genes which are associated with oxidative stress or the cell cycle in the redox-compromised *S. cerevisiae* EG110 cells, but not in the wild-type EG103 yeast cells. Results in this present study showed no aspirin-induced changes in the expression of any of the target genes in EG103 yeast cells cultivated for 48 hours (Figure 2.6), corroborating previous work which showed that in the presence of aspirin, these cells grow equally well relative to their aspirin-untreated counterparts (Balzan *et al.* 2004). On the other hand, of all the target gene expression data validated by qRT-PCR in Chapter 2, the expressions of the ROS-related genes *SNO1* and *SNZ1* were the most significantly downregulated by aspirin in EG110 yeast cells at 48 hours of cultivation (Figure 2.6 (g) and (h)). Thus, to better understand why aspirin targets these two genes in EG110, but not in EG103 yeast cells, it was necessary to explore the resultant aspirin-mediated impact of this downregulation on the metabolism of EG110 cells.

SNO1 and *SNZ1* encode proteins which are induced in response to nutrient depletion and oxidative stress (Padilla *et al.* 1998). Sno1 and Snz1 interact to form a glutamine amidotransferase complex which exhibits glutaminase activity (Dong *et al.* 2004). Glutaminases mediate the deamination of glutamine to form glutamate, which plays a central role in cell metabolism and function (Newsholme *et al.* 2003), and is critical for ROS mitigation and cell proliferation in redox-compromised and transformed cells (Gao *et al.* 2009, Gross *et al.* 2014, Wang *et al.* 2010a).

The aspirin-mediated downregulations of *SNO1* and *SNZ1* validated by this study (Figure 2.6 (g) and (h)), suggest that glutamate becomes depleted in aspirin-treated EG110 yeast cells (Figure 4.1). This hypothesis was confirmed by measuring the intracellular level of glutamate in aspirin-treated and untreated EG110 yeast cells (see section 3.3.1). Results showed that at 72 hours of cultivation, the intracellular level of glutamate in aspirin-treated EG110 cells starts to decline and progressively becomes significantly lower at 96 hours of cultivation (Figure 3.7). Since glutamate depletion has been linked to increased susceptibility to oxidative stress-induced apoptosis in yeast cells (Lee *et al.* 2012), and to growth suppression of various human cancer cells (Gao *et al.* 2009, Gross *et al.* 2014; Petronini *et al.* 1996, Wang *et al.* 2010a), it is likely that the depletion of intracellular glutamate in aspirin-treated EG110 yeast cells described in this study (Figure 3.7), contributes to their growth suppression and eventual apoptotic cell death. This is further supported by the fact that their aspirin-untreated counterparts, which maintained constant levels of intracellular glutamate (Figure 3.7), do not undergo the same fate and survive.

This study showed that the intracellular concentration of glutamate in aspirin-treated EG110 yeast cells grown for 96 hours (Figure 3.7), declined to a level which was insufficient to maintain cell growth (Figure 3.8) and viability (Figure 3.9) beyond this point. The addition of 100 mM and 200 mM L-glutamate substantially improved the growth of these cells, as determined by the growth curves (Figure 3.8), and significantly ameliorated the viability of aspirin-treated EG110 cells in a dose-dependent manner, as determined by CFU counts (Figure 3.9). These results are in line with the findings described by Wu *et al.* (2013) whereby they reported that glutamic acid caused wild-type yeast chronological
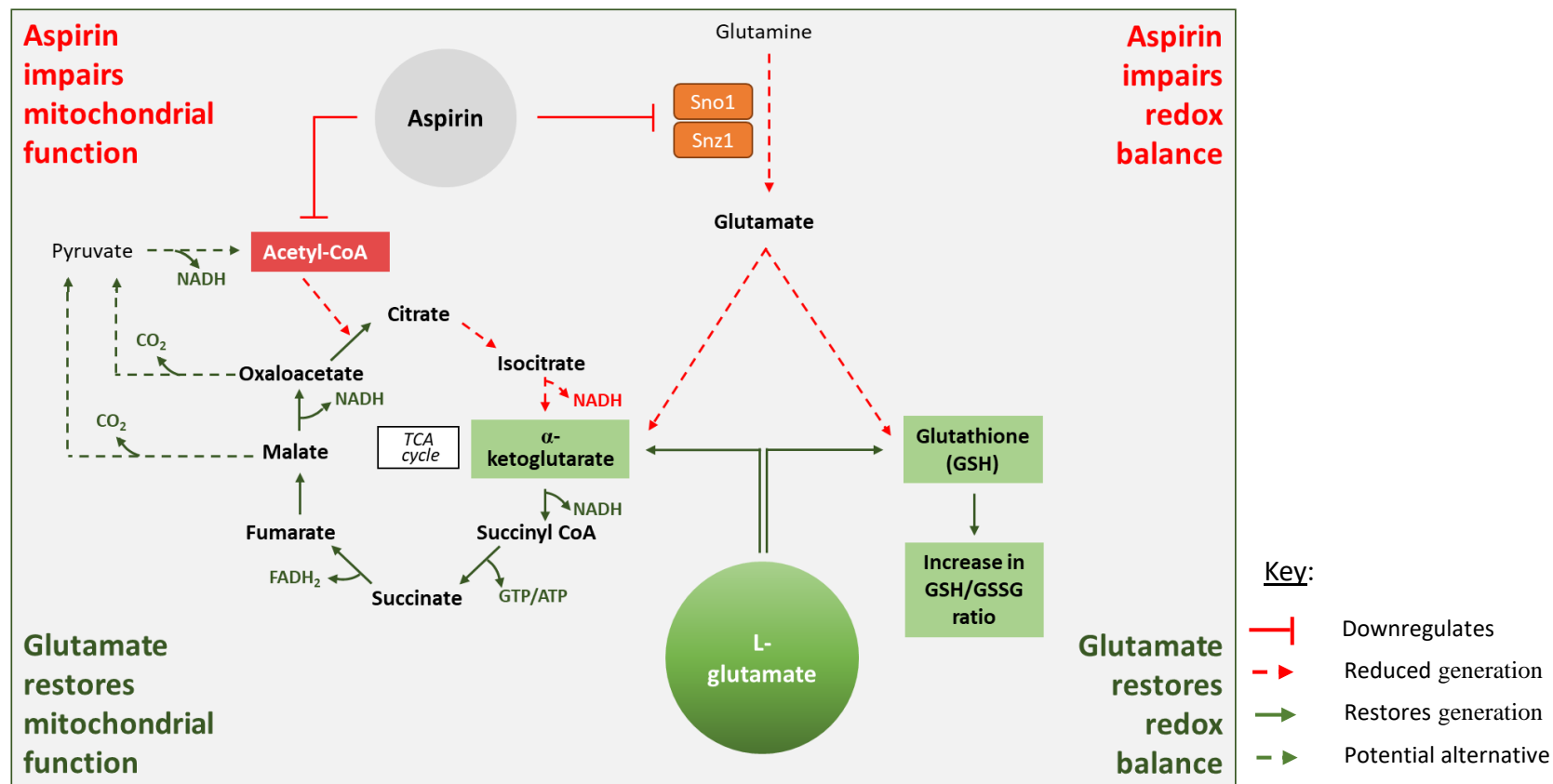
Figure 4.1 Aspirin-induced apoptosis in redox-compromised yeast cells may be brought about by glutamate depletion and is circumvented by the addition of L-glutamate. Aspirin downregulates the genes encoding Sno1 and Snz1 in redox-compromised yeast cells, impairing their ability to synthesise glutamate from glutamine, and glutamate's immediate metabolic products α-ketoglutarate and glutathione (GSH) in these cells. Aspirin downregulates the synthesis and transport of acetyl-CoA into the mitochondria (Farrugia *et al.* 2019). The resulting impaired mitochondrial function and lack of redox balance causes these cells to die by apoptosis. However, exogenous L-glutamate rescues aspirin-treated redox-compromised yeast cells from apoptosis by restoring mitochondrial function and redox balance through restored levels of α-ketoglutarate and GSH, respectively. The dotted green line represents two possible glutamate-dependent pathways to synthesize acetyl-CoA in the mitochondria *via* the decarboxylation of malate and oxaloacetate to pyruvate, which is converted to acetyl-CoA (as observed in SFxL glioma cells grown in glucose-deprived conditions in Yang *et al.* 2014). ATP, adenosine triphosphate, CoA, coenzyme A; FADH$_2$, reduced flavin adenine dinucleotide; GSH, glutathione, GSSG, oxidised glutathione; GTP, guanine triphosphate; L-glu, L-glutamate; NADH, reduced nicotinamide adenine dinucleotide; TCA, tricarboxylic acid.

158

lifespan extension in a dose-response manner and protected a *sod2*-null strain from cell death during chronological aging, especially when grown coupled with methionine and glucose restriction. Moreover, the addition of glutamate to mutant yeast cells unable to synthesise glutamate (Lee *et al.* 2012) and to cancerous cell lines (Petronini *et al.* 1996, Yang *et al.* 2018a) also rescued these cells from apoptotic cell death. Similarly, the present study also confirmed that L-glutamate rescues aspirin-treated EG110 yeast cells from apoptosis, as determined by annexin V-FITC and PI staining (Figure 3.10). Results showed that exogenous 200 mM L-glutamate: (i) ameliorated 10-fold the viability of aspirin-treated EG110 yeast cells at 96 hours of cultivation (Figure 3.10 (b) and (c)), and (ii) maintained their viability to a similar extent as that of aspirin-untreated EG110 yeast cells grown in YPE medium only (Figure 3.10 (a) and (c)). Taken together, these results further suggest that glutamate depletion may be a critical event during aspirin-induced apoptosis in redox-compromised yeast cells.

The anti-proliferative effects of aspirin, amongst other NSAIDs, have been attributed to its ability of inducing a G1/S arrest in cancer cells (see section 1.5.2.1), which tend to downregulate the antioxidant enzyme MnSOD (Dhar *et al.* 2011, Oberley, Buettner 1979), and hence are redox-compromised as are EG110 yeast cells. This work showed that the anti-proliferative effect of aspirin on EG110 cells was due to a cell cycle arrest at the G1/S checkpoint, since aspirin-treated EG110 yeast cells displayed a prominent peak associated with the G0/G1 phase, which was not observed in control EG110 yeast cells grown in YPE medium only (Figure 3.11). The aspirin-induced accumulation of cells in the G0/G1 fraction was similarly reported in a variety of aspirin-treated cancer cell lines including the oral squamous cell carcinoma TCA8113 and CAL27 cells (Zhang *et al.* 2018), the liver carcinoma

HepG2 cells (Raza *et al.* 2011) and the colorectal adenocarcinoma HCT116, HT-29 and SW480 cells (Lai *et al.* 2008, Luciani *et al*. 2007).

Further results in this work showed that the addition of 200 mM L-glutamate to aspirin-treated EG110 cells circumvents their aspirin-induced G0/G1 arrest and the cells proceed to the G2/M phase (Figure 3.11). The aspirin-induced G1/S cell cycle arrest in EG110 yeast cells may be linked to nutrient scarcity in budding yeast (Hartwell *et al.* 1974) and the inadequate supply of acetyl-CoA in these cells (Farrugia *et al.* 2019), since this metabolite is important for the transcription of the cyclin Cln3 that is responsible for the G1/S transition (Shi, Tu 2013) (see section 1.3.1). On the other hand, their glutamate-mediated evasion from cell cycle arrest may have been due to glutamate's anaplerotic conversion into acetyl-CoA *via* α-ketoglutarate, as observed in glucose-deprived mammalian cells (Yang *et al.* 2014) (Figure 4.1).

In addition, DNA content analyses revealed that aspirin-treated EG110 yeast cells also displayed a prominent sub-G0/G1 peak, which was absent in the cell cycle profiles of their glutamate-treated counterparts (Figure 3.11). The occurrence of a sub-G0/G1 peak in aspirin-treated EG110 yeast cells is indicative of DNA fragmentation which accompanies the later stages of apoptosis (Madeo *et al.* 1997; Carmona-Gutierrez *et al.* 2018). This observation corroborates previous results obtained by Balzan *et al.* (2004) who showed that these cells die by apoptosis. It also demonstrates that these cells evade apoptosis when supplemented with 200 mM L-glutamate. The occurrence of a sub-G1 peak in cells treated with aspirin is not limited to EG110 yeast cells, but was also reported for aspirin-treated cancer cells including breast cancer cells (Choi *et al.* 2013) and T-cell lymphoma cells (Kumar *et al.* 2012), which also die by apoptosis.

Interestingly, the cell cycle distribution profile of aspirin-treated EG110 yeast cells supplemented with L-glutamate (Figure 3.11) is very similar to that of the wild-type EG103 yeast cells treated with aspirin (Figure 3.12). In both cell cycle distribution profiles, cells temporarily accumulate at the G2/M phase at the expense of the G0/G1 phase, at 168 hours of cultivation. This striking similarity may be explained by the fact that aspirin behaves as an antioxidant in EG103 cells by increasing the mitochondrial NAD(P)H levels (Farrugia *et al.* 2013), which may act as a source of electrons to sustain the GSH system and protect redox homeostasis (Schafer, Buettner 2001, Spector *et al.* 2001, Wheeler, Grant 2004) (see section 1.2.2). Similarly, glutamate may protect mitochondrial function during oxidative stress in aspirin-treated EG110 cells by (i) acting as a precursor of α-ketoglutarate (Mullen *et al.* 2014, Yang *et al.* 2014), which feeds into the TCA cycle to further generate electron donors such as NADPH and FADH$_2$, as well as by (ii) being indispensable for the synthesis of the major antioxidant GSH (Lee *et al.* 2007, Whillier *et al.* 2011) (Figure 4.1).

To test these plausible hypotheses and further characterise the effect of aspirin on glutamate metabolism in the redox-compromised EG110 yeast cells, the levels of glutamate's immediate metabolic products, namely α-ketoglutarate and reduced GSH, were measured. Results showed that aspirin-treated EG110 yeast cells were found to contain lower concentrations of α-ketoglutarate at 96 hours of cultivation (Figure 3.13) and of reduced GSH at 72 and 96 hours of cultivation (Table 3.1) (Figure 4.1). The addition of 200 mM L-glutamate restored their levels to those in aspirin-untreated EG110 yeast cells grown in YPE medium only (Figure 3.13 and Table 3.1, respectively) (Figure 4.1). Hu *et al.* (2010) also observed that glutamate increased the α-ketoglutarate level and the amount of reduced GSH, and as a result reduced the ROS levels in H$_2$O$_2$-treated mammalian cells. Similarly, Lee *et al.* (2012) demonstrated the importance of glutamate as a precursor of glutathione by

rescuing *gdh3*-null yeast cells, which are compromised in synthesising glutamate in times of stress, *via* the addition of GSH or glutamate. Together, these results suggest that aspirin-treated EG110 yeast cells are not only depleted of glutamate but are also depleted of its vital products, which are important for mitochondrial function and protection against oxidative stress, particularly in these redox-compromised cells (Figure 4.1).

The decrease in the level of α-ketoglutarate in aspirin-treated EG110 yeast cells (Figure 3.13) may explain why aspirin was reported to inhibit cellular respiration in these cells, unlike their aspirin-untreated counterparts (Sapienza *et al.* 2008), and conforms to studies carried out in cells from various organisms, which reported that aspirin inhibits enzymes (Kaplan *et al.* 1954, Nulton-Persson *et al.* 2004) or limits the adequate supply of metabolites involved in cellular energy generation or biomass synthesis (Farrugia *et al.* 2019, Sandoval-Acuña *et al.* 2012, van Leeuwen *et al.* 2011; Vessey *et al.* 1996) (Figure 4.1). In the present study, the fact that the addition of L-glutamate restored the levels of α-ketoglutarate in aspirin-treated EG110 yeast cells (Figure 3.13) suggests that (i) reactions synthesising α-ketoglutarate from glutamate are still functional, and (ii) the limiting factor is the insufficient level of intracellular glutamate, which could be anaplerotically fed into the TCA cycle for proper mitochondrial function. In fact, these suggestions are supported by as yet unpublished results obtained by Professor Balzan's group, which show that exogenous L-glutamate restores considerably the mitochondrial respiration of aspirin-treated EG110 yeast cells.

Several anaplerotic routes exist by which glutamate or glutamate-derived α-ketoglutarate may serve as a source of carbon for the TCA cycle and sustain mitochondrial function. For example, glutamate may undergo transamination and generate α-ketoglutarate and

glutamate's structurally analogous amino acid, aspartate (Figure 3.1). Aspartate is a versatile amino acid, important for the synthesis of nucleotides and for mitochondrial function. It is particularly implicated in the maintenance of mitochondrial and cytosolic NAD/NADH *via* the malate-aspartate shuttle, the components of which have been associated with the regulation of lifespan extension in yeast cells (Easlon *et al.* 2008). However, synthesis of aspartate is rather limited in respiration-inhibited cells, due to the impairment of ETC reactions which cannot generate electron acceptors necessary for the synthesis of aspartate, and thus cell proliferation is inhibited (Sullivan *et al.* 2015).

Since aspirin-treated EG110 cells are also respiration-deficient (Sapienza *et al.* 2008), and aspartate is deemed important for mitochondrial function and cellular redox balance, it was interesting to determine whether the glutamate-mediated rescuing of aspirin-treated EG110 yeast cells (Figures 3.9, 3.10 and 3.11) was mediated by glutamate-derived aspartate. However, when fixed doses of L-aspartate were added to aspirin-treated EG110 yeast cells, their growth was not ameliorated to the same extent as when L-glutamate was added (Figure 3.14), especially after 96 hours of growth. This result may be explained by the fact that aspartate is not critical for growth of yeast cells on ethanol (Cavero *et al.* 2003) since in addition to the malate-aspartate shuttle, which is critical for growth of yeast cells on acetate and oleic acid (Cavero *et al.* 2003), ethanol-grown yeast cells may control the mitochondrial and cytosolic NAD/NADH ratio by operating the ethanol-acetaldehyde shuttle and the glycerol-3-phosphate shuttle (Larsson *et al.* 1998, Von Jagow, Klingenberg 1970).

The rescuing effect of L-glutamate in aspirin-treated EG110 yeast cells may also have been more effective than that of L-aspartate, since glutamate is also an indispensable precursor of GSH (Lee *et al.* 2007), an essential antioxidant in the cell (Gostimskaya, Grant

2016). More importantly, by increasing the reduced GSH, L-glutamate restores the

intracellular redox balance of aspirin-treated EG110 yeast cells, by increasing the GSH/GSSG

ratio (Table 3.1). The maintenance of the cellular redox environment (see section 1.2) is

crucial to avoid the cells' demise during oxidative stress, which may result in oxidative cell

damage to a variety of vital biomolecules (see section 1.1.2) and subcellular compartments

such as mitochondria. In fact, Raza and John (2012) emphasised the importance of the GSH-

dependent redox homeostasis in the human liver carcinoma HepG2 cells, which was critical

to preserve mitochondrial function and prevent oxidative stress caused by aspirin treatment.

According to Lee *et al.* (2012), during oxidative stress, glutamate is preferentially used for

GSH supply rather than for protein synthesis. In fact, GSH plays a crucial role in maintaining

a highly reducing intracellular redox potential (Østergaard *et al.* 2004), since the

mitochondrial thioredoxin system only provides a back-up system, but cannot bear the

redox load of the mitochondria on its own (Gostimskaya, Grant 2016). Specifically, GSH

provides a source of electrons for (i) glutathione peroxidase to detoxify hydrogen peroxide

and other hydroperoxides (Figure 1.2), and for (ii) glutaredoxins which are involved in

reducing oxidised amino acid side-chains in proteins, thereby maintaining protein

homeostasis (see section 1.2.2). The death of aspirin-treated EG110 yeast cells is preceded

by redox imbalance, as indicated by a lowered GSH/GSSG ratio (Table 3.1) and acute

oxidative stress (Farrugia *et al.* 2013), and is accompanied by a decreased respiratory rate

(Sapienza *et al.* 2008). Hence, the inadequate synthesis of GSH in aspirin-treated EG110 cells

due to insufficient glutamate (Table 3.1) further exacerbates oxidative stress and brings

about cell death in these redox-compromised cells (Figure 3.9 and 3.10).

GSH deficiency is also associated with a G1 cell cycle arrest in both lower eukaryotes such as yeast cells (Spector *et al.* 2001, Wanke *et al.* 1999), as well as in higher eukaryotes such as plant and mammalian cells (Dethlefsen *et al.* 1988, Russo *et al.* 1995, Vernoux *et al.* 2000). Hence, the aspirin-induced decrease in GSH levels (Table 3.1), resulting from an insufficient level of its precursor glutamate (Figure 3.7), may be another reason for the aspirin-induced G1 cell cycle arrest (Figure 3.11). In fact, the addition of L-glutamate to aspirin-treated EG110 yeast cells restored the cell cycle distribution of these cells (Figure 3.11). This could likely be due to the glutamate-mediated increase in the level of the antioxidant GSH (Table 3.1). Similarly, Wanke *et al.* (1999) showed that the addition of the antioxidant N-acetylcysteine (NAC) circumvented the G1 cell cycle arrest of GSH-deficient yeast cells.

Early-stage cancer cells, like EG110 yeast cells, are redox-compromised due to their characteristic reduction in the expression of the antioxidant enzyme MnSOD (Dhar *et al.* 2011, Oberley, Buettner 1979). These cells are also dependent on glutamate metabolism for energy production, biomass synthesis and redox homeostasis (Warburg 1956, DeBerardinis *et al.* 2007, 2008, Yang *et al.* 2017), especially under conditions of metabolic stress and oncogenic activation (Choi, Park 2018). Indeed, several cancer cells die rapidly if deprived of glutamate or its precursor glutamine (Cluntun *et al.* 2017, Jiang *et al.* 2019, Yuneva *et al.* 2007, Zhang *et al.* 2017).

Cancer cells alter their metabolism *via* transcriptional reprogramming, which includes the constitutive activation of Myc (Santoro *et al.* 2019) making them addicted to glutamine and its immediate products (Gao *et al.* 2009). Myc-dependent transformation entails: (i) the transcription of genes encoding glutamine transporters which enhance glutamine uptake, and (ii) the induction of the expression of glutaminase mRNA and protein levels, to convert

glutamine into glutamate (Gao *et al.* 2009, Hu *et al.* 2010, Lampa *et al.* 2017, Wise *et al.*

2008). Glutamate is subsequently converted to α-ketoglutarate to fuel the TCA cycle *via*

anaplerotic reactions, as well as to drive glutathione production (Le *et al.* 2012, Wise *et al.*

2008). Myc-dependent transformation is also responsible for the Warburg effect (Wise *et al.*

2008), whereby glucose-derived pyruvate is used to synthesise lactate rather than acetyl-

CoA, despite aerobic conditions (Warburg 1956).

The substantial reliance of cancer cells on glutamate has made its metabolism a

promising target to pharmacologically control their growth and proliferation. Several drugs

targeting glutamate metabolism have been developed in an attempt to slow down tumour

growth and prolong survival (Fung, Chan 2017, Xiang *et al.* 2015). These include the

glutaminase inhibitors CB-839 and bis-2-(5-phenylacetamido-1,3,4-thiadiazol-2-yl)ethyl

sulfide (BPTES) (Gao *et al.* 2009, Gross *et al.* 2014, Wang *et al.* 2010a), the glutamine analog

6-diazo-5-oxo-L-norleucine (DON), which inhibits glutamine-dependent enzymes (Peyton *et

al.* 2018) and other chemicals which disrupt glutamate-mediated anaplerosis (Korangath *et

al.*¸ 2015) or glutamine/glutamate uptake (Colas *et al.* 2015, Wang *et al.* 2015a).

This study explored aspirin's potential to selectively target the glutamate metabolism of

redox-compromised yeast cells, but not of healthy cells, to bring about their demise.

Specifically, this work demonstrated that the onset of apoptosis in the aspirin-treated,

redox-compromised EG110 yeast cells, which does not occur in their wild-type counterparts,

is accompanied by insufficient levels of glutamate and of its immediate metabolic products,

α-ketoglutarate and reduced GSH, and by changes to their cell cycle distribution. Since

early-stage cancer cells are similarly redox-compromised, it is likely that aspirin exerts its

chemopreventive roles by: inducing a cell cycle arrest, thereby limiting cell proliferation, and

by targeting biochemical pathways, which involve glutamate. In turn, the aspirin-mediated depletion of glutamate leads to (i) the depletion of vital metabolites, such as α-ketoglutarate and ii) the exacerbation of oxidative stress, causing further redox imbalance. Together, these findings reveal a novel target and chemopreventive mechanism of aspirin, which may contribute towards the development of better aspirin-like drugs for cancer prevention.

4.1 Further work

This work has extensively shown that glutamate counteracts the deleterious effects of aspirin in the MnSOD-deficient *S. cerevisiae* EG110 cells and ameliorates their growth (Figure 3.8) and viability (Figure 3.9). As a follow up of the present work, it would be interesting to determine whether exogenous L-glutamate similarly improves the growth and viability of both aspirin-treated and untreated wild-type EG103 yeast cells, even though aspirin does not limit their proliferation (Balzan *et al.* 2004). Growth curves and viability studies based on CFU counts will be carried out to demonstrate independent and combinational effects of L-glutamate and aspirin on the growth and viability of EG103 cells grown in YPE medium, in aspirin-treated YPE medium, in glutamate-treated YPE medium and in YPE medium supplemented with both aspirin and glutamate.

Furthermore, this work has shown that aspirin causes a cell cycle arrest at the G0/G1 phase in EG110 yeast cells at 168 hours of cultivation, accompanied by apoptosis, as indicated by a prominent sub-G0/G1 peak (Figure 3.11) and by the results obtained by annexin V-FITC/PI staining (Figure 3.10 (b)). As a follow up of the present work, it would be interesting to identify novel cell-cycle targets of aspirin to further unravel the mechanism by which aspirin causes a G0/G1 arrest in the redox-compromised EG110 yeast cells, but not in the wild-type EG103 yeast cells. Western blotting experiments of cell cycle-related proteins,

167

such as the G1/S cyclin Cln3 or the G1/S cyclin-dependent kinase inhibitor Sic1, may be

performed to describe which proteins are targeted by aspirin to mediate cell cycle arrest in

redox-compromised yeast cells. For instance, a reduction in the expression of Cln3 and/or an

increase in the protein expression of Sic1 may further explain why aspirin arrests the cell

cycle at the G1/S checkpoint. If these aspirin-induced changes are observed, the expressions

of these two genes can be measured by qRT-PCR at regular time intervals from 96 hours of

cultivation, when the characteristic apoptotic phenotype was observed (Sapienza *et al.*

2008), until 168 hours of cultivation.

In Chapter 2 the cell-cycle related target genes *ESP1* and *MCD1* were studied, since apart

from their role in the onset of anaphase (see section 1.4.2.2), they have also been tightly

linked to regulated cell death (Yang *et al.* 2008). The aspirin-induced changes in the gene

expression levels of *ESP1* and *MCD1* in EG110 yeast cells as determined by microarray

analysis (Farrugia *et al.* 2019), were not validated by qRT-PCR (Figure 2.6). However, it is

plausible that their pro-apoptotic function is manifested through post-translational

modifications, which would be interesting to explore. Yang *et al.* (2008) showed that the

induction of apoptosis by hydrogen peroxide liberates Esp1 from its inhibitor Pds1, which is

in turn degraded by the anaphase promoting complex (APC) (Figure 4.2 (i)). Subsequently,

the activated Esp1 acts as a caspase-like protease to mediate cleavage of Mcd1, *via* the

protein sequence of Esp1, which is similar to human caspase 1 at their conserved proteolytic

sites (Uhlmann *et al.*, 2000). In the presence of hydrogen peroxide, the C-terminal of Mcd1

is further cleaved and the truncated Mcd1 is translocated from the nucleus to the

mitochondria, acting as a nuclear signal for apoptosis (Figure 4.2 (ii)). This causes the release

of cytochrome *c* prior to a decrease in mitochondrial membrane potential and further

amplification of cell death signalling *via* increased cytochrome *c* release from the

mitochondria (Figure 4.2 (ii)). To study whether aspirin-mediated cell death in EG110 yeast

cells similarly involves the translocation of the truncated Mcd1 from the nucleus into the

mitochondria, this translocation can potentially be observed by performing parallel

immunoscreening experiments of nuclear/cytosolic and mitochondrial fractions extracted

from aspirin-treated EG110 yeast cells grown for 24, 48 and 96 hours of cultivation. The

expression of the truncated Mcd1 should decrease in the nuclear/cytosolic fraction and

concomitantly increase in the mitochondrial fraction over time. If aspirin indeed mediates

cell death *via* the translocation of truncated Mcd1 into the mitochondria, the subsequent

release of cytochrome *c* from the mitochondria into the cytosol may also be monitored by

immunoscreening at 24, 48 and 96 hours. The expression of cytochrome *c* should decrease

in the mitochondrial fraction and concomitantly increase in the cytosolic fraction over time.

The expression of the truncated Mcd1 in the mitochondrial fraction should be proportional

to the extent of cytochrome *c* released from the mitochondria into the cytosol.

Work on yeast cells has implicated that the release of cytochrome *c* is dependent on the

yeast metacaspase Yca1 during acetic acid-induced cell death (Guaragnella *et al.* 2010a).

Interestingly, Chen *et al.* (2000) observed that cytochrome *c* is released in two distinct

stages. The early release of low levels of cytochrome *c* into the cytosol is caspase-

independent whereas the late stage of cytochrome *c* release is caspase-dependent. Sapienza

et al. (2008) had shown that aspirin-mediated apoptotic cell death is accompanied by

cytochrome *c* release from the mitochondria into the cytosol. However, it is not yet known

whether cytochrome *c* release during aspirin-mediated apoptosis in EG110 yeast cells is

Yca1-dependent or not. In order to determine whether Yca1 acts upstream or downstream

of cytochrome *c* release, immunoscreening experiments may be carried out. An antibody

against cytochrome *c* may be used to measure the expression of cytochrome *c in* extracts

from aspirin-treated and untreated EG110 yeast cells grown in YPE medium treated with a general caspase inhibitor zVAD-fmk, which abolishes caspase activity in the cell. Hypothetically, if Yca1 is normally required for aspirin-mediated cytochrome *c* release, no cytochrome *c* should be observed in the cytosolic fractions. On the other hand, if Yca1 is usually activated after the aspirin-mediated cytochrome *c* release from the mitochondria into the cytosol, cytochrome *c* should still be observed in the cytosolic fractions, independent of Yca1's inhibited metacaspase activity. Such an experiment will determine whether Yca1 acts upstream or downstream of cytochrome *c* release in aspirin-treated EG110 yeast.
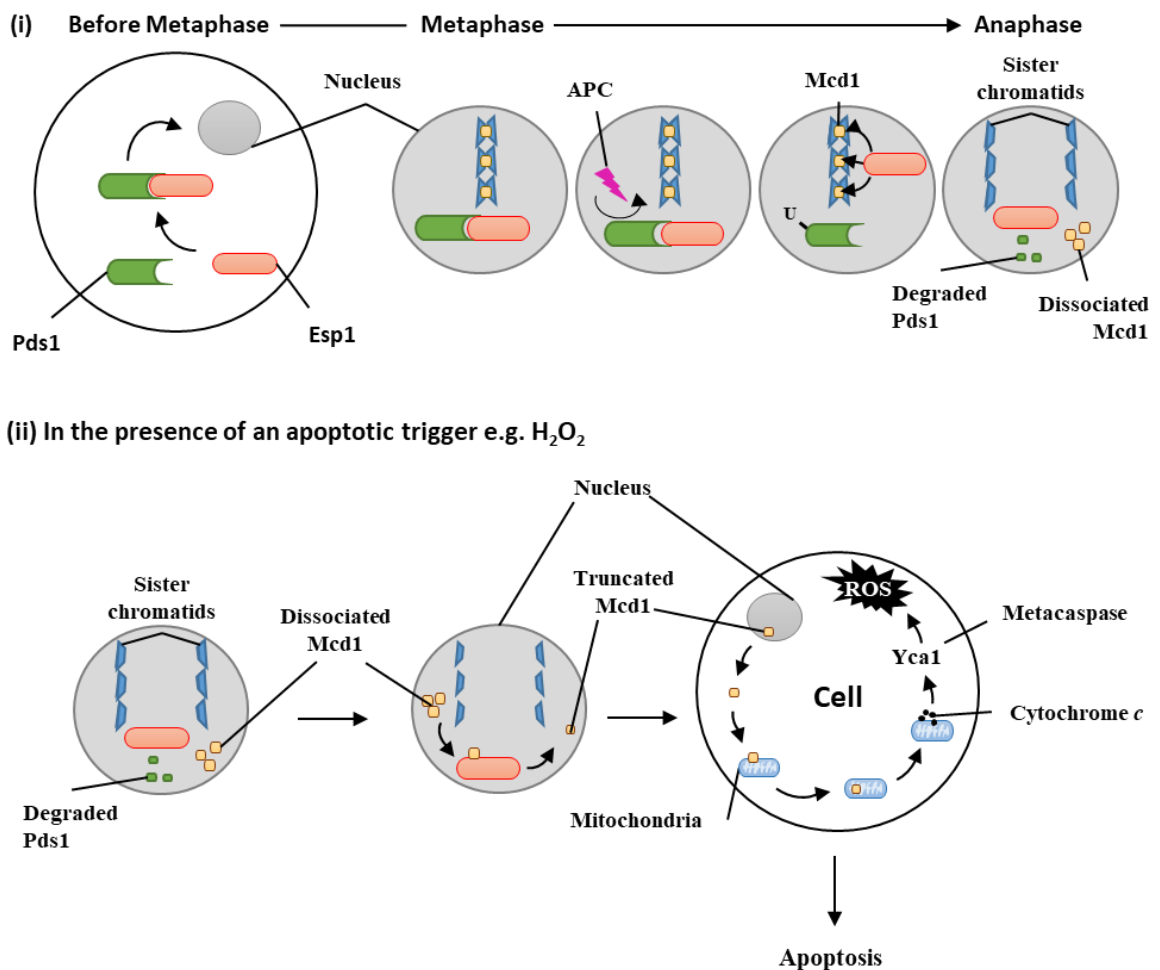
Figure 4.2 Cellular stress influences the interaction between the anaphase inhibitor securin, Pds1 and the anaphase-promoter protease Esp1 to commit yeast cells to apoptosis. (i) During normal cell division, before metaphase, cytoplasmic Esp1 must be chaperoned into the nucleus by binding Pds1. During metaphase, Pds1 is ubiquitinated by the action of Cdc20-APC, and is hence primed for degradation. The degradation of Pds1 liberates Esp1, thus allowing the dissociation of cohesin, Mcd1 from the two sister chromatids. This facilitates the onset of anaphase by enabling the separation and segregation of the two sister chromatids. (ii) Apoptotic triggers such as ROS (e.g. H_2O_2) mediate the degradation of Pds1 in the nucleus *via* improper APC activation. The activated Esp1 mediates the cleavage of the C-terminal of Mcd1. The truncated Mcd1 is then translocated from the nucleus to the mitochondria, and acts as a nuclear apoptotic signal. This results in the release of cytochrome *c*, which is associated with the activation of the yeast metacaspase Yca1 that effects apoptosis.

APC, anaphase-promoting complex; ROS, reactive oxygen species.

References

AGGARWAL, S., TANEJA, N., LIN, L., ORRINGER, M. B., REHEMTULLA, A. and BEER, D. G., 2000. Indomethacin-induced apoptosis in esophageal adenocarcinoma cells involves upregulation of Bax and translocation of mitochondrial cytochrome *c* independent of COX-2 expression. *Neoplasia*, *2,* 346-356.

AHLSKOG, J. K., BJÖRK, J. K., ELSING, A. N., ASPELIN, C., KALLIO, M., ROOS-MATTJUS, P. and SISTONEN, L., 2010. Anaphase-promoting complex/cyclosome participates in the acute response to protein-damaging stress. *Mol. Cell Biol., 30,* 5608-5620*.* https://doi.org/10.1128/MCB.01506-09.

AHMAD, W., IJAZ, B., SHABBIRI, K., AHMED, F. and REHMAN, S., 2017. Oxidative toxicity in diabetes and Alzheimer's disease: Mechanisms behind ROS / RNS generation. *J. Biomed. Sci., 24*, 76. https://doi.org/10.1186/s12929-017-0379-z

AHN, S. H., CHEUNG, W. L., HSU, J. Y., DIAZ, R. L., SMITH, M. M. and ALLIS, C. D., 2005. Sterile 20 kinase phosphorylates histone H2B at serine 10 during hydrogen peroxide-induced apoptosis in *S. cerevisiae*. *Cell, 120*, 25-36.

AHN, S. H., DIAZ, R. L., GRUNSTEIN, M. and ALLIS, C. D., 2006. Histone H2B deacetylation at lysine 11 is required for yeast apoptosis induced by phosphorylation of H2B at serine 10. *Mol. Cell.* 24, 211-20.

AL-NIMER, M. S., HAMEED, H. G. and MAHMOOD, M. M., 2015. Antiproliferative effects of aspirin and diclofenac against the growth of cancer and fibroblast cells: *In vitro* comparative study. *Saudi Pharm. J.*, 23, 483-486. https://doi.org/10.1016/j.jsps.2015.01.002.

ALBANO, F., ARCUCCI, A., GRANATO, G., ROMANO, S., MONTAGNANI, S., DE VENDITTIS, E. and RUOCCO, M. R., 2013. Markers of mitochondrial dysfunction during the diclofenac-induced apoptosis in melanoma cell lines. *Biochimie.*, *95*, 934-945. https://doi.org/10.1016/j.biochi.2012.12.012.

ALGRA, A. M. and ROTHWELL, P. M., 2012. Effects of regular aspirin on long-term cancer incidence and metastasis: a systematic comparison of evidence from observational studies versus randomised trials. *Lancet. Oncol., 13*, 518-527. https://doi.org/10.1016/S1470-2045(12)70112-2

ALIC, N., HIGGINS, V. J. and DAWES, I. W., 2001. Identification of a *Saccharomyces cerevisiae* gene that is required for G1 arrest in response to the lipid oxidation product linoleic acid hydroperoxide. *Mol. Biol. Cell, 12*, 1801-1810.

ALMEIDA, B., SILVA, A., MESQUITA, A., SAMPAIO-MARQUES, B., RODRIGUES, F. and LUDOVICO, P., 2008. Drug-induced apoptosis in yeast. *Biochim. Biophys. Acta*, *1783*, 1436-48. https://doi.org/10.1016/j.bbamcr.2008.01.005

ALTMAN, B. J., STINE, Z. E. and DANG, C. V., 2016. From Krebs to clinic: glutamine metabolism to cancer therapy. *Nat. Rev. Cancer*, *16*, 619–634. https://doi.org/10.1038/nrc.2016.71

ALVERS, A. L., FISHWICK, L. K., WOOD, M. S., HU, D., CHUNG, H. S., DUNN, W. A. JR. and ARIS, J. P., 2009. Autophagy and amino acid homeostasis are required for chronological longevity in *Saccharomyces cerevisiae. Aging Cell., 8*, 353-369. https://doi.org/10.1111/j.1474-9726.2009.00469.x.

AMARI, F., FETTOUCHE, A., SAMRA, M. A., KEFALAS, P., KAMPRANIS, S. C. and MAKRIS, A. M., 2008. Antioxidant small molecules confer variable protection against oxidative damage in yeast mutants. *J. Agric. Food Chem.*, *56*, 11740–11751. https://doi.org/10.1021/jf802829r

AMIGONI, L., FRIGERIO, G., MARTEGANI, E. and COLOMBO, S., 2016. Involvement of Aif1 in apoptosis triggered by lack of Hxk2 in the yeast *Saccharomyces cerevisiae. FEMS Yeast Res.*, *16*, 1-8. https://doi.org/10.1093/femsyr/fow016

AMORES-SÁNCHEZ, M. I. and MEDINA, M. A., 1999. Glutamine, as a precursor of glutathione, and oxidative stress. *Mol. Genet. Metab. 67*, 100-105.

ANTELMANN, H., BERNHARDT, J., SCHMID, R., MACH, H., VOELKER, U. and HECKER, M., 1997. First steps from a two-dimensional protein index towards a response-regulation map for *Bacillus subtilis. Electrophoresis, 18,* 1451-1463.

AVENDAÑO, A., DELUNA, A., OLIVERA, H., VALENZUELA, L. and GONZALEZ, A., 1997. *GDH3* encodes a glutamate dehydrogenase isozyme, a previously unrecognized route for glutamate biosynthesis in *Saccharomyces cerevisiae. J. Bacteriol.*, *179*, 5594-5597.

AVERY, A. M. and AVERY, S. V., 2001. *Saccharomyces cerevisiae* expresses three phospholipid hydroperoxide glutathione peroxidases. *J. Biol. Chem., 276*, 33730-33735. https://doi.org/10.1074/jbc.M105672200

AYALA, A., MUÑOZ, M. F. and ARGÜELLES, S., 2014. Lipid peroxidation: Production metabolism, and signalling mechanisms of malondialdehyde and 4-hydroxy-2-nonenal. *Oxid. Med. Cell. Longev., 2014,* 360438. https://doi.org/10.1155/2014/360438

AYYADEVARA, S., BHARILL, P., DANDAPAT, A., HU, C., KHAIDAKOV, M., MITRA, S., SHMOOKLER REIS, R. J. and MEHTA, J. L., 2013. Aspirin inhibits oxidant stress, reduces age-associated functional declines, and extends lifespan of *Caenorhabditis elegans*. *Antioxid. Redox Signal.*, *18*, 481–490.

AZAD, M. B., CHEN, Y. and GIBSON, S. B., 2009. Regulation of autophagy by reactive oxygen species (ROS): Implications for cancer progression and treatment. *Antioxid. Redox Signal., 11,* 777-790. https://doi.org/10.1089/ars.2008.2270

AZZOPARDI, M., FARRUGIA, G. and BALZAN, R., 2017. Cell-cycle involvement in autophagy and apoptosis in yeast. *Mech. Ageing Dev., 161*, 211-224. https://doi.org/10.1016/j.mad.2016.07.006

BAANDRUP, L., KJAER, S. K., OLSEN, J. H., DEHLENDORFF, C. and FRIIS, S., 2015. Low-dose aspirin use and the risk of ovarian cancer in Denmark. *Ann Oncol. 26,* 787-92. https://doi.org/10.1093/annonc/mdu578

BAEK, Y-U., KIM, Y-R., YIM, H-S. and KANG, S-O., 2004. Disruption of γ-glutamylcysteine synthetase results in absolute glutathione auxotrophy and apoptosis in *Candida albicans*. *FEBS Lett., 556*, 47-52. https://doi.org/10.1016/S0014-5793(03)01363-2

BAKKER, B. M., OVERKAMP, K. M., VAN MARIS, A. J., KÖTTER, P., LUTTIK, M. A., VAN DIJKEN, J. P. and PRONK, J. T., 2001. Stoichiometry and compartmentation of NADH metabolism in *Saccharomyces cerevisiae. FEMS Microbiol. Rev. 25*, 15-37.

BALTAZAR, M. T., DINIS-OLIVEIRA, R. J., DUARTE, J. A., BASTOS, M. L. and CARVALHO, F., 2011. Antioxidant properties and associated mechanisms of salicylates. *Curr. Med. Chem., 18*, 3252-3264. https://doi.org/10.2174/092986711796391552

BALZAN, R., SAPIENZA, K., GALEA, D. R., VASSALLO, N., FREY, H. and BANNISTER, W. H., 2004. Aspirin commits yeast cells to apoptosis depending on carbon source. *Microbiology, 150*, 109-115. https://doi.org/10.1099/mic.0.26578-0

BANK, A., YU, J. and ZHANG, L., 2008. NSAIDs downregulate Bcl-X(L) and dissociate BAX and Bcl-X(L) to induce apoptosis in colon cancer cells. *Nutr. Cancer, 60*, 98-103. https://doi.org/10.1080/01635580802381261. PubMed PMID: 19003586.

BARBER, S. C., MEAD, R. J. and SHAW, P. J., 2006. Oxidative stress in ALS: a mechanism of neurodegeneration and a therapeutic target. *Biochim. Biophys. Acta*, *1762*, 1051–1067. https://doi.org/10.1016/j.bbadis.2006.03.008

BARNUM, K. J. and O'CONNELL, M. J., 2014. Cell cycle regulation by checkpoints. *Methods Mol. Biol., 1170*, 29-40. https://doi.org/10.1007/978-1-4939-0888-2_2

BARON, J. A., COLE, B. F., SANDLER, R. S., HAILE, R. W., AHNEN, D., BRESALIER, R., MCKEOWN-EYSSEN, G., SUMMERS, R. W., ROTHSTEIN, R., BURKE, C. A., SNOVER, D. C., CHURCH, T. R., ALLEN, J. I., BEACH, M., BECK, G. J., BOND, J. H., BYERS, T., GREENBERG, E. R., MANDEL, J. S., … VAN STOLK, R. U., 2003. A randomized trial of aspirin to prevent colorectal adenomas. *N. Engl. J. Med.*, *348*, 891-899

BASIT, F., CRISTOFANON, S. and FULDA, S., 2013. Obatoclax (GX15-070) triggers necroptosis by promoting the assembly of the necrosome on autophagosomal membranes. *Cell Death Differ.*, *20*, 1161-73. https://doi.org/10.1038/cdd.2013.45

BASKERVILLE, C., SEGAL, M. and REED, S. I., 2008. The protease activity of yeast separase (Esp1) is required for anaphase spindle elongation independently of its role in cleavage of cohesin. *Genetics, 178*, 2361-2372. https://doi.org/10.1534/genetics.107.085308

BATTAGLIA, V., SALVI, M. and TONINELLO, A., 2005. Oxidative stress is responsible for mitochondrial permeability transition induction by salicylate in liver mitochondria. *J. Biol. Chem., 280*, 33864-33872. https://doi.org/10.1074/jbc.M502391200

BEARD, W. A., BATRA, V. K. A and ND WILSON, S. H., 2010. DNA polymerase structure-based insight on the mutagenic properties of 8-oxoguanine. *Mutat. Res., 703,* 18-23. https://doi.org/10.1016/j.mrgentox.2010.07.013

BENABDELLAH, K., AZCÓN-AGUILAR, C., VALDERAS, A., SPEZIGA, D., FITZPATRICK, T. B. AND FERROL, N., 2009. *GintPDX1* encodes a protein involved in vitamin B6 biosynthesis that is up-regulated by oxidative stress in the arbuscular mycorrhizal fungus *Glomus intraradices*. *New Phytol., 184*, 682-693. https://doi.org/10.1111/j.1469-8137.2009.02978.x

BENAMOUZIG, R., DEYRA, J., MARTIN, A., GIRARD, B., JULLIAN, E., PIEDNOIR, B., COUTURIER, D., COSTE, T., LITTLE, J. and CHAUSSADE, S., 2003. Daily soluble aspirin and prevention of colorectal adenoma recurrence: one-year results of the APACC trial. *Gastroenterology*, *125*, 328-36.

BERNDT, C., LILLIG, C. H. and FLOHÉ, L., 2014. Redox regulation by glutathione needs enzymes. *Front. Pharmacol., 5*, 168. https://doi.org/10.3389/fphar.2014.00168

BILSKI, P., LI, M. Y., EHRENSHAFT, M., DAUB, M. E. and CHIGNELL, C. F., 2000. Vitamin B6 (pyridoxine) and its derivatives are efficient singlet oxygen quenchers and potential fungal antioxidants. *Photochem. Photobiol., 71*, 129-134

BIN, P., HUANG, R. and ZHOU, X., 2017. Oxidation resistance of the sulfur amino acids: Methionine and cysteine. *Biomed. Res. Int., 2017,* 9584932. https://doi.org/10.1155/2017/9584932

BIN-UMER, M. A., MCLAUGHLIN, J. E., BUTTERFLY, M. S., MCCORMICK, S. and TUMER, N. E., 2014. Elimination of damaged mitochondria through mitophagy reduces mitochondrial oxidative stress and increases tolerance to trichothecenes. *Proc. Natl. Acad. Sci. U. S. A., 111,* 11798-11803. https://doi.org/10.1073/pnas.1403145111

BISSINGER, P. H., WIESER, R., HAMILTON, B. and RUIS, H., 1989. Control of *Saccharomyces cerevisiae* catalase T gene (*CTT1*) expression by nutrient supply via the *RAS-Cyclic* AMP pathway. *Mol. Cell. Biol., 9*, 1309-1315.

BLEIER, L. and DRÖSE, S., 2013. Superoxide generation by complex III: From mechanistic rationales to functional consequences. *Biochim. Biophys. Acta, 1827,* 578-587. https://doi.org/10.1016/j.bbabio.2012.12.002

BLESA, J., TRIGO-DAMAS, I., QURIOGA-VARELA, A. and JACKSON-LEWIS, V. R., 2015. Oxidative stress and Parkinson's disease. *Front. Neuroanat.*, *9,* 91. https://doi.org/10.3389/fnana.2015.00091

BOCK, J. M., MENON, S. G., GOSWAMI, P. C., SINCLAIR, L. L., BEDFORD, N. S., DOMANN, F. E. and TRASK, D. K., 2007. Relative non-steroidal anti-inflammatory drug (NSAID) antiproliferative activity is mediated through p21-induced G1 arrest and E2F inhibition. *Mol. Carcinog.*, *46* 857-864.

BORTNER, C. D., OLDENBURG, N. B. AN and D CIDLOWSKI, J. A., 1995. The role of DNA fragmentation in apoptosis. *Trends Cell Biol.*, *5*, 21-26.

BOS, J. L., 1989. ras oncogenes in human cancer: a review. *Cancer Res., 49*, 4682-4689.

BOSETTI, C., ROSATO, V., GALLUS, S., CUZICK, J. and LA VECCHIA, C., 2012. Aspirin and cancer risk: a quantitative review to 2011. *Ann. Oncol.*, *23*, 1403-1415. doi:10.1093/annonc/mds113

BOVERIS, A. and CHANCE, B., 1973. The mitochondrial generation of hydrogen peroxide. General properties and effect of hyperbaric oxygen. *Biochem. J., 134*, 707-716. https://doi.org/10.1042/bj1340707

BRANDUARDI, P., FOSSATI, T., SAUER, M., PAGANI, R., MATTANOVICH, D. and PORRO, D., 2007. Biosynthesis of vitamin C by teast leads to increased stress resistance. *PLoS One, 2,* e1092. https://doi.org/10.1371/journal.pone.0001092

BRAUER, M. J., SALDANHA, A. J., DOLINKSI, K. A and ND BOTSTEIN, D., 2005. Homeostatic adjustment and metabolic remodelling in glucose-limited yeast cultures. *Mol. Biol. Cell, 16,* 2503-2517. https://doi.org/10.1016/j.celrep.2014.03.057

BRAUN, E. L., FUGE, E. K., PADILLA, P. A. and WERNER-WASHBURNE, M., 1996. A stationary-phase gene in *Saccharomyces cerevisiae* is a member of a novel, highly conserved gene family. *J. Bacteriol., 178*, 6865-6872. https://doi.org/10.1128/jb.178.23.6865-6872.1996

BREEN, A. P. AN and D MURPHY, J. A., 1995. Reactions of oxyl radicals with DNA. *Free Radic. Bio. Med., 18*, 1033-1077. https://doi.org/10.1016/0891-5849(94)00209-3

BREITENBACH, M., RINNERTHALER, M., WEBER, M., BREITENBACH-KOLLER, H., KARL, T., CULLEN, P., BASU, S., HASKOVA, D. and HASEK, J., 2018. The defence and signalling role of NADH oxidases in eukaryotic cells. *Wien. Med. Wochenschr., 168,* 286-299. https://doi.org/10.1007/s10354-018-0640-4

BREMER, J. and DAVIS, E. J., 1975. Studies on the active transfer of reducing equivalents into mitochondria *via* the malate-aspartate shuttle. *Biochim. Biophys. Acta., 376*, 387-97.

BREVIARIO, D., HINNEBUSCH, A., CANNON, J., TATCHELL, K. and DHAR, R., 1986. Carbon source regulation of *RAS1* expression in *Saccharomyces cerevisiae* and the phenotypes of *ras2-* cells. *Proc. Natl. Acad. Sci. USA, 83*, 4152-4156.

BUENO, A and RUSSELL P., 1992. Dual functions of *CDC6*: a yeast protein required for DNA replication also inhibit nuclear division. *EMBO J., 11*, 2167-2176.

BURHANS, W. C. and WEINBERGER, M., 2007. Yeast endonuclease G: complex matters of death, and of life. *Mol. Cell., 25*, 323-325.

BURHANS, W. C. and WEINBERGER, M., 2009. Acetic acid effects on aging in budding yeast: Are they relevant to aging in higher eukaryotes? *Cell cycle, 8*, 2300-2302. https://doi.org/10.4161/cc.8.14.8852

BURHANS, W. C., WEINBERGER, M., MARCHETTI, M. A., RAMACHANDRAN, L., D'URSO, G. and HUBERMAN, J. A., 2003. Apoptosis-like yeast cell death in response to DNA damage and replication defects. *Mutat. Res., 532*, 227-243. https://doi.org/10.1016/j.mrfmmm.2003.08.019

BURN, J., BISHOP, D. T., CHAPMAN, P. D., ELLIOTT, F., BERTARIO, L., DUNLOP, M. G., ECCLES, D., ELLIS, A., EVANS, D. G., FODDE, R., MAHER, E. R., MÖSLEIN, G., VASEN, H. F., COAKER, J., PHILLIPS, R. K., BÜLOW, S. and MATHERS, J. C., 2011a. A randomized placebo-controlled prevention trial of aspirin and/or resistant starch in young people with familial adenomatous polyposis. Cancer Prev. Res., *4*, 655-65. https://doi.org/10.1158/1940-6207.CAPR-11-0106

BURN, J., GERDES, A. M., MACRAE, F., MECKLIN, J. P., MOESLEIN, G., OLSCHWANG, S., ECCLES, D., EVANS, D. G., MAHER, E. R., BERTARIO, L., BISGAARD, M. L., DUNLOP, M. G., HO, J. W., HODGSON, S. V., LINDBLOM, A., LUBINSKI, J., MORRISON, P. J., MURDAY, V., RAMESAR, R., … BISHOP, D. T., 2011b. Long-term effect of aspirin on cancer risk in carriers of hereditary colorectal cancer: an analysis from the CAPP2 randomised controlled trial. *Lancet., 378*, 2081-2087. https://doi.org/10.1016/S0140-6736(11)61049-0.

BURNETTI, A. J., AYDIN, M. and BUCHLER, N. E., 2016. Cell cycle Start is coupled to entry into the yeast metabolic cycle across diverse strains and growth rates. *Mol. Biol. Cell, 27*, 64-74. https://doi.org/10.1091/mbc.E15-07-0454

BÜTTNER, S., EISENBERG, T., CARMONA-GUTIERREZ, D., RULI, D., KNAUER, H., RUCKENSTUHL, C., SIGRIST, C., WISSING, S, KOLLROSER, M., FRÖHLICH, K. U., SIGRIST, S. and MADEO, F., 2007. Endonuclease G regulates budding yeast life and death. *Mol. Cell., 25*, 233-46.

BÜTTNER, S., EISENBERG, T., HERKER, E., CARMONA-GUTIERREZ, D., KROEMER, G. and MADEO, F., 2006. Why yeast cells can undergo apoptosis: death in times of peace, love, and war. *J. Cell Biol., 175*, 521-525.

BYUN, H. O., KIM, H. Y., LIM, J. J., SEO, Y. H. and YOON, G., 2008. Mitochondrial dysfunction by complex II inhibition delays overall cell cycle progression *via* reactive oxygen species production. *J. Cell Biochem., 104,* 1747-1759. https://doi.org/10.1002/jcb.21741

CABISCOL, E., PIULATS, E., ECHAVE, P., HERRERO, E. and ROS, J., 2000. Oxidative stress promotes specific protein damage in *Saccharomyces cerevisiae*. *J. Biol. Chem.*, *275*, 27393–27398. https://doi.org/10.1074/jbc.M003140200

CADET, J., DELATOUR, T., DOUKI, T., GASPARUTTO, D., POUGET, J.-P., RAVANAT, J.-L. and SAUVAIGO, S., 1999. Hydroxyl radicals and DNA base damage. *Mutat. Res., 424,* 9-21. https://doi.org/10.1016/S0027-5107(99)00004-4

CALZADA, A., SACRISTÁN, M., SÁNCHEZ, E. and BUENO, A., 2001. Cdc6 cooperates with Sic1 and Hct1 to inactivate mitotic cyclin-dependent kinases. *Nature*, *412*, 355-358.

CANLI, O., NICOLAS, A. M., GUPTA, J., FINKELMEIER, F., GONCHOVA, R. PESIC, M., NEUMAN, T., HORST, D., LOWER M., SAHIN, U. and GRETEN, F. R., 2017. Myeloid cell-derived reactive oxygen species induce epithelial mutagenesis. *Cancer cell, 32,* 869-883. https://doi.org/10.1016/j.ccell.2017.11.004

CARMONA-GUTIÉRREZ, D., BAUER, M. A., RING, J., KNAUER, H., EISENBERG, T., BÜTTNER, S., RUCKENSTUHL, C., REISENBICHLER, A., MAGNES, C., RECHBERGER, G. N., BIRNER-GRUENBERGER, R., JUNGWIRTH, H., FRÖHLICH, K. U., SINNER, F., KROEMER, G. and MADEO, F., 2011. The propeptide of yeast cathepsin D inhibits programmed necrosis. *Cell Death Dis.*, *2*, e161. https://doi.org/10.1038/cddis.2011.43

CARMONA-GUTIERREZ D, BAUER MA, ZIMMERMANN A, *et al.*, 2018. Guidelines and recommendations on yeast cell death nomenclature. *Microb. Cell.*, *5*, 4-31. https://doi.org/10.15698/mic2018.01.607

CASTAÑO, E., DALMAU, M., BARRAGÁN, M., PUEYO, G., BARTRONS, R. and GIL, J., 1999. Aspirin induces cell death and caspase-dependent phosphatidylserine externalization in HT-29 human colon adenocarcinoma cells. *Br. J. Cancer*, *81*, 294-299.

CASTELLANO, E. and DOWNWARD, J., 2011. RAS interaction with PI3K: More than just another effector pathway. *Genes Cancer*, *2*, 261–274. https://doi.org/10.1177/1947601911408079

CAVERO, S., VOZZA, A., DEL ARCO, A., PALMIERI, L., VILLA, A., BLANCO, E., RUNSWICK, M. J., WALKER, J. E., CERDÁN, S., PALMIERI, F. and SATRÚSTEGUI, J., 2003. Identification and metabolic role of the mitochondrial aspartate-glutamate transporter in *Saccharomyces cerevisiae*. *Mol. Microbiol.*, *50*, 1257–1269. https://doi.org/10.1046/j.1365-2958.2003.03742.x

CECARINI, V., GEE, J., FIORETTI, E., AMICI, M., ANGELETTI, M., ELEUTERI, A. M. and KELLER, J. N., 2006. Protein oxidation and cellular homeostasis: Emphasis on metabolism. *Biochim. Biophys. Acta, 1773,* 93-104. https://10.1016/j.bbamcr.2006.08.039

CHAN, T. A., MORIN, P. J., VOGELSTEIN, B. and KINZLER, K. W., 1998. Mechanisms underlying nonsteroidal antiinflammatory drug-mediated apoptosis. *Proc. Natl. Acad. Sci. U. S. A. 95*, 681-686.

CHANDRA, J., SAMALI, A. and ORRENIUS, S., 2000. Triggering and modulation of apoptosis by oxidative stress. *Free Radic. Biol. Med.*, *29*, 323-333.

CHANG, J. K., LI, C. J., LIAO, H. J., WANG, C. K., WANG, G. J. and HO, M. L., 2009. Anti-inflammatory drugs suppress proliferation and induce apoptosis through altering expressions of cell cycle regulators and pro-apoptotic factors in cultured human osteoblasts. *Toxicology*. *258,* 148-56. https://doi.org/10.1016/j.tox.2009.01.016.

CHARIZANIS, C., JUHNKE, H., KREMS, B. and ENTIAN, K-D., 1999. The oxidative stress response mediated via Pos9/Skn7 is negatively regulated by the Ras/PKA pathway in *Saccharomyces cerevisiae*. *Mol. Gen. Genet., 261*, 740-752. https://doi.org/10.1007/s004380050

CHEN, B., ZHAO, J., ZHANG, S., WU, W. and QI, R., 2012. Aspirin inhibits the production of reactive oxygen species by downregulating Nox4 and inducible nitric oxide synthase in human endothelial cells exposed to oxidized low-density lipoprotein. *J. Cardiovas. Pharmacol., 59*, 405-412. https://doi.org/10.1097/FJC.0b013e318248acba

CHEN, H. and XIONG, L., 2005. Pyridoxine is required for post-embryonic root development and tolerance to osmotic and oxidative stresses. *Plant J., 44*, 396-408. https://doi.org/10.1111/j.1365-313X.2005.02538.x

CHEN, Q., GONG, B. and ALMASAN, A., 2000. Distinct stages of cytochrome *c* release from mitochondria: evidence for a feedback amplification loop linking caspase activation to mitochondrial dysfunction in genotoxic stress induced apoptosis. *Cell Death Differ., 7,* 227-233.

CHEN, X., HE, W. T., HU, L., LI, J., FANG, Y., WANG, X., XU, X., WANG, Z., HUANG, K. and HAN, J., 2016a. Pyroptosis is driven by non-selective gasdermin-D pore and its morphology is different from MLKL channel-mediated necroptosis. *Cell Res*., *26,* 1007-1020. https://doi.org/10.1038/cr.2016.100

CHEN, X., MENGIJA, S., ZHANG, B. and ZHANG, Y., 2016b. Reactive oxygen species regulate T cell immune response in the tumour microenvironment. *Oxid. Med. Cell Longev., 2016,* 1580967. https://doi.org/10.1155/2016/1580967

CHEN, Y. H. and BOGENHAGEN, D. F., 1993. Effects of DNA lesions on transcription elongation by T7 RNA polymerase. *J. Biol. Chem., 268,* 5849-5855.

CHEN, Z., SILVA, H. and KLESSIG, D. F., 1993. Active oxygen species in the induction of plant systemic acquired resistance by salicylic acid. *Science*, *262*, 1883-1886.

CHENG, L., WATT, R. and PIPER, P. W., 1994. Polyubiquitin gene expression contributes to oxidative stress resistance in respiratory yeast (*Saccharomyces cerevisiae*). *Mol. Gen. Genet., 243,* 358-362. https://doi.org/10.1007/bf00301072

CHENG, R., LIU, Y-J., CUI, J-W., YANG, M., LIU, X-L., LI, P., WANG, Z., ZHU, L-Z., LU, S-Y., ZOU, L., WU, X-Q., LI, Y-X., ZHOU, Y., FANG, Z-Y. and WEI, W., 2017. Aspirin regulation of c-myc and cyclinD1 proteins to overcome tamoxifen resistance in estrogen receptor-positive breast cancer cells. *Oncotarget*, *8*, 30252-30264. https://doi.org/10.18632/oncotarget.16325

CHERVONEVA, I., LI, Y., SCHULZ, S., CROKER, S., WILSON, C., WALDMAN, S. A. and HYSLOP, T., 2010. Selection of optimal reference genes for normalization in quantitative RT-PCR. *BMC Bioinformatics, 11*, 253. https://doi.org/10.1186/1471-2105-11-253

CHINNAPAKA, S., ZHENG, G., CHEN, A. and MUNIRATHINAM, G., 2019. Nitro aspirin (NCX4040) induces apoptosis in PC3 metastatic prostate cancer cells *via* hydrogen peroxide (H_2O_2)-mediated oxidative stress. *Free Radic. Biol. Med., 143*, 494-509. https://doi.org/10.1016/j.freeradbiomed.2019.08.025.

CHIPUK, J. E., BOUCHIER-HAYES, L. and GREEN D. R., 2006. Mitochondrial outer membrane permeabilization during apoptosis: the innocent bystander scenario. *Cell Death Differ., 13*, 1396-1402.

CHIU, J. and DAWES, I. W., 2012. Redox control of cell proliferation. *Trends Cell Biol., 22*, 592-601. https://doi.org/10.1016/j.tcb.2012.08.002

CHIU, J., TACTACAN, C. M., TAN, S-X., LIN, R. C. Y., WOUTERS, M. A. and DAWES, I. W., 2011. Cell cycle sensing of oxidative stress in *Saccharomyces cerevisiae* by oxidation of a specific cysteine residue in the transcription factor Swi6p. *J. Biol. Chem., 286*, 5204-5214. https://doi.org/10.1074/jbc.M110.172973

CHOI, B. H., CHAKRABORTY, G., BAEK, K. and YOON, H. S., 2013. Aspirin-induced Bcl-2 translocation and its phosphorylation in the nucleus trigger apoptosis in breast cancer cells. *Exp. Mol. Med.*, *45*, e47. https://doi.org/10.1038/emm.2013.91

CHOI, J. Y., WON, N. H., PARK, J. D., JANG, S., EOM, C. Y., CHOI, Y., PARK, Y. I. and DONG, M. S., 2016. Ethylmercury-induced oxidative and endoplasmic reticulum stress-mediated autophagic cell death: Involvement of autophagosome-lysosome fusion arrest. *Toxicol Sci., 154*, 27-42.

CHOI, Y. K. and PARK, K. G., 2018. Targeting glutamine metabolism for cancer treatment. *Biomolecules and therapeutics*, *26*, 19–28. https://doi.org/10.4062/biomolther.2017.178

CHOO, A. Y., KIM, S. G., VANDER HEIDEN, M. G., MAHONEY, S. J., VU, H., YOON, S. O., CANTLEY, L. C. and BLENIS, J., 2010. Glucose addiction of TSC null cells is caused by failed mTORC1-dependent balancing of metabolic demand with supply. *Mol. Cell., 38,* 487-499. https://doi.org/10.1016/j.molcel.2010.05.007.

CLUNTUN, A. A., LUKEY, M. J., CERIONE, R. A. and LOCASALE, J. W., 2017. Glutamine metabolism in cancer: Understanding the heterogeneity. *Trends Cancer.,* 3, 169-180. https://doi.org/10.1016/j.trecan.2017.01.005.

COHEN, G., FESSL, F., TRACZYK, A., RYTKA, J. and RUIS, H., 1985. Isolation of the catalase A gene of *Saccharomyces cerevisiae* by complementation of the cta1 mutation. *Mol. Gen. Genet., 200,* 74-79. https://doi.org/10.1007/bf00383315

COHEN-FIX, O., PETERS, J. M., KIRSCHNER, M. W. and KOSHLAND, D., 1996. Anaphase initiation in *Saccharomyces cerevisiae* is controlled by the APC-dependent degradation of the anaphase inhibitor Pds1p. *Genes Dev.*, *10*, 3081-93.

COLAS, C., GREWER, C., OTTE, N. J., GAMEIRO, A., ALBERS, T., SINGH, K., SHERE, H., BONOMI, M., HOLST, J. and SCHLESSINGER, A., 2015. Ligand discovery for the alanine-serine-cysteine transporter (ASCT2, SLC1A5) from homology modeling and virtual screening. *PLoS Comput. Biol. 11,* e1004477. https://doi.org/10.1371/journal.pcbi.1004477.

COLEMAN, S. T., EPPING, E. A., STEGGARDA, S. M. and MOYE-ROWLEY, W.-S., 1999. Yap1p activates gene transcription in an oxidant-specific fashion. *Mol. Cell. Biol., 19,* 8302-8313. https://doi.org/10.1128/mcb.19.12.8302

COLEMAN, S. T., FANG, T. K., ROVINSKY, S. A., TURANO, F. J. and MOYE-ROWLEY, W. S., 2001. Expression of a glutamate decarboxylase homologue is required for normal oxidative stress tolerance in *Saccharomyces cerevisiae*. *J. Biol. Chem*. *276*, 244-50.

CONRAD, M., SCHOTHORST, J., KANKIPATI, H. N., VAN ZEEBROECK, G., RUBIO-TEXEIRA, M. and THEVELEIN, J. M., 2014. Nutrient sensing and signaling in the yeast *Saccharomyces cerevisiae. FEMS Microbiol. Rev.*, *38*, 254-99. https://doi.org/10.1111/1574-6976.12065.

COOPER, T. G., 1982. Nitrogen metabolism in *Saccharomyces cerevisiae*. In: Strathern, J. N., Jones, E. W., Broach, J. R., (Eds.). *The molecular biology of the yeast Saccharomyces.* New York, Cold Spring Harbor Laboratory Press. pp. 39 –99.

CORTÉS-ROJO, C., CHALDERÓN-CORTÉS, E., CLEMENTE-GUERRERO, M., ESTRADA-VILLAGÓMEZ, M., MANZO-AVALOS, S., MEJIA-ZEPEDA, R., BOLDOGH, I. and SAAVEDRA-MOLINA, A., 2009. Elucidation of the effects of lipoperoxidation on the mitochondrial electron transport chain using yeast mitochondria with manipulated fatty acid content. *J. Bioenerg. Biomembr.*, *41,* 15. https://doi.org/10.1007/s10863-009-9200-3

COSTA, V. M., AMORIM, M. A., QUINTANILHA, A. and MORADAS-FERREIRA, P., 2002. Hydrogen peroxide-induced carbonylation of key metabolic enzymes in *Saccharomyces cerevisiae:* the involvement of the oxidative stress response regulators Yap1 and Skn7. *Free Radic. Biol. Med., 33,* 1507-1515. https://doi.org/10.1016/s0891-5849(02)01086-9

COSTA, V., QUINTANILHA, A. and MORADAS-FERREIRA, P., 2007. Protein oxidation, repair mechanisms and proteolysis in *Saccharomyces cerevisiae. IUBMB Life, 59,* 293-298. https://doi.org/10.1080/15216540701225958

COVARRUBIAS-PINTO, A., MOLL, P., SOLIS-MALDONADO, M., ACUNA, A. I., RIVEROS, A., MIRO, M. P., PAPIC, E., BELTRAN, F. A., CEPEDA, C., CONCHA, I. I., BRAUCHI, S. and CASTRO, M. A., 2015. Beyond the redox imbalance: Oxidative stress contributes to an impaired *GLUT3* modulation in Huntington' disease. *Free Radic. Biol. Med., 89*, 1085-1096. https://doi.org/10.1016/j.freeradbiomed.2015.09.024

CROWELL, J. A., STEELE, V. E. and FAY, J. R., 2007. Targeting the AKT protein kinase for cancer chemoprevention. *Mol. Cancer Ther*., *6*, 2139-2148.

CUI, Y., ZHAO, S., WU, Z., DAI, P. and ZHOU, B., 2012. Mitochondrial release of the NADH dehydrogenase Ndi1 induces apoptosis in yeast. *Mol. Biol. Cell, 23,* 4373-4382. https://doi.org/10.1091/mbc.E12-04-0281

DACHINENI, R., AI, G., KUMAR, D. R., SADHU, S. S., TUMMALA, H. and BHAT, G. J., 2016. Cyclin A2 and CDK2 as novel targets of aspirin and salicylic acid: a potential role in cancer prevention. *Mol. Cancer Res*., *14*, 241-252. https://doi.org/10.1158/1541-7786.MCR-15-0360

DAVALLI, P., MITIC, T., CAPORALI, A., LAURIOLA, A. and D'ARCA, D., 2016. ROS, cell senescence, and novel molecular mechanisms in aging and age-related diseases. *Oxid. Med. Cell Longev*. *2016*, 3565127. https://doi.org/10.1155/2016/3565127

DAVIES, J. M. S., LOWRY, C. V. and DAVIES, K. J. A., 1995. Transient adaptation to oxidative stress in yeast. *Arch. Biochem. Biophys., 317,* 1-6. https://doi.org/10.1006/abbi.1995.1128

DAVIES, K. J. A., 2001. Degradation of oxidized proteins by the 20S proteasome. *Biochimie, 83,* 301-310. https://doi.org/10.1016/s0300-9084(01)01250-0

DE ARAÚJO, R. F., MARTINS, D. B. G., and BORBA, M. A. C., 2016. Oxidative stress and disease. In: J. A. Morales-Gonzáles and E. O. Madrigal-Santillán (Eds.), *A master regulator of oxidative stress - The transcription factor Nrf2*, (pp. 185 – 200). InTechOpen: London, UK. https://doi.org/10.5772/65366

DE GREY, A., 2002. HO_2: The forgotten radical. *DNA Cell Biol., 21,* 251-257. https://doi.org/10.1089/104454902753759672

DE LUNA-BERTOS, E., RAMOS-TORRECILLAS, J., GARCÍA-MARTÍNEZ, O., DÍAZ-RODRÍGUEZ, L. and RUIZ, C., 2012. Effect of aspirin on cell growth of human MG-63 osteosarcoma line. *Sci. World J.*, 2012, 834246. https://doi.org/10.1100/2012/834246.

DE SMIDT, O., DU PREEZ, J. C. and ALBERTYN, J., 2008. The alcohol dehydrogenases of *Saccharomyces cerevisiae*: a comprehensive review. *FEMS Yeast Res.*, *8,* 967-978. https://doi.org/10.1111/j.1567-1364.2008.00387.x

DE VRIES, S. and GRIVELL, L. A., 1988. Purification and characterisation of a rotenone-insensitive NADH:Q6 oxidoreductase from mitochondria of *Saccharomyces cerevisiae. Eur. J. Biochem., 176*, 377-384. https://doi.org/10.1111/j.1432-1033.1988.tb14292.x

DE VRIES, S. and MARRES, C. A., 1987. The mitochondrial respiratory chain of yeast. Structure and biosynthesis and the role in cellular metabolism. *Biochim. Biophys. Acta*, *895*, 205–239. https://doi.org/10.1016/s0304-4173(87)80003-4

DEL CARRATORE, R., DELLA CROCE, C., SIMILI, M., TACCINI, E., SCAVUZZO, M. and SBRANA, S., 2002. Cell cycle and morphological alterations as indicative of apoptosis promoted by UV irradiation in *S. cerevisiae. Mutat Res*., *513*, 183-91.

DEBERARDINIS, R. J. and CHANDEL, N. S., 2016. Fundamentals of cancer metabolism. *Sci Adv*., *2*, e1600200. https://doi.org/10.1126/sciadv.1600200.

DEBERARDINIS, R. J., LUM, J. J., HATZIVASSILIOU, G. and THOMPSON, C. B., 2008. The biology of cancer: Metabolic reprogramming fuels cell growth and proliferation. *Cell Metabolism, 7*, 11-20. https://doi.org/10.1016/j.cmet.2007.10.002

DEBERARDINIS, R. J., MANCUSO, A., DAIKHIN, E., NISSIM, I., YUDKOFF, M., WEHRLI, S. and THOMPSON, C. B., 2007. Beyond aerobic glycolysis: transformed cells can engage in glutamine metabolism that exceeds the requirement for protein and nucleotide synthesis. *Proc. Natl. Acad. Sci. U. S. A., 104*, 19345-19350. https://doi.org/10.1073/pnas.0709747104

DELAUNAY, A., ISNARD, A. D. and TOLEDANO, M. B., 2000. H_2O_2 sensing though oxidation of the Yap1 transcription factor. *EMBO J., 19*, 5157-5166. https://doi.org/10.1093/emboj/19.19.5157

DELAUNAY, A., PFLIEGER, D., BARRAULT, M. B., VINH, J. and TOLEDANO, M. B., 2002. A thiol peroxidase is an H_2O_2 receptor and redox-transducer in gene activation. *Cell, 111,* 471-481. https://doi.org/10.1016/s0092-8674(02)01048-6

DELCARDAYRÉ, S. B., STICK, K. P., NEWTON, G. L., FAHEY, R. C. and DAVIES, J. E., 1998. Coenzyme A disulphide reductase, the primary low molecular weight disulfide reductase from *Staphylococcus aureus.* Purification and characterisation of the native enzyme. *J. Biol. Chem., 273*, 5744-5751*.* https://doi.org/10.1074/jbc.273.10.5744

DELL'AGLIO, E., BOYCHEVA, S. and FITZPATRICK, T. B., 2017. The pseudoenzyme PDX1.2 sustains vitamin B_6 biosynthesis as a function of heat stress. *Plant Physiol.*, *174*, 2098-2112. https://doi.org/10.1104/pp.17.00531

DERISI, J. L., IYER, V. R. and BROWN, P. O., 1997. Exploring the metabolic and genetic control of gene expression on a genomic scale. *Science*, *278*, 680-686. https://doi.org/10.1126/science.278.5338.680

DETHLEFSEN, L. A., LEHMAN, C. M., BIAGLOW, J. E. and PECK, V. M., 1988. Toxic effects of acute glutathione depletion by buthionine sulfoximine and dimethylfumarate on murine mammary carcinoma cells. *Radiat. Res.*, *114*, 215–224.

DIAS, V., EUNSUNG, J. and MURAL MOURADIAN, M., 2013. The role of oxidative stress in Parkinson's disease. *J. Parkinsons Dis., 3,* 461-491. https://doi.org/10.3233/JPD-130230

DÍAZ-RODRÍGUEZ, L., GARCÍA-MARTÍNEZ, O., MORALES, M. A., RODRÍGUEZ-PÉREZ, L., RUBIO-RUIZ, B. and RUIZ, C., 2012. Effects of indomethacin, nimesulide, and diclofenac on human MG-63 osteosarcoma cell line. *Biol. Res. Nurs.*, *14*, 98-107.

DICKINSON, J. R. and SCHWEIZER, M. (Eds.), 1999. *The metabolism and molecular physiology of Saccharomyces cerevisiae*. London: Taylor and Francis.

DIERSSEN-SOTOS, T., GÓMEZ-ACEBO, I., DE PEDRO, M., PÉREZ-GÓMEZ, B., SERVITJA, S., MORENO, V., AMIANO, P., FERNANDEZ-VILLA, T., BARRICARTE, A., TARDON, A., DIAZ-SANTOS, M., PEIRO-PEREZ, R., MARCOS-GRAGERA, R., LOPE, V., GRACIA-LAVEDAN, E., ALONSO, M. H., MICHELENA-ECHEVESTE, M. J., GARCIA-PALOMO, A., … LLORCA, J., 2016. Use of non-steroidal anti-inflammatory drugs and risk of breast cancer: The Spanish Multi-Case-control (MCC) study. *BMC Cancer, 16*, 660. https://doi.org/10.1186/s12885-016-2692-4

DIKSHIT, P., CHATTERJEE, M., GOSWAMI, A., MISHRA, A. and JANA, N. R., 2006. Aspirin induces apoptosis through the inhibition of proteasome function. *J. Biol. Chem.*, *281*, 29228-29235. https://doi.org/10.1074/jbc.M602629200

DING, J. H., YUAN, L. Y., HUANG, R. B. and CHEN, G. A., 2014. Aspirin inhibits proliferation and induces apoptosis of multiple myeloma cells through regulation of Bcl-2 and Bax and suppression of VEGF. *Eur. J. Haematol.,* 93, 329-39. https://doi.org/10.1111/ejh.12352.

DIZDAROGLU, M., 1991. Chemical determination of free radical-induced damage to DNA. *Free Radic. Biol. Med., 10,* 225-242. https://doi.org/10.1016/0891-5849(91)90080-m

DHAR, S. K., TANGPONG, J., CHAISWING, L., OBERLEY, T. D. and ST CLAIR, D. K., 2011. Manganese superoxide dismutase is a p53-regulated gene that switches cancers between early and advanced stages. *Cancer Res., 71,* 6684-6695. https://doi.org/10.1158/0008-5472.CAN-11-1233.

DOAT, S., CÉNÉE, S., TRÉTARRE, B., REBILLARD, X., LAMY, P. J., BRINGER, J. P., IBORRA, F., MUREZ, T., SANCHEZ, M. and MENEGAUX, F., 2017. Nonsteroidal anti-inflammatory drugs (NSAIDs) and prostate cancer risk: results from the EPICAP study. *Cancer Med.*, *6*, 2461-2470. https://doi.org/10.1002/cam4.1186

DONDELINGER, Y., DECLERCQ, W., MONTESSUIT, S., ROELANDT, R., GONCALVES, A., BRUGGEMAN, I., HULPIAU, P., WEBER, K., SEHON, C. A., MARQUIS, R. W., BERTIN, J., GOUGH, P. J., SAVVIDES, S., MARTINOU, J. C., BERTRAND, M. J. and VANDENABEELE, P., 2014. MLKL compromises plasma membrane integrity by binding to phosphatidylinositol phosphates. *Cell Rep.*, *7*, 971-81. https://doi.org/10.1016/j.celrep.2014.04.026.

DONG, Y-X., SUEDA, S., NIKAWA, J-I and KONDO, H., 2004. Characterization of the products of the genes *SNO1* and *SNZ1* involved in pyridoxine synthesis in *Saccharomyces cerevisiae*. *Eur. J. Biochem., 271*, 745-752. https://doi.org/10.1111/j.1432-1033.2003.03973.x

DOUDICAN, N. A., SONG, B., SHADEL, G. S. and DEOTSCH, P. W., 2005. Oxidative DNA damage causes mitochondrial genomic instability in *Saccharomyces cerevisiae. 25,* 5196-5204. https://doi.org/10.1128/MCB.25.12.5196-5204.2005

DRÖSE, S. and BRANDT, U., 2012. Molecular mechanisms of superoxide production by the mitochondrial respiratory chain. *Adv. Exp. Med. Biol., 748*, 145-169. https://doi.org/10.1007/978-1-4614-3573-0_6

DU, L., YU, Y., CHEN, J., LIU, Y., XIA, Y., CHEN, Q. and LIU, X., 2007. Arsenic induces caspase- and mitochondria-mediated apoptosis in *Saccharomyces cerevisiae*. *FEMS Yeast Res.*, *7*, 860-865. https://doi.org/10.1111/j.1567-1364.2007.00274.x

DU, X., FU, X., YAO, K., LAN, Z., XU, H., CUI, Q. and YANG. E., 2017. Bcl-2 delays cell cycle through mitochondrial ATP and ROS. *Cell Cycle, 16*, 707-713. https://doi.org/10.1080/15384101.2017.1295182.

DUMONT, S. and RIVOAL, J., 2019. Consequences of oxidative stress on plant glycolytic and respiratory metabolism. *Front. Plant Sci., 10,* 166. https://doi.org/10.3389/fpls.2019.00166

DURNER, J. and KLESSIG, D. F., 1995. Inhibition of ascorbate peroxidase by salicylic acid and 2,6-dichloroisonicotinic acid, two inducers of plant defense responses. *Proc. Natl. Acad. Sci. U. S. A., 92,* 11312-11316.

EASLON, E., TSANG, F., SKINNER, C., WANG, C. and LIN, S. J., 2008. The malate-aspartate NADH shuttle components are novel metabolic longevity regulators required for calorie restriction-mediated life span extension in yeast. *Genes Dev.*, *22*, 931–944. https://doi.org/10.1101/gad.1648308

EBERHART, C. E., COFFEY, R. J., RADHIKA, A., GIARDIELLO, F. M., FERRENBACH, S. and DUBOIS, R. N., 1994. Up-regulation of cyclooxygenase 2 gene expression in human colorectal adenomas and adenocarcinomas. *Gastroenterology, 107*, 1183-8.

EHRENSHAFT, M. and DAUB, M. E., 2001. Isolation of *PDX2*, a second novel gene in the pyridoxine biosynthesis pathway of eukaryotes, archaebacteria, and a subset of eubacteria. *J. Bacteriol., 183*, 3383-3390. https://doi.org/10.1128/JB.183.11.3383-3390.2001

EISENBERG, T., BÜTTNER, S., KROEMER, G. and MADEO, F. (2007). The mitochondrial pathway in yeast apoptosis. *Apoptosis*, *12*, 1011-1023.

EISENBERG, T., CARMONA-GUTIERREZ, D., BÜTTNER, S., TAVERNARAKIS, N. and MADEO, F., 2010. Necrosis in yeast. *Apoptosis*, *15*, 257-68.

EISENBERG, T., KNAUER, H., SCHAUER, A., BÜTTNER, S., RUCKENSTUHL, C., CARMONA-GUTIERREZ, D., RING, J., SCHROEDER, S., MAGNES, C., ANTONACCI, L., FUSSI, H., DESZCZ, L., HARTL, R., SCHRAML, E., CRIOLLO, A., MEGALOU, E., WEISKOPF, D., LAUN, P., HEEREN, G., BREITENBACH … MADEO, F., 2009. Induction of autophagy by spermidine promotes longevity. *Nat. Cell Biol.*, *11*, :1305-1314. https://doi.org/10.1038/ncb1975.

EL SAYED, S. M., MAHMOUD, A. A., EL SAWY, S. A., ABDELAAL, E. A., FOUAD, A. M., YOUSIF, R. S., HASHIM, M. S., HEMDAN, S. B., KADRY, Z. M., ABDELMOATY, M. A., GABR, A. G., OMRAN, F. M., NABO, M. M. and AHMED, N. S., 2013. Warburg effect increases steady-state ROS condition in cancer cells through decreasing their antioxidant capacities (anticancer effects of 3-bromopyruvate through antagonizing Warburg effect). *Med. Hypotheses.*, *81*, 866-70. https://doi.org/10.1016/j.mehy.2013.08.024.

ELDER, D. J., HALTON, D. E., HAGUE, A. and PARASKEVA, C., 1997. Induction of apoptotic cell death in human colorectal carcinoma cell lines by a cyclooxygenase-2 (COX-2)-selective nonsteroidal anti-inflammatory drug: independence from COX-2 protein expression. *Clin. Cancer Res., 3*, 1679-1683.

ELGERSMA, Y., VAN ROERMUND, C. W., WANDERS, R. J. and TABAK, H. F., 1995. Peroxisomal and mitochondrial carnitine acetyltransferases of *Saccharomyces cerevisiae* are encoded by a single gene. *EMBO J.*, *14*, 3472-3479. https://doi.org/10.1002/j.1460-2075.1995.tb07353.x

ESTERBAUER, H., SCHAUR, R. J. and ZOLLNER, H., 1991. Chemistry and biochemistry of 4-hydroxynonenal, malonaldehyde and related aldehydes. *Free Radic. Biol. Med., 11,* 81-128. https://doi.org/10.1016/0891-5849(91)90192-6

EVAN, G. I. and VOUSDEN, K. H., 2001. Proliferation, cell cycle and apoptosis in cancer. *Nature, 411*, 342-348.

EVANS, M. V., TURTON, H. E., GRANT, C. M. and DAWES, I. W., 1998. Toxicity of linoleic acid hydroperoxide to *Saccharomyces cerevisiae:* involvement of a respiration-related process for maximal sensitivity and adaptive response. *J. Bacteriol., 180,* 483-490.

FABRIZIO, P. and LONGO, V. D., 2007. The chronological life span of *Saccharomyces cerevisiae. Methods Mol. Biol., 371*, 89-95.

FADOK, V. A., VOELKER, D. R., CAMPBELL, P. A., COHEN, J. J., BRATTON, D. L. and HENSON, P. M., 1992. Exposure of phosphatidylserine on the surface of apoptotic lymphocytes triggers specific recognition and removal by macrophages. *J. Immunol., 148*, 2207-2216.

FAHRENKROG, B., SAUDER, U. and AEBI, U., 2004. The *S. cerevisiae* HtrA-like protein Nma111p is a nuclear serine protease that mediates yeast apoptosis. *J. Cell Sci., 117*, 115-126. https://doi.org/10.1242/jcs.00848

FALLETTI, O., CADET, J., FAVIER, A. and DOUKI, T., 2007. Trapping of 4-hydroxynonenal by glutathione efficiently prevents formation of DNA adducts in human cells. *Free radical biology and medicine*, *42*(8), 1258–1269. https://doi.org/10.1016/j.freeradbiomed.2007.01.024

FANG, J. and BEATTIE, D. S., 2003. External alternative NADH dehydrogenase of *Saccharomyces cerevisiae:* a potential source of superoxide. *Free Radic. Biol. Med., 34,* 478-488. https://doi.org/10.1016/s0891-5849(02)01328-x

FANNJIANG, Y., CHENG, W. C., LEE, S. J., QI, B., PEVSNER, J., MCCAFFERY, J. M., HILL, R. B., BASAÑEZ, G. and HARDWICK, J. M., 2004. Mitochondrial fission proteins regulate programmed cell death in yeast. *Genes Dev., 18*, 2785-2797.

FARAH, M. E. and AMBERG, D. C., 2007. Conserved actin cysteine residues are oxidative stress sensors that can regulate cell death in yeast. *Mol. Biol. Cell, 18*, 1359-1365. https://doi.org/10.1091/mbc.E06-08-0718

FARRUGIA, G., AZZOPARDI, M., SALIBA, C., GRECH, G., GROSS, A. S., PISTOLIC, J., BENES, V., VASSALLO, N., BORG, J., MADEO, F., EISENBERG, T. and BALZAN, R., 2019. Aspirin impairs acetyl-coenzyme A metabolism in redox-compromised yeast cells. *Sci Rep., 9*, 6152. https://doi.org/10.1038/s41598-019-39489-4.

FARRUGIA, G., BANNISTER, W. H., VASSALLO, N. and BALZAN, R., 2013. Aspirin-induced apoptosis of yeast cells is associated with mitochondrial superoxide radical accumulation and NAD(P)H oxidation. *FEMS Yeast Res., 13*, 755-768. https://doi.org/10.1111/1567-1364.12075

FEDEROVA, M., BOLLINENI, R. C. and HOFFMANN, R., 2014. Protein carbonylation as a major hallmark of oxidative damage: Update of analytical strategies. *Mass Spectrom. Rev., 33,* 79-97. https://doi.org/10.1002/mas.21381

FEHÉR, A., ÖTVÖS, K., PASTERNAK, T. P. and SZANDTNER, A. P., 2008. The involvement of reactive oxygen species (ROS) in the activation (G_0-to-G_1 transition) of plant cells. *Plant Signal. Behav., 3,* 823-826. https://doi.org/10.4161/psb.3.10.5908

FENDT, S. M., BELL, E. L., KEIBLER, M. A., OLENCHOCK, B. A., MAYERS, J. R., WASYLENKO, T. M., VOKES, N. I., GUARENTE, L., VANDER HEIDEN, M. G. and STEPHANOPOULOS, G., 2013. Reductive glutamine metabolism is a function of the α-ketoglutarate to citrate ratio in cells. *Nat. Commun., 4,* 2236. https://doi.org/10.1038/ncomms3236

FENG, Y., HE, D., YAO, Z. and Klionsky, D. J., 2014. The machinery of macroautophagy. *Cell Res., 24*, 24-41. https://doi.org/10.1038/cr.2013.168

FENTON, H. J. H., 1894. Oxidation of tartaric acid in presence of iron. *J. Chem. Soc. Trans., 65,* 899-911. https://doi.org/10.1039/ct8946500899

FERNIE, A. R., CARRARI, F. and SWEETLOVE, L. J. (2004). Respiratory metabolism: Glycolysis, the TCA cycle and mitochondrial electron transport. *Curr. Opin. Plant Biol., 7*, 254-261. https://doi.org/10.1016/j.pbi.2004.03.007

FERRANDINA, G., LAURIOLA, L., ZANNONI, G. F., FAGOTTI, A., FANFANI, F., LEGGE, F., MAGGIANO, N., GESSI, M., MANCUSO, S., RANELLETTI, F. O. and SCAMBIA, G. (2002). Increased cyclooxygenase-2 (COX-2) expression is associated with chemotherapy resistance and outcome in ovarian cancer patients. *Ann. Oncol. 13*, 1205-1211.

FERRI, K. F. and KROEMER, G. (2001). Organelle-specific initiation of cell death pathways. *Nat. Cell Biol.*, 3, E255-E263.

FILOMENI, G., DE ZIO, D. and CECCONI, F. (2015). Oxidative stress and autophagy: The clash between damage and metabolic needs. *Cell Death Differ., 22*, 377-388. https://doi.org/10.1038/cdd.2014.150

FINKEL T. (2000). Redox-dependent signal transduction. *FEBS letters, 476*, 52–54. https://doi.org/10.1016/s0014-5793(00)01669-0

FINKEL T. (2011). Signal transduction by reactive oxygen species. *J. Cell Biol., 194*, 7–15. https://doi.org/10.1083/jcb.201102095

FISER, B., JÓJÁRT, B., CSIZMADIA, I. G. and VISKOLCZ, B. (2013). Glutathione--hydroxyl radical interaction: a theoretical study on radical recognition process. *PloS One, 8*, e73652. https://doi.org/10.1371/journal.pone.0073652

FLATTERY-O'BRIEN, J. A. and DAWES, I. W. (1998). Hydrogen peroxide causes *RAD9*-dependent cell cycle arrest in G2 in *Saccharomyces cerevisiae* whereas menadione causes G1 arrest independent of *RAD9* function. *J. Biol. Chem*., *273*, 8564-8571.

FOMENKO, D. E., KOC, A., AGISHEVA, N., JACOBSEN, M., KAYA, A., MALINOUSKI, M., RUTHERFORD, J. C., SIU, K. L., JIN, D. Y., WINGE, D. R. and GLADYSHEV, V. N. (2011). Thiol peroxidases mediate specific genome-wide regulation of gene expression in response to hydrogen peroxide. *Proc. Natl. Acad. Sci. USA. 108*, 2729-2734. https://doi.org/10.1073/pnas.1010721108.

FONG, C. S., TEMPLE, M. D., ALIC, N., CHIU, J., DURCHDEWALD, M., THORPE, G. W., HIGGINS, V. J. and DAWES, I. W. (2008). Oxidant-induced cell-cycle delay in *Saccharomyces cerevisiae*: The involvement of the SWI6 transcription factor. *FEMS Yeast Res., 8*, 386-399. https://doi.org/10.1111/j.1567-1364.2007.00349.x

FORSBURG, S. L. and NURSE, P. (1991). Cell cycle regulation in the yeasts *Saccharomyces cerevisiae* and *Schizosaccharomyces pombe*. *Annu. Rev. Cell Biol*., *7*, 227-256.

FRIIS, S., RIIS, A. H., ERICHSEN, R., BARON, J. A. and SØRENSEN, H. T., 2015. Low-dose aspirin or nonsteroidal anti-inflammatory drug use and colorectal cancer risk: A population-based, case-control study. *Ann. Intern. Med.* 2015 Sep 1;163(5):347-55. https://doi/org/10.7326/M15-0039.

FRÖHLICH, K.-U., FUSSI, H., and RUCKENSTUHL, C., 2007. Yeast apoptosis – from genes to pathways. *Semin. Cancer Biol., 17,* 112-121. https://doi.org/10.1016/j.semcancer.2006.11.006

FUGE, E. K., BRAUN, E. L. and WERNER-WASHBURNE, M., 1994. Protein synthesis in long-term stationary-phase cultures of *Saccharomyces cerevisiae*. *J. Bacteriol., 176*, 5802-5813. https://doi.org/10.1128/jb.176.18.5802-5813.1994

FULDA, S., 2010. Evasion of apoptosis as a cellular stress response in cancer. *Int. J. Cell Biol.*, *2010*, 370835. https://doi.org/10.1155/2010/370835.

FULDA, S., GORMAN, A. M., HORI, O. and SAMALI, A., 2010. Cellular stress responses: cell survival and cell death. *Int. J. Cell Biol,* 2010, 214074. https://doi.org/10.1155/2010/214074.

FUNG, M. K. L. and CHAN, G. C., 2017. Drug-induced amino acid deprivation as strategy for cancer therapy. *J. Hematol. Oncol., 10*, 144. https://doi.org/10.1186/s13045-017-0509-9.

GALANO, A. and ALVAREZ-IDABOY, J. R., 2011. Glutathione: mechanism and kinetics of its non-enzymatic defence action against free radicals. *RSC Adv., 1*, 1763-1771. https://doi.org/10.1039/c1ra00474c

GALLOGLY, M. M. and MIEYAL, J. J., 2007. Mechanisms of reversible protein glutathionylation in redox signalling and oxidative stress. *Curr. Opin. Pharmacol., 7,* 381-391. https://doi.org/10.1016/j.coph.2007.06.003

GALLUZZI, L., VITALE, I., AARONSON, S. A., ABRAMS, J. M., ADAM, D., AGOSTINIS, P., … KROEMER G., 2018. Molecular mechanisms of cell death: recommendations of the Nomenclature Committee on Cell Death 2018. *Cell Death Differ. 25,* 486-541. https://doi.org/10.1038/s41418-017-0012-4.

GALPERIN, M. Y. and KOONIN, E. V. (1997). Sequence analysis of an exceptionally CONSERVED OPERON suggests enzymes for a new link between histidine and purine biosynthesis. *Mol. Microbiol., 24*, 443-445. https://doi.org/10.1046/j.1365-2958.1997.3671706.x

GAO, P., TCHERNYSHYOV, I., CHANG, T. C., LEE, Y. S., KITA, K., OCHI, T., ZELLER, K. I., DE MARZO, A. M., VAN EYK, J. E., MENDELL, J. T. and DANG, C. V., 2009. c-Myc suppression of miR-23a/b enhances mitochondrial glutaminase expression and glutamine metabolism. *Nature, 458*, 762–765. https://doi.org/10.1038/nature07823

GAO, L. AND WILLIAMS, J. L., 2012. Nitric oxide-donating aspirin induces G2/M phase cell cycle arrest in human cancer cells by regulating phase transition proteins. *Int. J. Oncol.,* 41, 325-330. https://doi.org/10.3892/ijo.2012.1455.

GASCH, A. P., SPELLMAN, P. T., KAO, C. M., CARMEL-HAREL, O., EISEN, M. B., STORZ, G., BOTSTEIN, D. and BROWN, P. O. (2000). Genomic expression programs in the response of yeast cells to environmental changes. *Mol. Biol. Cell, 11,* 4241-4257. https://doi.org/10.1091/mbc.11.12.4241

GASCHLER, M. M. and STOCKWELL, B. R. (2017). Lipid peroxidation in cell death. *Biochem. Biophys. Res. Commun., 482*, 419-425. https://doi.org/10.1016/j.bbrc.2016.10.086

GHOSH, N., DAS, A., CHAFFEE, S., ROY, S. and SEN, C. K., 2018. Reactive oxygen species, oxidative damage and cell death. In: S. Chatterjee, W. Jugraithmayr and D. Bagchi (Eds.). *Immunity and Inflammation in Health and Disease: Emerging Roles of Nutraceuticals and Functional Foods in Immune Support. (*pp. 45-55). Academic Press https://doi.org/10.1016/B978-0-12-805417-8.00004-4

GIANNATTASIO, S., ATLANTE, A., ANTONACCI, L., GUARAGNELLA, N., LATTANZIO, P., PASSARELLA, S., and MARRA, E., 2008. Cytochrome *c* is released from coupled mitochondria of yeast *en route* to acetic acid-induced programmed cell death and can work as an electron donor and a ROS scavenger. *FEBS Lett., 582,* 1519-1525. https://doi.org/10.1016/j.febslet.2008.03.048

GIANNATTASIO, S., GUARAGNELLA, N., CORTE-REAL, M., PASSARELLA, S. and MARRA, E., 2005. Acid stress adaptation protects *Saccharomyces cerevisiae* from acetic acid-induced programmed cell death. *Gene, 354,* 93-98. https://doi.org/10.1016/j.gene.2005.03.030

GODON, C. LAGNIEL, G., LEE, J., BUHLER, J. M., KIEFFER, S., PERROT, M., BOUCHERIE, H., TOLEDANO, M. B. and LABARRE, J., 1998. The H_2O_2 stimulon in *Saccharomyces cerevisiae. J. Biol. Chem, 273,* 22480-22489. https://doi.org/10.1074/jbc.273.35.22480

GOEL, A., CHANG, D. K., RICCIARDIELLO, L., GASCHE, C. and BOLAND, C. R., 2003. A novel mechanism for aspirin-mediated growth inhibition of human colon cancer cells. *Clin. Cancer Res., 9*, 383-390.

GOMES, P., SAMPAIO-MARQUES, B., LUDOVICO, P., RODRIGUES, F. and LEÃO, C., 2007. Low auxotrophy-complementing amino acid concentrations reduce yeast chronological life span. *Mech. Ageing Dev., 128*, 383-391.

GOODALL, M. L., FITZWALTER, B. E., ZAHEDI, S., WU, M., RODRIGUEZ, D., MULCAHY-LEVY, J. M., GREEN, D. R., MORGAN, M., CRAMER, S. D. and THORBURN, A., 2016. The autophagy machinery controls cell death switching between apoptosis and necroptosis. *Dev Cell*. *37*, 337-349. https://doi.org/10.1016/j.devcel.2016.04.018

GONÇALVES, A. P. and VIDEIRA, A., 2015. Mitochondrial type II NAD(P)H dehydrogenase in fungal cell death. *Microb. Cell, 2*, 68-73. https://doi.org/10.15698/mic2015.03.192

GONOS, E. S., KAPETANOU, M., SEREIKAITE, J., BARTOSZ, G., NAPARŁO, K., GRZESIK, M. and SADOWSKA-BARTOSZ, I., 2018. Origin and pathophysiology of protein carbonylation, nitration and chlorination in age-related brain diseases and aging. *Aging*, *10*, 868–901. https://doi.org/10.18632/aging.101450

GÖRNER, W., DUCRCHSCHLAG, E., MARTINEZ-PASTOR, M. T., ESTRUCH, F., AMMERER, G., HAMILTON, B., RUIS, H. and SCHULLER, C., 1998. Nuclear localization of the C2H2-zinc finger protein Msn2p is regulated by stress and protein kinase A activity. *Genes Dev., 12,* 586-597. https://doi.org/10.1101/gad.12.4.586

GOSTIMSKAYA, I. and GRANT, C. M., 2016. Yeast mitochondrial glutathione is an essential antioxidant with mitochondrial thioredoxin providing a back-up system. *Free Rad. Biol. Med.*, *94*, 55–65. https://doi.org/10.1016/j.freeradbiomed.2016.02.015

GRANT, C. M., 2001. Role of the glutathione/glutaredoxin and thioredoxin systems in yeast growth and response to stress conditions. *Mol. Microbiol., 39*, 533-541. https://doi.org/10.1046/j.1365-2958.2001.02283.x

GRANT, C. M., COLLINSON, L. P., ROSE, J.-H. and DAWES, I. W., 1996a. Yeast glutathione reductase is required for protection against oxidative stress and is a target gene for yAP-1 transcriptional regulation. *Mol. Microbiol., 21,* 171-179. https://doi.org/10.1046/j.1365-2958.1996.6351340.x

GRANT, C. M., MACIVER, F. H. and DAWES, I. W., 1996b. Glutathione is an essential metabolite required for resistance to oxidative stress in the yeast *Saccharomyces cerevisiae*. *Curr. Genet., 29*, 511-515. https://doi.org/10.1007/BF02426954

GRANT, C. M., MACIVER, F. H. and DAWES, I. W., 1997. Glutathione synthetase is dispensable for growth under both normal and oxidative stress conditions in the yeast *Saccharomyces cerevisiae* due to an accumulation of the dipeptide gamma-glutamylcysteine. *Mol. Biol. Cell.,* 8, 1699-1707.

GRANT, C. M., QUINN, K. A. and DAWES, I. W., 1999. Differential protein S-thiolation of glyceraldhyde-3-phosphate dehydrogenase isoenzymes influences sensitivity to oxidative stress. *Mol. Cell. Biol., 19*, 2650-2656. https://doi.org/10.1128/mcb.19.4.2650

GREEN, D. R. and EVAN, G. I., 2002. A matter of life and death. *Cancer Cell*, *1,* 19-30.

GREEN, D. R. and LLAMBI, F., 2015. Cell death signalling. *Cold Spring Harb. Perspect. Biol., 7*, a006080. https://doi.org/10.1101/cshperspect.a006080.

GREENSPAN, E. J., MADIGAN, J. P., BOARDMAN, L. A. and ROSENBERG, D. W., 2011. Ibuprofen inhibits activation of nuclear β-catenin in human colon adenomas and induces the phosphorylation of GSK-3β. *Cancer Prev. Res.,* 4, 161-171. https://doi.org/10.1158/1940-6207.CAPR-10-0021.

GREETHAM, D. and Grant, C. M., 2009. Antioxidant activity of the yeast mitochondrial one-Cys peroxiredoxin is dependent on thioredoxin reductase and glutathione *in vivo. Mol. Cell. Biol., 29,* 3229-3240. https://doi.org/10.1128/MCB.01918-08

GRIFFITH, O.W., 1980. Determination of glutathione and glutathione disulfide using glutathione reductase and 2-vinylpyridine. *Anal. Biochem*., 106, 207-212.

GRIFFITH, O.W., 1985. Glutathione and glutathione disulfide In H. U. Bergmeyer (Ed.), *Methods of Enzymatic Analysis*, 3rd Ed., Vol. 8., pp. 521-529. Verlag Chemie, Weinheim.

GROEGER, G., QUINEY, C. and Cotter, T. G., 2009. Hydrogen peroxide as a cell-survival signaling molecule. *Antioxid. Redox Signal.,11*, 2655-2671. https://doi.org/10.1089/ARS.2009.2728

GROSS, M. I., DEMO, S. D., DENNISON, J. B., CHEN, L., CHERNOV-ROGAN, T., GOYAL, B., JANES, J. R., LAIDIG, G. J., LEWIS, E. R., LI, J., MACKINNON, A. L., PARLATI, F., RODRIGUEZ, M. L., SHWONEK, P. J., SJOGREN, E. B., STANTON, T. F., WANG, T., YANG, J., ZHAO, F. and BENNETT, M. K., 2014. Antitumor activity of the glutaminase inhibitor CB-839 in triple-negative breast cancer. *Mol. Cancer Therap.*, *13*, 890–901. https://doi.org/10.1158/1535-7163.MCT-13-0870

GROSSER, N. and SCHRODER, H., 2003. Aspirin protects endothelial cells from oxidant damage via the nitric oxide-cGMP pathway. *Arterioscler. Thromb. Vasc. Biol., 23*, 1345-1351. https://doi.org/10.1161/01.ATV.0000083296.57581.AE

GU, Q., WANG, J. D., XIA, H. H., LIN, M. C., HE, H., ZOU, B., TU, S. P., YANG, Y., LIU, X. G., LAM. S. K., WONG, W. M., CHAN, A. O., YUEN, M. F., KUNG, H. F. and WONG, B. C., 2005. Activation of the caspase-8/Bid and Bax pathways in aspirin-induced apoptosis in gastric cancer. *Carcinogenesis, 26*, 541-546.

GUARAGNELLA, N., BOBBA, A., PASSARELLA, S., MARRA, E. and GIANNATTASIO, S, (2010a. Yeast acetic acid-induced programmed cell death can occur without cytochrome *c* release which requires metacaspase YCA1. *FEBS Lett*.¸ *584*, 224-228. doi:10.1016/j.febslet.2009.11.072

GUARAGNELLA, N., PASSARELLA, S., MARRA, E. and GIANNATTASIO, S., 2010b. Knock-out of metacaspase and/or cytochrome *c* results in the activation of a ROS-independent acetic acid-induced programmed cell death pathway in yeast. *FEBS Lett.*, 584, 3655-3660. https://doi.org/10.1016/j.febslet.2010.07.044.

GUILLAMÓN, J. M., VAN RIEL, N. A., GIUSEPPIN, M. L. and VERRIPS, C. T., 2001. The glutamate synthase (GOGAT) of *Saccharomyces cerevisiae* plays an important role in central nitrogen metabolism. *FEMS Yeast Res.*, *1,* 169-175.

GUS'KOVA, R. A., IVANOV, I. I., KOL'TOVER, V. K., AKHOBADZE, V. V. and RUBIN, A. B., 1984. Permeability of bilayer lipid membranes for superoxide (O_2^-) radicals. *Biochim. Biophys. Acta, 778,* 579-585. https://doi.org/10.1016/0005-2736(84)90409-7

HAASE, S.B. and LEW, D.J., 1997. Flow cytometric analysis of DNA content in budding yeast. *Cell Cycle Control*, 283, 322-332. https://doi.org/10.1016/s0076-6879(97)83026-1

HABER, F. and WEISS, J., 1934. The catalytic decomposition of hydrogen peroxide by iron salts. *Proc. R. Soc. Lond. A. Math*. *Phys. Sci., 147*¸ 332-351. https://doi.org/10.1098/rspa.1934.0221

HAENEN, G. R. M. M. and Bast, A., 2014. Glutathione revisited: a better scavenger than previously thought. *Front. Pharmacol., 5*, 260. https://doi.org/10.3389/fphar.2014.00260

HALLIWELL, B. and GUTTERIDGE, J. M. C., 2015. Free radicals in biology and medicine. 5th edn., New York: Oxford University Press.

HANIF, R., PITTAS, A., FENG, Y., KOUTSOS, M. I., QIAO, L., STAIANO-COICO, L., SHIFF, S. I. and Rigas, B., 1996. Effects of nonsteroidal anti-inflammatory drugs on proliferation and on induction of apoptosis in colon cancer cells by a prostaglandin-independent pathway. *Biochem. Pharmacol., 52*, 237-245.

HARDWICK, J. C., VAN SANTEN, M., VAN DEN BRINK, G. R., VAN DEVENTER, S. J. and PEPPELENBOSCH, M. P., 2004. DNA array analysis of the effects of aspirin on colon cancer cells: involvement of Rac1. *Carcinogenesis*, *25*, 1293-1298.

HARRIS, R. E., BEEBE-DONK, J., DOSS, H. and BURR DOSS, D., 2005. Aspirin, ibuprofen, and other non-steroidal anti-inflammatory drugs in cancer prevention: a critical review of non-selective COX-2 blockade. *Oncol. Rep.*, *13,* 559-583.

HARRIS, R. E., BEEBE-DONK, J. and SCHULLER, H. M., 2002. Chemoprevention of lung cancer by non-steroidal anti-inflammatory drugs among cigarette smokers. *Oncol. Rep., 9*, 693-695.

HARRIS, R. E., CHLEBOWSKI, R. T., JACKSON, R. D., FRID, D. J., ASCENSEO, J. L., ANDERSON, G., LOAR, A., RODABOUGH, R. J., WHITE, E. and MCTIERNAN, A., 2003. Breast cancer and nonsteroidal anti-inflammatory drugs: prospective results from the Women's Health Initiative. *Cancer Res.*, *63*, 6096-6101.

HARTWELL, L. H., CULOTTI, J., PRINGLE, J. R. and REID, B. J., 1974. Genetic control of the cell division cycle in yeast. *Science*, *183*, 46-51.

HARTWELL, L. H., CULOTTI, J. and REID, B. (1970). Genetic control of the cell-division cycle in yeast. I. Detection of mutants. *Proc. Natl. Acad. Sci. U. S. A.*, 66, 352-359.

HARTWELL, L. H. and WEINERT, T. A., 1989. Checkpoints: controls that ensure the order of cell cycle events. *Science, 246,* 629-634. https://doi.org/10.1126/science.2683079

HE, W., WANG, Q., SRINIVASAN, B., XU, J., PADILLA, M. T., LI, Z., WANG, X., LIU, Y., GOU, X., SHEN, H. M., XING, C. and LIN, Y., 2014. A JNK-mediated autophagy pathway that triggers c-IAP degradation and necroptosis for anticancer chemotherapy. *Oncogene*, 33, 3004-3013. https://doi.org/10.1038/onc.2013.256

HEGDE, R., SRINIVASULA, S. M., ZHANG, Z., WASSELL, R., MUKATTASH, R., CILENTI, L., DUBOIS, G., LAZEBNIK, Y., ZERVOS, A. S., FERNANDES-ALNEMRI, T. and ALNEMRI, E. S., 2002. Identification of Omi/HtrA2 as a mitochondrial apoptotic serine protease that disrupts inhibitor of apoptosis protein-caspase interaction. *J. Biol. Chem.*, *277*, 432–438. https://doi.org/10.1074/jbc.M109721200

HEKIMI, S., LAPOINTE, J. and WEN, Y., 2011. Taking a "good" look at free radicals in the aging process. *Trends Cell Biol., 21,* 569-576. https://doi/org/10.1016/j.tcb.2011.06.008.

HERKER, E., JUNGWIRTH, H., LEHMANN, K. A., MALDENER, C., FRÖHLICH, K. U., WISSING, S., BÜTTNER, S., FEHR, M., SIGRIST, S. and MADEO, F., 2004. Chronological aging leads to apoptosis in yeast. *J. Cell Biol.*, *164*, 501–507. https://doi.org/10.1083/jcb.200310014

HERMANN, M., KAPIOTIS, S., HOFBAUER, R., SEELOS, C., HELD, I. and GMEINER, B., 1999. Salicylate promotes myeloperoxidase-initiated LDL oxidation: antagonization by its metabolite gentisic acid. *Free Radic. Biol. Med., 26*, 1253-1260. https://doi.org/10.1016/S0891-5849(98)00322-0

HERRERA-VÁSQUEZ, A., SALINAS, P. and HOLUIGUE, L., 2015. Salicylic acid and reactive oxygen species interplay in the transcriptional control of defense genes expression. *Front. Plant Sci.*, 6, 171. https://doi.org/10.3389/fpls.2015.00171.

HIDA, T., YATABE, Y., ACHIWA, H., MURAMATSU, H., KOZAKI, K., NAKAMURA, S., OGAWA, M., MITSUDOMI, T., SUGIURA, T. and TAKAHASHI, T., 1998. Increased expression of cyclooxygenase 2 occurs frequently in human lung cancers, specifically in adenocarcinomas. *Cancer Res., 58*, 3761-4.

HILTUNEN, J. K., MURSULA, A. M., ROTTENSTEINER, H., WIERENGA, R. K., KASTANIOTIS, A. J. and GURITZ, A., 2003. The biochemistry of peroxisomal β-oxidation in the yeast *Saccharomyces cerevisiae. FEMS Microbiol. Rev., 27,* 35-64. https://doi.org/10.1016/s0168-6445(03)00017-2

HIRAO, A., KONG, Y-Y., MATSUOKA, S., WAKEHAM, A., RULAND, J., YOSHIDA, H., LIU, D., ELLEDGE, J. and MAK, T. W., 2000) DNA damage-induced activation of p53 by the checkpoint kinase Chk2. *Science*, *287*, 1824-1827. https://doi.org/10.1126/science.287.5459.1824

HLAVATÁ, L., NACHIN, L., JEŽEK, P. and NYSTRÖM, T., 2008. Elevated Ras/protein kinase A activity in *Saccharomyces cerevisiae* reduces proliferation rate and lifespan by two different reactive oxygen species-dependent routes. *Aging Cell, 7*, 148-157. https://doi.org/10.111/j.1474-9726.2007.00361.x

HO, Y. H., SHISHKOVA, E., HOSE, J., COON, J. J. and GASCH, A. P., 2018. Decoupling yeast cell division and stress defense implicates mRNA repression in translational reallocation during stress. *Curr. Biol.*, *28*, 2673-2680. https://doi.org/10.1016/j.cub.2018.06.044.

HOCKENBERY, D. M., OLTVAI, Z. N., YIN, X.-M., MILLIMAN, C. L. and Korsmeyer, S. J., 1993. Bcl-2 functions in an antioxidant pathway to prevent apoptosis. *Cell, 75*, 241-51; http://dx.doi.org/10.1016/0092-8674(93)80066-N

HOFMAN-BANG, J., 1999. Nitrogen catabolite repression in *Saccharomyces cerevisiae. Mol. Biotechnol., 12*, 35-73.

HOLLER, N., ZARU, R., MICHEAU, O., THOME, M., ATTINGER, A., VALITUTTI, S., BODMER, J. L., SCHNEIDER, P., SEED, B. and TSCHOPP, J., 2000. Fas triggers an alternative, caspase-8-independent cell death pathway using the kinase RIP as effector molecule. *Nat. Immunol.*, *1*, 489-95.

HORVATH, S. E. and DAUM, G., 2013. Lipids of mitochondria. *Prog. Lipid Res., 52,* 590-614. https://doi.org/10.1016/j.plipres.2013.07.002

HOSIOS, A. M. and VANDER HEIDEN, M. G., 2018. The redox requirements of proliferating mammalian cells. *J. Biol. Chem. 293*, 7490-7498. https://doi.org/10.1074/jbc.TM117.000239.

HOSSAIN, M. A., KIM, D. H., JANG, J. Y., KANG, Y. J., YOON, J. H., MOON, J. O., CHUNG, H. Y., KIM, G. Y., CHOI, Y. H., COPPLE, B. L. and KIM, N. D., 2012. Aspirin induces apoptosis *in vitro* and inhibits tumor growth of human hepatocellular carcinoma cells in a nude mouse xenograft model. *Int. J. Oncol., 40*, 1298-304. https://doi.org/10.3892/ijo.2011.1304.

HU, H., HAN, T., ZHUO, M., WU, L. L., YUAN, C., WU, L., LEI, W., JIAO, F. and WANG, L. W., 2017. Elevated COX-2 expression promotes angiogenesis through EGFR/p38-MAPK/Sp1-dependent signalling in pancreatic cancer. *Sci. Rep., 7,* 470. https://doi.org/10.1038/s41598-017-00288-4.

HU, W., ZHANG, C., WU, R., SUN, Y., LEVINE, A. and FENG, Z., 2010. Glutaminase 2, a novel p53 target gene regulating energy metabolism and antioxidant function. *Proc. Natl. Acad. Sci. U. S. A., 107*, 7455–7460. https://doi.org/10.1073/pnas.1001006107

HUANG, Y. C., CHUANG, L. Y. and HUNG, W. C., 2002. Mechanisms underlying nonsteroidal anti-inflammatory drug-induced p27Kip1 expression. *Mol. Pharmacol., 62*, 1515-1521. https://doi.org/10.1124/mol.62.6.1515

HUH, W. K., LEE, B. H., KIM, S. T., KIM, Y. R., RHIE, G. E., BAEK, Y. W., HWANG, C. S., LEE, J. S. and KANG, S. O., 1998. D-erythroascorbic acid is an important antioxidant molecule in *Saccharomyces cerevisiae. Mol. Microbiol., 30,* 895-903. https://doi.org/10.1046/j.1365-2958.1998.01133.x

HWANG, D., SCOLLARD, D., BYRNE, J. and LEVINE, E., 1998. Expression of cyclooxygenase-1 and cyclooxygenase-2 in human breast cancer. *J. Natl. Cancer Inst*., *90*, 455-460.

IMOTO, Y., YOSHIDA, Y., YAGISAWA, F., KUROIWA, H. and KUROIWA, T., 2011. The cell cycle, including the mitotic cycle and organelle division cycles, as revealed by cytological observations. *J. Electron Microsc. (Tokyo), 60,* S117-S136. https://doi.org/10.1093/jmicro/dfr034

INAI, Y. and NISHIKIMI, M., 2002. Increased degradation of oxidized proteins in yeast defective in 26S proteasome assembly. *Arch. Biochem. Biophys., 404,* 279-284. https://doi.org/10.1016/s0003-9861(02)00336-3

INOUE, Y., MATSUDA, T., SUGIYAMA, K-I, IZAWA, S. and KIMURA, A., 1999. Genetic analysis of glutathione peroxidase in oxidative stress response of *Saccharomyces cerevisiae*. *J. Biol. Chem., 274*, 27002-27009. https://doi.org/10.1074/jbc.274.38.27002

IRAQUI, I., KIENDA, G., SOEUR, J., FAYE, G., BALDACCI, G., KOLODNER, R. D. and HUANG, M. E., 2009. Peroxiredoxin Tsa1 is the key peroxidase suppressing genome instability and protecting against cell death in *Saccharomyces cerevisiae. PLoS Genet*., *5*, e1000524. https://doi.org/10.1371/journal.pgen.1000524

ISHIKAWA, H., WAKABAYASHI, K., SUZUKI, S., MUTOH, M., HIRATA, K., NAKAMURA, T., TAKEYAMA, I., KAWANO, A., GONDO, N., ABE, T., TOKUDOME, S., GOTO, C., MATSUURA, N. and SAKAI, T., 2013. Preventive effects of low-dose aspirin on colorectal adenoma growth in patients with familial adenomatous polyposis: double-blind, randomized clinical trial. *Cancer Med.,* 2, 50-56. https://doi.org/10.1002/cam4.46.

IZAWA, S., MAEDA, K., SUGIYAMA, K., MANO, J., INOUE, Y. and KIMURA, A., 1999. Thioredoxin deficiency causes the constitutive activation of Yap1, an AP-1-like transcription factor in *Saccharomyces cerevisiae. J. Biol. Chem., 274,* 28459-28565. https://doi.org/10.1074/jbc.274.40.28459

JAIN, S. K. and LIM, G., 2001. Pyridoxine and pyridoxamine inhibit superoxide radicals and prevent lipid peroxidation, protein glycolysation, and $(Na^{++}K^{++})$-ATPase activity reduction in high glucose-treated human erythrocytes. *Free Radic. Biol. Med., 30*, 232-237

JAMIESON, D. J., 1992. *Saccharomyces cerevisiae* has distinct adaptive response to both hydrogen peroxide and menadione. *J. Bacteriol., 174,* 6678-6681.

JAMNIK, P. and RASPOR, P., 2005. Methods for monitoring oxidative stress response in yeasts. *J. Biochem. Mol. Toxicol., 19*, 195-203. https://doi.org/10.1002/jbt.20091

JANUMYAN, Y., CUI, Q., YAN, L., SANSAM, C. G., VALENTIN, M. and YANG, E., 2008. G0 function of BCL2 and BCL-xL requires BAX, BAK, and p27 phosphorylation by Mirk, revealing a novel role of BAX and BAK in quiescence regulation. *J. Biol. Chem., 2*83, 34108-34120. http://dx.doi.org/10.1074/jbc.M806294200

JANUMYAN, Y. M., SANSAM, C. G., CHATTOPADHYAY, A., CHENG, N., SOUCIE, E. L., PENN, L. Z., ANDREWS, D., KNUDSON, C. M. and YANG, E., 2003. Bcl-xL/Bcl-2 coordinately regulates apoptosis, cell cycle arrest and cell cycle entry. *EMBO J.*, 22, 5459-5470. http://dx.doi.org/10.1093/emboj/cdg533

JEGGO, P. A. and LOBRICH, M., 2007. DNA double-strand breaks: Their cellular and clinical impact? *Oncogene, 26*, 7717-7719. https://doi.org/10.1038/sj.onc.1210868

JIANG, J., SRIVASTAVA, S. and ZHANG, J., 2019. Starve cancer cells of glutamine: Break the spell or make a hungry monster? *Cancers*, *11*, E804. https://doi.org/10.3390/cancers11060804.

JONCKHEERE, A. I., SMEITINK, J. A. and RODENBURG, R. J., 2012. Mitochondrial ATP synthase: architecture, function and pathology. *J. Inherit. Metab. Dis*.,*35*, 211-25. https://doi.org/10.1007/s10545-011-9382-9.

JONES, D. P., 2002. Redox potential of GSH/GSSG couple: assay and biological significance. *Methods Enzymol*., *348*, 93-112.

JONES, R. P. and GREENFIELD, P. F., 1987. Ethanol and the fluidity of the yeast plasma membrane. *3*, 223-232. https://doi.org/10.1002/yea.320030403

JUNG, Y. R., KIM, E. J., CHOI, H. J., PARK, J-J., KIM, H-S., LEE, Y-J., PARK, M-J. and LEE, M., 2015. Aspirin targets SIRT1 and AMPK to induce senescence of colorectal carcinoma cells. *Mol. Pharmacol., 88*, 708-719. https://doi.org/10.1124/mol.115.098616

JÜRGENSMEIER, J. M., KRAJEWSKI, S., ARMSTRONG, R. C., WILSON, G. M., OLTERSDORF, T., FRITZ, L. C., REED, J. C. and OTTILIE, S., 1997. Bax- and bak-induced cell death in the fission yeast *Schizosaccharomyces pombe*. *Mol. Biol. Cell, 8*, 325-339.

KAGAN, V. E., TYURIN, V. A., JIANG, J., TYRUINA, Y. Y., RITOV, V. B., AMOSCATO, A. A., OSIPOV, N., BELIKOVA, N. A., KAPRALOV, A. A., KINI, V., VLASOVA, I. I., ZHAO, Q., ZOU, M., DI, P., SYISTUNENKO, D. A., KURNIKOV, I. V. and BORISENKO, G. G., 2005. Cytochrome *c* acts as a cardiolipin oxygenase required for release of proapoptotic factors. *Nat. Chem. Biol., 1*, 223-232. https://doi.org/10.1038/nchembio727

KALUCKA, J., MISSIAEN, R., GEORGIADOU, M., SCHOORS, S., LANGE, C., DE BOCK, K., DEWERCHIN, M. and CARMELIET, P., 2015. Metabolic control of the cell cycle. *Cell Cycle*, *14*, 3379-88. https://doi.org/10.1080/15384101.2015.1090068.

KANE, D. J., SARAFIAN, T. A., ANTON, R., HAHN, H., GRALLA, E. B., VALENTINE, J. S., ORD, T. and BREDESEN, D. E., 1993. Bcl-2 inhibition of neural death: decreased generation of reactive oxygen species. *Science,* 262, 1274-1277. http://dx.doi.org/10.1126/science.8235659

KANKI, T. and KLIONSKY, D. J., 2008. Mitophagy in yeast occurs through a selective mechanism. *J. Biol. Chem., 283,* 32386-32393. https://doi.org/10.1074/jbc.M802403200

KANNAN, K. and JAIN, S. K., 2004. Effect of vitamin B6 on oxygen radicals, mitochondrial membrane potential, and lipid peroxidation in H_2O_2-treated U937 monocytes. *Free Radic. Biol. Med., 36,* 423-428

KAPLAN, E. H., KENNEDY, J. and DAVIS, J., 1954. Effects of salicylate and other benzoates on oxidative enzymes of the tricarboxylic acid cycle in rat tissue homogenates. *Arch. Biochem Biophys. 51*, 47-61.

KASHFI, K., 2015. Utility of nitric oxide and hydrogen sulfide-releasing chimeras as anticancer agents. *Redox Biol*., *5*, 420. https://doi.org/10.1016/j.redox.2015.09.030.

KATAOKA, T., POWERS, S., MCGILL, C., FASANO, O., STRATHERN, J., BROACH, J. and WIGLER, M. (1984). Genetic analysis of yeast *RAS1* and *RAS2* genes. *Cell, 37*, 437-445. https://doi.org/10.1016/0092-8674(84)90374-X

KAWAMORI, T., UCHIYA, N., SUGIMURA, T. and WAKABAYASHI, K., 2003. Enhancement of colon carcinogenesis by prostaglandin E2 administration. *Carcinogenesis*, *24*, 985-990.

KAZEMZADEH, L., CVIJOVIC, M. and PETRANOVIC, D., 2012. Boolean model of yeast apoptosis as a tool to study yeast and human apoptotic regulations. *Front. Physiol., 3*, 446. https://doi.org/10.3389/fphys.2012.00446

KE, J., YANG, Y., CHE, Q., JIANG, F., WANG, H., CHEN, Z., ZHU, M., TONG, H., ZHANG, H., YAN, X., WANG, X., WANG, F., LIU, Y., DAI, C. and WAN, X., 2016. Prostaglandin E2 (PGE2) promotes proliferation and invasion by enhancing SUMO-1 activity via EP4 receptor in endometrial cancer. *Tumour Biol.*, 37, 12203-12211.

KEHRER, J. P., 2000. Cause-effect of oxidative stress and apoptosis. *Teratology, 62*, 235-236. https://doi.org/10.1002/1096-9926(200010)62:4<235::AID-TERA11>3.0.CO;2-3

KHAN, M. A., CHOCK, P. B. and STADTMAN, E. R., 2005. Knockout of caspase-like gene, *YCA1*, abrogates apoptosis and elevates oxidized proteins in *Saccharomyces cerevisiae*. *Proc. Natl. Acad. Sci. U. S. A., 102,* 17326-31

KHARAZIHA, P., CHIOUREAS, D., BALTATZIS, G., FONSECA, P., RODRIGUEZ, P., GOGVADZE, V., LENNARTSSON, L., BJÖRKLUND, A. C., ZHIVOTOVSKY, B., GRANDÉR, D., EGEVAD, L., NILSSON, S. and PANARETAKIS, T., 2015. Sorafenib-induced defective autophagy promotes cell death by necroptosis. *Oncotarget*, 6, 37066-37082. https://doi.org/10.18632/oncotarget.5797

KHOURY, C. M., YANG, Z., LI, X. Y., VIGNALI, M., FIELDS, S. and GREENWOOD, M. T., 2008. A TSC22-like motif defines a novel antiapoptotic protein family. *FEMS Yeast Res., 8*, 540-563. https://doi.org/10.1111/j.1567-1364.2008.00367.x

KIM, I. S., HY, S. and JIN, I., 2011. Adaptive stress response to menadione-induce oxidative stress in *Saccharomyces cerevisiae KNU5377. J. Microbiol., 49,* 816-823. https://doi.org/10.1007/s12275-011-1154-6

KIM, J.-H., SEDLAK, M., GAO, Q., RILEY, C. P., REGNIER, F. E. and ADAMEC, J., 2010. Dynamics of protein damage in yeast frataxin mutant exposed to oxidative stress. *OMICS, 14*, 689-699. https://https.doi.org/10.1089/omi.2010.0051

KIM, S., SHORE, D. L., WILSON, L. E., SANNIEZ, E. I., KIM, J. H., TAYLOR, J. A. and SANDLER, D. P., 2015. Lifetime use of nonsteroidal anti-inflammatory drugs and breast cancer risk: results from a prospective study of women with a sister with breast cancer. *BMC Cancer.,* 15, 960. https://doi.org/10.1186/s12885-015-1979-1.

KING, K. L. and CIDLOWSKI, J. A., 1998. Cell cycle regulation and apoptosis. *Annu. Rev. Physiol., 60*, 601-617.

KLEIN, M., SWINNEN, S., THEVELEIN, J. M. and NEVOIGT, E., 2017. Glycerol metabolism and transport in yeast and fungi: Established knowledge and ambiguities. *Env. Microbiol., 19*, 878-893. https://doi.org/10.1111/1462-2920.13617

KLESSIG, D. F., DURNER, J., NOAD, R., NAVARRE, D. A., WENDEHENNE, D., KUMAR, D., ZHOU, J. M., SHAH, J., ZHANG, S., KACHROO, P., TRIFA, Y., PONTIER, D., LAM, E. and SILVA, H., 2000. Nitric oxide and salicylic acid signaling in plant defense. *Proc. Natl. Acad. Sci. USA, 97*, 8849-8855. https://doi.org/10.1073/pnas.97.16.8849

KNÖCKEL, J., MÜLLER, I. B.B, BUTZLOFF, S., BERGMANN, B., WALTER, R. D. and WRENGER, C., 2012. The antioxidative effect of the *de novo* generated vitamin B_6 in *Plasmodium falciparium* validated by protein interreference. *Biochem. J., 443,* 397-405. https://doi.org/10.1042/BJ20111542

KNORRE, D. A., SMIRNOVA, E. A. and SEVERIN, F. F., 2005. Natural conditions inducing programmed cell death in the yeast *Saccharomyces cerevisiae*. *Biochemistry* (*Mosc*), *70*, 264-266.

KOELINK, P. J., MIEREMET-OOMS, M. A., CORVER, W. E., WOLANIN, K., HOMMES, D. W., LAMERS, C. B. and VERSPAGET, H. W., 2010. 5-aminosalicylic acid interferes in the cell cycle of colorectal cancer cells and induces cell death modes. *Inflamm. Bowel Dis*., 16, 379-389. https://doi.org/10.1002/ibd.21086.

KOGA, H., SAKISAKA, S., OHISHI, M., KAWAGUCHI, T., TANIGUCHI, E., SASATOMI, K., HARADA, M., KUSABA, T., TANAKA, M., KIMURA, R., NAKASHIMA, Y., NAKASHIMA, O., KOJIRO, M., KUROHIJI, T., and SATA, M., 1999. Expression of cyclooxygenase-2 in human hepatocellular carcinoma: relevance to tumor dedifferentiation. *Hepatology, 29*, 688-696.

KÖNCZÖL, M., WEISS, A., STANGENBERG, E., GMINSKI, R., GARCIA-KÄUFER, M., GIERÉ, R., MERFORT, I. and MERSCH-SUNDERMANN, V., 2013. Cell-cycle changes and oxidative stress response to magnetite in A549 human lung cells. *Chem. Res. Toxicol.*, *26*, 693-702. https://doi.org/10.1021/tx300503q

KORANGATH, P., TEO, W. W., SADIK, H., HAN, L., MORI, N., HUIJTS, C. M., WILDES, F., BHARTI, S., ZHANG, Z., SANTA-MARIA, C. A., TSAI, H., DANG, C. V., STEARNS, V., BHUJWALLA, Z. M. and SUKUMAR, S., 2015. Targeting glutamine metabolism in breast cancer with aminooxyacetate. *Clin. Cancer Res*., 21, 3263-3273. https://doi.org/10.1158/1078-0432.CCR-14-1200. Epub 2015

KOROVILA, I., HUGO, M., CASTRO, J. P., WEBER, D., HOHN, A., GRUNE, T. and JUNG, T., 2017. Proteostasis, oxidative stress and aging. *Redox Biol., 13,* 550-567. https://doi.org/10.1016/j.redox.2017.07.008

KORYTOWSKI, W., BASOVA, L. V., PILAT, A., KERNSTOCK, R. M. and GIROTTI, A. W., 2011. Permeabilization of the mitochondrial outer membrane by Bax/truncated Bid (tBid) proteins as sensitized by cardiolipin hydroperoxide translocation: Mechanistic implications for the intrinsic pathway of oxidative apoptosis. *J. Biol. Chem., 286*, 26334-26343. https://doi.org/10.1074/jbc.M110.188516

KRATZER, S. and SCHÜLLER, H. J., 1995. Carbon source-dependent regulation of the acetyl-coenzyme A synthetase-encoding gene ACS1 from *Saccharomyces cerevisiae. Gene*, *161*, 75–79. https://doi.org/10.1016/0378-1119(95)00289-i

KREMS, B., CHARIZANIS, C. and ENTIAN, K. D., 1996. The response regulator-like protein Pos9/Skn7 of *Saccharomyces cerevisiae* is involved in oxidative stress resistance. *Curr. Genet., 29,* 327-334. https://doi.org/10.1007/bf02208613

KUGE, S. and JONES, N., 1994. *YAP1* dependent activation of *TRX2* is essential for the response of *Saccharomyces cerevisiae* to oxidative stress by hydroperoxides. *EMBO J., 13,* 655-664. https://doi.org/10.1002/j.1460-2075.1994.tb06304.x

KUGE, S., JONES, N. and NOMOTO, A., 1997. Regulation of yAP-1 nuclear localization in response to oxidative stress. *EMBO J., 16*, 1710-1720. https://doi.org/10.1093/emboj/16.7.1710

KUMAR, A., VISHVAKARMA, N. K., TYAGI, A., BHARTI, A. C. and SINGH, S. M., 2012. Anti-neoplastic action of aspirin against a T-cell lymphoma involves an alteration in the tumour microenvironment and regulation of tumour cell survival. *Biosci. Rep.*, *32*, 91–104. https://doi.org/10.1042/BSR20110027

KUMARI, S., BADANA, A. K., G, M. M., G, S. and MALLA, R., 2018. Reactive oxygen species: A key constituent in cancer survival. *Biomark. insights*, *13*, 1177271918755391. https://doi.org/10.1177/1177271918755391

LAI, M. Y., HUANG, J. A., LIANG, Z. H., JIANG, H. X. and TANG, G. D., 2008. Mechanisms underlying aspirin-mediated growth inhibition and apoptosis induction of cyclooxygenase-2 negative colon cancer cell line SW480. *World J. Gastroenterol., 14*, 4227-4233.

LAMPA, M., ARLT, H., HE, T., OSPINA, B., REEVES, J., ZHANG, B., MURTIE, J., DENG, G., BARBERIS, C., HOFFMANN, D., CHENG, H., POLLARD, J., WINTER, C., RICHON, V., GARCIA-ESCHEVERRIA, C., ADRIAN, F., WIEDERSCHAIN, D. and SRINIVASAN, L., 2017. Glutaminase is essential for the growth of triple-negative breast cancer cells with a deregulated glutamine metabolism pathway and its suppression synergizes with mTOR inhibition. *PloS One*, *12*, e0185092. https://doi.org/10.1371/journal.pone.0185092

LANDSKRON, G., DE LA FUENTE, M., THUWAJIT, P., THUWAJIT, C. and HERMOSO, M. A., 2014. Chronic inflammation and cytokines in the tumor microenvironment. *J. Immunol. Res.,* 2014, 149185. https://doi.org/10.1155/2014/149185.

LANE N., 2002. Oxygen-the Molecule that made the World. Oxford: Oxford University Press, London.

LARSSON, C., PÅHLMAN, I. L., ANSELL, R., RIGOULET, M., ADLER, L. and GUSTAFSSON, L., 1998. The importance of the glycerol 3-phosphate shuttle during aerobic growth of *Saccharomyces cerevisiae. Yeast*, *14*, 347–357. https://doi.org/10.1002/(SICI)1097-0061(19980315)14:4<347::AID-YEA226>3.0.CO;2-9

LAU, E., TSUJI, T., GUO, L., LU, S-H. and JIANG, W., 2007. The role of pre-replicative complex (pre-RC) components in oncogenesis. *FASEB J., 21*, 3786-3794. https://doi.org/10.1096/fj.07-8900rev

LAUN, P., PICHOVA, A., MADEO, F., FUCHS, J., ELLINGER, A., KOHLWEIN, S., DAWES, I., FRÖHLICH, K. U. and BREITENBACH, M., 2001. Aged mother cells of *Saccharomyces cerevisiae* show markers of oxidative stress and apoptosis. *Mol. Microbiol.,39,* 1166-1173.

LE, A., LANE, A. N., HAMAKER, M., BOSE, S., GOUW, A., BARBI, J., TSUKAMOTO, T., ROJAS, C. J., SLUSHER, B. S., ZHANG, H., ZIMMERMAN, L. J., LIEBLER, D. C., SLEBOS, R. J., LORKIEWICZ, P. K., HIGASHI, R. M., FAN, T. W. and DANG, C. V., 2012. Glucose-independent glutamine metabolism via TCA cycling for proliferation and survival in B cells. *Cell metabolism*, *15*(1), 110–121. https://doi.org/10.1016/j.cmet.2011.12.009

LE MOAN, N., CLEMENT, G., LE MAOUT, S., TACNET, F. and TOLEDANO, M. B., 2006. The *Saccharomyces cerevisiae* proteome of oxidised protein thiols: Contrasted functions for the thioredoxin and glutathione pathways. *J. Biol. Chem., 281,* 10420-10430. https://doi.org/10.1074/jbc.M513346200

LEADSHAM, J. E., MILLER, K., AYSCOUGH, K. R., COLOMBO, S., MARTEGANI, E., SUDBERY, P. and GOURLAY, C. W., 2009. Whi2p links nutritional sensing to actin-dependent Ras-cAMP-PKA regulation and apoptosis in yeast. *J. Cell Sci., 122*, 706-715. https://doi.org/10.1242/jcs.042424

LEADSHAM, J. E., SANDERS, G., GIANNAKI, S., BASTOW, E. L., HUTTON, R., NAEIMI, W. R., BREITENBACH, M. and GOURLAY, C. W., 2013. Loss of cytochrome *c* oxidase promotes RAS-dependent ROS production from the ER resident NADPH oxidase, Yno1p, in yeast. *Cell Metab., 18*, 279-286. https://doi.org/10.1016/j.cmet.2013.07.005

LEE, E. F., HARRIS, T. J., TRAN, S., EVANGELISTA, M., ARULANANDA, S., JOHN, T., RAMNAC, C., HOBBS, C., ZHU, H., GUNASINGH, G., SEGAL, D., BEHREN, A., CEBON, J., DOBROVIC, A., MARIADASON, J. M., STRASSER, A., ROHRBECK, L., HAASS, N. K., HEROLD, M. J. and FAIRLIE, W. D., 2019. BCL-XL and MCL-1 are the key BCL-2 family proteins in melanoma cell survival. *Cell Death Dis*., *10*, 342. https://doi.org/10.1038/s41419-019-1568-3.

LEE, J., GODON, C., LAGNIEL, G., SPECTOR, D., GARIN, J., LABARRE, J. and TOLEDANO, M. B., 1999. Yap1 and Skn7 control two specialized oxidative stress response regulons in yeast. *J. Biol. Chem., 274*, 16040-16046. https://doi.org/10.1074/jbc.274.23.16040

LEE, R. E. C., BRUNETTE, S., PUENTE, L. G. and Megeney, L. A., 2010. Metacaspase Yca1 is required for clearance of insoluble protein aggregates. *Proc. Natl. Acad. Sci. U.S.A., 107,* 13348-13353. https://doi.org/10.1073/pnas.1006610107

LEE, R. E. C., PUENTE, L. G., KAERN, M. and MEGENEY, L. A., 2008. A non-death role of the yeast metacaspase: Yca1p alters cell cycle dynamics. *PloS One, 3*, e2956. https://doi.org/10.1371/journal.pone.0002956

LEE, Y. J., HOE, K. L. and MAENG, P. J., 2007. Yeast cells lacking the *CIT1*-encoded mitochondrial citrate synthase are hypersusceptible to heat- or aging-induced apoptosis. *Mol. Biol. Cell*, *18,* 3556-3567.

LEE, Y. J., KIM, K. J., KANG, H. Y., KIM, H. R. and MAENG, P. J., 2012. Involvement of *GDH3*-encoded NADP+-dependent glutamate dehydrogenase in yeast cell resistance to stress-induced apoptosis in stationary phase cells. *J. Biol. Chem., 287*, 44221-44233. https://doi.org/10.1074/jbc.M112.375360

LEMASTERS, J. J., 2005. Selective mitochondrial autophagy, or mitophagy, as a targeted defence against oxidative stress, mitochondrial dysfunction, and aging. *Rejuvenation Res., 8,* 3-5. https://doi.org/10.1089/rej.2005.8.3

LEMASTERS, J. J., QIAN, T., HE, L., KIM, J. S., ELMORE, S. P., CASCIO, W. E. and BRENNER, D. A., 2002. Role of mitochondrial inner membrane permeabilization in necrotic cell death, apoptosis, and autophagy. *Antioxid. Redox Signal., 4*, 769–781. https://doi.org/10.1089/152308602760598918

LEMIRE B. D. and OYEDOTUN K. S., 2002. The *Saccharomyces cerevisiae* mitochondrial succinate:ubiquinone oxidoreductase. *Biochim. Biophys. Acta*. *1553*, 102-116. https://doi.org/10.1016/s0005-2728(01)00229-8

LEROY, C., MANN, C. and MARSOLIER, M.-C., 2001. Silent repair accounts for cell cycle specificity in the signaling of oxidative DNA lesions. *EMBO J., 20*, 2896-2906. https://doi.org/10.1093/emboj/20.11.2896

LI, P., NIJHAWAN, D., BUDIHARDJO, I., SRINIVASULA, S. M., AHMAD, M., ALNEMRI, E. S. and WANG, X., 1997. Cytochrome *c* and dATP-dependent formation of Apaf-1/caspase-9 complex initiates an apoptotic protease cascade. *Cell*, *91*, 479-489.

LI, W., SUN, L., LIANG, Q., WENG, J., MO, W. and ZHOU, B., 2006. Yeast AMID homologue Ndi1p displays respiration-restricted apoptotic activity and is involved in chronological aging. *Mol. Biol. Cell, 17,* 1802-1811. https://doi.org/10.1091/mbc.E05-04-0333

LIANG, Q. and ZHOU, B., 2007. Copper and manganese induce yeast apoptosis *via* differentpathways. *Mol Biol Cell*., *12*, 4741-4749.

LIGR, M., MADEO, F., FRÖHLICH, E., HILT, W., FRÖHLICH, K. U. and WOLF, D. H., 1998. Mammalian Bax triggers apoptotic changes in yeast. *FEBS Lett., 438*, 61-65. https://doi.org/10.1016/S0014-5793(98)01227-7

LINETTE, G. P., LI, Y., ROTH, K. and KORSMEYER, S. J., 1996. Cross talk between cell death and cell cycle progression: BCL-2 regulates NFAT-mediated activation. *Proc. Natl. Acad. Sci.U. S. A*, *93*, 9545–9552. https://doi.org/10.1073/pnas.93.18.9545

LIU, C. C. and Chen, R. H., 2016. KLHL20 links the ubiquitin-proteasome system to autophagy termination. *Autophagy*, *12*, 890–891. https://doi.org/10.1080/15548627.2016.1157243

LIVNAT-LEVANON, N., KEVEI, E., KRUTAUZ, D., SEGREF, A., RINALDI, T., ERPAPAZOGLOU, Z., COHEN, M., REIS, N., HOPPE, T. and GLICKMAN, M. H., 2014. Reversible 26S proteasome disassembly upon mitochondrial stress. *Cell Rep., 7,* 1371-1380. https://doi.org/10.1016/j.celrep.2014.04.030

LLOYD, D., MORRELL, S., CARLSEN, H. N., DEGN, H., JAMES, P. E. and ROWLANDS, C. C., 1993. Effects of growth with ethanol on fermentation and membrane fluidity of *Saccharomyces cerevisiae. Yeast, 9,* 825-833. https://doi.org/10.1002/yea.320090803

LOGAN, R. F., GRAINGE, M. J., SHEPHERD, V. C., ARMITAGE, N. C. and MUIR, K. R., 2008. Aspirin and folic acid for the prevention of recurrent colorectal adenomas. *Gastroenterology*, *134*, 29-38.

LOGUE, S. E. and MARTIN, S. J., 2008. Caspase activation cascades in apoptosis. *Biochem. Soc. Trans.,* 36, 1-9. https://doi.org/10.1042/BST0360001

LONGO, V. D., ELLERBY, L. M., BREDESEN, D. E., VALENTINE, J. S. and GRALLA, E. B., 1997. Human Bcl-2 reverses survival defects in yeast lacking superoxide dismutase and delays death of wild-type yeast. *J. Cell Biol., 137*, 1581-1588.

LONGO, V. D., GRALLA, E. B. and VALENTINE, J. S., 1996. Superoxide dismutase activity is essential for stationary phase survival in *Saccharomyces cerevisiae*. Mitochondrial production of toxic oxygen species *in vivo. J. Biol. Chem, 271,* 12275-12280. https://doi.org/10.1074/jbc.271.21.12275

LONGO, V. D., LIOU, L. L., VALENTINE, J. S. and GRALLA, E. B., 1999. Mitochondrial superoxide decreases yeast survival in stationary phase. *Arch. Biochem. Biophys., 365,* 131-142. https://doi.org/10.1006/abbi.1999.1158

LOWE, S. W. and LIN, A. W., 2000. Apoptosis in cancer. *Carcinogenesis*, *21*, 485-95.

LU, M., STROHECKER, A., CHEN, F., KWAN, T., BOSMAN, J., JORDAN, V. C. and CRYNS, V. L., 2008. Aspirin sensitizes cancer cells to TRAIL-induced apoptosis by reducing survivin levels. *Clin. Cancer Res., 14*, 3168-3176. https://doi.org/10.1158/1078-0432.CCR-07-4362.

LUCIANI, M. G., CAMPREGHER, C. and GASCHE, C., 2007. Aspirin blocks proliferation in colon cells by inducing a G1 arrest and apoptosis through activation of the checkpoint kinase ATM. *Carcinogenesis*, *28*, 2207-2217.

LUDOVICO, P., RODRIGUES, F., ALMEIDA, A., SILVA, M. T., BARRIENTOS, A. and CÔRTE-REAL, M., 2002. Cytochrome *c* release and mitochondria involvement in programmed cell death induced by acetic acid in *Saccharomyces cerevisiae*. *Mol. Biol. Cell*, 13, 2598-2606.

LUDOVICO, P., SOUSA, M. J., SILVA, M. T., LEÃO, C. and CÔRTE-REAL, M., 2001. *Saccharomyces cerevisiae* commits to a programmed cell death process in response to acetic acid. *Microbiology*, *147*, 2409-2415.

LUSCHAK, V. I. and GOSPODARYOV, D. V., 2005. Catalases protect cellular proteins from oxidative modification in *Saccharomyces cerevisiae. Cell Biol. Int., 29,* 187-192. https://doi.org/10.1016/j.cellbi.2004.11.001

LUTTIK, M. A., OVERKAMP, K. M., KOTTER, P., DE VRIES, S., VAN DIJKEN, J. P. and PRONK, J. T., 1998. The *Saccharomyces cerevisiae NDE1* and *NDE2* genes encode separate mitochondrial NADH dehydrogenases catalyzing the oxidation of cytosolic NADH. *J. Biol. Chem., 273,* 24529-24534. https://doi.org/10.1074/jbc.273.38.24529

MADAMANCHI, N. R., VENDROV, A. and RUNGE, M. S., 2005. Oxidative stress and vascular disease. *Arterioscler. Thromb. Vasc. Biol., 25,* 29-38. https://doi.org/10.1161/01.ATV.0000150649.39934.13

MADEO, F., CARMONA-GUTIERREZ, D., RING, J., BÜTTNER, S., EISENBERG, T. and KROEMER, G., 2009. Caspase-dependent and caspase-independent cell death pathways in yeast. *Biochem. Biophys. Res. Comm.*, *382*, 227–231. https://doi.org/10.1016/j.bbrc.2009.02.117

MADEO, F., FRÖHLICH, E. and FRÖHLICH, K.-U., 1997. A yeast mutant showing diagnostic markers of early and late apoptosis. *J. Cell Biol., 139*, 729-734. https://doi.org/10.1083/jcb.139.3.729

MADEO, F., FRÖHLICH, E., LIGR, M., GREY, M., SIGRIST, S. J., WOLF, D. H. and FROHLICH, K-U., 1999. Oxygen stress: a regulator of apoptosis in yeast. *J. Cell Biol., 145*, 757-767. https://doi.org/10.1083/jcb.145.4.757

MADEO, F., HERKER, E., MALDENER, C., WISSING, S., LÄCHELT, S., HERLAN, M., FEHR, M., LAUBER, K., SIGRIST, S. J., WESSELBORG, S. and FRÖHLICH, K. U., 2002. A caspase-related protease regulates apoptosis in yeast. *Mol. Cell., 9,* 911-927.

MADEO, F., HERKER, E., WISSING, S., JUNGWIRTH, H., EISENBERG, T. and FRÖHLICH, K.-U., 2004. Apoptosis in yeast. *Curr. Opin. Microbiol., 7*, 655-660. https://doi.org/10.1016/j.mib.2004.10.012

MAGASANIK, B., 1992. Regulation of nitrogen utilization. In: *The Molecular and Cellular Biology of the Yeast Saccharomyces: Gene Expression* (Jones E. W., Pringle J. R., Broach J.R., Eds.), pp. 283 –317. Cold Spring Harbor Laboratory Press, Cold Spring Harbor, NY.

MAGER, W. H. and WINDERICKX, J., 2005. Yeast as a model for medical and medicinal research. *Trends Pharmacol. Sci.*, *26*, 265-73.

MAGIERA, M. M., GUEYDON, E. and SCHWOB, E., 2014. DNA replication and spindle checkpoints cooperate during S phase to delay mitosis and preserve genome integrity. *J. Cell Biol.,* 204, 165-175. https://doi.org/10.1083/jcb.201306023.

MAHARJAN, S., OKU, M., TSUDA, M., HOSEKI, J. and SAKAI, Y., 2014. Mitochondrial impairment triggers cytosolic oxidative stress and cell death following proteasome inhibition. *Sci. Rep., 4,* 5896. https://doi.org/10.1038/srep05896

MAIESE, K. (2015). New insights for oxidative stress and diabetes mellitus. *Oxid. Med. Cell. Longev.*, *2015*, 875961. https://doi.org/10.1155/2015/875961

MALLICK, S., PATIL, R., GYANCHANDANI, R., PAWAR, S., PALVE, V., KANNAN, S., PATHAK, K. A., CHOUDHARY, M. and TENI, T. R., 2009. Human oral cancers have altered expression of Bcl-2 family members and increased expression of the anti-apoptotic splice variant of Mcl-1. *J. Pathol.*, *217*, 398-407. https://doi.org/10.1002/path.2459

MALSY, M., GRAF, B. and BUNDSCHERER, A., 2017. Effects of metamizole, MAA, and paracetamol on proliferation, apoptosis, and necrosis in the pancreatic cancer cell lines PaTu 8988 t and Panc-1. *BMC Pharmacol. Toxicol., 18*, 77. https://doi.org/10.1186/s40360-017-0185-y.

MANON, S., 2004. Utilization of yeast to investigate the role of lipid oxidation in cell death. *Antiox. Redox Signal., 6,* 259-267. https://doi.org/10.1089/152308604322899323

MANON, S., CHAUDHURI, B. and GUÉRIN, M., 1997. Release of cytochrome *c* and decrease of cytochrome *c* oxidase in Bax-expressing yeast cells, and prevention of these effects by coexpression of Bcl-x_L. *FEBS Lett., 415*, 29-32. https://doi.org/10.1016/S0014-5793(97)01087-9

MANOOCHEHRI, M., KARBASI, A., BANDEHPOUR, M. and KAZEMI, B., 2014. Down-regulation of BAX gene during carcinogenesis and acquisition of resistance to 5-FU in colorectal cancer. *Pathol. Oncol. Res.,* 20, 301-307. https://doi.org/10.1007/s12253-013-9695-0

MARCHETTI, M., RESNICK, L., GAMLIEL, E., KESARAJU, S., WEISSBACH, H., and BINNINGER, D., 2009. Sulindac enhances the killing of cancer cells exposed to oxidative stress. *PLoS One.*, 4, e5804. https://doi.org/10.1371/journal.pone.0005804.

MARCHETTI, M. A., WEINBERGER, M., MURAKAMI, Y., BURHANS, W. C. and HUBERMAN, J. A., 2006. Production of reactive oxygen species in response to replication stress and inappropriate mitosis in fission yeast. *J. Cell Sci, 119*, 124-131. https://doi.org/10.1242/jcs.02703

MARIMUTHU, S., CHIVUKULA, R. S., ALFONSO, L. F., MORIDANI, M., HAGEN, F. K. and BHAT, G. J., 2011. Aspirin acetylates multiple cellular proteins in HCT-116 colon cancer cells: Identification of novel targets. *Int. J. Oncol., 39*, 1273–1283. https://doi.org/10.3892/ijo.2011.1113

MARINHO, H. S., REAL, C., CYRNE, L., SOARES, H. and ANTUNES, F., 2014. Hydrogen peroxide sensing, signalling and regulation of transcription factors. *Redox Biol., 2*, 535-562. https://doi.org/10.1016/j.redox.2014.02.006

MARKOVIC, J., BORRÁS, C., ORTEGA, Á., SASTRE, J., VIÑA, J. and PALLARDÓ, F. V., 2007. Glutathione is recruited into the nucleus in early phases of cell proliferation. *J. Biol. Chem., 282*, 20416-20424. https://doi.org/10.1074/jbc.M609582200

MARQUES, M., MOJZITA, D., AMORIM, M. A., ALMEIDA, T., HOHMANN, S., MORADAS-FERREIRA, P. and COSTA, V., 2006. The Pep4p vacuolar proteinase contributes to the turnover of oxidized proteins but PEP4 overexpression is not sufficient to increase chronological lifespan in *Saccharomyces cerevisiae*. *Microbiology, 152,* 3595-3605. https://doi.org/10.1099/mic.0.29040-0

MARRES, C. A., DE VRIES, S. and GRIVELL, L. A., 1991. Isolation and inactivation of the nuclear gene encoding the rotenone-insensitive internal NADH: ubiquinone oxidoreductase of mitochondria from *Saccharomyces cerevisiae. Eur. J. Biochem., 195,* 857-862. https://doi.org/10.1111/j.1432-1033.1991.tb15775.x

MARTIN, S. J., REUTELINGSPERGER, C. P., MCGAHON, A. J., RADER, J. A., VAN SCHIE, R. C., LAFACE, D. M. and GREEN, D. R., 1995. Early redistribution of plasma membrane phosphatidylserine is a general feature of apoptosis regardless of the initiating stimulus: inhibition by overexpression of Bcl-2 and Abl. *J. Exp. Med., 182*, 1545-1556.

MARTINS, I., GALLUZI, L. and KROEMER, G., 2011. Hormesis, cell death and aging. *Aging, 3*, 821-828. https://doi.org/10.18632/aging.100380

MARTINEZ-PASTOR, M. T., MARCHLER, G., SCHÜLLER, C., MARCHLER-BAUER, A., RUIS, H. and ESTRUCH, F., 1996. The *Saccharomyces cerevisiae* zinc finger proteins Msn2p and Msn4p are required for transcriptional induction through the stress response element (STRE). *EMBO J., 15,* 2227-2235.

MÁRTON, M., TIHANYI, N., GYULVÁRI, P., BÁNHEGYI, G. and KAPUY, O., 2018. NRF2-regulated cell cycle arrest at early stage of oxidative stress response mechanism. *PLoS One, 13,* e0207949. https://doi.org/10.1371/journal.pone.0207949

MARUYAMA, Y., Ito, T., KODAMA, H. and MATSUURA, A., 2016. Availability of amino acids extends chronological lifespan by suppressing hyper-acidification of the environment in *Saccharomyces cerevisiae. PLoS One, 11*, e0151894. https://doi.org/10.1371/journal.pone.0151894

MCLAIN, A. L., SZWEDA, P. A. and SZWEDA, L. I., 2011. α-ketoglutarate dehydrogenase: A mitochondrial redox sensor. *Free Radic. Res., 45,* 29-36. https://doi.org/10.3109/10715762.2010.534163

MEADEN, P. G., DICKINSON, F. M., MIFSUD, A., TESSIER, W., WESTWATER, J., BUSSEY, H. and MIDGLEY, M., 1997. The *ALD6* gene of *Saccharomyces cerevisiae* encodes a cytosolic, Mg^{2+}-activated acetaldehyde dehydrogenase. *Yeast, 13*, 1319-1327. https://doi.org/10.1002/(SICI)1097-0061(199711)13:14<1319::AID-YEA183>3.0.CO;2-T

MENDENHALL, M. D. and HODGE, A. E., 1998. Regulation of Cdc28 cyclin-dependent protein kinase activity during the cell cycle of the yeast *Saccharomyces cerevisiae*. *Microbiol. Mol. Biol. Rev., 62*, 1191-1243.

MESQUITA. A., WEINBERGER, M., SILVA, A., SAMPAIO-MARQUES, B., ALMEIDA, B., LEÃO, C., COSTA, V., RODRIGUES, F., BURHANS, W. C. and LUDOVICO, P., 2010. Caloric restriction or catalase inactivation extends yeast chronological lifespan by inducing H_2O_2 and superoxide dismutase activity. *Proc. Natl. Acad. Sci. U. S. A.*, 107, 15123-15128. https://doi.org/10.1073/pnas.1004432107.

MILLER, S. M. and MAGASANIK, B., 1990. Role of NAD-linked glutamate dehydrogenase in nitrogen metabolism in *Saccharomyces cerevisiae. J. Bacteriol. 172*, 4927-4935.

MIQUEL, J., 1991. An integrated theory of aging as the result of mitochondrial-DNA mutation in differentiated cells. *Arch. Gerentol. Geriatr., 12,* 99-117. https://doi.org/10.1016/0167-4943(91)90022-i

MITSUI, K., NAKAGAWA, D., NAKAMURA, M., OKAMOTO, T. and TSURUGI, K., 2005. Valproic acid induces apoptosis dependent of Yca1p at concentrations that mildly affect the proliferation of yeast. *FEBS Lett*., *579*, 723-727.

MITTAL, M., SIDDIQUI, M. R., TRAN, K., REDDY, S. P. and MALIK, A. B., 2014. Reactive oxygen species in inflammation and tissue injury. *Antioxid. Redox Signal., 20,* 1126-1167. https://doi.org/10.1089/ars.2012.5149

MIZUNUMA, M., TSUBAKIYAMA, R., OGAWA, T., SHITAMUKAI, A., KOBAYASHI, Y., INAI, T., KUME, K. and HIRATA, D., 2013. Ras/cAMP-dependent protein kinase (PKA) regulates multiple aspects of cellular events by phosphorylating the Whi3 cell cycle regulator in budding yeast. *J. Biol. Chem., 288,* 10558-10566. https://doi.org/10.1074/jbc.M112.402214

MOCCAND, C., BOYCHEVA, S., SURRIABRE, P., TAMBASCO-STUDART, M., RASCHKE, M., JAUFMANN, M. and FITZPATRICK, T.B., 2014. The pseudoenzyme PDX1.2 boosts vitamin B_6 biosynthesis under heat and oxidative stress in *Arabidopsis*. *J. Biol. Chem., 289*, 8203-8216. https://doi.org/10.1074/jbc.M113.540526

MOLDOGAZIEVA, N. T., MOKHOSOEV, I. M., FELDMAN, N. B. and LUTSENKO, S. V., 2018. ROS and RNS signalling: adaptive redox switched through oxidative/nitrosative protein modifications. *Free Rad. Res., 52,* 507-543. https://doi.org/10.10808*10715762.2018.1457217

MONJAZEB, A. M., HIGH, K. P., CONNOY, A., HART, L. S., KOUMENIS, C. and CHILTON, F. H., 2006. Arachidonic acid-induced gene expression in colon cancer cells. *Carcinogenesis*, *27*, 1950-1960.

MONTEIRO, G., HORTA, B. B., PIMENTA, D. C., AUGUSTO, O. and NETTO, L. E., 2007. Reduction of 1-Cys peroxiredoxins by ascorbate changes the thiol-specific antioxidant paradigm, revealing another function of vitamin C. *Proc. Natl. Acad. Sci. U. S. A., 104,* 4886-4891. https://doi.org/10.1073/pnas.0700481104

MORGAN, B. A., BANKS, G. R., TOONE, W. M., RAITT, D., KUGE, S. and JOHNSTON, H., 1997. The skn7 response regulator controls gene expression in the oxidative stress response of the budding yeast *Saccharomyces cerevisiae. EMBO J., 16,* 1035-1044. https://doi.org/10.1093/emboj/16.5.1035

MOSKOVITZ, J., BERLETT, B. S., POSTON, J. M. and STADTMAN, E. R., 1999. Methionine sulfoxide reductase in antioxidant defense. *Methods Enzymol., 300,* 239-244. h-https://doi.org/10.1016/S0076-6879(99)00130-5

MOYE, W. S., AMURO, N., RAO, J. K. and ZALKIN, H., 1985. Nucleotide sequence of yeast *GDH1* encoding nicotinamide adenine dinucleotide phosphate-dependent glutamate dehydrogenase. *J. Biol. Chem.,* 260, 8502-8508.

MULFORD, K. E. and FASSLER, J. S., 2011. Association of the Skn7 and Yap1 transcription factors in the *Saccharomyces cerevisiae* oxidative stress response. *Eukaryot.. Cell, 10*, 761-769. https://doi.org/10.1128/EC.00328-10

MULLEN, A. R., HU, Z., SHI, X., JIANG, L., BOROUGHS, L. K., KOVACS, Z., BORIACK, R., RAKHEJA, D., SULLIVAN, L. B., LINEHAN, W. M., CHANDEL, N. S. and DEBERARDINIS, R. J., 2014. Oxidation of alpha-ketoglutarate is required for reductive carboxylation in cancer cells with mitochondrial defects. *Cell rep., 7*, 1679–1690. https://doi.org/10.1016/j.celrep.2014.04.037

MULLER, E. G. D., 1991. Thioredoxin deficiency in yeast prolongs S phase and shortens the G1 interval of the cell cycle. *J. Biol. Chem., 266*, 9194-9202.

MULLER, E. G. D., 1996. A glutathione reductase mutant of yeast accumulates high levels of oxidized glutathione and requires thioredoxin for growth. *Mol. Biol. Cell, 7*, 1805-1813.

MULLER, F. L., LIU, Y. and VAN REMMEN, H., 2004. Complex III releases superoxide to both sides of the inner mitochondrial membrane. *J. Biol. Chem., 279,* 49064-49073. https://10.1074/jbc.M407715200

MULLER, F. L., LUSTGARTEN, M. S., JANG, Y., RICHARDSON, A. and VAN REMMEN, H., 2007. Trends in oxidative aging theories. *Free Radic. Biol. Med., 43*, 477-503. https://doi.org/10.1016/j.freeradbiomed.2007.03.034

MURILLO, M. M., RANA, S., SPENCER-DENE, B., NYE, E., STAMP, G. and DOWNWARD, J., 2018. Disruption of the interaction of RAS with PI 3-Kinase induces regression of EGFR-mutant-driven lung cancer. *Cell Rep.*, *25*, 3545-3553.e2. https://doi.org/10.1016/j.celrep.2018.12.003.

NARENDRA, D. P., JIN, S. M., TANAKA, A., SUEN, D. F., GAUTIER, C. A., SHEN, J., COOKSON, M. R. and YOULE, R. J., 2010. PINK1 is selectively stabilized on impaired mitochondria to activate Parkin. *PLoS Biol.,8*, e1000298. https://doi.org/10.1371/journal.pbio.1000298

NARENDRA, D., TANAKA, A., SUEN, D. F. and YOULE, R. J., 2008. Parkin is recruited selectively to impaired mitochondria and promotes their autophagy. *J. Cell Biol.*, *183*, 795-803. https://doi.org/10.1083/jcb.200809125

NARGUND, A. M., AVERY, S. V. and HOUGHTON, J. E., 2008. Cadmium induces a heterogeneous and caspase-dependent apoptotic response in *Saccharomyces cerevisiae*. *Apoptosis*, 13, 811-821. Https://doi.org/10.1007/s10495-008-0215-8

NAUSEEF, W. M., 2008. Biological roles for the NOX family NADPH oxidases. *J. Biol. Chem., 283,* 16961-16965. https://doi.org/10.1074/jbc.R700045200

NAVARRO-TAPIA, E., QUEROL, A. and PEREZ-TORRADO, R., 2018. Membrane fluidification by ethanol stress activates unfolded protein response in yeasts. *Microb. Biotechnol., 11,* 465-475. https://doi.org/10.1111/1751-7915.13032

NEMES, Z. JR., FRIIS, R. R., AESCHLIMANN, D., SAURER, S., PAULSSON, M. and FÉSÜS, L., 1996. Expression and activation of tissue transglutaminase in apoptotic cells of involuting rodent mammary tissue. *Eur. J. Cell Biol.*, *70*, 125-133.

NEUHARD, J. and KELLN. R. A., 1996. Biosynthesis and conversion of pyrimidines. In Neidhardt, F. C., Curtiss III, R., Ingraham, J. L., Linn, E. C. C., Low, K. B., Magasanik, B., Reznikoff, W. S., Riley, M., Schaechter, M., and Umbarger, H. E. (Eds.), *Escherichia coli and Salmonella: cellular and molecular biology*, (2nd ed.). (p. 580–599). Washington D.C., USA: ASM Press.

NEWSHOLME, P., PROCOPIO, J., LIMA, M. M., PITHON-CURI, T. C. and CURI, R., 2003. Glutamine and glutamate-Their central role in cell metabolism and function. *Cell Biochem. Funct.*, *21*, 1–9. https://doi.org/10.1002/cbf.1003

NG, C.-H., TAN, S.-X., PERRONE, G. G., THORPE, G. W., HIGGINS, V. J. and DAWES, I. W., 2008. Adaptation to hydrogen peroxide in *Saccharomyces cerevisiae:* The role of NADPH-generating systems and the *SKN7* transcription factor. *Free Rad. Biol. Med., 44,* 1131-1145. https://doi.org/10.1016/j.freeradbiomed.2007.12.008

NIKOLOVA, I., MARINOV, L., GEORGIEVA, A. RENATA, T., MALCHEV, M, VOYNIKOV, Y. and KOSTADINOVA, I., 2018. Metamizole (dipyrone) – cytotoxic and antiproliferative effects on HeLa, HT-29 and MCF-7 cancer cell lines. *Biotechnol. Biotechnol. Equip., 32,* 1327-1337. https://doi.org/10.1080/13102818.2018.1511382

NITA, M. and GRZYBOWSKI, A., 2016. The role of the reactive oxygen species and oxidative stress in the pathomechanism of the age-related ocular diseases and other pathologies of the anterior and posterior eye segments in adults. *Oxid. Med. Cell Longev., 2016*, 3164734. https://doi.org/10.1155/2016/3164734

NOSEK, J. and FUKUHARA, H., 1994. NADH dehydrogenase subunit genes in the mitochondrial DNA yeasts. *J. Bacteriol., 176,* 5622-5630. https://doi.org/10.1128/jb.176.18.5622-5630.1994

NULTON-PERSSON, A. C., SZWEDA, L. I. and SADEK, H. A., 2004. Inhibition of cardiac mitochondrial respiration by salicylic acid and acetylsalicylate. *J. Cardiovasc. Pharmacol.*, *44*, 591–595. https://doi.org/10.1097/00005344-200411000-0001

NÚÑEZ, L., VALERO, R. A., SENOVILLA, L., SANZ-BLASCO, S., GARCÍA-SANCHO, J. and VILLALOBOS, C., 2006. Cell proliferation depends on mitochondrial Ca^{2+} uptake: inhibition by salicylate. *J. Physiol., 571*, 57-73.

NURSE, P., 2000. A long twentieth century of the cell cycle and beyond. *Cell, 100,* 71-78. https://doi.org/10.1016/S0092-8674(00)81684-0

NYSTRÖM, T., 2005. Role of oxidative carbonylation in protein quality control and senescence. *EMBO J., 24,* 1311-1317. https://10.1038/sj.emboj.7600599

OBERLEY, L. W. and BUETTNER, G. R., 1979. Role of superoxide dismutase in cancer: a review. *Cancer Res.,* 39, 1141-1149.

ODAT, O., MATTA, S., KHALIL, H., KAMPRANIS, S. C., PFAU, R., TSICHLIS, P. N. and MAKRIS, A. M., 2007. Old yellow enzymes, highly homologous FMN oxidoreductases with modulating roles in oxidative stress and programmed cell death in yeast. *J. Biol. Chem., 282*, 36010-36023. https://doi.org/10.1074/jbc.M704058200

OFENGEIM, D., ITO, Y., NAJAFOV, A., ZHANG, Y., SHAN, B., DEWITT, J. P., YE, J., ZHANG, X., CHANG, A., VAKIFAHMETOGLU-NORBERG, H., GENG, J., PY, B., ZHOU, W., AMIN, P., BERLINK LIMA, J., QI, C., YU, Q., TRAPP, B. and YUAN, J., 2015. Activation of necroptosis in multiple sclerosis. *Cell Rep., 10,* 1836-1849.

OLSEN, J. H., FRIIS, S., POULSEN, A. H., FRYZEK, J., HARVING, H., TJØNNELAND, A., SØRENSEN, H. T. and BLOT, W., 2008. Use of NSAIDs, smoking and lung cancer risk. *Br. J. Cancer.*, 98, 232-237.

ØSTERGAARD, H., TACHIBANA, C. and WINTHER, J. R., 2004. Monitoring disulfide bond formation in the eukaryotic cytosol. *J. Cell Biol.*, *166*, 337–345. https://doi.org/10.1083/jcb.200402120

PADILLA, P. A., FUGE, E. K., CRAWFORD, M. E., ERRETT, A. and WERNER-WASHBURNE, M., 1998. The highly conserved, coregulated *SNO* and *SNZ* gene families in *Saccharomyces cerevisiae* respond to nutrient limitation. *J. Bacteriol., 180*, 5718-5726

PALLARDÓ, F. V., MARKOVIC, J., GARCÍA, J. L. and VIÑA, J., 2009. Role of nuclear glutathione as a key regulator of cell proliferation. *Mol. Aspects Med., 30*, 77-85. https://doi.org/10.1016/j.mam.2009.01.001

PAN, M. R., CHANG, H. C. and HUNG, W. C., 2008. Non-steroidal anti-inflammatory drugs suppress the ERK signaling pathway via block of Ras/c-Raf interaction and activation of MAP kinase phosphatases. *Cell. Signal.*, *20*, 1134–1141. https://doi.org/10.1016/j.cellsig.2008.02.004

PANDEY, P., SINGH, J., ACHARY, V. M. M. and REDDY, M. K., 2015. Redox homeostasis *via* gene families of ascorbate-glutathione pathway. *Front. Environ. Sci., 3,* 25. https://doi.org/10.3389/fenvs.2015.00025

PATHI, S., JUTOORU, I., CHADALAPAKA, G., NAIR, V., LEE, S. O. and SAFE, S., 2012. Aspirin Inhibits colon cancer cell and tumor growth and downregulates specificity protein (Sp) transcription factors. *PLoS One*, 7, e48208. https://doi.org/10.1371/journal.pone.0048208.

PELICANO, H., CARNEY, D. and HUANG, P., 2004. ROS stress in cancer cells and therapeutic implications. *Drug Resist. Updat*., 7, 97-110.

PEREIRA, C., CHAVES, S., ALVES, S. SALIN, B., CAMOUGRAND, N., MANON, S., SOUSA, M. J., and CORTE-REAL, M., 2010. Mitochondrial degradation in acetic acid-induced yeast apoptosis the role of Pep4 and the ADP/ATP carrier. *Mol. Microbiol., 76,* 1398-13410. https://doi.org/10.1111/j.1365-2958.2010.07122x

PERKINS, G., DRURY, L. S. and DIFFLEY, J. F., 2001. Separate SCF(CDC4) recognition elements target Cdc6 for proteolysis in S phase and mitosis. *The EMBO journal*, *20*, 4836–4845. https://doi.org/10.1093/emboj/20.17.4836

PERRONE, G. G., TAN, S.-X. and DAWES, I. W., 2008. Reactive oxygen species and yeast apoptosis. *Biochim. Biophys. Acta, 1783*, 1354-1368. https://doi.org/10.1016/j.bbamcr.2008.01.023

PERUGINI, R. A., MCDADE, T. P., VITTIMBERGA, F. J. JR., DUFFY, A. J. and CALLERY, M. P., 2000. Sodium salicylate inhibits proliferation and induces G1 cell cycle arrest in human pancreatic cancer cell lines. *J. Gastrointest. Surg.*, *4*, 24-32.

PETKOVA, M. I., PUJOL-CARRION, N., ARROYO, J., GARCÍA-CANTALEJO, J. and ANGELES DE LA TORRE-RUIZ, M., 2010. Mtl1 is required to activate general stress response through Tor1 and Ras2 inhibition under conditions of glucose starvation and oxidative stress. *J. Biol. Chem.*, *285*, 19521-19531. https://doi.org/10.1074/jbc.M109.085282

PETRANOVIC, D. and NIELSEN, J., 2008. Can yeast systems biology contribute to the understanding of human disease? *Trends Biotechnol.*, *26*, 584-590. https://doi.org/10.1016/j.tibtech.2008.07.008.

PETRANOVIC, D., TYO, K., VEMURI, G. N. and NIELSEN, J., 2010. Prospects of yeast systems biology for human health: integrating lipid, protein and energy metabolism. *FEMS Yeast Res., 10,* 1046-1059. doi:10.1111/j.1567-1364.2010.00689.x

PETRONINI, P. G., URBANI, S., ALFIERI, R., BORGHETTI, A. F. and GUIDOTTI, G. G., 1996. Cell susceptibility to apoptosis by glutamine deprivation and rescue: survival and apoptotic death in cultured lymphoma-leukemia cell lines. *J. Cell. Physiol.*, *169*, 175–185. https://doi.org/10.1002/(SICI)1097-4652(199610)169:1<175::AID-JCP18>3.0.CO;2-C

PETROVA, V. Y., DRESCHER, D., KUJUMDZIEVA, A. V. and SCHMITT, M. J., 2004. Dual targeting of yeast catalase A to peroxisomes and mitochondria. *Biochem. J., 380,* 393-400. https://doi.org/10.1042/BJ20040042

PEYTON, K. J., LIU, X. M., YU, Y., YATES, B., BEHNAMMANESH, G. and DURANTE, W., 2018. Glutaminase-1 stimulates the proliferation, migration, and survival of human endothelial cells. *Biochem. Pharmacol.,* 156, 204-214. https://doi.org/10.1016/j.bcp.2018.08.032.

PHULL, A.-R., NASIR, B., UL HAQ, I. and KIM, S. J., 2018. Oxidative stress, consequences and ROS mediated cellular signalling in rheumatoid arthritis. *Chem.-Biol. Interact., 281,* 121-136. https://doi.org/10.1016/j.cbi.2017.12.024

PIAZZA, G. A., ALBERTS, D. S., HIXSON, L. J., PARANKA, N. S., LI, H., FINN, T., BOGERT, C., GUILLEN, J. M., BRENDEL, K., GROSS, P. H., SPERL, G., RITCHIE, J., BURT, R. W., ELLSWORTH, L., AHNEN, D. J. and PAMUKCU, R., 1997. Sulindac sulfone inhibits azoxymethane-induced colon carcinogenesis in rats without reducing prostaglandin levels. *Cancer Res., 57*, 2909-2915.

PIAZZA, G. A., RAHM, A. L., KRUTZSCH, M., SPERL, G., PARANKA, N. S., GROSS, P. H., BRENDEL, K., BURT, R. W., ALBERTS, D. S. and PAMUKCU, R., 1995. Antineoplastic drugs sulindac sulfide and sulfone inhibit cell growth by inducing apoptosis. *Cancer Res.*, *55*, 3110–3116.

PIPER, P.W., 1999. Yeast superoxide dismutase mutants reveal a pro-oxidant action of weak organic acid food preservatives. *Free Radic. Biol. Med., 27,* 1219-1227. https://doi.org/10.1016/s0891-5849(99)00147-1

POLJSAK, B., SUPUT, D. and MILISAV, I., 2013. Achieving the balance between ROS and antioxidants: When to use the synthetic antioxidants. *Oxid. Med. Cell Longev., 2013*, 956792. https://doi.org/10.1155/2013/956792

POMPEIA, C., HODGE, D. R., PLASS, C., WU, Y. Z., MARQUEZ, V. E., KELLEY, J. A. and FARRAR, W. L., 2004. Microarray analysis of epigenetic silencing of gene expression in the KAS-6/1 multiple myeloma cell line. *Cancer Res*., *64*, 3465-73.

POSTNIKOFF, S. D., MALO, M. E., WONG, B. and HARKNESS, T. A., 2012. The yeast forkhead transcription factors fkh1 and fkh2 regulate lifespan and stress response together with the anaphase-promoting complex. *PLoS Genet., 8,* e1002583. https://doi.org/10.1371/journal.pgen.1002583

PRAMILA, T., WU, W., MILES, S., NOBLE, W. S. and BREEDEN, L. L., 2006. The Forkhead transcription factor Hcm1 regulates chromosome segregation genes and fills the S-phase gap in the transcriptional circuitry of the cell cycle. *Genes Dev*., *20*, 2266-2278.

PREYA, U.H., LEE, K-T., KIM, N-J., LEE, J-Y., JANG, D. S. and CHOI, J-H., 2017. The natural terthiophene α-terthienylmethanol induces S phase cell cycle arrest of human ovarian cancer cells *via* the generation of ROS stress. *Chem. Biol. Interact., 272*, 72-79. https://doi.org/10.1016/j.cbi.2017.05.011

PRIAULT, M., BESSOULE, J.-J., GRELAUD, C, A., CAMOUGRAND, N. and MANON, S., 2002. Bax-induced cell death in yeast depends on mitochondrial lipid oxidation. *Eur. J. Biochem., 269*, 5440-5450. https://doi.org/10.1046/j.1432.2002.03234.x

PRIAULT, M., CAMOUGRAND, N., KINNALLY, K. W., VALLETTE, F. M. and MANON, S., 2003. Yeast as a tool to study Bax/mitochondrial interactions in cell death. *FEMS Yeast Res., 4*, 15-27. https://doi.org/10.1016/S1567-1356(03)00143-0

PRIAULT, M., SALIN, B. SCHAEFFER, J., VALLETTE, F. M., RAGO, J.-P. and MARTINOU, J.-C., 2005. Impairing the bioenergetic status and the biogenesis of mitochondria triggers mitophagy in yeast. *Cell Death Differ., 12,* 1613-1621. https://doi.org/10.1038/sj.cdd.4401697

PRIZMENT, A. E., FOLSOM, A. R. and ANDERSON, K. E., 2010. Nonsteroidal anti-inflammatory drugs and risk for ovarian and endometrial cancers in the Iowa Women's Health Study. *Cancer Epidemiol. Biomarkers Prev.,* 19, 435-442. https://doi.org/10.1158/1055-9965.EPI-09-0976.

PROFILO, E., PEÑA-ALTAMIRA, L. E., CORRICELLI, M., CASTEGNA, A., DANESE, A., AGRIMI, G., PETRALLA, S., GIANNUZZI, G., PORCELLI, V., SBANO, L., VISCOMI, C., MASSENZIO, F., PALMIERI, E. M., GIORGI, C., FIERMONTE, G., VIRGILI, M., PALMIERI, L., ZEVIANI, M., PINTON, P., MONTI, B., PALMIERI, F. and LASORSA, F. M., 2017. Down-regulation of the mitochondrial aspartate-glutamate carrier isoform 1 *AGC1* inhibits proliferation and N-acetylaspartate synthesis in Neuro2A cells. *Biochim. Biophys. Acta Mol. Basis Dis.*, *1863*, 1422-1435. https://doi.org/10.1016/j.bbadis.2017.02.022.

PYO, C. W., CHOI, J. H., OH, S. M. and CHOI, S. Y., 2013. Oxidative stress-induced cyclin D1 depletion and its role in cell cycle processing. *Biochim. Biophys. Acta, 1830*, 5316-5325. https://doi.org/10.1016/j.bbagen.2013.07.030

QIAO, L., HANIF, R., SPHICAS, E., SHIFF, S. J. and RIGAS, B., 1998. Effect of aspirin on induction of apoptosis in HT-29 human colon adenocarcinoma cells. *Biochem. Pharmacol., 55*, 53-64. doi:10.1016/S0006-2952(97)00400-0

RAI, N., SARKAR, M. and RAHA, S., 2015. Piroxicam, a traditional non-steroidal anti-inflammatory drug (NSAID) causes apoptosis by ROS mediated Akt activation. *Pharmacol. Rep., 67*, 1215-1223. https;//doi.org/10.1016/j.pharep.2015.05.012.

RAITT, D. C., JOHNSON, A. L., ERKINE, A. M., MAKINO, K., MORGAN, B., GROSS, D. S. and JOHNSTON, L. H., 2000. The skn7 response regulator of *Saccharomyces cerevisiae* interacts with Hsf1 *in vivo* and is required for the induction of heat shock genes by oxidative stress. *Mol. Biol. Cell, 11*, 2335-2347. https://doi.org/10.1091/mbc.11.7.2335

RAO, S. K., PAVICEVIC, Z., DU, Z., KIM, J. G., FAN, M., JIAO, Y., ROSEBUSH, M., SAMANT, S., GU, W., PFEFFER, L. M. and NOSRAT, C. A., 2010. Pro-inflammatory genes as biomarkers and therapeutic targets in oral squamous cell carcinoma. *J. Biol. Chem.*, 285, 32512-32521. https://doi.org/10.1074/jbc.M110.150490

RASCHKE, M., BOYCHEVA, S., CRÈVECOEUR, M., NUNES-NESI, A., WITT, S., FERNIE, A. R., AMRHEIN, N. and FITZPATRICK, T.B., 2011. *Plant J., 66,* 414-432. https://doi.org/10.1111/j.1365-313X.2011.04499.x

RAZA, H. and JOHN, A., 2012. Implications of altered glutathione metabolism in aspirin-induced oxidative stress and mitochondrial dysfunction in HepG2 cells. *PloS one*, *7*, e36325. https://doi.org/10.1371/journal.pone.0036325

RAZA, H., JOHN, A. and BENEDICT, S., 2011. Acetylsalicylic acid-induced oxidative stress, cell cycle arrest, apoptosis and mitochondrial dysfunction in human hepatoma HepG2 cells. *Eur. J. Pharmacol., 668*, 15-24. https://doi.org/10.1016/j.ejphar.2011.06.016

REDDY, B. S., KAWAMORI, T., LUBET, R. A., STEELE, V. E., KELLOFF, G. J., and RAO, C. V., 1999. Chemopreventive efficacy of sulindac sulfone against colon cancer depends on time of administration during carcinogenic process. *Cancer Res., 59*, 3387–3391.

REEKMANS, R., DE SMET, K., CHEN, C., VAN HUMMELEN, P. and CONTRERAS, R., 2005. Old yellow enzyme interferes with Bax-induced NADPH loss and lipid peroxidation in yeast. *FEMS Yeast Res., 5,* 711-725. https://doi.org/10.1016/j.femsyr.2004.12.010

REINACHER-SCHICK, A., SCHOENECK, A., GRAEVEN, U., SCHWARTE-WALDHOFF, I. and SCHMIEGEL, W., 2003. Mesalazine causes a mitotic arrest and induces caspase-dependent apoptosis in colon carcinoma cells. *Carcinogenesis*, *24*, 443-451.

RINNERTHALER, M., BUTTNER, S., LAUN, P., HEEREN, G., FELDER, T. K, KLINGER, H., WEINBERGER, M., STOLZE, J., GROUSL, T., HASEK, J., BENADA, O., FRYDLOVA, I., KLOCKER, A., SIMON-NOBBE, B., JANSKO, B., BREITENBACH-KOLLER, H., EISENBERG, T., GOURLAY, C. W., MADEO, F., BURHAND, W. C. and BREITENBACH, M., 2012. Yno1p/Aim14p, a NADPH-oxidase ortholog, controls extramitochondrial reactive oxygen species generation, apoptosis, and actin cable formation in yeast. *Proc. Natl. Acad. Sci. U. S. A., 109,* 8658-8663. https://doi.org/10.1073/pnas.1201629109

ROBERTS, H. R., SMARTT, H. J., GREENHOUGH, A., MOORE, A. E., WILLIAMS, A. C. and PARASKEVA, C., 2011. Colon tumour cells increase PGE(2) by regulating COX-2 and 15-PGDH to promote survival during the microenvironmental stress of glucose deprivation. *Carcinogenesis*, *32*, 1741-1747. https://doi.org/10.1093/carcin/bgr210

RODRIGUES, F., LUDOVICO, P. and LEÃO, C., 2006. Sugar metabolism in yeasts: An overview of aerobic and anaerobic glucose catabolism. In: Péter, G. and Rosa, C. (Eds.), *Biodiversity and Ecophysiology of Yeasts. The Yeast Handbook. (*pp.101-121). Springer, Berlin, Heidelberg. https://doi.org/10.1007/3/540/30985/3_6

RODRIGUEZ-COLMAN, M. J., REVERTER-BRANCHAT, G., SOROLLA, M. A., TAMARIT, J., ROS, J. and CABISCOL, E., 2010. The forkhead transcription factor Hcm1 promotes mitochondrial biogenesis and stress resistance in yeast. *J. Biol. Chem., 285*, 37092-37101. https://doi.org/10.1074/jbc.M110.174763

RODRÍGUEZ-NAVARRO, S., LLORENTE, B., RODRÍGUEZ-MANZANEQUE, M. T., RAMNE, A., UBER, G., MARCHESAN, D., DUJON, B., HERRERO, E., SUNNERHAGEN, P. and PÉREZ-ORTÍN, J. E., 2002. Functional analysis of yeast gene families involved in metabolism of vitamins B_1 and B_6. *Yeast, 19*, 1261-1276. doi:10.1002/yea.916

ROELOFS, H. M., TE MORSCHE, R. H., VAN HEUMEN, B. W., NAGENGAST, F. M. and PETERS, W. H., 2014. Over-expression of COX-2 mRNA in colorectal cancer. *BMC Gastroenterol., 14*, 1. https://doi.org/10.1186/1471-230X-14-1

ROTHWELL, P. M., WILSON, M., ELWIN, C. E., NORRVING, B., ALGRA, A., WARLOW, C. P. and MEADE, T. W., 2010. Long-term effect of aspirin on colorectal cancer incidence and mortality: 20-year follow-up of five randomised trials. *Lancet*, *376*, 1741-1750. https://doi.org/10.1016/S0140-6736(10)61543-7.

ROTTENBERG, H., COVIAN, R. and TRUMPOWER, B. L., 2009. Membrane potential greatly enhances superoxide generation by the cytochrome bc_1 complex reconstituted into phospholipid vesicles. *J. Biol. Chem., 284,* 19203-19210. https://doi.org/10.1074/jbc.M109.017376

RUDER, E. H., LAIYEMO, A. O., GRAUBARD, B. I., HOLLENBECK, A. R., SCHATZKIN, A. and CROSS, A. J., 2011. Non-steroidal anti-inflammatory drugs and colorectal cancer risk in a large, prospective cohort. *Am. J. Gastroenterol.,* 106, 1340-1350. https://doi.org/10.1038/ajg.2011.38.

RUSSO, T., ZAMBRANO, N., ESPOSITO, F., AMMENDOLA, R., CIMINO, F., FISCELLA, M., JACKMAN, J., O'CONNOR, P. M., ANDERSON, C. W. and APPELLA, E., 1995. A p53-independent pathway for activation of WAF1/CIP1 expression following oxidative stress. *J. Biol. Chem., 270*, 29386-29391. https://doi.org/10.1074/jbc.270.49.29386

SAHARAN, R. K., KANWAL, S. and SHARMA, S. C., 2010. Role of glutathione in ethanol stress tolerance in yeast *Pachysolen tannophilus*. *Biochem. Biophys. Res. Commun., 397*, 307-310. https://doi.org/10.1016/j.bbrc.2010.05.107

SAINT-PRIX, F., BONQUIST, L. and DEQUIN, S., 2004. Functional analysis of the ALD gene family of *Saccharomyces cerevisiae* during anaerobic growth on glucose: The NADP+-dependent Ald6p and Ald5p isoforms play a major role in acetate formation. *Microbiology, 150*, 2209-2220. https://doi.org/10.1099/mic.0.26999-0

SAITO, K., THIELE, D. J., DAVIO, M., LOCKRIDGE, O. and MASSEY, V., 1991. The cloning and expression of a gene encoding Old Yellow Enzyme from *Saccharomyces carlsbergensis*. *J. Biol. Chem.*, *266*, 20720–20724.

SAMBROOKE, J., FRITSCH, E.F. and MANIATIS, T., 1989. *Molecular cloning: A Laboratory Manual, 2nd Ed*. New York: Cold Spring Harbor Laboratory Press.

SANDLER, R. S., HALABI, S., BARON, J. A., BUDINGER, S., PASKETT, E., KERESZTES, R., PETRELLI, N., PIPAS, J. M., KARP, D. D., LOPRINZI, C. L., STEINBACH, G. and SCHILSKY, R., 2003. A randomized trial of aspirin to prevent colorectal adenomas in patients with previous colorectal cancer. *N. Engl. J. Med.*, 348, 883-890.

SANDOVAL-ACUÑA, C., LOPEZ-ALARCÓN, C., ALIAGA, M. E. and SPEISKY, H., 2012. Inhibition of mitochondrial complex I by various non-steroidal anti-inflammatory drugs and its protection by quercetin *via* a coenzyme Q-like action. *Chem. Biol. Interact.*, 199, 18-28. https://doi.org/10.1016/j.cbi.2012.05.006.

SANKPAL, U. T., ABDELRAHIM, M., CONNELLY, S. F., LEE, C. M., MADERO-VISBAL, R., COLON, J., SMITH, J., SAFE, S., MALIAKAL, P. and BASHA, R., 2012. Small molecule tolfenamic acid inhibits PC-3 cell proliferation and invasion in vitro, and tumor growth in orthotopic mouse model for prostate cancer. *Prostate, 72*, 1648-58. https://doi.org/10.1002/pros.22518.

SANTA-GONZALEZ, G. A., GOMEZ-MOLINA, A., ARCOS-BURGOS, M., MEYER, J. N. and CAMARGO, M., 2016. Distinctive adaptive response to repeated exposure to hydrogen peroxide associated with upregulation of DNA repair genes and cell cycle arrest. *Redox Biol.*, *9*, 124–133.

SANTORO, A., VLACHOU, T., LUZI, L., MELLONI, G., MAZZARELLA, L., D'ELIA, E., AOBULI, X., PASI, C. E., REAVIE, L., BONETTI, P., PUNZI, S., CASOLI, L., SABÒ, A., MORONI, M. C., DELLINO, G. I., AMATI, B., NICASSIO, F., LANFRANCONE, L. and PELICCI, P. G., 2019. p53 loss in breast cancer leads to Myc activation, increased cell plasticity, and expression of a mitotic signature with prognostic value. *Cell Rep., 26*, 624-638.e8. https://doi.org/10.1016/j.celrep.2018.12.071.

SANTRA, M., DILL, K. A. and DE GRAFF, M. R., 2019. Proteostasis collapse is a driver of cell aging and death. *Proc. Natl. Acad. Sci. U. S. A., 116,* 22173-22178. https://doi.org/10.1073/PNAS.1906592116

SAPIENZA, K. and BALZAN, R., 2005. Metabolic aspects of aspirin-induced apoptosis in yeast. *FEMS Yeast Res., 5*, 1207-1213. https://doi.org/10.1016/femsyr.2005.05.001

SAPIENZA, K., BANNISTER, W. and BALZAN, R., 2008. Mitochondrial involvement in aspirin-induced apoptosis in yeast. *Microbiology*, *154*, 2740-2747. https://doi.org/10.1099/mic.0.2008/017228-0

SAXOWSKY, T. T. and DOETSCH, P. W., 2006. RNA polymerase encounters with DNA damage: Transcription-coupled repair or transcriptional mutagenesis? *Chem. Rev., 106*, 474-488. https://doi.org/10.1021/cr040466q

SCHAFER, F. Q. and BUETTNER, G. R., 2001. Redox environment of the cell as viewed through the redox state of the glutathione disulfide/glutathione couple. *Free Radic. Biol. Med., 30*, 1191-1212. https://doi.org/10.1016/S0891-5849(01)00480-4

SCHIEBER, M. and CHANDEL, N. S., 2014. ROS function in redox signalling and oxidative stress. *Curr. Biol., 24*, R453-R462. https://doi.org/10.1016/j.cub.2014.03.034

SCHNELL, N., KREMS, B. and ENTIAN, K. D., 1992. The *PAR1* (*YAP1/SNQ3*) gene of *Saccharomyces cerevisiae*, a c-*jun* homologue, is involved in oxygen metabolism. *Curr. Genetics, 21*, 269-273. https://doi.org/10.1007/BF00351681

SCHULZ, T. J., ZARSE, K., VOIGT, A., URBAN, N., BIRRINGER, M. and RISTOW, M., 2007. Glucose restriction extends *Caenorhabditis elegans* life span by inducing mitochondrial respiration and increasing oxidative stress. *Cell Metab., 6,* 280-293.

SELVENDIRAN, K., BRATASZ, A., TONG, L., IGNARRO, L. J. and KUPPUSAMY, P., 2008. NCX-4016, a nitro-derivative of aspirin, inhibits EGFR and STAT3 signalling and modulates Bcl-2 proteins in cisplatin-resistant human ovarian cancer cells and xenografts. *Cell Cycle,* 7, 81-88.

SENGUPTA, R. and HOLMGREN, A., 2014. Thioredoxin and glutaredoxin-mediated redox regulation of ribonucleotide reductase. *World J. Biol. Chem., 5*, 68-74. https://doi.org/10.4331/wjbc.v5.i1.68

SEO, B. B., KITAJIMA-IHARA, T., CHAN, E. K. L., SCHEFFLER, I. E., MATSUNO-YAGI, A. and YAGI, T., 1998. Molecular remedy of complex I defects: Rotenone-insensitive internal NADH-quinone oxidoreductase of *Saccharomyces cerevisiae* mitochondrial restores the NADH oxidase activity of complex I-deficient mammals. *Proc. Natl. Acad. Sci. U. S. A., 95,* 9167-9171.

SEO, B. B., MATSUNO-YAGI, A. and YAGI, T., 1999. Modulation of oxidative phosphorylation of human kidney 293 cells by transfection with the internal rotenone-insensitive NADH-quinone oxidoreductase (*NDI1)* gene of *Saccharomyces cerevisiae. Biochim. Biophys. Acta, 1412,* 56-65. https://doi.org/10.1016/s0005-2728(99)00051-1

SEVERIN, F. F. and HYMAN, A. A., 2002. Pheromone induces programmed cell death in *S. cerevisiae. Curr. Biol., 12*, R233-R235.

SHACKELFORD, R. E., KAUFMANN, W. K. and PAULES, R. S., 2000. Oxidative stress and cell cycle checkpoint function. *Free Radic. Biol. Med., 28*, 1387-404.

SHAO, J. and FENG, G., 2013. Selective killing effect of oxytetracycline, propafenone and metamizole on A549 or Hela cells. *Chin. J. Cancer Res*., 25, 662-570. https://doi.org/10.3978/j.issn.1000-9604.2013.11.05.

SHAPIRA, M., SEGAL, E. and BOTSTEIN, D., 2004. Disruption of yeast forkhead-associated cell cycle transcription by oxidative stress. *Mol. Biol. Cell*., 15, 5659-5669.

SHARMA, A., BOISE, L. H. and SHANMUGAM, M., 2019. Cancer metabolism and the evasion of apoptotic cell death. *Cancers*, *11*, E1144. https://doi.org/10.3390/cancers11081144.

SHI, J., LENG, W., ZHAO, L., XU, C., WANG, J., CHEN, X., WANG, Y. and PENG, X., 2017. Nonsteroidal anti-inflammatory drugs using and risk of head and neck cancer: a dose-response meta-analysis of prospective cohort studies. *Oncotarget., 8*, 99066-99074. https://doi.org/10.18632/oncotarget.21524.

SHI, L. and TU, B. P., 2013. Acetyl-CoA induces transcription of the key G1 cyclin *CLN3* to promote entry into the cell division cycle in *Saccharomyces cerevisiae*. *Proc. Natl. Acad. Sci. U. S. A*., 110, 7318-7323. https://doi.org/10.1073/pnas.1302490110.

SHIDOJI, Y., HAYASHI, K., KOMURA, S., OHISHI, N. and YAGI, K., 1999. Loss of molecular interaction between cytochrome *c* and cardiolipin due to lipid peroxidation. *Biochem. Biophys. Res. Commun., 264,* 343-347. https://doi.org.10.1006/bbrc.1999.1410

SHIFF, S. J., KOUTSOS, M. I., QIAO, L. and RIGAS, B., 1996. Nonsteroidal antiinflammatory drugs inhibit the proliferation of colon adenocarcinoma cells: effects on cell cycle and apoptosis. *Exp. Cell Res., 222*, 179-188. https://doi.org/10.1006/excr.1996.0023

SHIFF, S. J., QIAO, L., TSAI, L. L. and RIGAS, B., 1995. Sulindac sulfide, an aspirin-like compound, inhibits proliferation, causes cell cycle quiescence, and induces apoptosis in HT-29 colon adenocarcinoma cells. *J. Clin. Invest.*, *96*, 491-503.

SHIMADA, K., PASERO, P and GASSER, S. M., 2002. ORC and the intra-S-phase checkpoint: a threshold regulates Rad53p activation in S phase. *Genes Dev., 16*, 3236-3252.

SHIRAHIGE, K., HORI, Y., SHIRAISHI, K., YAMASHITA, M., TAKAHASHI, K., OBUSE, C., TSURIMOTO, T. and YOSHIKAWA, H., 1998. Regulation of DNA-replication origins during cell-cycle progression. *Nature*, *395*, 618-621.

SIMON, H. U., HAJ-YEHIA, A. and LEVI-SCHAFFER, F., 2000. Role of reactive oxygen species (ROS) in apoptosis induction. *Apoptosis*, *5*, 415-418.

SIMON, J. A. and BEDALOV, A., 2004. Yeast as a model system for anticancer drug discovery. *Nat. Rev. Cancer*, *4*, 481-92. https://doi.org/10.1038/nrc1372.

SINGH, A., KUKRETI, R., SASO, L. and KUKRETI, S., 2019. Oxidative stress: A key modulator in neurodegenerative diseases. *Molecules, 24*, E1583. https://www.doi.org/10.3390/molecules24081583.

SIVASUBRAMANIAM, S., VANNIASINGHAM, V. M., TAN, C. T. and CHUA, N. H., 1995. Characterisation of *HEVER*, a novel stress-induced gene from *Hevea brasiliensis*. *Plant Mol. Biol., 29*, 173-178. https://doi.org/10.1007/BF00019129

SJ, S., VEERABHADRAPPA, B., SUBRAMANIYAN, S. and DYAVAIAH, M., 2019. Astaxanthin enhances the longevity of *Saccharomyces cerevisiae* by decreasing oxidative stress and apoptosis. *FEMS Yeast Res.*, *19*, 1-11. https://doi.org/10.1093/femsyr/foy113

SJÖBERG, L., ERIKSEN, T. E. and RÉVÉSZ, L., 1982. The reaction of the hydroxyl radical with glutathione in neutral and alkaline aqueous solution. *Radiat. Res., 89*, 255-263.

SKULACHEV, V. P., 2006. Bioenergetic aspects of apoptosis, necrosis and mitoptosis. *Apoptosis*. *11,* 473– 485. https://doi.org/10.1007/s10495-006-5881-9

SMALL, W. C. and MCALISTER-HENN, L., 1998. Identification of a cytosolically directed NADH dehydrogenase in mitochondria of *Saccharomyces cerevisiae. J. Bacteriol., 180,* 4051-4055

SON, J., LYSSIOTIS, C. A., YING, H., WANG, X., HUA, S., LIGORIO, M., PERERA, R. M., FERRONE, C. R., MULLARKY, E., SHYH-CHANG, N., KANG, Y., FLEMING, J. B., BARDEESY, N., ASARA, J. M., HAIGIS, M. C., DEPINHO, R. A., CANTLEY, L. C. and KIMMELMAN, A. C., 2013. Glutamine supports pancreatic cancer growth through a *KRAS*-regulated metabolic pathway. *Nature*, *496*, 101–105. https://doi.org/10.1038/nature12040

SPECTOR, D., LABARRE, J. and TOLEDANO, M. B., 2001. A genetic investigation of the essential role of glutathione: mutations in the proline biosynthesis pathway are the only suppressors of glutathione auxotrophy in yeast. *J. Biol. Chem., 276*, 7011-7016. https://doi.org/10.1074/jbc.M009814200

ST. PIERRE, J., BUCKINGHAM, J. A., ROEBUCK, S. J. and BRAND, M. D., 2002. Topology of superoxide production form different sites in the mitochondrial electron transport chain. *J. Biol. Chem., 277,* 44784-44790. https://doi.org/10.1074/jbc.M207217200

STADTMAN, E. R. and LEVINE, R. L., 2003. Free radical-mediated oxidation of free amino acids and amino acid residues in proteins. *Amino acids, 25,* 207-218. https:/10.1007/s00726-003-0011-2

STEPHEN, D. W. S. and JAMIESON, D. J., 1997. Amino-acid-dependent regulation of the *Saccharomyces cerevisiae GSH1* gene by hydrogen peroxide. *Mol. Microbiol., 23,* 203-210. https://doi.org/10.1046/j.1365-2958.1997.2081572.x

SUBBEGOWDA, R. and FROMMEL, T. O., 1998. Aspirin toxicity for human colonic tumor cells results from necrosis and is accompanied by cell cycle arrest. *Cancer Res.,* 58, 2772-2776.

SULLIVAN, L. B., GUI, D. Y., HOSIOS, A. M., BUSH, L. N., FREINKMAN, E. and VANDER HEIDEN, M. G., 2015. Supporting aspartate biosynthesis is an essential function of respiration in proliferating cells. *Cell*, *162*, 552–563. https://doi.org/10.1016/j.cell.2015.07.017

SUN, Y., TANG, X. M., HALF, E., KUO, M. T. and SINICROPE, F. A., 2002. Cyclooxygenase-2 overexpression reduces apoptotic susceptibility by inhibiting the cytochrome *c*-dependent apoptotic pathway in human colon cancer cells. *Cancer Res.*, 62, 6323-6328.

SURAWEERA, A., MÜNCH, C., HANSSUM, A and BERTOLOTTI, A., 2012. Failure of amino acid homeostasis causes cell death following proteasome inhibition. *Mol. Cell, 48,* 242-253. https://doi.org/10.1016/j.molcel.2012.08.003

SUSIN, S. A., LORENZO, H. K., ZAMZAMI, N., MARZO, I., SNOW, B. E., BROTHERS, G. M., MANGION, J., JACOTOT, E., COSTANTINI, P., LOEFFLER, M., LAROCHETTE, N., GOODLETT, D. R., AEBERSOLD, R., SIDEROVSKI, D. P., PENNINGER, J. M. and KROEMER, G., 1999. Molecular characterization of mitochondrial apoptosis-inducing factor. *Nature, 397*, 441-446.

SUSIN, S. A., ZAMZAMI, N., CASTEDO, M., HIRSCH, T., MARCHETTI, P., MACHO, A., DAUGAS, E., GEUSKENS, M. and KROEMER, G., 1996. Bcl-2 inhibits the mitochondrial release of an apoptogenic protease. *J. Exp. Med.*, *184*, 1331-1341.

SUZUKI, K., KUBOTA, Y., SEKITO, T. and OHSUMI, Y., 2007. Hierarchy of Atg proteins in pre-autophagosomal structure organization. *Genes Cells*, *12,* 209-218.

SUZUKI, Y., IMAI, Y., NAKAYAMA, H., TAKAHASHI, K., TAKIO, K. and TAKAHASHI, R., 2001. A serine protease, HtrA2, is released from the mitochondria and interacts with XIAP, inducing cell death. *Mol. Cell.*, *8*, 613-21.

SWIEGERS. J. H., DIPPENAAR, N., PRETORIUS, I. S. and BAUER, F. F., 2001. Carnitine-dependent metabolic activities in *Saccharomyces cerevisiae:* three carnitine acetyltransferases are essential in a carnitine-dependent strain. *Yeast, 18*, 858-895. https://doi.org/10.1002/yea.712

SZATROWSKI, T. P. and NATHAN, C. F., 1991. Production of large amounts of hydrogen peroxide by human tumor cells. *Cancer Res., 51*, 794-798.

TAKAHASHI, M.-A. and ASADA, K., 1983. Superoxide anion permeability of phospholipid membranes and chloroplast thylakoids. *Arch. Biochem. Biophys., 226,* 558-566. https://doi.org/10.1016/00003-9861(83)90325-9

TAKESHIGE, K., BABA, M., TSUBOI, S., NODA, T. and OHSUMI, Y., 1992. Autophagy in yeast demonstrated with proteinase-deficient mutants and conditions for its induction. *J. Cell Biol., 119,* 301-311. https://doi.org/10.1083/jcb.119.2.301

TAO, W., KURSCHNER, C. and MORGAN, J. I., 1997. Modulation of cell death in yeast by the Bcl-2 family of proteins. *J. Biol. Chem.*, *272*, 15547-52.

TATCHELL, K., ROBINSON, L. C. and BREITENBACH, M., 1985. *RAS2* of *Saccharomyces cerevisiae* is required for gluconeogenic growth and proper response to nutrient limitation. *Proc. Natl. Acad. Sci. U. S. A., 82*, 3785-3789.

TEWARI, D., MAJUMDAR, D., VALLABHANENI, S. and BERA, A. K., 2017. Aspirin induces cell death by directly modulating mitochondrial voltage-dependent anion channel (VDAC). *Sci Rep., 7,* 45184. https://doi.org/10.1038/srep45184.

THORNBERRY, N. A. and LAZEBNIK, Y., 1998. Caspases: enemies within. *Science*, *281*, 1312- 1316.

THORPE, G. W., FONG, C. S., ALIC, N., HIGGINS, V. J. and DAWES, I. W., 2004. Cells have distinct mechanisms to maintain protection against different reactive oxygen species: Oxidative-stress-response genes. *Proc. Natl. Acad. Sci. U.S.A, 101,* 6564-6569. https:/doi.org/10.1073/pnas.0305888101

TITIZ, O., TAMBASCO-STUDART, M., WARZYCH, E., APEL, K., AMRHEIN, N., LALOI, C. and FITZPATRICK, T.B., 2006. PDX1 is essential for vitamin B_6 biosynthesis, development and stress tolerance in *Arabidopsis. Plant J., 48*, 933-946. https://doi.org/10.1111/j.1365-313X.2006.02928.x

TODA, T., UNO, I., ISHIKAWA, T., POWERS, S., KATAOKA, T., BROEK, D., CAMERON, S., BROACH, J., MATSUMOTO, K. and WIGLER, M., 1985. In yeast, *RAS* proteins are controlling elements of adenylate cyclase. *Cell, 40*, 27-36. doi:0092-8674(85)90305-8

TOMODA, T., TAKEDA, K., KURASHIGE, T., ENZAN, H. and MIYAHARA, M., 1994. Acetylsalicylate (ASA)-induced mitochondrial dysfunction and its potentiation by Ca2+. *Liver, 14,* 103-108.

TRABERT, B., NESS, R. B., LO-CIGANIC, W. H., MURPHY, M. A., GOODE, E. L., POOLE, E. M., BRINTON, L. A., WEBB, P. M., NAGLE, C. M., JORDAN, S. J., RISCH, H. A., ROSSING, M. A., DOHERTY, J. A., GOODMAN, M. T., LURIE, G., KJÆR, S. K., HOGDALL. E., JENSEN, A., CRAMER, D. W., TERRY, K. L., … WENTZENSEN, N., 2014. Aspirin, nonaspirin nonsteroidal anti-inflammatory drug, and acetaminophen use and risk of invasive epithelial ovarian cancer: a pooled analysis in the Ovarian Cancer Association Consortium. *J. Natl. Cancer Inst., 106*, djt431. https://doi.org/10.1093/jnci/djt431.

TRANCÍKOVÁ, A., WEISOVÁ, P., KISSOVÁ, I., ZEMAN, I. and KOLAROV, J., 2004. Production of reactive oxygen species and loss of viability in yeast mitochondrial mutants: protective effect of Bcl-xL. *FEMS Yeast Res., 5*, 149–156. https://doi.org/10.1016/j.femsyr.2004.06.014

TRINCHIERI, G., 2012. Cancer and inflammation: an old intuition with rapidly evolving new concepts. *Annu. Rev. Immunol., 30*, 677-706. https://doi.org/10.1146/annurev-immunol-020711-075008.

TSANG, C. K., LIU, Y., THOMAS, J., ZHANG, Y. and ZHENG, X. F. S., 2014. Superoxide dismutase 1 acts as a nuclear transcription factor to regulate oxidative stress resistance. *Nat. Commun., 5,* 3446. https://doi.org/10.1038/ncomms4446

TSUJII, M. and DUBOIS, R. N., 1995. Alterations in cellular adhesion and apoptosis in epithelial cells overexpressing prostaglandin endoperoxide synthase 2. *Cell, 83,* 493-501. https://doi.org/10.1016/0092-8674(95)90127-2

TSUJII, M., KAWANO, S. and DUBOIS, R. N., 1997. Cyclooxygenase-2 expression in human colon cancer cells increase metastatic potential. *Proc Natl Acad Sci U. S. A*. 94, 3336-3340.

TUCKER, O. N., DANNENBERG, A. J., YANG, E. K., ZHANG, F., TENG, L., DALY, J. M., SOSLOW, R. A., MASFERRER, J. L., WOERNER, B. M., KOKI, A. T. and FAHEY, T. J., 1999. Cyclooxygenase-2 expression is up-regulated in human pancreatic cancer. *Cancer Res., 59,* 987-990.

TURCOTTE, B., LIANG, X. B., ROBERT, F. and SOONTORNGUN, N., 2009. Transcriptional regulation of non-fermentable carbon utilization in budding yeast. *FEMS Yeast Res., 10,* 2-13, https://doi.org/10.1111/j.1567-1364.2009.00555.x

TURTON, H. E., DAWES, I. W. and GRANT, C. M., 1997. *Saccharomyces cerevisiae* exhibits a yAP-1-mediated adaptive response to malondialdehyde. *J. Bacteriol., 179,* 1096-1101. https://doi.org/10.1128/jb.179.4.1096-1101.1997

TYSON, J. J. and NOVAK, B., 2008. Temporal organization of the cell cycle. *Curr. Biol., 18,* R759-R768. https://doi.org/10.1016/j.cub.2008.07.001

UBERSAX, J. A., WOODBURY, E. L., QUANG, P. N., PARAZ, M., BLETHROW, J. D., SHAH, K., SHOKAT, K. M. and Morgan, D. O., 2003. Targets of the cyclin-dependent kinase Cdk1. *Nature, 425*, 859-64.

UCHIDA, K., 2003. 4-hydroxyl-2nonenal: a product and mediator of oxidative stress. *Prog. Lipid Res.*, *42*, 318-343. https://doi.org/10.1016/s0163-7827(03)00014-6

UHLMANN, F., LOTTSPEICH, F. and NASMYTH, K., 1999. Sister-chromatid separation at anaphase onset is promoted by cleavage of the cohesin subunit Scc1. *Nature*, *400*, 37-42.

UHLMANN, F., WERNIC, D., POUPART, M. A., KOONIN, E. V. and NASMYTH, K., 2000. Cleavage of cohesin by the CD clan protease separin triggers anaphase in yeast. *Cell,* 103, 375-386.

UNTERGASSER, A., NIJVEEN, H., RAO, X., BISSELING, T., GEURTS, R. and LEUNISSEN, J.A.M., 2007. Primer3Plus, an enhanced web interface to Primer3. *Nucleic Acids Res.*, 35, W71-W74. https://doi.org/10.1093/nar/gkm306

UREN, A. G., O'ROURKE, K., ARAVIND, L. A., PISABARRO, M. T., SESHAGIRI, S., KOONIN, E. V. and DIXIT, V. M., 2000. Identification of paracaspases and metacaspases: two ancient families of caspase-like proteins, one of which plays a key role in MALT lymphoma. *Mol. Cell. 6,* 961-7.

VÁCHOVÁ, L. and PALKOVÁ, Z., 2005. Physiological regulation of yeast cell death in multicellular colonies is triggered by ammonia. *J. Cell Biol., 169*, 711-717.

VAHSEN, N., CANDÉ, C., BRIÈRE, J. J., BÉNIT, P., JOZA, N., LAROCHETTE, N., MASTROBERARDINO, P. G., PEQUIGNOT, M. O., CASARES, N., LAZAR, V., FERAUD, O., DEBILI, N., WISSING, S., ENGELHARDT, S., MADEO, F., PIACENTINI, M., PENNINGER, J. M., SCHÄGGER, H., RUSTIN, P., and KROEMER, G., 2004. AIF deficiency compromises oxidative phosphorylation. *EMBO J.*, 23, 4679-4689.

VALENZUELA, L., BALLARIO, P., ARANDA, C., FILETICI, P. and GONZÁLEZ. A., 1998. Regulation of expression of *GLT1*, the gene encoding glutamate synthase in *Saccharomyces cerevisiae*. *J. Bacteriol., 180*, 3533-3540.

VALLE, B. L., D'SOUZA, T., BECKER, K. G., WOOD, W. H., ZHANG, Y., WERSTO, R. P. and MORIN, P. J., 2013. Non-steroidal anti-inflammatory drugs decrease E2F1 expression and inhibit cell growth in ovarian cancer cells. *PLoS One, 8,* e61836. https://doi.org/10.1371/journal.pone.0061836

VAN LEEUWEN, J. S., ORIJ, R., LUTTIK, M. A., SMITS, G. J., VERMEULEN, N. P. and VOS, J. C., 2011. Subunits Rip1p and Cox9p of the respiratory chain contribute to diclofenac-induced mitochondrial dysfunction. *Microbiology,* 157, 685-694. https://doi.org/10.1099/mic.0.044578-0.

VAN LOO, G., VAN GURP, M., DEPUYDT, B., SRINIVASULA, S. M., RODRIGUEZ, I., ALNEMRI, E. S., GEVAERT, K., VANDEKERCKHOVE, J., DECLERCQ, W. and VANDENABEELE, P., 2002. The serine protease Omi/HtrA2 is released from mitochondria during apoptosis. Omi interacts with caspase-inhibitor XIAP and induces enhanced caspase activity. *Cell Death Differ., 9,* 20-26.

VANDESOMPELE, J., DE PRETER, K., PATTYN, F., POPPE, B., VAN ROY, N., DE PAEPE, A. and SPELEMAN, F., 2002. Accurate normalization of real-time quantitative RT-PCR data by geometric averaging of multiple internal control genes. *Genome Biol., 3*, research0034.1

VANE, J. R. (1971). Inhibition of prostaglandin synthesis as a mechanism of action for aspirin-like drugs. *Nat. New Biol., 231*, 232-235.

VAZQUÉZ, J., GRILLITSCH, K., DAUM, G., MAS, A., TORIJA, M.-J. and BELTRAN, G. (2018). Melatonin minimizes the impact of oxidative stress induced by hydrogen peroxide in *Saccharomyces* and non-conventional yeast. *Front. Microbiol.,* 8, 1066. https://doi.org/10.3389/fmicb.2017.01066

VEAL, E. A., DAY, A. M. and MORGAN, B. A. (2007). Hydrogen peroxide sensing and signalling. *Mol. Cell*, *26*, 1-14. https://doi.org/10.1016/j.molcel.2007.03.016

VERBON, E. H., POST, J. A. and BOONSTRA, J. (2012). The influence of reactive oxygen species on cell cycle progression in mammalian cells. *Gene, 511,* 1-6. https://doi.org/10.1016/j.gene.2012.08.038

VERDONE, L., WU, J., VAN RIPER, K., KACHEROVSKY, N., VOGELAUER, M., YOUNG, E. T., GRUNSTEIN, M., DI MAURO, E. and CASERTA, M. (2002). Hyperacetylation of chromatin at the *ADH2* promoter allows Adr1 to bind in repressed conditions. *EMBO J., 21*, 1101-1111. https://doi.org/10.1093/emboj/21.5.1101

VERHAGEN, A. M., SILKE, J., EKERT, P. G., PAKUSCH, M., KAUFMANN, H., CONNOLLY, L. M., DAY, C. L., TIKOO, A., BURKE, R., WROBEL, C., MORITZ, R. L., SIMPSON, R. J. and VAUX, D. L. (2002). HtrA2 promotes cell death through its serine protease activity and its ability to antagonize inhibitor of apoptosis proteins. *J. Biol. Chem*. *277*, 445-54.

VERNOUX, T., WILSON, R. C., SEELEY, K. A., REICHHELD, J-P., MUROY, S., BROWN, S., MAUGHAN, S. C., COBBETT, C. S., MONTAGU, M. V., INZÉ, D., MAY, M. J. and SUNG, Z. R. (2000). The root meristemless1/cadmium sensitive2 gene defines a glutathione-dependent pathway involved in initiation and maintenance of cell division during postembryonic root development. *Plant Cell, 12*, 97-109.

VESSEY, D. A., HU, J. and KELLEY, M., 1996. Interaction of salicylate and ibuprofen with the carboxylic acid: CoA ligases from bovine liver mitochondria. *J. Biochem. Toxicol*., *11*, 73-78.

VIDAL, A. C., HOWARD, L. E., MOREIRA, D. M., CASTRO-SANTAMARIA, R., ANDRIOLE, G. L. and FREEDLAND, S. J., 2015. Aspirin, NSAIDs, and risk of prostate cancer: results from the REDUCE study. *Clin. Cancer Res., 21*, 756-762. https://doi.org/10.1158/1078-0432.CCR-14-2235.

VIRCHOW, R., 1863. *Cellular Pathology as Based Upon Physiological and Pathological Histology*. Philadelphia, PA, USA: J. B. Lippincott.

VIVANCOS, P. D., DONG, Y., ZIEGLER, K., MARKOVIC, J., PALLARDÓ, F. V., PELLNY, T. K., VERRIER, P. J. and FOYER, C. H. (2010). Recruitment of glutathione into the nucleus during cell proliferation adjusts whole-cell redox homeostasis in *Arabidopsis thaliana* and lowers the oxidative defence shield. *Plant Journal, 64*, 825-838. https://doi.org/10.1111/j.1365-313X.2010.04371.x

VOGT, T., MCCLELLAND, M., JUNG, B., POPOVA, S., BOGENRIEDER, T., BECKER, B., RUMPLER, G., LANDTHALER, M. and STOLZ, W., 2001. Progression and NSAID-induced apoptosis in malignant melanomas are independent of cyclooxygenase II. *Melanoma Res*., *11*, 587-599.

VON JAGOW, G. and KLINGENBERG, M., 1970. Pathways of hydrogen in mitochondria of *Saccharomyces carlsbergensis*. *Eur. J. Biochem.*, *12*, 583–592. https://doi.org/10.1111/j.1432-1033.1970.tb00890.x

VRANOVÀ, E. INZE, D. and BREUSEGEM, F. V., 2002. Signal transduction during oxidative stress. *J. Exp. Bot., 53,* 1227-1236. https://doi.org/10.1093/jexbot/53.372.1227

WALTER, D., WISSING, S., MADEO, F. and FAHRENKROG, B., 2006. The inhibitor-of-apoptosis protein Bir1p protects against apoptosis in S. cerevisiae and is a substrate for the yeast homologue of Omi/HtrA2. *J. Cell Sci., 119*, 1843-1851.

WALTHER, K. and SCHÜLLER, H. J., 2001. Adr1 and Cat8 synergistically activate the glucose-regulated alcohol dehydrogenase gene *ADH2* of the yeast *Saccharomyces cerevisiae. 147*, 2037-2044. https://doi.org/10.1099/00221287-147-8-2037

WANG, H., SUN, L., SU, L., RIZO, J., LIU, L., WANG, L. F., WANG, F. S. and WANG, X., 2014. Mixed lineage kinase domain-like protein MLKL causes necrotic membrane disruption upon phosphorylation by RIP3. *Mol Cell*., *54*, 133-146. https://doi.org/10.1016/j.molcel.2014.03.003.

WANG, J. B., ERICKSON, J. W., FUJI, R., RAMACHANDRAN, S., GAO, P., DINAVAHI, R., WILSON, K. F., AMBROSIO, A. L., DIAS, S. M., DANG, C. V. and CERIONE, R. A., 2010a. Targeting mitochondrial glutaminase activity inhibits oncogenic transformation. *Cancer Cell*, *18*, 207–219. https://doi.org/10.1016/j.ccr.2010.08.009

WANG, Q., HARDIE, R. A., HOY, A. J., VAN GELDERMALSEN, M., GAO, D., FAZLI, L., SADOWSKI, M. C., BALABAN, S., SCHREUDER, M., NAGARAJAH, R., WONG, J. J., METIERRE, C., PINELLO, N., OTTE, N. J., LEHMAN, M. L., GLEAVE, M., NELSON, C. C., BAILEY, C. G., RITCHIE, W., RASKO, J. E., … HOLST, J., 2015. Targeting ASCT2-mediated glutamine uptake blocks prostate cancer growth and tumour development. J. Pathol., *236*, 278–289. https://doi.org/10.1002/path.4518

WANG, Q., LU, D., FAN, L., LI, Y., LIU, Y., YU, H., WANG, H., LIU, J. and SUN, G., 2019. COX-2 induces apoptosis-resistance in hepatocellular carcinoma cells via the HIF-1α/PKM2 pathway. *Int. J. Mol. Med*., *43*, 475-488. https://doi.org/10.3892/ijmm.2018.3936.

WANG, X., Yen, J., Kaiser, P. and Huang, L., 2010b. Regulation of the 26S proteasome complex during oxidative stress. *Sci. Signal., 3*, ra88. https://doi.org/10.1126/scisignal.2001232

WANKE, V., Accorsi, K., Porro, D., Esposito, F., Russo, T. and Vanoni, M., 1999. In budding yeast, reactive oxygen species induce both RAS-dependent and RAS-independent cell cycle-specific arrest. *Mol. Microbiol., 32,* 753-764.

WARBURG, O., 1956. On the origin of cancer cells. *Science, 123*, 309-314.

WEINBERGER, M., RAMACHANDRAN, L., FENG, L., SHARMA, K., SUN, X., MARCHETTI, M., HUBERMAN, J. A. and BURHANS, W. C., 2005. Apoptosis in budding yeast caused by defects in initiation of DNA replication. *J. Cell Sci*., 118, 3543-3553.

WEMMIE, J. A., STEGGERDA, S. M. and MOYE-ROWLEY, W. S., 1997. The *Saccharomyces cerevisiae* AP-1 protein discriminates between oxidative stress elicited by the oxidants H_2O_2 and diamide. *J. Biol. Chem., 272,* 7908-7914. https://doi.org/10.1074/jbc.272.12.7908

WENZ, T., COVIAN, R., HELLWIG, P., MACMILLAN, F., MEUNIER, B., TRUMPOWER, B. L. and HUNTE, C., 2007. Mutational analysis of cytochrome b at the ubiquinol oxidation site of yeast complex III. *J. Biol. Chem., 282*, 3977-3988. https://doi.org/10.1074/jbc.M606482200

WHEELER, G. L. and GRANT, C. M., 2004. Regulation of redox homeostasis in the yeast *Saccharomyces cerevisiae. Physiol. Plant., 120*, 12–20. https://doi.org/10.1111/j.0031-9317.2004.0193.x

WHILLIER, S., GARCIA, B., CHAPMAN, B. E., KUCHEL, P. W. and RAFTOS, J. E., 2011. Glutamine and α-ketoglutarate as glutamate sources for glutathione synthesis in human erythrocytes. *FEBS J., 278*, 3152–3163. https://doi.org/10.1111/j.1742-4658.2011.08241.x

WIATROWSKI, H. A. and CARLSON, M., 2003. Yap1 accumulates in the nucleus in response to carbon stress in *Saccharomyces cerevisiae. Eukaryot. Cell, 2,* 19-26. https://doi.org/10.1128/EC.2.1.19-26.2003

WILKINSON, D. and RAMSDALE, M. Proteases and caspase-like activity in the yeast *Saccharomyces cerevisiae.*, 2011. *Biochem. Soc. Trans.*, 39, 1502-1508. https://doi.org/10.1042/BST0391502.

WINKLER, B. S., ORSELLI, S. M. and REX, T. S., 1994. The redox couple between glutathione and ascorbic acid: a chemical and physiological perspective. *Free Radic. Biol. Med., 17,* 333-349. https://doi.org/10.1016/0891-5849(94)90019-1

WINTERBOURN, C. C. and METODIEWA, D. (1999). Reactivity of biologically important thiol compounds with superoxide and hydrogen peroxide. *Free Radic. Biol. Med., 27*, 322-328. https://doi.org/10.1016/S0891-5849(99)00051-9

WISE, D. R., DEBERARDINIS, R. J., MANCUSO, A., SAYED, N., ZHANG, X. Y., PFEIFFER, H. K., NISSIM, I., DAIKHIN, E., YUDKOFF, M., MCMAHON, S. B. and THOMPSON, C. B., 2008. Myc regulates a transcriptional program that stimulates mitochondrial glutaminolysis and leads to glutamine addiction. *Proc. Natl. Acad. Sci. U. S. A., 105*, 18782-18787. https://doi.org/10.1073/pnas.0810199105.

WISSING, S., LUDOVICO, P., HERKER, E., BÜTTNER, S., ENGELHARDT, S. M., DECKER, T., LINK, A., PROKSCH, A., RODRIGUES, F., CORTE-REAL, M., FRÖHLICH, K. U., MANNS, J., CANDÉ, C., SIGRIST, S. J., KROEMER, G., and MADEO, F., 2004. An AIF orthologue regulates apoptosis in yeast. *J. Cell Biol., 166*, 969-974.

WOLAK, N., KOWALSKA, E., KOZIK, A. and RAPALA-KOZIK, M., 2014. Thiamine increases the resistance of baker's yeast *Saccharomyces cerevisiae* against oxidative, osmotic and thermal stress, through mechanisms partly independent of thiamine diphosphate-bound enzymes. *FEMS yeast research*, *14*(8), 1249–1262. https://doi.org/10.1111/1567-1364.12218

WOLFF, S. P. and DEAN, R. T., 1986. Fragmentation of proteins by free radicals and its effect on their susceptibility to enzymic hydrolysis. *Biochem. J., 234,* 399-403. https://doi.org/10.1042/bj2340399

WONISCH, W., KOHLWEIN, S. D., SCHAUR, J., TATZBER, F., GUTTENBERGER, H. ZARKOVIC, N., WINKLER, R. and ESTERBAUER, H., 1998. Treatment of the budding yeast *Saccharomyces cerevisiae* with the lipid peroxidation product 4-HNE provokes a temporary cell cycle arrest in G1 phase. *Free Radic. Biol. Med., 25,* 682-687. https://doi.org/10.1016/s0891-5849(98)00110-5

WU, A. L. and MOYE-ROWLEY, W. S., 1994. *GSH1,* which encodes γ-glutamylcysteine synthetase, is a target gene for yAP-1 transcriptional regulation. *Mol. Cell Biol., 14,* 5832-5839. https://doi.org/10.1128/MCB.14.9.5832

WU, Z., SONG, L., LIU, S. Q. and HUANG, D., 2013. Independent and additive effects of glutamic acid and methionine on yeast longevity. *PloS One*, *8*, e79319. https://doi.org/10.1371/journal.pone.0079319

XIA, B., FANG, S., CHEN, X., HU, H., CHEN, P., WANG, H. and GAO, Z., 2016. MLKL forms cation channels. *Cell Res*. *26*, 517-28. https://doi.org/10.1038/cr.2016.26.

XIANG, Y., STINE, Z. E., XIA, J., LU, Y., O'CONNOR, R. S., ALTMAN, B. J., HSIEH, A. L., GOUW, A. M., THOMAS, A. G., GAO, P., SUN, L., SONG, L., YAN, B., SLUSHER, B. S., ZHUO, J., OOI, L. L., LEE, C. G., MANCUSO, A., MCCALLION, A. S., LE, A., MILONE, M. C., RAYPORT, S., FELSHER, D. W. and DANG, C. V., 2015. Targeted inhibition of tumor-specific glutaminase diminishes cell-autonomous tumorigenesis. *J. Clin. Invest., 125*, 2293-2306. https://doi.org/10.1172/JCI75836.

XU, J., XU, X., SHI, S., WANG, Q., SAXTON, B., HE, W., GOU, X., JANG, J. H., NYUNOYA, T., WANG, X., XING, C., ZHANG, L. and LIN, Y., 2016. Autophagy-mediated degradation of IAPs and c-FLIP(L) potentiates apoptosis induced by combination of TRAIL and Chal-24*. J. Cell Biochem*., *117*, 1136-1144. https://doi.org/10.1002/jcb.25397

YAACOB, N., ALI, M. S. M., SALLEH, A. B. and RAHMAN, N. A. A., 2016. Effects of glucose, ethanol and acetic acid on regulation of *ADH2* gene from *Lachancea fermentati. PeerJ., 4,* e1751. https://doi.org/10.7717/peerj.1751

YAMAKI, M., UMEHARA, T., CHIMURA, T. and HORIKOSHI, M., 2001. Cell death with predominant apoptotic features in *Saccharomyces cerevisiae* mediated by deletion of the histone chaperone ASF1/CIA1. *Genes Cells*, *6,* 1043-1054.

YANG, C., KO, B., HENSLEY, C. T., JIANG, L., WASTI, A. T., KIM, J., SUDDERTH, J., CALVARUSO, M. A., LUMATA, L., MITSCHE, M., RUTTER, J., MERRITT, M. E. and DEBERARDINIS, R. J., 2014. Glutamine oxidation maintains the TCA cycle and cell survival during impaired mitochondrial pyruvate transport. *Mol. Cell*, *56*, 414–424. https://doi.org/10.1016/j.molcel.2014.09.025

YANG, C., SUDDERTH, J., DANG, T., BACHOO, R. M., MCDONALD, J. G. and DEBERARDINIS, R. J., 2009. Glioblastoma cells require glutamate dehydrogenase to survive impairments of glucose metabolism or Akt signaling. *Cancer Res., 69*, 7986-7993. https://doi.org/10.1158/0008-5472.CAN-09-2266.

YANG, C. S., STAMPOULOGLOU, E., KINGSTON, N. M., ZHANG, L., MONTI, S. and VARELAS, X., 2018a. Glutamine-utilizing transaminases are a metabolic vulnerability of TAZ/YAP-activated cancer cells. *EMBO reports*, *19*, e43577. https://doi.org/10.15252/embr.201643577

YANG, H., REN, Q. and ZHANG, Z., 2008. Cleavage of Mcd1 by caspase-like protease Esp1 promotes apoptosis in budding yeast. *Mol. Biol. Cell.,*19, 2127-2134. https://doi.org/10.1091/mbc.E07-11-1113.

YANG, H., VILLANI, R. M., WANG, H., SIMPSON, M. J., ROBERTS, M. S., TANG, M. and LIANG, X., 2018b. The role of cellular reactive oxygen species in cancer chemotherapy. *J. Exp. Clin. Cancer Res., 37*, 266. https://doi.org/10.1186/s13046-018-0909-x

YANG, L., VENNETI, S. and NAGRATH, D., 2017. Glutaminolysis: a hallmark of cancer metabolism. *Annu. Rev. Biomed. Eng., 19,* 163-194. https://doi.org/10.1146/annurev-bioeng-071516-044546

YANG, L., ZHU, H., LIU, D., LIANG, S., XU, H., CHEN, J., WANG, X. and XU, Z., 2011. Aspirin suppresses growth of human gastric carcinoma cell by inhibiting survivin expression. *J. Biomed. Res.*, 25, 246-253. https://doi.org/10.1016/S1674-8301(11)60033-X.

YANG, Q. H., CHURCH-HAJDUK, R., REN, J., NEWTON, M. L. and DU, C., 2003. Omi/HtrA2 catalytic cleavage of inhibitor of apoptosis (IAP) irreversibly inactivates IAPs and facilitates caspase activity in apoptosis. *Genes Dev.*, *17*, 1487-96.

YANG, W. and HEKIMI, S., 2010. A mitochondrial superoxide signal triggers increased longevity in *Caenorhabditis elegans*. *PLoS Biol., 8,* e1000556. https://doi.org/10.1371/journal.pbio.1000556

YANG, Z., KHOURY, C., JEAN-BAPTISTE, G. and GREENWOOD, M. T., 2006. Identification of mouse sphingomyelin synthase 1 as a suppressor of Bax-mediated cell death in yeast. *FEMS Yeast Res., 6,* 751-762. https://doi.org/10.1111/j.1567-1364.2006.00052.x

YAROSZ, E. L. and CHANG, C.-H., 2018. The role of reactive oxygen species in regulating T cell mediated immunity and disease. *Immune Netw., 18*, e14. https://doi.org/10.4110/in.2018.18.e14

YE, J., COULOURIS, G., ZARETSKAYA, I., CUTCUTACHE, I., ROZEN, S. and MADDEN, T.L., 2012. Primer-BLAST: A tool to design target-specific primers for polymerase chain reaction. *BMC Bioinform.*, 13: 134. https://doi.org/10.1186/1471-2105-13-134

YE, S., LEE, M., LEE, D., HA, E. H. and CHUN, E. M., 2019. Association of long-term use of low-dose aspirin as chemoprevention with risk of lung cancer. *JAMA Netw. Open. 2,* e190185. https://doi.org/10.1001/jamanetworkopen.2019.0185.

YI, D.-G., HONG, S. and HUH, W.-K., 2018. Mitochondrial dysfunction reduces yeast replicative lifespan by elevating RAS-dependent ROS production by the ER-localised NADPH oxidase Yno1. *PLoS One, 13,* e0198619. https://doi.org/10.1371/journal.pone.0198619

YIANNAKOPOULOU, E. C. and TILIGADA, E., 2009. Protective effect of salicylates against hydrogen peroxide stress in yeast. *J. App. Microbiol., 106*, 903-908. https://doi.org/10.1111/j.1365-2672.2008.04061.x

YIN, H., XU, H., ZHAO, Y., YANG, W., CHENG, J. and ZHOU, Y., 2006. Cyclooxygenase-independent effects of aspirin on HT-29 human colon cancer cells, revealed by oligonucleotide microarrays. *Biotechnol. Lett., 28,* 1263-1270.

YIN, Z., PASCUAL, C. and KLIONSKY, D. J., 2016. Autophagy: machinery and regulation. *Microb. Cell, 3,* 588-596. https://doi.org/10.15698/mic2016.12.546

YIP-SCHNEIDER, M. T., SWEENEY, C. J., JUNG, S. H., CROWELL, P. L. and MARSHALL, M. S., 2001. Cell cycle effects of nonsteroidal anti-inflammatory drugs and enhanced growth inhibition in combination with gemcitabine in pancreatic carcinoma cells. *J. Pharmacol. Exp. Ther., 298,* 976-985.

YOUNG, M. M., TAKAHASHI, Y., KHAN, O., PARK, S., HORI, T., YUN, J., SHARMA, A. K., AMIN, S., HU, C. D., ZHANG, J., KESTER, M. and WANG, H. G., 2012. Autophagosomal membrane serves as platform for intracellular death-inducing signaling complex (iDISC)-mediated caspase-8 activation and apoptosis. *J. Biol. Chem*., *287*, 12455-12468. https://doi.org/10.1074/jbc.M111.309104

YU, L., WAN, F., DUTTA, S., WELSH, S., LIU, Z., FREUNDT, E., BAEHRECKE, E. H. and LENARDO, M., 2006. Autophagic programmed cell death by selective catalase degradation. *Proc. Natl. Acad. Sci. U. S. A., 103*, 4952-4957.

YU, S. W., WANG, Y., FRYDENLUND, D. S., OTTERSEN, O. P., DAWSON, V. L. and DAWSON, T. M., 2009. Outer mitochondrial membrane localization of apoptosis-inducing factor: mechanistic implications for release. *ASN Neuro*., *1*, e00021. https://doi.org/10.1042/AN20090046

YUNEVA, M., ZAMBONI, N., OEFNER, P., SACHIDANANDAM, R. and LAZEBNIK, Y., 2007. Deficiency in glutamine but not glucose induces MYC-dependent apoptosis in human cells. *J. Cell Biol., 178*, 93-105.

ZALKIN H. and NYGAARD P., 1996. Biosynthesis of purine nucleotides. In: Neidhardt F. C., Curtiss, R., Ingraham, J. L., Lin, E. C. C., Low, K. B., Magasanik, B., Reznikoff, W. S., Riley, M., Schaechter, M. and Umbarger, H. E. (Eds.), *Escherichia coli* and *Salmonella*: cellular and molecular biology. (2nd ed.). Washington D.C.: ASM Press. pp. 561–579.

ZARA, S., ANTONIO FARRIS, G., BUDRONI, M. and BAKALINSKY, A. T., 2002. HSP12 is essential for biofilm formation by a Sardinian wine strain of *S. cerevisiae*. *Yeast*, *19*, 269-276.

ZHA, H., FISK, H. A., YAFFE, M. P., MAHAJAN, N., HERMAN, B. and REED, J. C., 1996. Structure-function comparisons of the proapoptotic protein Bax in yeast and mammalian cells. *Mol. Cell. Biol., 16*, 6494-6508. https://doi.org/10.1128/MCB.16.11.6494

ZHANG, D. W., SHAO, J., LIN, J., ZHANG, N., LU, B. J., LIN, S. C., DONG, M. Q. and HAN, J., 2009. RIP3, an energy metabolism regulator that switches TNF-induced cell death from apoptosis to necrosis. *Science*, *325*, 332-336. https://doi.org/10.1126/science.1172308

ZHANG, J., PAVLOVA, N. N. and THOMPSON, C. B., 2017. Cancer cell metabolism: the essential role of the nonessential amino acid, glutamine. *EMBO J*, *36*, 1302-1315. https://doi.org/10.15252/embj.201696151.

ZHANG, X., FENG, H., LI, Z., GUO, J. and LI, M., 2018. Aspirin is involved in the cell cycle arrest, apoptosis, cell migration, and invasion of oral squamous cell carcinoma. *Int. J. Mol. Sci.*, *19*, E2029. https://doi.org/10.3390/ijms19072029.

ZHAO, W., ZHOU, T., ZHENG, H. Z., QIU, K. P., CUI, H. J., YU, H. and LIU, X. G., 2018. Yeast polyubiquitin gene *UBI4* deficiency leads to early induction of apoptosis and shortened replicative lifespan. *Cell Stress Chaperones*, *23*, 527-537. https://doi.org/10.1007/s12192-017-0860-3

ZHIVOTOSKY, B. and ORRENIUS, S., 2001. Assessment of apoptosis and necrosis by DNA fragmentation and morphological criteria. *Curr. Protoc. Cell Biol., 12,* 18.3.1-18.3.23, https://doi.org/10.1002/0471143030.cb1803s12

ZHENG, J., WINDERICKX, J., FRANSSENS, V. and LIU, B., 2018. A mitochondria-associated oxidative stress perspective on Huntington's disease. *Front. Mol. Neurosci.*, *11*, 329. https://doi.org/10.3389/fnmol.2018.00329

ZHOU, Y., TOZZI, F., CHEN, J., FAN, F., LING, X., WANG, J., GAO, G., ZHANG, A., XIA, X., BRASHER, H., WIDGER, W., ELLIS, L. M. and WEIHUA, Z., 2012. Intracellular ATP levels are a pivotal determinant of chemoresistance in colon cancer cells. *Cancer Res.*, *72,* 304-314. https://doi.org/10.1158/0008-5472.CAN-11-1674

ZYRINA, A. N., SMIRNOVA, E. A., MARKOVA, O. V., SEVERIN, F. F. and KNORRE, D. A, 2017. Mitochondrial superoxide dismutase and Yap1p act as a signalling module contributing to ethanol tolerance of the yeast *Saccharomyces cerevisiae. App. Env. Microbiol., 83,* e02759-16. https://doi.org/10.1128/AEM.02759-16

Publications related to this work

AZZOPARDI, M., FARRUGIA, G. and BALZAN, R. (2017). Cell-cycle involvement in autophagy and apoptosis in yeast. *Mech. Ageing Dev., 161*, 211-224. https://doi.org/10.1016/j.mad.2016.07.006

FARRUGIA, G., AZZOPARDI, M., SALIBA, C., GRECH, G., GROSS, A. S., PISTOLIC, J., BENES, V., VASSALLO, N., BORG, J., MADEO, F., EISENBERG, T. and BALZAN, R. (2019). Aspirin impairs acetyl-coenzyme A metabolism in redox-compromised yeast cells. *Sci Rep.,* 9, 6152. https://doi.org/10.1038/s41598-019-39489-4.
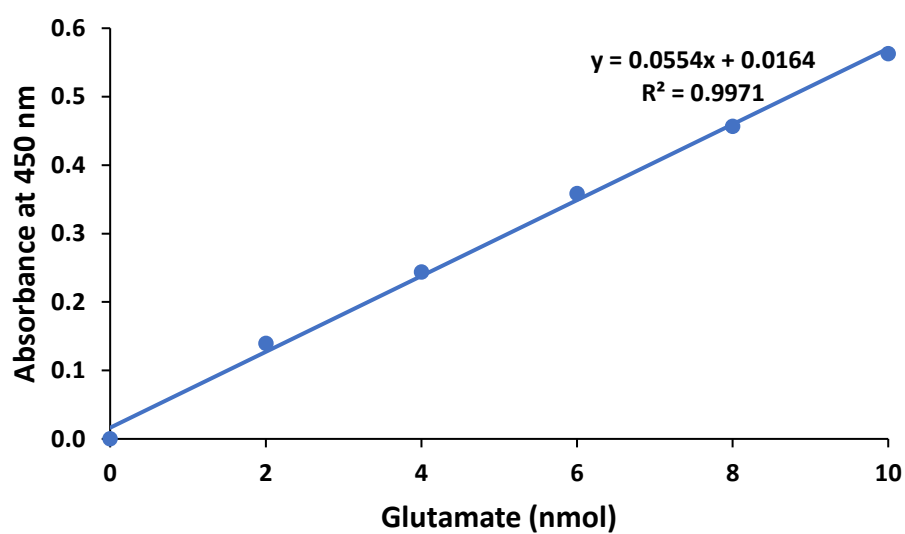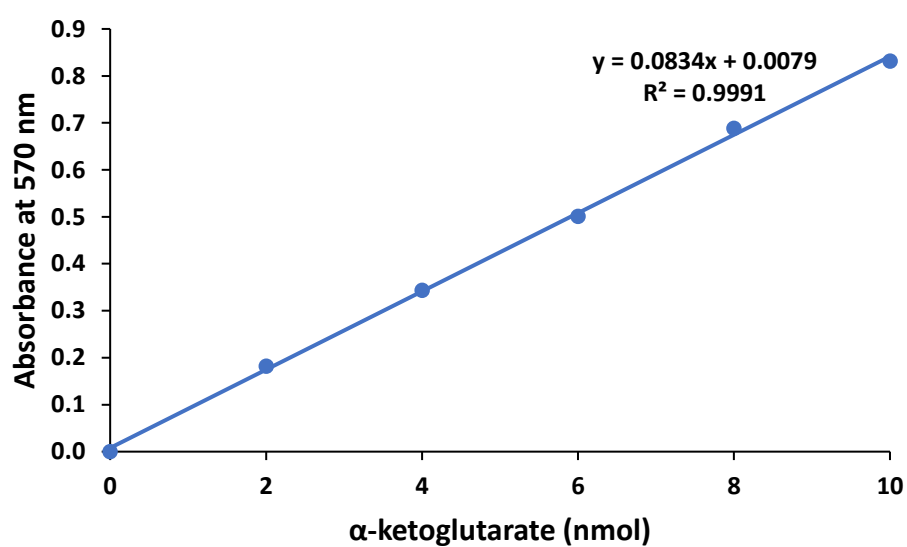
SUPPLEMENTARY FIGURES
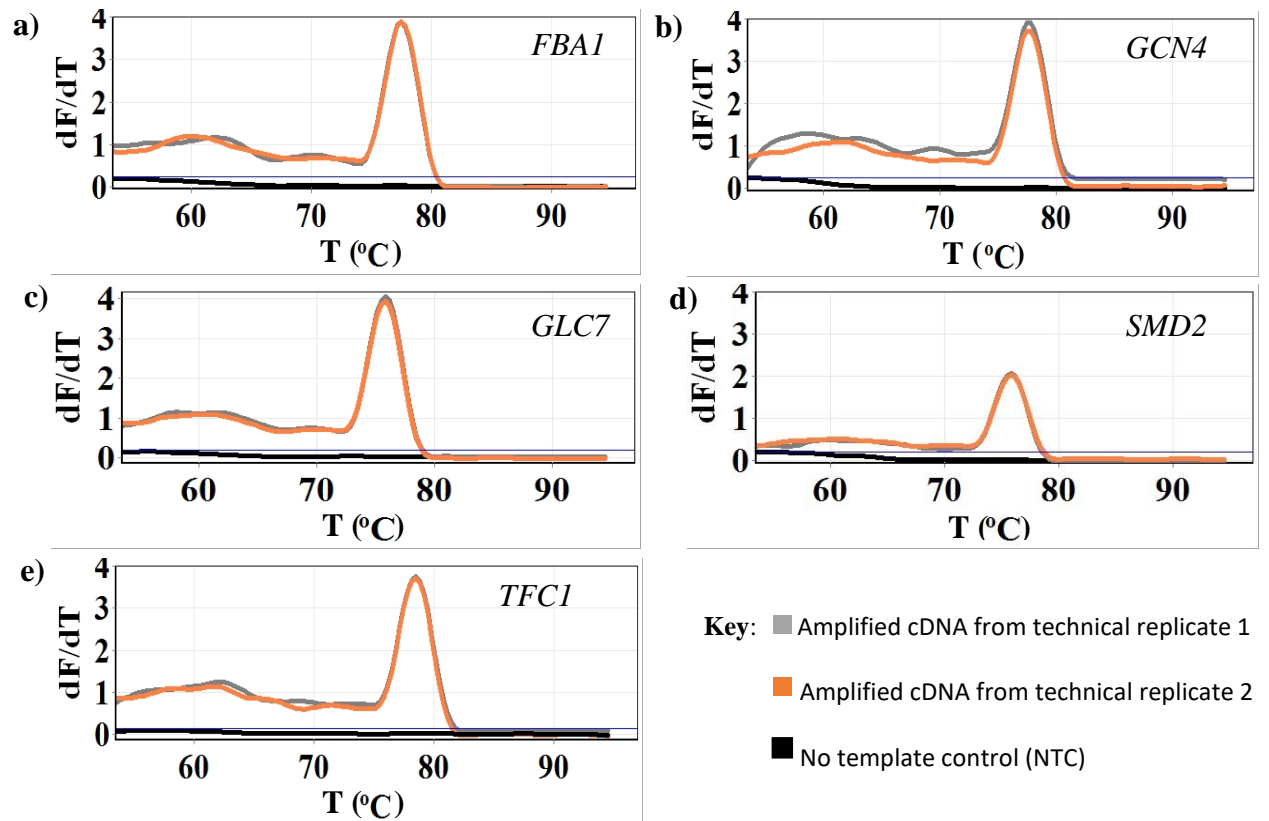
Supplementary Figure 1: The melting behaviour of the double-stranded cDNA amplicons in plots of the derivative of fluorescence versus temperature (d*F*/d*T* vs *T*) for the reference genes a) *FBA1* **b)** *GCN4* **c)** *GLC7* **d)** *SMD2* **and e)** *TFC1*. Each plot shows a prominent singular peak of the curve confirming the presence of a single amplification product for each primer pair. Each plot shows two technical replicates (grey and orange curves) and a no template control (NTC) in black (close to dF/dT = 0) to ensure the absence of contaminant DNA in any of the reagents or during sample preparation. cDNA, complementary DNA.
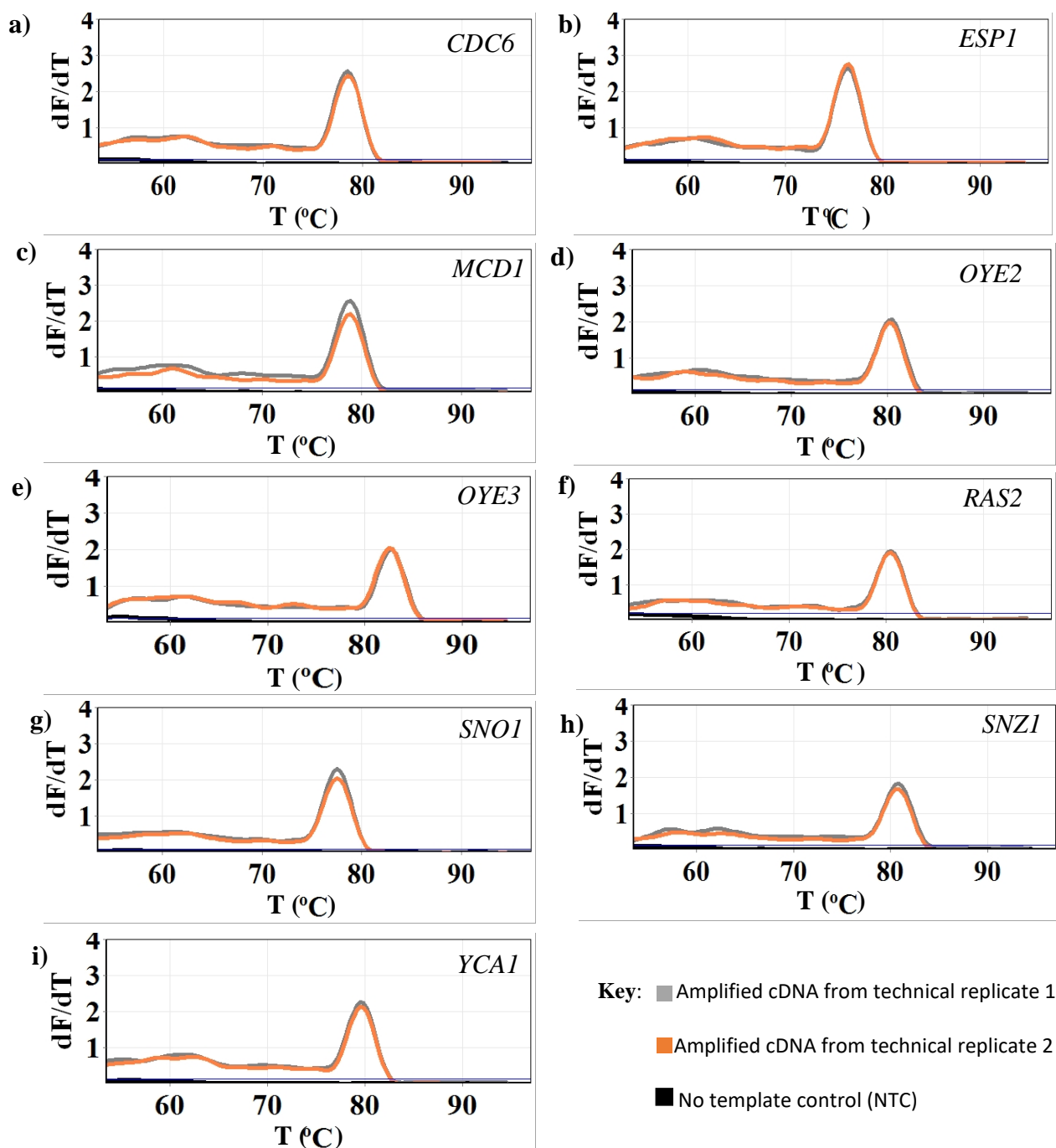
Supplementary Figure 2: The melting behaviour of the double-stranded cDNA amplicons in plots of the derivative of fluorescence versus temperature (d*F*/d*T* vs *T)* for the target genes a) *CDC6* **b)** *ESP1* **c)** *MCD1* **d)** *OYE2* **e)** *OYE3* **f)** *RAS2* **g)** *SNO1* **h)** *SNZ1* **and i)** *YCA1.* Each plot shows a prominent singular peak of the curve confirming the presence of a single amplification product for each primer pair. Each plot shows two technical replicates (grey and orange curves) and a no template control (NTC) in black (close to dF/dT = 0) to ensure the absence of contaminant DNA in any of the reagents or during sample preparation. cDNA, complementary DNA.

Supplementary Figure 3: Standard calibration curve for the measurement of L-glutamate content in total yeast cell extracts. A graph of absorbance at 450 nm against amount (nmol) of glutamate in each standard well was plotted, and this gave a straight line. Regression analysis was then used to determine the glutamate content (nmol) in total yeast cell lysates.

$$y = 0.0834x + 0.0079$$
$$R^2 = 0.9991$$

Supplementary Figure 4: Standard calibration curve for the measurement of α-ketoglutarate in yeast cells. A graph of absorbance at 570 nm against amount (nmol) of α-ketoglutarate in each sample well was plotted, and this gave a straight line through the origin. Regression analysis was then used to determine the α-ketoglutarate content (nmol) in total yeast cell lysates.
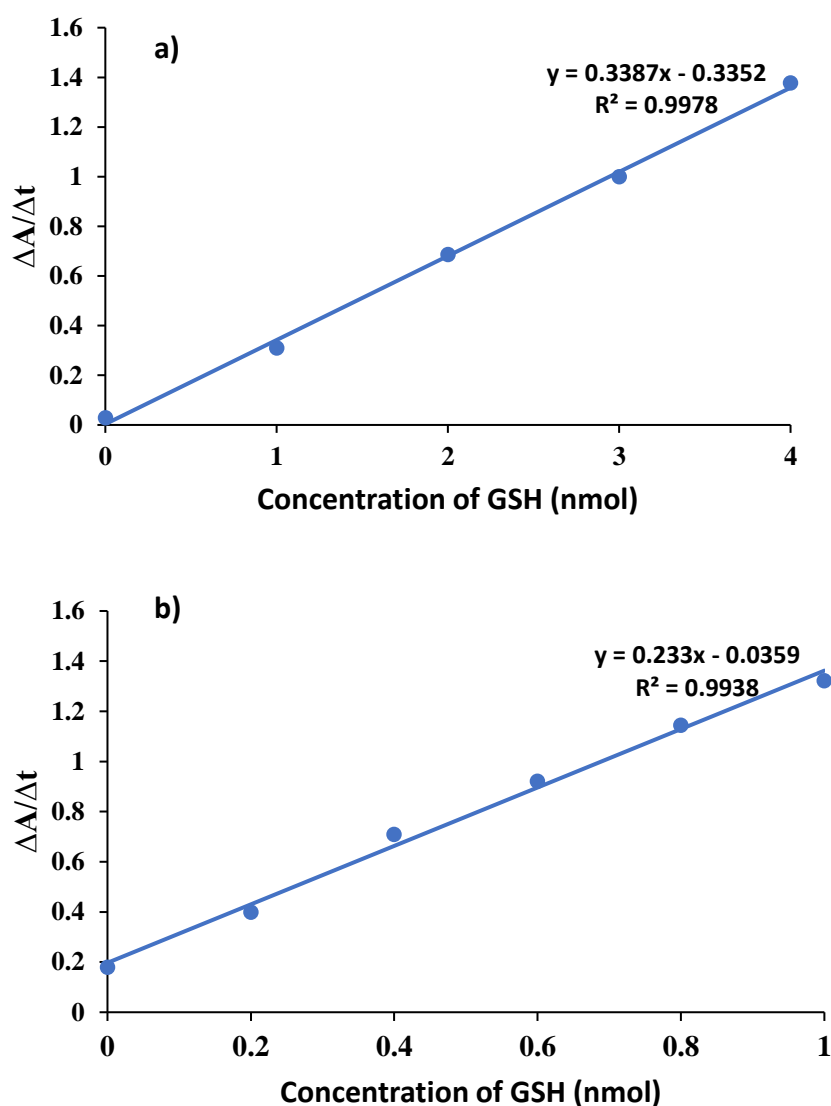
Supplementary Figure 5: Calibration curves for the measurement of a) total glutathione content (GSH + GSSG) and b) oxidised glutathione content (GSSG) in yeast cells. a) A graph of ΔA/Δt against GSH (nmol) was plotted, and this gave a straight line passing through 0.03 min^{-1} on the ordinate, and ΔA/Δt of 1.0 min^{-1} at 3 nmol GSH. b) A graph of ΔA/Δt against GSH (nmol) was plotted, and this gave a straight line passing through 0.18 min^{-1} on the ordinate, and ΔA/Δt of 1.3 min^{-1} at 1.0 nmol GSH. Regression analysis was then used to determine the total glutathione and oxidised glutathione content (nmol) in the protein-free cell lysates.

GSH, reduced glutathione, GSSG, oxidised glutathione